Photodissociation Studies of Transition Metal Oxide Cluster Cations

by

Karen Virginia Sinclair Molek

(Under the direction of Michael A. Duncan)

Abstract

Transition-metal oxide cation clusters, $M_nO_m^+$ (M = V, Nb, Ta, Cr, Fe), are produced in a molecular beam using laser vaporization in a pulsed nozzle cluster source and detected with time-of-flight mass spectrometry. The mass spectrum for each metal exhibits a limited number of stoichiometries for each value of n, where $m \geq n$. The cluster cations are mass selected and photodissociated using the second (532 nm) or third (355 nm) harmonic of a Nd:YAG laser. All of these clusters require multiphoton conditions for dissociation, consistent with their expected strong bonding. Dissociation occurs by either elimination of oxygen or by fission processes producing stable cation species and/or eliminating stable neutrals, repeatedly producing clusters having the same specific stoichiometries. In oxygen elimination, vanadium, chromium and iron species tend to lose units of O_2, whereas niobium and tantalum lose O atoms. For each metal increment, n, oxygen elimination proceeds until a terminal stoichiometry is reached. Clusters having this stoichiometry do not eliminate more oxygen, but rather undergo fission, producing smaller $M_nO_m^+$ species. The smaller clusters produced as fission products represent the corresponding terminal stoichiometries for those smaller n values. This behavior suggests that these clusters have stable bonding networks at their core, but additional excess oxygen at their periphery. Chromium and iron also shows a strong preference for eliminating specific stable neutral clusters such as FeO, CrO_3, Cr_2O_5, or Cr_4O_{10}. Specific cation clusters are identified to be stable because they are produced

repeatedly in the decomposition of larger clusters. These combined results determine that $M_2O_4^+$, $M_3O_7^+$, $M_4O_9^+$, $M_5O_{12}^+$, $M_6O_{14}^+$, and $M_7O_{17}^+$ have the greatest stability for V, Nb, and Ta oxide clusters. The Cr clusters determined to have the greatest relative stability are $Cr_2O_4^+$, $Cr_3O_6^+$, $Cr_3O_7^+$, $Cr_4O_9^+$ and $Cr_4O_{10}^+$ and the most stable iron clusters are $n = m$ clusters of $Fe_nO_m^+$, where n=2-13.

The most stable cation clusters have been calculated using density functional theory to be ring or cage structures comprised on M-O-M-O networks. The inferred neutral clusters eliminated are also noteworthy as their stoichiometries are found in the corresponding bulk materials. In addition our data implies that the vanadium group and iron oxide clusters exhibit oxidation states which are commonly found in the corresponding bulk oxides. The vanadium group clusters imply oxidation states of +4 and +5 whereas the iron clusters suggest the commonly found +2 and +3 states. In contrast, the most stable chromium clusters suggest +4 and +5 oxidation states which are not commonly found in the corresponding solid oxide materials. These results have provided insights into the similarities and differences between the oxide clusters and their corresponding nanoparticle and bulk oxides which are useful for nanomaterial isolation experiments.

INDEX WORDS: Laser vaporization, Molecular Beams, Mass Spectrometry, Photodissociation, Metal Oxide Clusters

Photodissociation Studies of Transition Metal Oxide Cluster Cations

by

Karen Virginia Sinclair Molek

B.S., Mercer University, 2001

A Dissertation Submitted to the Graduate Faculty
of The University of Georgia in Partial Fulfillment
of the
Requirements for the Degree

Doctor of Philosophy

Athens, Georgia

2007

Photodissociation Studies of Transition Metal Oxide Cluster Cations

by

Karen Virginia Sinclair Molek

Approved:

Major Professor: Michael A. Duncan

Committee: Nigel G. Adams
Geoffrey D. Smith

Electronic Version Approved:

Maureen Grasso
Dean of the Graduate School
The University of Georgia
August 2007

Dedication

First and foremost, I dedicate all of my accomplishments no matter how large or small to my heavenly Father and Savior Jesus Christ. He is majestic and flawless yet He loves us imperfections and all. I care not to even imagine how different my life would be without Christ's perfect love and provision.

I also dedicate my Ph.D to Franklin Sinclair. Some would describe him as a simple farmer from rural Georgia who encountered many obstacles in life, both in and out of his control. I call him Granddaddy, a man I love dearly. He passed away in 1996, but not before I was accepted to college. He was so proud of me. It was him who taught me how to work my first algebra problem but somehow I still thought I was smarter than him. Time and time again he proved me wrong. We had contests to see who could do math in their head the quickest. He always won! He could even do math quicker in his head than I could do it using a calculator and I am certain he would still beat me today. He and I shared another special bond. He was the one I would always call to come and pull my Jimmy out of the ditch when I had been driving too fast down the dirt road after it rained. He always came and pulled me out and I made him promise not to tell my Daddy. He did his best to keep me out of trouble and thankfully, it worked most of the time, on the dirt roads anyway. He told me if I was going to play hard I also had to work hard. I can still hear him knocking on my bedroom window at 8 am trying to get me out of the bed because I would not answer the door, I didn't want to pick vegetables out of the garden at that hour of the morning. He certainly wasn't a perfect man but he had a good heart until the day he died. His life has taught me many lessons but most of all it still challenges me today to love people the most that I possibly can. He used to tell me to always let people know how much I love them and

not just assume they know it. So I dedicate this to him to let him know how much he is missed and how much I love him.

Last but definitely not least, I dedicate this to my parents, Darrell and Donna Sinclair. Words can not describe how much of a role they have in my life and have had throughout my life. They can take all of the credit for me being here today because without them I would have stayed closer to home for college and probably would not have ever considered going to graduate school. They pushed me when I wanted to quit and loved me when I felt like a failure.

Acknowledgments

I thank Christ for all that He has done. He has provided for me when I thought it was not possible. Without Him I am nothing and with Him I am everything. These two scriptures were a crucial part of my graduate school journey as I have learned to surrender my life to His will more than I even new possible.

"This I declare of the Lord:
He alone is my refuge, my place of safety;
he is my God, and I am trusting him."
- Psalms 91:2

"You thrill me, Lord, with all you have done for me!
I sing for joy because of what you have done."
- Pslams 92:4

Next is my wonderful husband and best friend Christopher David. Words simply cannot describe how much I love and appreciate him. He was the last thing I was looking for in graduate school and the first thing I found. He is the absolute perfect for me. A mere two months prior to us meeting I was told that I would never get married because I was looking for perfection that could never be found. Comically, only six days after our first date Chris asked me to marry him. I've never been as sure of anything in my life as I am about how much I love him. He has supported me through this journey, held me when I cried, laughed with me but mostly at me and accepted me with my many flaws. Chris I appreciate you being such a wonderful husband and man of God. Oh how Geoff's Kinetics class changed my life forever!

Mom and dad, or as I like to call them Darrell and Donna, thank you! I certainly haven't made your lives easy over the years, especially the college years and yet you have always loved me! As long as I can remember you have both been my role models in life and in fact, as I have gotten older you have become even more of a role model for me. I have never once doubted your unconditional love for me. There is truly only one way to sum up how much I appreciate and love you both. I pray daily that Chris and I will be the parents to our children that you have been to me. If we achieve that level of love and acceptance, as parents we will have done our jobs. You are truly the hardest working, most intelligent, wisest, most generous, and definitely the most loving people I know. I have watched you literally work your way to where you are today while maintaining integrity, character, generosity and your loving nature. Without you both behind me supporting me and believing in me I would not be where I am today. You believed in me when I did not believe in myself. I know you aren't perfect (whew do I ever know that ◡̈) but you are both as close to it as parents come. Thank you! Thank you for who you are and for loving me with a love as close to perfection as I believe is humanly possible.

Thank you to my family! You all know who you are and Lord knows there's too many of you to name individually. I love each and every one of you and your support has been so important to me throughout the past 10 years. It certainly has not been easy being the only one living away from home but you have all made it so much more bearable! Granny and Ninny, you will always hold a special place in my heart! Ninny, you practically raised me and I obviously think you did a pretty good job. I love you so much and appreciate everything you have done for me. You are really a second mom to me and I am so thankful for our times together. Granny, there is no way to describe in a paragraph or even a book how much I treasure our relationship. You are the woman of God I strive to be. You are kind, loving, accepting, gentle, wise, but most of all you are faithful! I can always count on you to pray for me and teach me what it means to have faith. Our talks have been unparalleled over the past 10 years. I know you don't always agree with me and probably even think I'm off my rocker

sometimes, but you always listen to me like what I have to say is of the up most importance. Don't worry I know that part of that laughter in our conversations is you laughing at me rather than with me. Thank you for teaching me daily what it means to love Christ and keep him at the center of my life.

And to my friends and family in Macon and Athens, thank you too. Stacy you have been there to love me through it all. We have grown up together and while we live our separate lives this just would not be complete without expressing my appreciation for all you have done for me. Your friendship has been invaluable to me. You have always believed in me and supported me. What would I have done without you? Thank you and you will always be my best friend regardless of circumstances. Angelina, Caryn and Rod thank you so much for encouraging Chris and I throughout this process and for being so proud of us. Don't worry Caryn I might not apply to Mercer but I'm recruiting other people for you. To "my people", my small group, PRAISE GOD this is over so I can see you again! We will never be able to replace you and you will always hold a special place in our hearts. I am constantly amazed at how five couples can become family in a mere year. Thank you for accepting and loving Chris and I like family. Girls pack your beach bags! Paul and Sarah, Joe and Lisa, and Dalila you have all been such great friends to us. I appreciate your support and the many, many talks about life and science with all of you. You have each played individual roles in this process and I am so grateful to have overlapped with each of you! Dalila, Kotyn and Mr. Mistoffelees say thank you too. Joe, what am I going to do without the talks, laughs, teaching, fun, anger, etc.?

Last but certainly not least, a thank you to everyone in the department. Obviously none of this would have been possible without an advisor who believed in me. Mike Duncan, I know we've had our share of "interesting" conversations but I truly appreciate all that you have done to guide me through this process. Your charisma and passion for science never ceases to amaze me. I have a rekindled passion for science because of our talks about science over the past few months. Thank you for all of your help, especially over the past couple of

months. I look forward to working with you in the future and seeking your expertise when I start my own teaching career. Nigel Adams, I simply can't express how much I appreciate all of your encouragement and helpful talks over the past five years. Thank you for investing your time into my career and life when I thought it would be easier to just quit. Geoff Smith, I also appreciate your time and helpful talks. I must say there was something magical about that Kinetics class. Butch Atwood and Chuck Kutal, you both provided invaluable help, resources and guidance regarding teaching over the past five years. You are both amazing professors and I aspire to have my students enjoy my class as I have seen them enjoy your classes. Mamie Watson and all the ladies in the front office, I appreciate all of the help and fun over the past few years. You make that department a little more cheerful. Best wishes to all of you in the Duncan and Adams lab. Jason and Brian I hope you get finished soon. Allen, don't kill yourself being crazy in the lab before you finish.

One parting comment, thank you to everyone whom I have not named here. It's impossible to name everyone but please know that I appreciate all of you who I have interacted with throughout this journey. PRAISE GOD IT'S OVER!!!

Table of Contents

List of Figures

List of Tables

Chapter 1

Introduction and Literature Review

1.1 Applications of Bulk Oxide Materials

Transition metal oxides are ubiquitous throughout catalysis, ceramics, electronics, and magnetic materials.[1–11] Transition metal oxides exhibit several different oxidation states while maintaining their chemical stability, making them ideal candidates for catalysis and electronics.[8] These oxidation states allow the oxidation processes used to form various alcohols, aldehydes, acids, ketones, and anhydrides to be selectively controlled.[9] Recent catalysis experiments have tried using magnetite, Fe_3O_4 in an attempt to lower the temperature at which the water gas shift reaction occurs.[11] These oxides are perhaps even more renowned for their utility in electronics.[1–3] The defect structures of zinc oxide, ZnO, are used in gas sensors and semiconductors making it one of the most well studied oxide systems.[8] More recently there have been speculations of whether ZnO can be used in spintronics, where the electron spins are exploited for data storage rather than the charges.[12] Other materials such as capacitors used in automotive electronics, electronic devices, and high speed tools are comprised of tantalum oxide, Ta_2O_5.[1–3] These oxides are also found in magnetic applications. Magnetite, Fe_3O_4, is the most magnetic of all the naturally occurring minerals on earth making it particularly useful in magnetic materials used for data recording.[1–3]

1.2 Nanoparticle Applications

Recently, nanoparticle studies have further expanded the applications of transition metal oxides into magnetism, catalysis and biotechnology.[13–27] Perhaps the first observation of micron-sized particles came from Michael Faraday in 1857 when he theorized that the red color of gold colloids was due to their microscopic size.[28] Even smaller particles can be studied today in the nano regime. These nanoparticles do exhibit classical bulk like properties yet in some ways still maintain properties of the material from which they originate.[13] This alludes to their intermediate behavior which is between the corresponding bulk solid as well as the atoms and molecules which makeup that solid. Thus, their size can have a large influence

on the chemical reactivity, stability, magnetic, optical and electrical properties. Reactivity, stability, and optical properties are related to the fraction of the total number of atoms which are found on the surface of these nanoparticles. This change in stability is found where transition metal oxides are used as supports for solid metal catalysts.[10] For example, small clusters of gold supported on titanium dioxide are well known for their efficacy in CO oxidation.[6,10] The relationship between the magnetic and electrical properties of these particles and the corresponding bulk material is not so intuitive.[13] Extensive investigations have proven that while some of the magnetic and electrical properties change, others remain very similar. For example, α-Fe_2O_3 behaves like typical antiferromagnetic bulk materials at sizes > 14 nm, whereas smaller crystals < 9 nm show ferromagnetic behavior.[8] However, chromium oxide, Cr_2O_3, which is antiferromagnetic in the bulk solid has ferromagnetic properties in the nanoparticle size regime.[29] ZnO quantum dots is another example of nanoparticles which are considered a hybrid of molecules and bulk materials. Quantum dots exhibit some of the same properties as the corresponding bulk material as well as quantum behavior found at the molecular level.[13] Probing physical properties of these oxides is therefore vital to our understanding of these systems. Gas phase metal oxide clusters are model systems which can be used to probe stability, geometry, and reactivity at the molecular level. This work focuses on the determination of stable cation clusters using photodissociation studies. The results can be compared to those from a variety of experimental investigations and density functional theory (DFT), providing insights into the bonding, structure, stability and possibly magnetic properties of these systems. These results will provide valuable information which can then be used in isolating nanocluster materials.

1.3 Cluster Production

Experiments have been used to generate and detect clusters for decades, thus there is an enormous amount of information available discussing the results provided by these techniques. For this reason, disadvantages and advantages of specific sources and techniques

will be discussed in relation to the present investigations. Subsequently, techniques used to study metal oxide clusters will be discussed providing justification and advantages of our experimental techniques.

It is instructive to first discuss the overall physical properties of transition metal oxides. This will be useful in understanding the advantage and disadvantages of the techniques which can be used to produce gas phase clusters. Bulk solids of transition metal oxides are highly refractory materials with boiling points ranging from 2000 K for zinc oxide to 4000 K for chromium oxide.[1–3] The bond energies of these clusters are in the range of 3 - 7 eV.[30–32] The ionization potentials of the oxide clusters have only been measured for FeO, which is about 8.5 eV.[33] Theory has been used to calculate the ionization potentials of iron[34] and vanadium[35] oxides which are also thought to be approximately 8 eV. Zinc is the only oxide with a measurable conductivity while most other oxides are insulators.[1–3] Lastly, most of these bulk oxides are considered chemically inert due to their inherent stability. All of these properties combined necessitate a technique which can overcome the physical properties allowing gas phase clusters to be produced and studied.

Historically clusters have been generated by synthetic methods, high temperature ovens known as Knudsen cells, and ion sputtering. Alivisatos and coworkers have used synthetic methods to produce nanoparticle clusters of cobalt, cadmium selenide and iron oxide.[19,35] Hill and coworkers have even synthesized transition metal oxygen anion clusters, known as polyoxometalates or "POMs".[15,36] However these methods are limited to forming large clusters as well as to those that can be produced in solution. It is useful to produce small gas phase clusters which can be used to study fundamental properties such as bonding, structure, and reactivity. Generating gas phase clusters consists of 4 processes: 1) vaporization which produces gas phase atoms or molecules, 2) nucleation where condensation of these atoms occur forming small clusters, 3) growth where additional atoms are added to the initial cluster, and 4) coalescence where the smaller clusters merge to form larger clusters. In addition to growth, clusters can also shrink due to evaporative cooling or even fragmentation

from internally hot clusters.[37] Thus, the type of source utilized determines the size distributions of clusters. The initial step in gas phase cluster formation, vaporization, requires high-temperatures which are provided by only a few methods. Knudsen cells and ion sputtering are two sources which operate at high enough temperatures to produce gas phase clusters. A Knudsen cell involves heating a volatile solid or liquid in a high temperature oven which has an aperture small enough that it does not disturb the equilibrium between the gas and condensed phases within the cell.[37] Heating the sample creates a low enough vapor pressure that the evaporated atoms, molecules, or clusters within the cell can effuse through the aperture. The high temperature required creates internally hot clusters which undergo fragmentation generating smaller clusters.[37] An additional problem is the aperture diameter necessary to maintain equilibrium in the oven can cause clogging for less volatile solids. Recknagle and coworkers evaded the problems of creating hot clusters by filling the Knudsen cell with helium gas and enclosing it in a liquid nitrogen cooled condensation cell. This is known as inert gas condensation.[38] Antimony, bismuth and lead clusters were detected containing between 2 and 500 atoms using this source.[38] Martin and coworkers used this method to generate alkali metal clusters,[39] alkali - halide clusters,[39] and even small oxygen deficient alkali oxide clusters.[39] Although development of inert gas condensation was an improvement over traditional Knudsen cells, there are still disadvantages. As mentioned previously, most transition metal oxides have extremely high boiling points, up to 4000 K, which would be impossible to study using this source. For example, aluminum oxide cluster can be initially formed in this cell, however, discontinuities in the evaporation rate were noted which alters the clusters produced.[39] Ion sputtering sources can generate clusters of high refractory materials. Target materials are bombarded with high energy inert gas ions from an ion gun.[40] Heavier inert gases are typically used as sputtering ions with energies of approximately 20 keV.[41] The clusters produced are hot and therefore undergo evaporative cooling so that the most abundant clusters are those with larger binding energies. This method can be used for high melting materials but it cannot be used for those materials which are reactive, like

transition metals. Thus, this method is mainly used with gold and silver which are considered inert metals.[40,41] An alternative to the previously described technique is laser ablation, or sometimes called laser vaporization. In laser ablation high powered pulsed lasers are focused onto a solid target vaporizing the material instantaneously.[42] The advantage of this source is that practically any solid can be studied confining the limitations to the creativity of the user rather than the chemical species. In addition this source produces neutral, cation and anion clusters which are all contained in the clusters expansion adding further versatility to the manifold of clusters which can be studied.

1.4 Cluster Detection

Various detection methods have been utilized to ionize and detect clusters produced by the aforementioned sources. Traditionally electron impact ionization (EI), and photoionization (PI) were used to ionize neutral clusters in order to detect the generated clusters. Electron impact has been used with Knudsen cell[38,39] and ion sputtering[40,41] sources to detect antimony, bismuth, lead, alkali metal, alkali - halide, and small alkali oxide clusters. This process efficiently produces ions where the electron energy is above the ionization potential.[43] However, the excess energy required to produce ions with high ionization potentials, like transition metal oxides, results in internal heating as well as extensive fragmentation of these clusters. Originally laser vaporization was used in the investigations of photoionized neutral clusters.[42] The advantages of laser vaporization allowed numerous systems to be studied, however photoionization suffers from similar disadvantages as EI. As mentioned previously, the measured ionization potential of FeO is approximately 8.5 eV[32] and the calculated ionization potentials for iron[33] and vanadium[34] oxides are approximately the same. These potentials show that multiphoton conditions are required in order to detect the neutral clusters using 193 nm and 355 nm. VUV photoionization, 118 nm, has the best chance to ionize clusters without fragmentation, and thus may be able to detect the most abundant neutral clusters formed. However photoionization with VUV could also be detecting those

clusters which are easier to ionize as opposed to those that are the most stable. This possible bias in the photoionization measurements makes it impossible to truly obtain neutral cluster distributions. In order to avoid these disadvantages cations can be measured out of the jet using laser ablation. A supersonic expansion containing cold cations is produced by coupling this source with a pulsed nozzle.[44–53] This not only circumvents the disadvantages of ionization methods but adds the ability to seed ligands of interest directly into the expansion gas. This technique produces weakly bound metal ion-ligand complexes or strongly bound transition metal oxide and metal carbide clusters, as shown by our group.[51–53]

1.5 Survey of Transition Metal Oxide Experiments

Several detection methods and experimental techniques have been combined with laser vaporization in order to study gas phase transition metal oxide clusters.[29–33,54–67] Cluster stoichiometries and relative abundances of various transition metal oxide clusters have been determined using mass spectrometry. Equilibrium measurements have been performed on the small vanadium oxide clusters.[54] Castleman and coworkers measured mass spectra for vanadium, niobium, tantalum, and chromium oxide cation clusters.[29] These spectra show that oxide clusters exhibit several stoichiometries for each metal increment, as opposed to "magic numbers" like metal carbides.[73–79] Armentrout and coworkers determined the binding energies for small chromium and iron oxide clusters are in the range of 3-5 eV via the thresholds for energetic oxidation reactions.[60] Castleman and co-workers have also investigated collision induced dissociation of both vanadium oxide cluster cations and anions,[29] as well as niobium oxide cations.[30] The binding energies of vanadium, niobium and tantalum oxides were determined to be 3-6 eV.[29,30] In addition, the stable clusters were determine to be $V_2O_{4-6}^{+/-}$, $V_3O_{6-9}^{+/-}$, $V_4O_{8-10}^{+/-}$, $V_5O_{11-13}^{+/-}$, $V_6O_{13-15}^{+/-}$, and $V_{17}O_{16-18}^{+/-}$ and the stable neutral leaving groups were determined to be VO_2, VO_3 and V_2O_5 for both cation and anion clusters.[29,30] The same patterns were observed for the niobium oxide cation clusters.[30] This same group also measured the photodissociation of $V_nO_m^+$ clusters for $n < 7$.[29] Although the data is not as

complete, the same stable clusters were measured. These CID and photodissociation studies were used to determine the stable cluster cations for vanadium and niobium oxide clusters where similar stoichiometries were found.[29,30]

Additional experiments by Bernstein and co-workers investigated neutral mass distributions for the vanadium group and iron oxides using laser photoionization at vacuum ultraviolet[33,56] and x-ray wavelengths.[57] While cross sections are not known for any of these species, the ionization potential of FeO has been measured by Leone and coworkers to be 8.56 eV.[32] Additionally Khanna and co-workers calculated the ionization potentials to be approximately 7.5 eV for n=m FeO clusters, where n = 2-6.[33] VUV photoionization is the best way to ionize these clusters without fragmentation, allowing the possible detection of the most abundant neutral clusters formed. The most abundant clusters detected with 118 nm photoionization studies were V_2O_5, V_3O_7, V_4O_9, V_5O_{12}, V_6O_{14}, and V_7O_{17} with small amounts of V_8O_{19}.[33,56] Whereas the most abundant clusters for all three group V metals detected using 26.5 eV were of the form $(MO_2)_{0,1}(M_2O_5)_y$ corresponding to M_2O_5, M_3O_7, M_4O_{10}, M_5O_{12}, M_6O_{15}, M_7O_{17}, M_8O_{20}, and M_9O_{22}.[57] This same photoionization technique was used to measure photoionized Fe_nO_m neutral clusters using three different wavelengths, 355 nm, 193 nm, and 118nm.[56] All three wavelengths show distributions where $n = m$, or 1:1, species are the most intense features within the mass spectra.

The dissociation patterns of small iron oxide cation clusters, where m $\leq$ 4, were measured by Schwarz and co-workers using collisional activated mass spectrometry.[31] These results showed preferential inferred losses of FeO from the 1:1 clusters and losses of O_2 from the more oxygen rich clusters. The thermochemical data presented by Schwarz and co-workers for the smaller clusters, suggest the loss of FeO from Fe_3O_3 is $\sim$ 20 kcal/mole lower energy than the competitive channels of dissociation to FeO + O_2 and FeO_2 + FeO and $\sim$ 30 kcal/mole lower energy than the dissociation to Fe_3O_2 + O.[31]

The combined results from these experiments provide evidence for the relative stabilities of some oxide species. However all of these measurements use mass spectrometry, where

problems due to unknown ionization potentials, fragmentation processes, and size-dependent cross sections are of concern. Cation experiments using energy-variable collision induced dissociation or photodissociation to determine the thresholds for bond breaking also have problems. Photodissociation relies on the absorption of light, which may not be efficient in the threshold region, and collisional measurements may suffer from significant kinetic shift effects at the threshold, especially for strongly bound clusters. These same issues generally make it difficult to measure the relative concentrations of neutral clusters detected by mass spectrometry, regardless of the ionization method employed. Ionization methods may detect clusters which are easier to ionize as opposed to those that are the most stable. Clusters that are the most stable as cations often have low ionization potentials, making it conceivable that the VUV ionization detects low IP clusters more easily than stable neutral clusters. The measured and calculated potentials show that multiphoton conditions are required in order to detect the neutral clusters using 193 nm and 355 nm. VUV photoionization, 118 nm, has the best chance to ionize clusters without fragmentation, and thus may be able to detect the most abundant neutral clusters formed. The x-ray laser at 26.5 eV does not require multiphoton conditions, but the excess energy could create internally hot clusters which could result in their fragmentation before detection. This possible bias in the photoionization makes it impossible at present to resolve the issue of cation versus neutral stabilities.

Castleman and coworkers have reported extensive studies of transition metal oxides and the *reactivity* of the group V oxide cations and small iron oxide anion clusters with small hydrocarbons and carbon monoxide, respectively.[30] The stable cations previously reported for the group V oxides were found to be less reactive, for the most part, than their more oxygen-rich counterparts. In the oxygen-rich clusters, reactions often lead to the loss of oxygen and the formation of smaller oxide clusters, which typically correspond to those reported as having the largest relative stability. From these studies Castleman also concluded that the overall oxide cluster stabilities are as follows, V<Nb<Ta.[30] The reactivity of iron oxide anions was very limited as only the small clusters (where n=1-2) were probed.[30] However, these

results showed that $Fe_2O_2^-$ was less reactive than its oxygen rich counterparts. Castleman also reported the repetitive inferred loss of molecular oxygen with subsequent inferred losses FeO or FeO_2.[30]

The spectroscopy of small oxides has been studied with rare gas matrix isolation and photoelectron spectroscopy (PES) of mass-selected ions. Matrix isolation studies of small iron, chromium, nickel and noble metal oxides have been combined with DFT to determine isomeric structures of these small species.[61] Such experiments do not employ mass-selection making it difficult to accurately determine the clusters studied. PES has determined the electronic structures of small anion oxide clusters of copper, manganese, iron, cobalt, nickel, chromium, vanadium, tungsten and molybdenum.[62–64] The vibrationally resolved spectra obtained from this experiment provide vibrational frequencies for the small mass selected clusters. The limitations of this experiment are the requirement of anion clusters and ultraviolet light. Because the binding energies are high for metal oxide clusters a source with more energy per photon would be useful. Both of these techniques are useful for elucidating structures of the small oxide clusters but not the large ones.

Infrared experiments have been used to determine structures using vibrational spectroscopy. Our group in collaboration with Meijer and coworkers, used IR-resonance enhanced multiphoton ionization (IR-REMPI) to obtain the IR spectra for several metal carbide[76] and oxide[65] cluster systems. The most applicable work in this area are the new infrared photodissociation experiments using the FELIX free electron laser.[66,67] FELIX has been used to measure vibrational patterns of mass selected clusters which are compared to the patterns predicted by theory[68,71] for different cluster geometries. Since these clusters require multiphoton conditions to dissociate, these experiments work the best. Asmis and co-workers used FELIX to measure the mass-selected infrared photodissociation spectra of $V_4O_{10}^+$,[67] as well as infrared multiple photon dissociation (IRMPD) of vanadium oxide anion clusters $(V_2O_5)_n$(where n=1-4).[67] The spectra from both experiments reveal compelling evidence that these anion clusters have polyhedral cage structures as suggest by theory.[67] Asmis

and coworkers have also used rare gas tagging experiments to study the VO_2^+ and $V_2O_4^+$ cations.[67] Rare gas tagging experiments rely on the elimination of the tag atoms rather than fragmentation of the oxide cluster itself. There is excellent agreement between the calculated structures and those measured via tagging and IRMPD, however the experimental data is still very limited for these oxides.

While these IR methods have proven to be useful, they are not without their limitations. The free electron laser has a rather broad spectral resolution which is usually greater than 20 cm^{-1}. In addition, particularly high laser energies are required to dissociate large transition metal oxide clusters. This creates internally hot clusters which can result in fragmentation prior to probing their vibrational spectra or broadening if the spectra are recorded. Because these clusters are strongly bound they also require multiphoton conditions in order to dissociate. With bond energies on the order of 4 eV and the frequencies for M=O stretches around 1000 cm^1, a simple calculation shows that about 32 photons of light at 1000 cm^{-1} are required to dissociate and observe such a vibration. This is impossible except with free electron lasers. For these reasons experimental studies determining the structure of these oxides clusters are limited.

Measurements of stability can aid in the determination of possible structural motifs for these systems, and to date no thorough studies determining the relative stability of such clusters exist for these transition metal oxides. Our group has shown repeatedly that photofragmentation studies of cluster cations can be used to determine relative stabilities.[55,74,80] Stable clusters are difficult to dissociate, however, they are often produced as fragment ions upon the dissociation of larger clusters. Although stable neutrals are not detected, they can be inferred from the neutral leaving groups via mass conservation. These methods have been used previously in our lab to study metal carbide[74] and metal oxide clusters.[55] The work presented here focuses on the using photodissociation studies to determine the most stable clusters for V, Nb, Ta, Cr, and Fe oxide cluster cations. The stable cations cluster can then be

compared to the results of the aforementioned experiments as well as the structures obtained by theory.[68–72]

1.6 References

[1] Rao, C. N.; Raveau, B. *Transition Metal Oxides*; Wiley: New York, 1998.

[2] Cox, P. A. *Transition Metal Oxides*; Clarendon: Oxford, 1992.

[3] Cotton, F. A.; Wilkinson, G.; Murillo, C. A.; Bochmann, M. *Advanced Inorganic Chemistry*, Sixth ed.; John Wiley and Sons: New York, 1999.

[4] Hayashi, C.; Uyeda, R.; Tasaki, A. *Ultra-Fine Particles*; Noyes: Westwood, 1997.

[5] Gates, B. C. "Supported Metal-Clusters - Synthesis, Structure, and Catalysis," *Chem. Rev.* **1995**, *95*, 511.

[6] Street, S. C.; Xu, C.; Goodman, D. W. "The physical and chemical properties of ultrathin oxide films," *Annu. Rev. Phys. Chem.* **1997**, *48*, 43. Rainer, D. R.; Goodman, D. W. "Metal clusters on ultrathin oxide films: model catalysts for surface science studies," *J. Mol. Catal. A: Chem.* **1998**, *131*, 259. St. Clair, T. P.; Goodman, D. W. "Metal nanoclusters supported on metal oxide thin films: bridging the materials gap," *Top. Catal.* **2000**, *13*, 5. Wallace, W. T.; Min, B. K.; Goodman, D. W. "The nucleation, growth, and stability of oxide-supported metal clusters," *Top. Catal.* **2005**, *34*, 17. Chen, M. S.; Goodman, D. W. "Catalytically active gold: From nanoparticles to ultrathin films," *Acc. Chem. Res.* **2006**, *39*, 739. Chen, M. S., Luo, K., Kumar, D., Wallace, W. T., Yi, C.-W., Gath, K. K., Goodman, D. W. "The Structure of ordered Au films on TiOx " *Surf. Sci.* **2007**, *601*, 632.

[7] Wachs, I. E.; Briand, L. E.; Jehng, J. M.; Burcham, L.; Gao, X. T. "Molecular structure and reactivity of the group V metal oxides," *Catal. Today* **2000**, *57*, 323. Chen, Y. S.; Wachs, I. E. "Tantalum oxide-supported metal oxide (Re2O7, CrO3, MoO3, WO3, V2O5, and Nb2O5) catalysts: synthesis, Raman characterization and chemically probed by methanol oxidation," *J. Catal.* **2003**, *217*, 468. Wachs, I. E. "Recent conceptual advances in the catalysis science of mixed metal oxide catalytic materials," *Catal.*

Today **2005**, *100*, 79. Wachs, I. E.; Jehng, J. M.; Ueda, W. "Determination of the chemical nature of active surface sites present on bulk mixed metal oxide catalysts," *J. Phys. Chem. B* **2005**, *109*, 2275. Tian, H. J.; Ross, E. I.; Wachs, I. E. "Quantitative determination of the speciation of surface vanadium oxides and their catalytic activity," *J. Phys. Chem. B* **2006**, *110*, 9593.

[8] Henrich, V. E.; Cox, P. A. *The Surface Science of Metal Oxides*; Cambridge University Press: Cambridge, 1994.

[9] *Transition Metal Oxides: Surface Chemistry and Catalysis*; Kung, H. H., Ed.; Elsevier: New York, 1989; Vol. 45.

[10] Somorjai, G. A. *Introduction to Surface Chemistry and Catalysis*; Wiley-Interscience: New York, 1994.

[11] Liu, Q. S., Ma, W. P., He, R. X. , Mu, Z. J. "Reaction and characterization studies of an industrial Cr-free iron-based catalyst for high-temperature water gas shift reaction," *Catal. Today* **2005**, *106*, 52.

[12] Spintronics; Nanotechnology Now, 2006.

[13] *Nanopartcles*; Schmid, G., Ed.; WILEY-VCH: Weinheim, 2004.

[14] *Nanomaterials for Medical Diagnosis and Therapy*; 1st ed.; Kumar, C. S. S. R., Ed.; WILEY-VCH: Weinheim, 2007; Vol. 10.

[15] Pope, M. T.; Mller, A. *Poloyoxometalate Chemistry From Topology via Self-Assembly to Applications*; Kluwer: Boston, 2001.

[16] *Metal Nanoparticles: Synthesis, Characterization, and Applications*; Feldheim, D. L.; Foss, C. A. J., Eds.; Marcel Dekker: New York, 2002.

[17] Crans, D. C.; Smee, J. J.; Gaidamauskas, E.; Yang, L. Q. "The chemistry and biochemistry of vanadium and the biological activities exerted by vanadium compounds," *Chem. Rev.* **2004**, *104*, 849.

[18] Dimitrov, D. V. U., K., Hadjipanayis, G. C.; Papaefthymiou, V.; Simopoulos, A. "Ferrimagnetism and defect clustes in Fe1-xO films," *Phys. Rev. B* **1999**, *59*, 499. Dimitrov, D. V. U., K., Hadjipanayis, G. C.; Papaefthymiou, V.; Simopoulos, A. "Defect clusters in Fe1-xO and their ferromagnetic properties," *Journal of Appled Physics* **2000**, *87*, 7022.

[19] Rockenberger, J.; Scher, E. C.; Alivisatos, A. P. "A new nonhydrolytic single-precursor approach to surfactant-capped nanocrystals of transition metal oxides," *J. Am. Chem. Soc.* **1999**, *121*, 11595. Puntes, V. F.; Krishnan, K. M.; Alivisatos, A. P. "Colloidal nanocrystal shape and size control: The case of cobalt," *Science* **2001**, *291*, 2115. Nolting, F.; Luning, J.; Rockenberger, J.; Hu, J.; Alivisatos, A. P. "A PEEM study of small agglomerates of colloidal iron oxide nanocrystals," *Surf. Rev. Lett.* **2002**, *9*, 437. Jun, Y. W.; Casula, M. F.; Sim, J. H.; Kim, S. Y.; Cheon, J.; Alivisatos, A. P. "Surfactant-assisted elimination of a high energy facet as a means of controlling the shapes of TiO2 nanocrystals," *J. Am. Chem. Soc.* **2003**, *125*, 15981. Casula, M. F.; Jun, Y. W.; Zaziski, D. J.; Chan, E. M.; Corrias, A.; Alivisatos, A. P. "The concept of delayed nucleation in nanocrystal growth demonstrated for the case of iron oxide nanodisks," *J. Am. Chem. Soc.* **2006**, *128*, 1675. Farrell, D.; Majetich, S. A.; Wilcoxon, J. P. "Preparation and characterization of monodisperse Fe nanoparticles," *J. Phys. Chem. B* **2003**, *107*, 11022.

[20] Ayers, T. M.; Fye, J. L.; Li, Q.; Duncan, M. A. "Synthesis and isolation of titanium metal cluster complexes and ligand-coated nanoparticles with a laser vaporization flowtube reactor," *J. Cluster Sci.* **2003**, *14*, 97.

[21] Roesky, H. W.; Haiduc, I.; Hosmane, N. S. "Organometallic oxides of main group and transition elements downsizing inorganic solids to small molecular fragments," *Chem. Rev.* **2003**, *103*, 2579.

[22] Redl, F. X.; Black, C. T.; Papaefthymiou, G. C.; Sandstrom, R. L.; Yin, M.; Zeng, H.; Murray, C. B.; O'Brien, S. P. "Magnetic, electronic, and structural characterization of nonstoichiometric iron oxides at the nanoscale," *J. Am. Chem. Soc.* **2004**, *126*, 14583.

[23] Cushing, B. L.; Kolesnichenko, V. L.; O'Connor, C. J. "Recent advances in the liquid-phase syntheses of inorganic nanoparticles," *Chem. Rev.* **2004**, *104*, 3893.

[24] Kang, E.; Park, J.; Hwang, Y.; Kang, M.; Park, J. G.; Hyeon, T. "Direct synthesis of highly crystalline and monodisperse manganese ferrite nanocrystals," *J. Phys. Chem. B* **2004**, *108*, 13932.

[25] Fernandez-Garcia, M.; Martinez-Arias, A.; Hanson, J. C.; Rodriguez, J. A. "Nanostructured oxides in chemistry: Characterization and properties," *Chem. Rev.* **2004**, *104*, 4063.

[26] Suzdalev, I. P. M., Y. V.; Imshennik, V. K.; Novichikhin, S. V.; Mateev, V. V.; Tretyakov, Y. D.; Lukashin, A. V.; Eliseev, A. A.; Avramenko, N. V.; Mayygin, A. A.; Sosnov, E. A. . "Formation and properties of the nanocluster structure of iron oxides," *Russian Chem. Bulletin, Int. Ed* **2006**, *55*, 1755.

[27] Faraday, M. "The Bakerian Lecture: Experimental Relations of Gold (and Other Metals) to Light " *Philosophical Transactions* **1857**, *147*, 145.

[28] Baobre-Lpez, M., Vzquez-Vzquez, C., Rivas, J., Lpez-Quintela, M.A. "Magnetic properties of chromium (III) oxide nanoparticles," *Nanotechnology* **2003**, *14*, 318.

[29] a) Kooi, S. E.; Castleman, A. W. "Photofragmentation of vanadium oxide cations," *J. Phys. Chem. A* **1999**, *103*, 5671. b) Bell, R. C.; Zemski, K. A.; Justes, D. R.; Castleman,

A. W. "Formation, structure and bond dissociation thresholds of gas-phase vanadium oxide cluster ions," *J. Chem. Phys.* **2001**, *114*, 798.

[30] a) Deng, H. T.; Kerns, K. P.; Castleman, A. W. "Formation, structures, and reactivities of niobium oxide cluster ions," *J. Phys. Chem.* **1996**, *100*, 13386. b) Bell, R. C.; Zemski, K. A.; Kerns, K. P.; Deng, H. T.; Castleman, A. W. "Reactivities and collision-induced dissociation of vanadium oxide cluster cations," *J. Phys. Chem. A* **1998**, *102*, 1733. c) Bell, R. C.; Zemski, K. A.; Castleman, A. W. "Size-specific reactivities of vanadium oxide cluster cations," *J. Cluster Sci.* **1999**, *10*, 509. d) Zemski, K. A.; Bell, R. C.; Castleman, A. W. "Reactivities of tantalum oxide cluster cations with unsaturated hydrocarbons," *Int. J. Mass. Spectrom.* **1999**, *184*, 119. e) Zemski, K. A.; Bell, R. C.; Castleman, A. W. "Reactions of tantalum oxide cluster cations with 1-butene, 1,3-butadiene, and benzene (vol 104A, pg 5733, 2000)," *J. Phys. Chem. A* **2000**, *104*, 7408. f) Zemski, K. A.; Justes, D. R.; Bell, R. C.; Castleman, A. W. "Reactions of niobium and tantalum oxide cluster cations and anions with n-butane," *J. Phys. Chem. A* **2001**, *105*, 4410. g) Zemski, K. A.; Justes, D. R.; Castleman, A. W. "Reactions of group V transition metal oxide cluster ions with ethane and ethylene," *J. Phys. Chem. A* **2001**, *105*, 10237. h) Zemski, K. A.; Justes, D. R.; Castleman, A. W. "Studies of metal oxide clusters: Elucidating reactive sites responsible for the activity of transition metal oxide catalysts," *J. Phys. Chem. B* **2002**, *106*, 6136. i) Justes, D. R.; Mitric, R.; Moore, N. A.; Bonacic-Koutecky, V.; Castleman, A. W. "Theoretical and experimental consideration of the reactions between VxOy+ and ethylene," *J. Am. Chem. Soc.* **2003**, *125*, 6289. j) Justes, D. R.; Moore, N. A.; Castleman, A. W. "Reactions of vanadium and niobium oxides with methanol," *J. Phys. Chem. B* **2004**, *108*, 3855. k) Bergeron, D. E.; Castleman, A. W., Jr.; Jones, N. O.; Khanna, S. N. "Stable Cluster Motifs for Nanoscale Chromium Oxide Materials," *Nano Lett.* **2004**, *4*, 261. l) Kimble, M. L.; Castleman, A. W. "Gas-phase studies of AunOm+ interacting with carbon monoxide," *Int. J. Mass. Spectrom.* **2004**, *233*, 99. m) Kimble, M. L.; Castleman, A. W., Jr.; Mitric, R.; Buergel, C.; Bonacic-Koutecky, V. "Reactivity

of Atomic Gold Anions toward Oxygen and the Oxidation of CO: Experiment and Theory," *J. Am. Chem. Soc.* **2004**, *126*, 2526. n) Sun, Q.; Rao, B. K.; Jena, P.; Stolcic, D.; Kim, Y. D.; Gantefor, G.; Castleman, A. W. "Appearance of bulk properties in small tungsten oxide clusters," *J. Chem. Phys.* **2004**, *121*, 9417. o) Sun, Q.; Rao, B. K.; Jena, P.; Stolcic, D.; Kim, Y. D.; Gantefor, G.; Castleman, A. W. "Appearance of bulk properties in small tungsten oxide clusters (vol 121, pg 9417, 2004)," *J. Chem. Phys.* **2005**, *122*. p) Kimble, M. L.; Castleman, A. W.; Burgel, C.; Bonacic-Koutecky, V. "Interactions of CO with AunOm- (n ¿= 4)," *Int. J. Mass. Spectrom.* **2006**, *254*, 163. q) Kimble, M. L.; Moore, N. A.; Johnson, G. E.; Castleman, A. W.; Burgel, C.; Mitric, R.; Bonacic-Koutecky, V. "Joint experimental and theoretical investigations of the reactivity of Au2On- and Au3On- (n=1-5) with carbon monoxide," *J. Chem. Phys.* **2006**, *125*. r) Moore, N. A.; Mitric, R.; Justes, D. R.; Bonacic-Koutecky, V.; Castleman, A. W., Jr. "Kinetic Analysis of the Reaction between (V2O5)n=1,2+ and Ethylene," *J. Phys. Chem. B* **2006**, *110*, 3015. s) Reilly, N. M., Reveles, J. U., Johnson, G. E., Khanna, S. N., Castleman, A.W. Jr. "Influence of charge state on the reaction of $FeO_3^{+/-}$ with carbon monoxide," *Chem. Phys, Lett.* **2007**, *435*, 295. t) Reilly, N. M., Reveles, J. U., Johnson, G. E., Khanna, S. N., Castleman, A.W. Jr. "Experimental and Theoretical Study of the Structures and Reactivity of $Fe_{1-2}O_{\leq 6}^-$ Clusters with CO," *J. Phys. Chem. A*. **2007**, *111*, 4158.

[31] a) Harvey, J. N.; Diefenbach, M.; Schroder, D.; Schwarz, H. "Oxidation properties of the early transition-metal dioxide cations MO2+ (M = Ti, V, Zr, Nb) in the gas-phase," *Int. J. Mass. Spectrom.* **1999**, *183*, 85. b) Schrder, D.; Schwarz, H.; Shaik, S. "Characterization, orbital description, and reactivity patterns of transition-metal oxo species in the gas phase," *Struct. Bonding* **2000**, *97*, 91. c) Jackson, P.; Fisher, K. J.; Willett, G. D. "The catalytic activation of primary alcohols on niobium oxide surfaces unraveled: the gas phase reactions of NbxOy- clusters with methanol and ethanol," *Chem. Phys.* **2000**, *262*, 179. d) Schrder, D.; Jackson, P.; Schwarz, H. "Dissociation

patterns of small FemOn+ (m=1-4, n ¡= 6) cluster cations formed upon chemical ionization of Fe(CO)(5)/O-2 mixtures," *Eur. J. Inorg. Chem.* **2000**, 1171. e) Jackson, P.; Harvey, J. N.; Schrder, D.; Schwarz, H. "Structure and reactivity of the prototype iron-oxide cluster Fe2O2+," *Int. J. Mass. Spectrom.* **2001**, *204*, 233. f) Schroder, D.; Engeser, M.; Schwarz, H.; Harvey, J. N. "Energetics of the ligated vanadium dications VO2+, VOH2+, and [V,O,H-2](2+)," *Chemphyschem* **2002**, *3*, 584. g) Engeser, M.; Schlangen, M.; Schroder, D.; Schwarz, H.; Yumura, T.; Yoshizawa, K. "Alkane oxidation by VO2+ in the gas phase: A unique dependence of reactivity on the chain length," *Organometallics* **2003**, *22*, 3933. h) Engeser, M.; Schroder, D.; Schwarz, H. "Gas-phase dehydrogenation of methanol with mononuclear vanadium-oxide cations," *Chemistry-a European Journal* **2005**, *11*, 5975. i) Koszinowski, K.; Schlangen, M.; Schroder, D.; Schwarz, H. "Formation, structure, and reactivity of gaseous Ni2O2+," *Eur. J. Inorg. Chem.* **2005**, 2464. j) Feyel, S.; Dobler, J.; Schroder, D.; Sauer, J.; Schwarz, H. "Thermal activation of methane by tetranuclear [V4O10](+)," *Angewandte Chemie-International Edition* **2006**, *45*, 4681. k) Feyel, S.; Schroder, D.; Rozanska, X.; Sauer, J.; Schwarz, H. "Gas-phase oxidation of propane and 1-butene with [V3O7](+): Experiment and theory in concert," *Angewandte Chemie-International Edition* **2006**, *45*, 4677. l) Feyel, S.; Schroder, D.; Schwarz, H. "Gas-phase oxidation of isomeric butenes and small alkanes by vanadium-oxide and -hydroxide cluster cations," *J. Phys. Chem. A* **2006**, *110*, 2647.

[32] Metz, R. B.; Nicolas, C.; Ahmed, M.; Leone, S. R. "Direct determination of the ionization energies of FeO and CuO with VUV radiation," *J. Chem. Phys.* **2005**, *123*.

[33] a) Jones, N. O.; Reddy, B. V.; Rasouli, F.; Khanna, S. N. "Structural growth in iron oxide clusters: Rings, towers, and hollow drums," *Phys. Rev. B* **2005**, *72*. b) Jones, N. O.; Reddy, B. V.; Rasouli, F.; Khanna, S. N. "Structural growth in iron oxide clusters: Rings, towers, and hollow drums (vol 72, pg 165411, 2005)," *Phys. Rev. B* **2006**, *73*.

[34] Matsuda, Y.; Bernstein, E. R. "Identification, structure, and spectroscopy of neutral

vanadium oxide clusters," *J. Phys. Chem. A* **2005**, *109*, 3803.

[35] a) Puntes, V. F.; Krishnan, K. M.; Alivisatos, A. P. "Colloidal nanocrystal shape and size control: The case of cobalt," *Science* **2001**, *291*, 2115. b) Johnston-Halperin E., A. D. D., Crooker S. A., Efros A. L., Rosen M., Peng X., Alivisatos A. P. "Spin spectroscopy of dark excitons in CdSe quantum dots to 60 T," *Phys. Rev. B* **2001**, *63* 5310. c) Peng, X., Manna, L., Yang, W., Wickham, J., Scher, E., Kadavanich, A., Alivisatos, A.P. "Shape control of CdSe nanocrystals," *Nature* **2000**, *404*, 6773.

[36] a) Hill, C. L., Prosser-McCartha, C. M. "Homogeneous catalysis by transition metal oxygen anion clusters," *Coord. Chem. Rev.* **1995**, *143*, 407. b) Rhule, J. T., Hill, C. L., Judd, D. A. "Polyoxometalates in Medicine," *Chem. Rev.* **1998**, *98*, 327. c) Hill, C. L. "Progress and challenges in polyoxometalate-based catalysis and catalytic materials chemistry," *Journal of Molecular Catalysis A: Chemical* **2007**, *262*, 2.

[37] *Clusters of Atoms and Molecules Vol. I*; Haberland, H., Ed.; Springer: Berlin, 1995; Vol. 52.

[38] a) Sattler, K., Muhlbach, J., Recknagel, E. "Generation of Metal Clusters from 2 to 500 Atoms," *Phys. Rev. Lett.* **1980**, *45*, 821. b) Muhlbach, J., Pfau, P., Recknagel, E., Sattler, K. "Cluster Emission From the Surfaces OF Bi, Sb, and Se," *Surf. Sci.* **1980**, *106*, 18.

[39] a) Martin, T. P., Schaber, H. "Matrix isolated alkali halide monomers and clusters," *J. Chem. Phys.* **1978**, *68*, 4299. b) Martin, T. P. "Compound clusters produced by the reaction of elemental vapors," *J. Chem. Phys* **1984**, *81*, 4426.

[40] Johnston, R. L. *Atomic and Molecular Clusters*; Taylor & Francis: London, 2002.

[41] Hofer, W. O. *Sputtering by Particle Bombardment III*; Springer: Berlin, 1991.

[42] a) Dietz, T.G.; Duncan, M.A.; Powers, D.E.; Smalley, R.E. J. Chem. Phys. 1981, 74, 6511. b) Zheng, L.S.; Brucat, P.J.; Pettiette, C.L.; Yang, S.; Smalley, R.E. J. Chem.

Phys. 1985, 83, 4273. c) Brucat, P.J.; Zheng, L.S.; Pattiette, C.L.; Yang, S.; Smalley, R.E. J. Chem. Phys. 1986, 84, 3078. d) Zheng, L.S.; Carner, C.M.; Brucat, P.J.; Yang, S.H.; Pettiette, C.L.; Craycraft, M.J.; Smalley, R.E. J. Chem. Phys. 1986, 85, 1681. e) Chesnovsky, O.; Yang, S.H.; Pettiette, C.L.; Craycraft, M.J.; Liu, Y.; Smalley, R.E. Chem. Phys. Lett. 1987, 138, 119. f) Yang, S.; Taylor, K.J.; Craycraft, M.J.; Conceicao, J.; Pettiette, C.L.; Chesnovsky, O.; Smalley, R.E. Chem. Phys. Lett. 1988, 144, 431. g) Chesnovsky, O.; Taylor, K.J.; Conceicao, J.; Smalley, R.E. Phys. Rev. Lett. 1990, 64, 1785. h) Jin, C.; Taylor, K.J.; Conceicao, J.; Smalley, R.E. Chem. Phys. Lett, 1990, 175, 17.

[43] Massey, H.S.W. *Electron Collisions with Molecules and Photoionization*, Oxford University Press, Oxford, 1969. 14.

[44] a) Leuchtner, R. E.; Harms, A. C.; Castleman, A. W., Jr. *J. Chem. Phys.* **1990**, *92*, 6527. b) Guo, B. C.; Kerns, K. P.; Castleman, A. W., Jr. *Science* **1992**, *255*, 1411. c) Guo, B. C.; Castleman, A. W., Jr. *J. Am. Chem. Soc.* **1992**, *114*, 6152. d) Cartier, S. F.; May, B. D.; Castleman, A.W., Jr. *J. Am. Chem. Soc.* **1994**, *116*, 5295. e) Kerns, K. P.; Guo, B. C.; Deng, H. T.; Castleman, A. W., Jr. *J. Am. Chem. Soc.* **1995**, *117*, 4026. f) Kerns, K. P.; Guo, B. C.; Deng, H. T.; Castleman, A. W. Jr. *J. Phys. Chem.* **1996**, *100*, 16817. g) Vann, W. D.; Wagner, R. L.; Castleman, A. W. Jr. *J. Phys. Chem. A* **1998**, *102*, 1708. h) Zemski, K. A.; Justes, D. R.; Castleman, A. W., Jr. *J. Phys. Chem. B* **2002**, *106*, 6136.

[45] a) Beyer, M.; Berg, C.; Grlitzer, H.W.; Schindler, T.; Achatz, U.; Albert, G.; Niedner-Schatteburg, G.; Bondybey, V.E. *J. Am. Chem. Soc.* **1996**, *118,* 7386. b) Beyer, M.; Achatz, U.; Berg, C.; Joos, S.; Niedner-Schatteburg, G.; Bondybey, V.E. *J. Phys. Chem. A* **1999**, *103*, 671. c) Bondybey, V.E.; Beyer, M.K. *Int. Rev. Phys. Chem.* **2002**, *21*, 277. d) Fox, B.S.; Balteanu, I.; Balaj, O.P.; Liu, H.; Beyer, M.K; Bondybey, V.E. *Phys. Chem. Chem. Phys.* **2002**, *4*, 2224. e) Berg C.; Achatz, U.; Beyer, M.; Joos, S.; Albert,

G.; Schindler, T.; Niedner-Schattburg, G.; Bondybey, V.E. *Int. J. Mass Spectrom.* **1997**, *167*, 723. f) Berg, C.; Beyer, M.; Achatz, U.; Joos, S.; Niedner-Schattburg, G.; Bondybey, V.E. *Chem. Phys.* **1998**, *239*, 379.

[46] a) Schalley, C.; Schroeder, D.; Schwarz, H. Organometallics **1995**, 14, 316. b) Schwarz, J.; Heinemann, C.; Schwarz, H. J. Phys. Chem. **1995**, 99, 11405. c) Schalley, C.A.; Wesendrup, R.; Schroeder, D.; Schwarz, H. Organometallics **1996**, 15, 678. d) Schroeter, K.; Schalley, C.A.; Wesendrup, R.; Schroeder, D.; Schwarz, H. Organometallics **1997**, 16, 986. e) Schroeder, D.; Kretzschmar, I.; Schwarz, H.; Rue, C.; Armentrout, P.B. Inorg. Chem. **1999**, 38, 3474. f) Jackson, P.; Harvey, J.N.; Schroeder, D.; Schwarz, H. Int. J. Mass Spectrom. **2001**, 204, 233. g) Schwarz, H. Ang. Chem., Int. Ed. **2003**, 42, 4442.

[47] a) Kemper, P.R.; Hsu, M.T.; Bowers, M.T. J. Phys. Chem. **1991**, 95, 10600. b) Bushnell, J.E.; Kemper, P.R.; Maitre, P.; Bowers, M.T. J. Am. Chem. Soc. **1994**, 116, 9710. c) Bushnell, J.E.; Kemper, P.R.; Bowers, M.T. J. Phys. Chem. **1995,** 99, 15602. d) Kemper, P.R.; Weis, P.; Bowers, M.T. Int. J. Mass Spectrom. Ion Proc. **1997**, 160, 17. e) Weis, P.; Kemper, P.R.; Bowers, M.T., J. Phys. Chem. A **1997**, 101, 8207. f) Kemper, P.R.; Bushnell, J.; Bowers, M.T.; Gellene, G.I. J. Phys. Chem. A. **1998**, 102, 8590. g) Zhang, Q.; Kemper, P. R.; Shin, S. K.; Bowers, M. T. Int. J. Mass Spectrom. **2001**, 204, 281. f) Zhang, Q.; Kemper, P.R.; Bowers, M.T. Int. J. Mass Spectrom. **2001**, 210, 265. h) Manard, M.J.; Kemper, P.R.; Carpenter, C.J.; Bowers, M.T. Int. J. Mass Spectrom. **2005**, 241, 99. i) Manard, M.J.; Kemper, P.R.; Bowers, M.T. Int. J. Mass Spectrom. **2005**, 241, 109.

[48] a) Aristov, N.; Armentrout, P. B. *J. Am. Chem. Soc.* **1986**, *108*, 1806. b) Georgiadis, R.; Armentrout, P. B. *Int. J. Mass Spectrom. Ion Proc.* **1989**, *89*, 227. c) Fisher, E. R.; Armentrout, P. B. *J. Phys. Chem.* **1990**, *94*, 1674. d) Chen, Y.M.; Armentrout, P.B., *Chem. Phys. Lett.* **1993**, *210*, 123. e) Clemmer, D. E.; Chen, Y.-M.; Aristov, N.; Armentrout, P. B. *J. Phys. Chem.* **1994**, *98*, 7538. f) Dalleska, N. F.; Honma, K.;

Sunderlin, L. S.; Armentrout, P. B. *J. Am. Chem. Soc.* **1994**, *116*, 3519. g) Meyer, F.; Khan, F. A.; Armentrout, P. B. *J. Am. Chem. Soc.* **1995**, *117*, 9740. h) Sievers, M. R.; Jarvis, L. M.; Armentrout, P. B. *J. Am. Chem. Soc.* **1998**, *120*, 1891. i) Sievers, M. R.; Chen, Y.-M.; Haynes, C. L.; Armentrout, P. B. *Int. J. Mass Spectrom.* **2000**, *195*, 149. j) Shoeib, T.; Milburn, R.K.; Koyanagi, G.K.; Lavrov, V.V.; Bohme, D.K.; Siu, K.W.M.; Hopkinson, A.C. *Int. J. Mass Spectrom.* **2000**, *201*, 87. k) Koizumi, H.; Larson, M.; Muntean, F.; Armentrout, P. B. *Int. J. Mass Spectrom.* **2003**, *228*, 221.

[49] a) Ho, Y.P.; Yang, Y.C.; Klippenstein, S.J.; Dunbar, R.C., *J. Phys. Chem. A* **1997**, *101*, 3338. b) Petrie, S.; Dunbar, R.C. *J. Phys. Chem. A.* **2000**, *104*, 4480. Petrie, S. *J. Phys. Chem.* **2002**, *106*, 7034.

[50] a) Schroeder, D.; Hruk, J.; Hertwig, R.; Koch, W.; Schwerdtfeger, P.; Schwarz, H. *Organometallics* **1995**, *14*, 312. b) Stoeckigt, D.; Hruk, J.; Schwarz, H. *Int. J. Mass Spectrom. Ion Proc.* **1995**, *149*, 1. c) Schroeder, D.; Schwarz, H.; Hruk, J.; Pyykkoe, P. *Inorg. Chem.* **1998**, *37*, 624.

[51] a) Willey, K. F.; Cheng, P. Y.; Yeh, C. S.; Robbins, D. L.; Duncan, M. A. *J. Chem. Phys.* **1991**, *95*, 6249. b) Yeh, C. S.; Robbins, D. L.; Pilgrim, J. S.; Duncan, M. A. *Chem. Phys. Lett.* **1993**, *206*, 509. c) Brock, L. R.; Pilgrim, J. S.; Duncan, M. A. *Chem. Phys. Lett.* **1994**, *230*, 93. d) Pilgrim, J. S.; Duncan, M. A. *Chem. Phys. Lett.* **1995**, *232*, 335. e) Brock, L. R.; Knight, A. M.; Reddic, J. E.; Pilgrim, J. S.; Duncan, M. A. *J. Chem. Phys.* **1997**, *106*, 6268. f) Berry, K. R.; Duncan, M. A. *Chem. Phys. Lett.* **1997**, *279*, 44. g) Stangassinger, A.; Knight, A. M.; Duncan, M. A. *J. Phys. Chem. A* **1999**, *103*, 1547.

[52] a) Willey, K.F.; Yeh, C.S; Robbins, D.L.; Pilgrim, J.S.; Duncan, M.A. *J. Chem. Phys.* **1992**, *97*, 8886. b) Yeh, C. S.; Willey, K. F.; Robbins, D. L.; Pilgrim, J. S.; Duncan, M. A. *Chem. Phys. Lett.* **1992**, *196*, 233. c) Pilgrim, J. S.; Yeh, C. S.; Duncan, M. A. *Chem. Phys. Lett.* **1993**, *210*, 322. d) Pilgrim, J. S.; Yeh, C. S.; Berry, K. R.; Duncan,

M. A. *J. Chem. Phys.* **1994**, *100*, 7945. e) Scurlock, C. T.; Pilgrim, J. S.; Duncan, M. A. *J. Chem. Phys.* **1995**, *103*, 3293. f) Yeh, C. S.; Pilgrim, J. S.; Willey, K. F.; Robbins, D. L.; Duncan, M. A. *Int. Rev. Phys. Chem.* **1994**, *13*, 231. g) Yeh, C. S.; Willey, K. F.; Robbins, D. L.; Duncan, M. A. *J. Phys. Chem.* **1992**, *96*, 7833. h) Willey, K. F.; Yeh, C. S.; Robbins, D. L.; Duncan, M. A. *Chem. Phys. Lett.* **1992**, *192*, 179. i) Yeh, C.S.; Willey, K.F.; Robbins, D.L.; Duncan, M.A. *J. Chem. Phys.* **1993**, *98*, 1867. j) Robbins, D.L.; Brock, L.R.; Pilgrim, J.S.; Duncan, M.A. *J. Chem. Phys.* **1995**, *102*, 1481. k) France, M.R.; Pullins, S.H.; Duncan, M.A. *Chem. Phys.* **1998**, *239*, 447. l) Reddic, J.E.; Duncan, M.A. *Chem. Phys. Lett.* **1999**, *312*, 96. m) Reddic, J.E.; Duncan, M.A. *J. Chem. Phys.* **1999**, *110*, 9948.

[53] a) Scurlock, C.T.; Pullins, S.H.; Reddic, J.E.; Duncan, M.A. *J. Chem. Phys.* **1996**, *104*, 4591. b) Pullins, S.H.; Scurlock, C.T.; Reddic, J.E.; Duncan, M.A. *J. Chem. Phys.* **1996**, *104*, 7518. c) Velasquez, J.; Kirschner, K.N.; Reddic, J.E.; Duncan, M.A. *Chem. Phys. Lett.* **2001**, *343*, 613. d) Reddic, J.E.; Duncan, M.A. *J. Chem. Phys.* **2000**, *112*, 4974. e) Scurlock, C.T.; Pullins, S.H.; Duncan, M.A. *J. Chem. Phys.* **1996**, *105*, 3579. f) Kirschner, K.N.; Ma, B.; Bowen, J.P.; Duncan, M.A. *Chem. Phys. Lett.* **1998**, *295*, 204. g) Pullins, S.H.; Reddic, J.E.; France, M.R.; Duncan, M.A. *J. Chem. Phys.* **1998**, *108*, 2725. h) Weslowski, S. S.; King, R. A.; Schaefer, H. F.; Duncan, M. A. *J. Chem. Phys.* **2000**, *113*, 701. i) France, M. R.; Pullins, S. H.; Duncan, M. A. *J. Chem. Phys.* **1998**, *108*, 7049. j) France, M. R.; Pullins, S. H.; Duncan, M. A. *J. Chem. Phys.* **1998**, *109*, 8842.

[54] a) Berkowitz, J.; Chupka, W. A.; Inghram, M. G. "Thermodynamics of the V-O System - Dissociation Energies of VO and VO_2," *J. Chem. Phys.* **1957**, *27*, 87. b) Inghram, M. G.; Chupka, W. A.; Berkowitz, J. "Thermodynamics of the Ta-O System - Dissociation Energies of Tao and Tao2," *J. Chem. Phys.* **1957**, *27*, 569.

[55] a) France, M. R.; Buchanan, J. W.; Robinson, J. C.; Pullins, S. H.; Tucker, J. L.; King, R.

B.; Duncan, M. A. "Antimony and Bismuth Oxide Clusters: Growth and Decomposition of New Magic Number Clusters," *J. Phys. Chem. A* **1997**, *101*, 6214.

[56] a) Foltin, M.; Stueber, G. J.; Bernstein, E. R. "On the growth dynamics of neutral vanadium oxide and titanium oxide clusters," *J. Chem. Phys.* **1999**, *111*, 9577. b) Foltin, M.; Stueber, G. J.; Bernstein, E. R. "Investigation of the structure, stability, and ionization dynamics of zirconium oxide clusters," *J. Chem. Phys.* **2001**, *114*, 8971. c) Matsuda, Y.; Shin, D. N.; Bernstein, E. R. "On the zirconium oxide neutral cluster distribution in the gas phase: Detection through 118 nm single photon, and 193 and 355 nm multiphoton, ionization," *J. Chem. Phys.* **2004**, *120*, 4142. d) Matsuda, Y.; Shin, D. N.; Bernstein, E. R. "On the copper oxide neutral cluster distribution in the gas phase: Detection through 355 nm and 193 nm multiphoton and 118 nm single photon ionization," *J. Chem. Phys.* **2004**, *120*, 4165. e) Matsuda, Y.; Bernstein, E. R. "On the titanium oxide neutral cluster distribution in the gas phase: Detection through 118 nm single-photon and 193 mn multiphoton ionization," *J. Phys. Chem. A* **2005**, *109*, 314. f) Matsuda, Y.; Bernstein, E. R. "Identification, structure, and spectroscopy of neutral vanadium oxide clusters," *J. Phys. Chem. A* **2005**, *109*, 3803. g) Dong, F.; Heinbuch, S.; He, S. G.; Xie, Y.; Rocca, J. J.; Bernstein, E. R. "Formation and distribution of neutral vanadium, niobium, and tantalum oxide clusters: Single photon ionization at 26.5 eV," *J. Chem. Phys.* **2006**, *125*, 164318. h) Shin, D. N.; Matsuda, Y.; Bernstein, E. R. "On the iron oxide neutral cluster distribution in the gas phase. I. Detection through 193 nm multiphoton ionization," *J. Chem. Phys.* **2004**, *120*, 4150. i) Shin, D. N.; Matsuda, Y.; Bernstein, E. R. "On the iron oxide neutral cluster distribution in the gas phase. II. Detection through 118 nm single photon ionization," *J. Chem. Phys.* **2004**, *120*, 4157.

[57] Dong, F.; Heinbuch, S.; He, S. G.; Xie, Y.; Rocca, J. J.; Bernstein, E. R. "Formation and distribution of neutral vanadium, niobium, and tantalum oxide clusters: Single photon ionization at 26.5 eV," *J. Chem. Phys.* **2006**, *125*.

[58] Wang, X.; Neukermans, S.; Vanhoutte, F.; Janssens, E.; Verschoren, G.; Silverans, R. E.; Lievens, P. "Stability patterns and ionization potentials of CrnOm clusters (n=3-50, m=0, 1, 2)," *Appl. Phys. B: Lasers Opt.* **2001**, *73*, 417.

[59] Fielicke, A.; Rademann, K. "Stability and reactivity patterns of medium-sized vanadium oxide cluster cations $V_xO_y^+$ (4 ¡= x ¡= 14)," *Phys. Chem. Chem. Phys.* **2002**, *4*, 2621.

[60] a) Griffin, J. B.; Armentrout, P. B. "Guided ion beam studies of the reactions of Fe-n(+) (n=2-18) with O-2: Iron cluster oxide and dioxide bond energies," *J. Chem. Phys.* **1997**, *106*, 4448. b) Xu, J.; Rodgers, M. T.; Griffin, J. B.; Armentrout, P. B. "Guided ion beam studies of the reactions of V-n(+) (n=2-17) with O-2: Bond energies and dissociation pathways," *J. Chem. Phys.* **1998**, *108*, 9339. c) Griffin, J. B.; Armentrout, P. B. "Guided ion beam studies of the reactions of Cr-n(+) (n=2-18) with O-2: Chromium cluster oxide and dioxide bond energies," *J. Chem. Phys.* **1998**, *108*, 8062. d) Vardhan, D.; Liyanage, R.; Armentrout, P. B. "Guided ion beam studies of the reactions of Ni-n(+) (n=2-18) with O-2: Nickel cluster oxide and dioxide bond energies," *J. Chem. Phys.* **2003**, *119*, 4166. e) Liu, F. Y.; Li, F. X.; Armentrout, P. B. "Guided ion-beam studies of the reactions of Co-n(+) (n=2-20) with O-2: Cobalt cluster-oxide and -dioxide bond energies," *J. Chem. Phys.* **2005**, *123*.

[61] a) Chertihin, G. V.; Saffel, W.; Yustein, J. T.; Andrews, L.; Neurock, M.; Ricca, A.; Bauschlicher, C. W. "Reactions of laser-ablated iron atoms with oxygen molecules in condensing argon. Infrared spectra and density functional calculations of iron oxide product molecules," *J. Phys. Chem.* **1996**, *100*, 5261. b) Chertihin, G. V.; Bare, W. D.; Andrews, L. "Reactions of laser-ablated chromium atoms with dioxygen. Infrared spectra of CrO, OCrO, CrOO, CrO3, Cr(OO)(2), Cr2O2, Cr2O3 and Cr2O4 in solid argon," *J. Chem. Phys.* **1997**, *107*, 2798. c) Zhou, M. F.; Andrews, L. "Infrared spectra and density functional calculations of the CrO2-, MoO2-, and WO2- molecular anions in solid neon," *J. Chem. Phys.* **1999**, *111*, 4230. d) Andrews, L.; Rohrbacher, A.; Laperle,

C. M.; Continetti, R. E. "Laser desorption/ionization of transition metal atoms and oxides from solid argon," *J. Phys. Chem. A* **2000**, *104*, 8173. e) Wang, X.; Andrews, L. "Precious Metal-Molecular Oxygen Complexes: Neon Matrix Infrared Spectra and Density Functional Calculations for M(O2), M(O2)2 (M = Pd, Pt, Ag, Au)," *J. Phys. Chem. A* **2001**, *105*, 5812. f) Danset, D.; Manceron, L.; Andrews, L. "Vibrational Spectra of Nickel and Platinum Dioxide Molecules Isolated in Solid Argon," *J. Phys. Chem. A* **2001**, *105*, 7205.

[62] a) Fan, J. W.; Wang, L. S. "Photoelectron-Spectroscopy of Feo- and Feo2- - Observation of Low-Spin Excited-States of Feo and Determination of the Electron-Affinity of Feo2," *J. Chem. Phys.* **1995**, *102*, 8714. b) Wang, L. S.; Wu, H. B.; Desai, S. R. "Sequential oxygen atom chemisorption on surfaces of small iron clusters," *Phys. Rev. Lett.* **1996**, *76*, 4853. c) Wu, H. B.; Desai, S. R.; Wang, L. S. "Observation and photoelectron spectroscopic study of novel mono- and diiron oxide molecules: FeO_y^- (y=1-4) and $Fe_2O_y^-$ (y=1-5)," *J. Am. Chem. Soc.* **1996**, *118*, 7434. d) Wang, L.-S.; Wu, H.; Desai, S. R.; Lou, L. "Electronic structure of small copper oxide clusters: from Cu2O to Cu2O4," *Phys. Rev. B: Condens. Matter* **1996**, *53*, 8028. e) Gutsev, G. L.; Rao, B. K.; Jena, P.; Li, X.; Wang, L.-S. "Experimental and theoretical study of the photoelectron spectra of MnOx- (x=1-3) clusters," *J. Chem. Phys.* **2000**, *113*, 1473. f) Sun, Q.; Sakurai, M.; Wang, Q.; Yu, J. Z.; Wang, G. H.; Sumiyama, K.; Kawazoe, Y. "Geometry and electronic structures of magic transition-metal oxide clusters M9O6 (M = Fe, Co, and Ni)," *Phys. Rev. B* **2000**, *62*, 8500. g) Gutsev, G. L.; Jena, P.; Zhai, H.-J.; Wang, L.-S. "Electronic structure of chromium oxides, CrOn- and CrOn (n = 1-5) from photoelectron spectroscopy and density functional theory calculations," *J. Chem. Phys.* **2001**, *115*, 7935. h) Zhai, H.-J.; Wang, L.-S. "Electronic structure and chemical bonding of divanadium-oxide clusters (V2Ox, x=3-7) from anion photoelectron spectroscopy," *J. Chem. Phys.* **2002**, *117*, 7882. i) Gutsev, G. L.; Bauschlicher, C. W., Jr.; Zhai, H.-J.; Wang, L.-S. "Structural and electronic properties of iron monoxide clusters FenO and FenO- (n = 2-6): a combined

photoelectron spectroscopy and density functional theory study," *J. Chem. Phys.* **2003**, *119*, 11135. j) Zhai, H.-J.; Kiran, B.; Cui, L.-F.; Li, X.; Dixon, D. A.; Wang, L.-S. "Electronic Structure and Chemical Bonding in MOn- and MOn Clusters (M = Mo, W; n = 3-5): A Photoelectron Spectroscopy and ab Initio Study," *J. Am. Chem. Soc.* **2004**, *126*, 16134. k) Yang, X.; Waters, T.; Wang, X.-B.; O'Hair, R. A. J.; Wedd, A. G.; Li, J.; Dixon, D. A.; Wang, L.-S. "Photoelectron Spectroscopy of Free Polyoxoanions Mo6O192- and W6O192- in the Gas Phase," *J. Phys. Chem. A* **2004**, *108*, 10089. l) Zhai, H. J.; Huang, X.; Waters, T.; Wang, X. B.; O'Hair, R. A. J.; Wedd, A. G.; Wang, L. S. "Photoelectron spectroscopy of doubly and singly charged group VIB dimetalate anions: M2O72-, MM ' O-7(2-), and M2O7- (M, M ' = Cr, Mo, W)," *J. Phys. Chem. A* **2005**, *109*, 10512. m) Zhai, H.-J.; Huang, X.; Cui, L.-F.; Li, X.; Li, J.; Wang, L.-S. "Electronic and Structural Evolution and Chemical Bonding in Ditungsten Oxide Clusters: W2On- and W2On (n = 1-6)," *J. Phys. Chem. A* **2005**, *109*, 6019. n) Huang, X.; Zhai, H. J.; Li, J.; Wang, L. S. "On the structure and chemical bonding of tri-tungsten oxide clusters W3On- and W3On (n=7-10): W3O8 as a potential molecular model for O-deficient defect sites in tungsten oxides," *J. Phys. Chem. A* **2006**, *110*, 85. o) Zhai, H. J.; Wang, L. S. "Probing the electronic properties of dichromium oxide clusters Cr2On- (n=1-7) using photoelectron spectroscopy," *J. Chem. Phys.* **2006**, *125*.

[63] a) Wenthold, P. G.; Jonas, K. L.; Lineberger, W. C. "Ultraviolet photoelectron spectroscopy of the chromium dioxide negative ion," *J. Chem. Phys.* **1997**, *106*, 9961. b) Ramond, T. M.; Davico, G. E.; Hellberg, F.; Svedberg, F.; Salen, P.; Soderqvist, P.; Lineberger, W. C. "Photoelectron spectroscopy of nickel, palladium, and platinum oxide anions," *J. Mol. Spectrosc.* **2002**, *216*, 1. c) Ichino, T.; Gianola, A. J.; Andrews, D. H.; Lineberger, W. C. "Photoelectron spectroscopy of AuO- and AuS-," *J. Phys. Chem. A* **2004**, *108*, 11307.

[64] a) Pramann, A.; Nakamura, Y.; Nakajima, A.; Kaya, K. "Photoelectron Spectroscopy of Yttrium Oxide Cluster Anions: Effects of Oxygen and Metal Atom Addition," *J.*

Phys. Chem. A **2001**, *105*, 7534. b) Pramann, A.; Koyasu, K.; Nakajima, A.; Kaya, K. "Photoelectron spectroscopy of cobalt oxide cluster anions," *J. Phys. Chem. A* **2002**, *106*, 4891. c) Pramann, A.; Koyasu, K.; Nakajima, A.; Kaya, K. "Anion photoelectron spectroscopy of VnOm- (n=4-15; m=0-2)," *J. Chem. Phys.* **2002**, *116*, 6521.

[65] a) von Helden, G.; Kirilyuk, A.; van Heijnsbergen, D.; Sartakov, B.; Duncan, M. A.; Meijer, G. "Infrared spectroscopy of gas-phase zirconium oxide clusters," *Chem. Phys.* **2000**, *262*, 31. b) van Heijnsbergen, D.; von Helden, G.; Meijer, G.; Duncan, M. A. "Infrared resonance-enhanced multiphoton ionization spectroscopy of magnesium oxide clusters," *J. Chem. Phys.* **2002**, *116*, 2400. c) van Heijnsbergen, D.; Demyk, K.; Duncan, M. A.; Meijer, G.; von Helden, G. "Structure determination of gas phase aluminum oxide clusters," *Phys. Chem. Chem. Phys.* **2003**, *5*, 2515.

[66] a) Fielicke, A.; Meijer, G.; von Helden, G. "Infrared spectroscopy of niobium oxide cluster cations in a molecular beam: Identifying the cluster structures," *J. Am. Chem. Soc.* **2003**, *125*, 3659. b) Fielicke, A.; Meijer, G.; von Helden, G. "Infrared multiple photon dissociation spectroscopy of transition metal oxide cluster cations - Comparison of group Vb (V, Nb, Ta) metal oxide clusters," *European Physical Journal D* **2003**, *24*, 69. c) Fielicke, A.; Mitric, R.; Meijer, G.; Bonacic-Koutecky, V.; von Helden, G. "The structures of vanadium oxide cluster-ethene complexes. A combined IR multiple photon dissociation spectroscopy and DFT calculation study," *J. Am. Chem. Soc.* **2003**, *125*, 15716. d) Demyk, K.; van Heijnsbergen, D.; von Helden, G.; Meijer, G. "Experimental study of gas phase titanium and aluminum oxide clusters," *Astronomy & Astrophysics* **2004**, *420*, 547.

[67] a) Asmis, K. R.; Bruemmer, M.; Kaposta, C.; Santambrogio, G.; von Helden, G.; Meijer, G.; Rademann, K.; Woeste, L. "Mass-selected infrared photodissociation spectroscopy of $V_4O_{10}^+$," *Phys. Chem. Chem. Phys.* **2002**, *4*, 1101. b) Brummer, M.; Kaposta, C.; Santambrogio, G.; Asmis, K. R. "Formation and photodepletion of cluster ion-messenger

atom complexes in a cold ion trap: Infrared spectroscopy of VO^+, VO_2^+, and VO_3^+," *J. Chem. Phys.* **2003**, *119*, 12700. c) Asmis, K. R.; Meijer, G.; Bruemmer, M.; Kaposta, C.; Santambrogio, G.; Woeste, L.; Sauer, J. "Gas phase infrared spectroscopy of mono- and divanadium oxide cluster cations," *J. Chem. Phys.* **2004**, *120*, 6461. d) Asmis, K. R.; Santambrogio, G.; Brummer, M.; Sauer, J. "Polyhedral vanadium oxide cages: Infrared spectra of cluster anions and size-induced d electron localization," *Angewandte Chemie-International Edition* **2005**, *44*, 3122. e) Janssens, E.; Santambrogio, G.; Brummer, M.; Woste, L.; Lievens, P.; Sauer, J.; Meijer, G.; Asmis, K. R. "Isomorphous substitution in bimetallic oxide clusters," *Phys. Rev. Lett.* **2006**, *96*.

[68] a) Sambrano, J. R.; Andres, J.; Beltran, A.; Sensato, F.; Longo, E. "Theoretical study of the structure and stability of Nb_xO_y and $Nb_xO_y^+$ (x = 1-3; y = 2-5, 7, 8) clusters," *Chem. Phys. Lett.* **1998**, *287*, 620. b) Calatayud, M.; Silvi, B.; Andres, J.; Beltran, A. "A theoretical study on the structure, energetics and bonding of VOx+ and VOx (x=1-4) systems," *Chem. Phys. Lett.* **2001**, *333*, 493. c) Calatayud, M.; Andres, J.; Beltran, A. "A systematic density functional. theory study of VxOy+ and VxOY (X=2-4, Y=2-10) systems," *J. Phys. Chem. A* **2001**, *105*, 9760. d) Sambrano, J. R.; Gracia, L.; Andres, J.; Berski, S.; Beltran, A. "A theoretical study on the gas phase reactions of the anions NbO3-, NbO5-, and NbO2(0H)(2)(-) with H2O and O-2," *J. Phys. Chem. A* **2004**, *108*, 10850. e) Sambrano, J. R.; Andres, J.; Gracia, L.; Safont, V. S.; Beltran, A. "DFT study of the water-assisted tautomerization process between hydrated oxide, MO(H2O)(+), and dihydroxide, M(OH)(2)(+) cations (M = V, Nb and Ta)," *Chem. Phys. Lett.* **2004**, *384*, 56. f) Gracia, L.; Andres, J.; Safont, V. S.; Beltran, A. "DFT study of the reaction between VO2+ and C2H6," *Organometallics* **2004**, *23*, 730.

[69] a) Veliah, S.; Xiang, K. H.; Pandey, R.; Recio, J. M.; Newsam, J. M. "Density functional study of chromium oxide clusters: Structures, bonding, vibrations, and stability," *J. Phys. Chem. B* **1998**, *102*, 1126. b) Xiang, K. H.; Pandey, R.; Recio, J. M.; Francisco,

E.; Newsam, J. M. "A theoretical study of the cluster vibrations in Cr2O2,Cr2O3, and Cr2O4," *J. Phys. Chem. A* **2000**, *104*, 990.

[70] a) Reddy, B. V.; Khanna, S. N. "Chemically induced oscillatory exchange coupling in chromium oxide clusters," *Phys. Rev. Lett.* **1999**, *83*, 3170. b) Morisato, T.; Jones, N. O.; Khanna, S. N.; Kawazoe, Y. "Stable aluminum and chromium oxide clusters as precursors to nanoscale materials," *Comp. Mater. Sci.* **2006**, *35*, 366. c) Jones, N. O.; Reddy, B. V.; Rasouli, F.; Khanna, S. N. "Structural growth in iron oxide clusters: Rings, towers, and hollow drums," *Phys. Rev. B* **2005**, *72*. d) Jones, N. O.; Reddy, B. V.; Rasouli, F.; Khanna, S. N. "Structural growth in iron oxide clusters: Rings, towers, and hollow drums (vol 72, pg 165411, 2005)," *Phys. Rev. B* **2006**, *73*

[71] a) Vyboishchikov, S. F.; Sauer, J. "Gas-phase vanadium oxide anions: Structure and detachment energies from density functional calculations," *J. Phys. Chem. A* **2000**, *104*, 10913. b) Vyboishchikov, S. F.; Sauer, J. "(V2O5)(n) gas-phase clusters (n=1-12) compared to V2O5 crystal: DFT calculations," *J. Phys. Chem. A* **2001**, *105*, 8588. c) Vyboishchikov, S. F. "Gas-phase reactions of V2O5+ and V2O6+ ions with CH3CF3 studied by density functional theory," *Journal of Molecular Structure-Theochem* **2005**, *723*, 53.

[72] a) Shiroishi, H.; Oda, T.; Hamada, I.; Fujima, N. "Structure and magnetism on iron oxide clusters Fe_nO_m (n=1-5): Calculation from first principles," *European Physical Journal D* **2003**, *24*, 85. b) Shiroishi, H.; Oda, T.; Hamada, I.; Fujima, N. "Structure and magnetism on sanion iron oxide clusters $Fe_nO_m^-$ (n=1-2)," *Molecular Simulation* **2004**, *30*, 911.

[73] a) Guo, B. C.; Kerns, K. P.; Castleman, A. W., Jr. "Ti8C12+-metallo-carbohedrenes: a new class of molecular clusters?," *Science* **1992**, *255*, 1411. b) Guo, B. C.; Wei, S.; Purnell, J.; Buzza, S.; Castleman, A. W., Jr. "Metallo-carbohedrenes [M8C12+ (M = vanadium, zirconium, hafnium, and titanium)]: a class of stable molecular cluster ions,"

Science **1992**, *256*, 515. c) Guo, B. C.; Castleman, A. W., Jr. "Metallo-carbohedrenes: a new class of molecular clusters," *Adv. Met. Semicond. Clusters* **1994**, *2*, 137. d) Cartier, S. F.; May, B. D.; Castleman, A. W., Jr. "Formation, Structure, and Stabilities of Metallocarbohedrenes," *J. Phys. Chem.* **1996**, *100*, 8175.

[74] a) Pilgrim, J. S.; Duncan, M. A. "Beyond metallo-carbohedrenes: growth and decomposition of metal-carbon nanocrystals," *J. Am. Chem. Soc.* **1993**, *115*, 9724. b) Pilgrim, J. S.; Duncan, M. A. "Metallo-carbohedrenes: chromium, iron, and molybdenum analogs," *J. Am. Chem. Soc.* **1993**, *115*, 6958. c) Duncan, M. A. "Synthesis and characterization of metal-carbide clusters in the gas phase," *J. Cluster Sci.* **1997**, *8*, 239.

[75] Rohmer, M.-M.; Benard, M.; Poblet, J.-M. "Structure, Reactivity, and Growth Pathways of Metallocarbohedrenes M8C12 and Transition Metal/Carbon Clusters and Nanocrystals: A Challenge to Computational Chemistry," *Chem. Rev.* **2000**, *100*, 495.

[76] a) van Heijnsbergen, D.; von Helden, G.; Duncan, M. A.; van Roij, A. J. A.; Meijer, G. "Vibrational spectroscopy of gas-phase metal-carbide clusters and nanocrystals," *Phys. Rev. Lett.* **1999**, *83*, 4983. b) von Helden, G.; van Heijnsbergen, D.; Meijer, G. "Resonant ionization using IR light: A new tool to study the spectroscopy and dynamics of gas-phase molecules and clusters," *J. Phys. Chem. A* **2003**, *107*, 1671.

[77] Gueorguiev, G. K.; Pacheco, J. M. "Structural identification of metcars," *Phys. Rev. Lett.* **2002**, *88*; Gueorguiev, G. K.; Pacheco, J. M. "Shapes of cagelike metal carbide clusters: First-principles calculations," *Phys. Rev. B* **2003**, *68*.

[78] a) Liu, P.; Rodriguez, J. A.; Hou, H.; Muckerman, J. T. "Chemical reactivity of metcar Ti8C12, nanocrystal Ti14C13 and a bulk TiC(001) surface: A density functional study," *J. Chem. Phys.* **2003**, *118*, 7737. b) Liu, P.; Rodriguez, J. A.; Muckerman, J. T. "The chemical activity of metal compound nanoparticles: Importance of electronic and steric effects in M8C12 (M=Ti, V, Mo) metcars," *J. Chem. Phys.* **2004**, *121*, 10321. c) Liu, P.;

Lightstone, J. M.; Patterson, M. J.; Rodriguez, J. A.; Muckerman, J. T.; White, M. G. "Gas-phase interaction of thiophene with the Ti8C12+ and Ti8C12 met-car clusters," *J. Phys. Chem. B* **2006**, *110*, 7449.

[79] Varganov, S. A.; Gordon, M. S. "Effects of strong electron correlations in Ti8C12 Met-Car," *Chem. Phys.* **2006**, *326*, 97; Varganov, S. A.; Dudley, T. J.; Gordon, M. S. "Predicted IR spectra of Ti8C12 and Ti8C12+," *Chem. Phys. Lett.* **2006**, *429*, 49.

[80] a) Ticknor, B. W. D.; M. A. "Photodissociation of size-selected silicon carbide cluster cations," *Chem. Phys. Lett* **2005**, *405*, 214. b) Jaeger, J. B. J., T. D.; Duncan, M. A. " Photodissociation of Metal-Silicon Clussters: Encapsulated versus Surface-Bound Metal," *J. Phys. Chem. A* **2006**, *110*, 9310.

Chapter 2

Experimental

Clusters are produced and studied in a specially designed molecular beam machine which is shown in Figure 2.1. The machine contains two chambers which are differentially pumped. The one where clusters are formed is known as the "source" chamber. It is held at a constant pressure of $\sim 10^{-6}$ torr by a VHS-10 (Varian) diffusion pump. Clusters are produced by laser vaporization of a rotating metal rod in a pulsed nozzle cluster source. The clusters produced are skimmed into a molecular beam through a skimmer cone which separates the two chambers. The second chamber, known as the "detection" chamber houses the reflectron time-of-flight mass spectrometer (TOF-MS) where the clusters are mass analyzed.[1,2] This chamber is held at a constant pressure of $\sim 10^{-8}$ torr by a VHS-6 (Varian) diffusion pump. Figure 2.1 shows a schematic of our apparatus including the chamber where clusters are formed and the differentially pumped reflectron TOF-MS.

The laser vaporization source is shown in Figure 2.2a. The second harmonic (532 nm) of a pulsed Nd:YAG laser (Spectra Physics GCR-11) is used to vaporize a 1/4 metal rod. Typical vaporization laser energies used are 20-60 mJ/pulse with a 5 - 10 ns pulse duration and a 10 Hz repetition rate. The timing and synchronization of our entire experiment is controlled by digital delay generators (Stanford Research Systems DG535). The metal rod is held in a homemade holder where an aperture allows the vaporized material to intersect with a helium buffer gas which is seeded with 1 to 20% oxygen. A General Valve (series 9) with backing pressures of 60 to 150 psi is used to pulse in the gas mixture creating a supersonic expansion where cluster growth occurs. The clusters formed are cooled via collisions with the helium mixture. Cooling the expansion too quickly essentially freezes the clusters thus spoiling the growth of large, strongly bound ones. For this reason a 1 inch growth channel, with a 5mm diameter, is attached to the end of the regular rod holder, as shown in Figure 2.2a. A photograph of the entire nozzle assembly is shown in Figure 2.2b. This growth channel allows the clusters more time to cool and find their thermodynamically favored state. The channel also introduces turbulence into the flow creating more collisions between the metal and oxygen and thus there are more opportunities to grow larger clusters. Although the

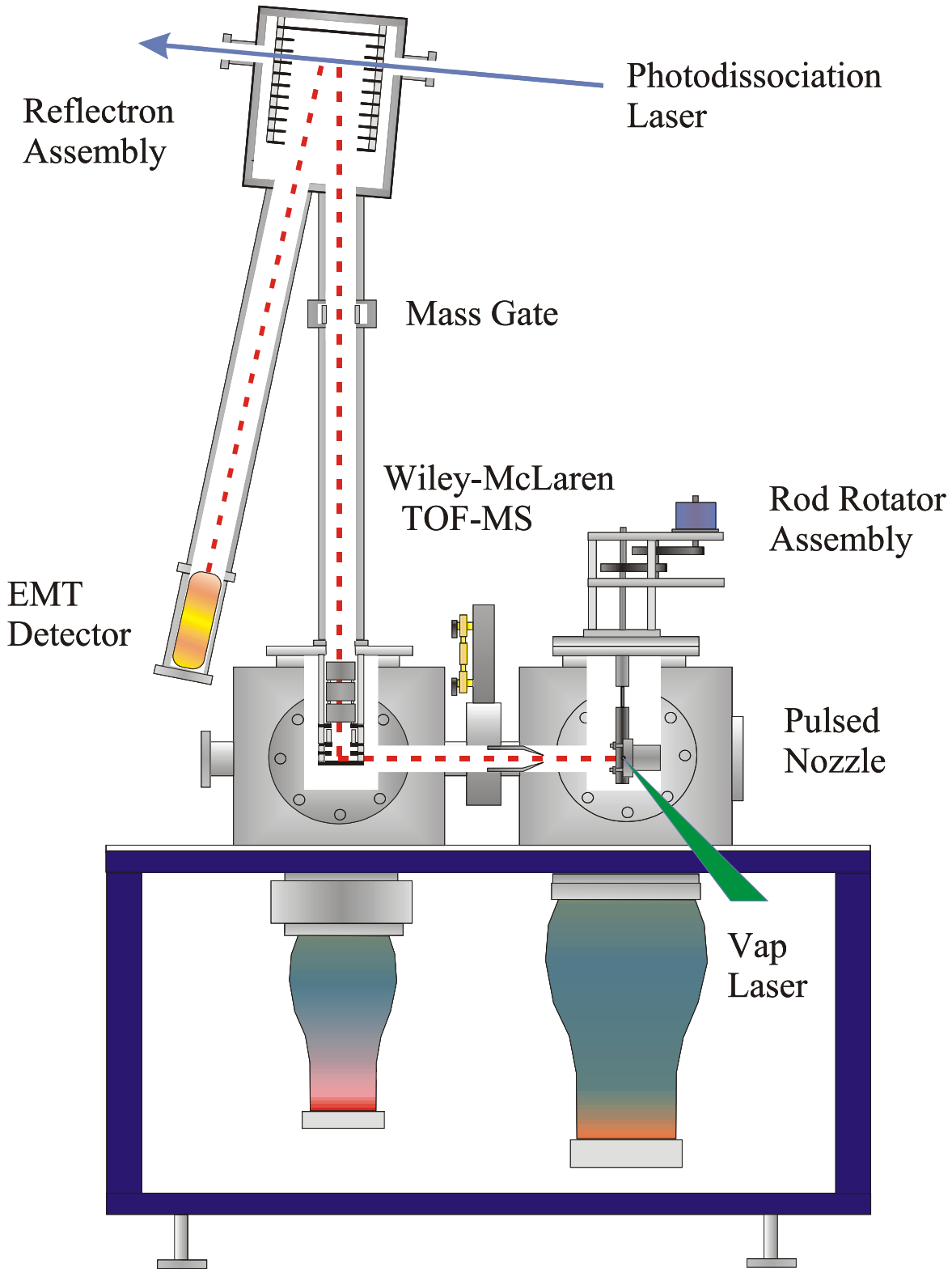

Figure 2.1: The molecular beam machine with the reflectron time-of-flight mass spectrometer (TOF-MS).

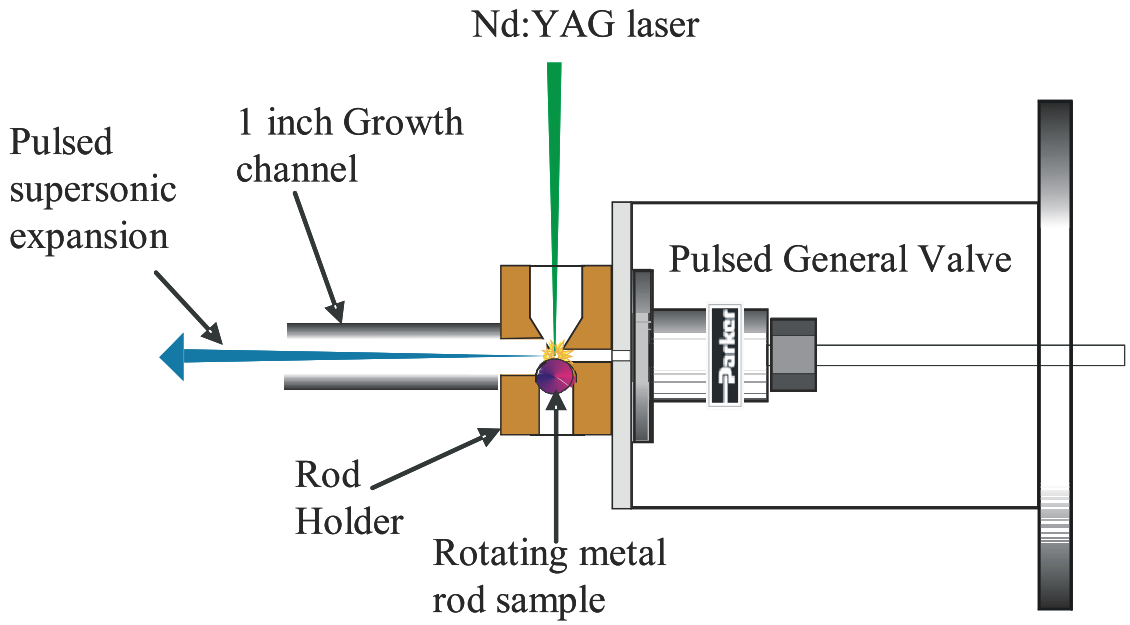

(a) The laser vaporization cluster source showing the *General Valve* pulsed nozzle, the rotating rod, and the rod holder with a one inch growth channel.

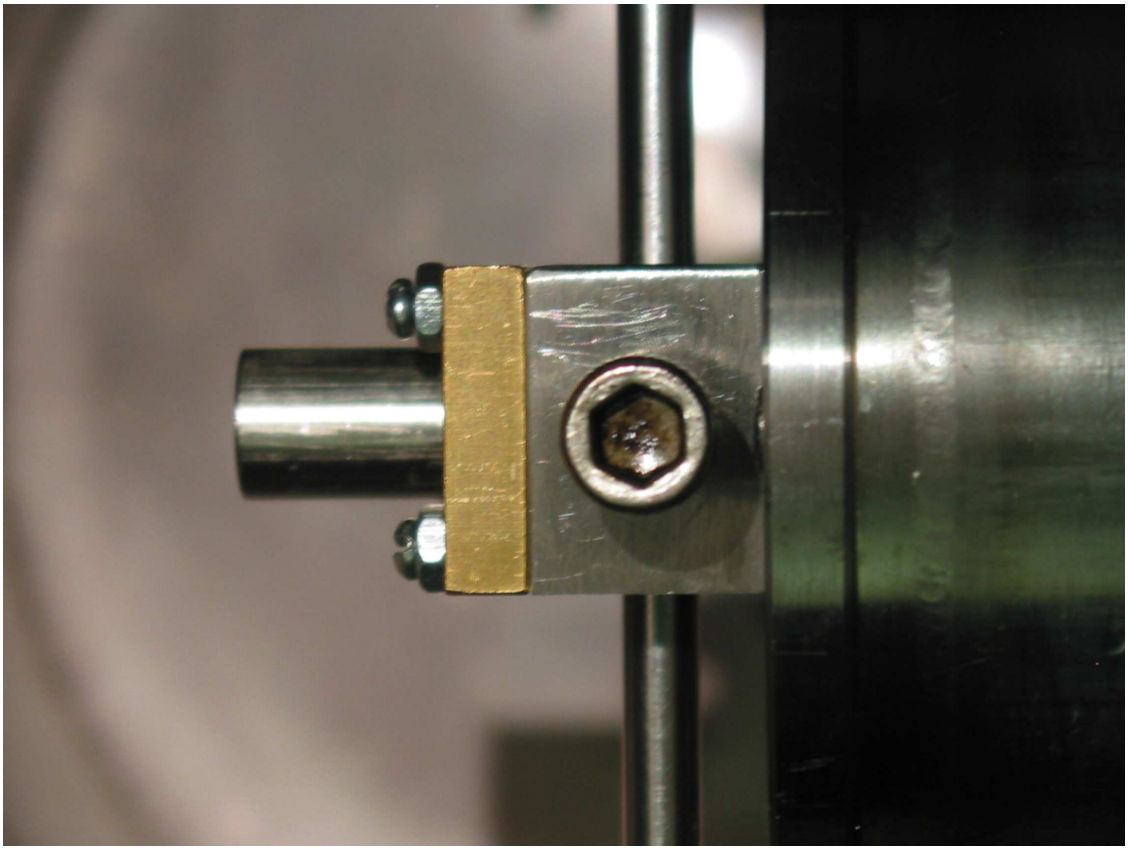

(b) Photograph of the entire nozzle assembly with a metal rod in place.

Figure 2.2

resulting expansion has an overall neutral charge, it contains cations, anions, electrons, and neutral species alike. The expansion is skimmed into the differentially pumped TOF-MS chamber creating a collimated molecular beam of clusters containing the helium buffer gas as well as the clusters of interest. A photograph of the cluster source including the nozzle assembly and skimmer cone is shown in Figure 2.3.

After entering the mass spectrometer chamber, the cation clusters are detected with a TOF mass spectrometer. To do this, ions are accelerated, perpendicular from the initial direction of beam flow, down the first flight tube with a Wiley McLaren[3] type source. The acceleration region consists of a repeller plate, a draw-out-grid (DOG), and a ground plate. The repeller plate and DOG are pulsed with voltages of 1000V and 900V respectively, while the ground plate is held at a constant 0 V. The plates are timed properly using digital delay generators and switched using fast high voltage transistor switches (Behlke HTS-500). The plate voltages and amount of spatial separation between the plates creates two electric fields whose ratio is adjusted to achieve optimized resolution. As the ions move through the electric field they are accelerated into the first flight tube. Clusters, which all have some remaining velocity in the direction of the molecular beam, are steered into the first flight tube using deflection plates. An additional lens, known as the einzel lens, is used to further focus the ions.

Once the ions enter the first flight tube they are separated in time based on their mass. In the first flight tube the ions encounter a "mass gate" which is a plate that can be left at 0 V or held at 200 V and pulsed down to 0 V, depending on the mode of operation. When a mass spectrum is being collected in order to determine what clusters are being formed in the source, the mass gate is left at 0 V allowing all clusters to pass through. When mass selection is being used the plates are held at 200 V to reject any undesired ions. The plates are switched back to 0 V at the precise time the ion of interest passes through, after which the plates are switched back to 200 V, rejecting later cluster ions.

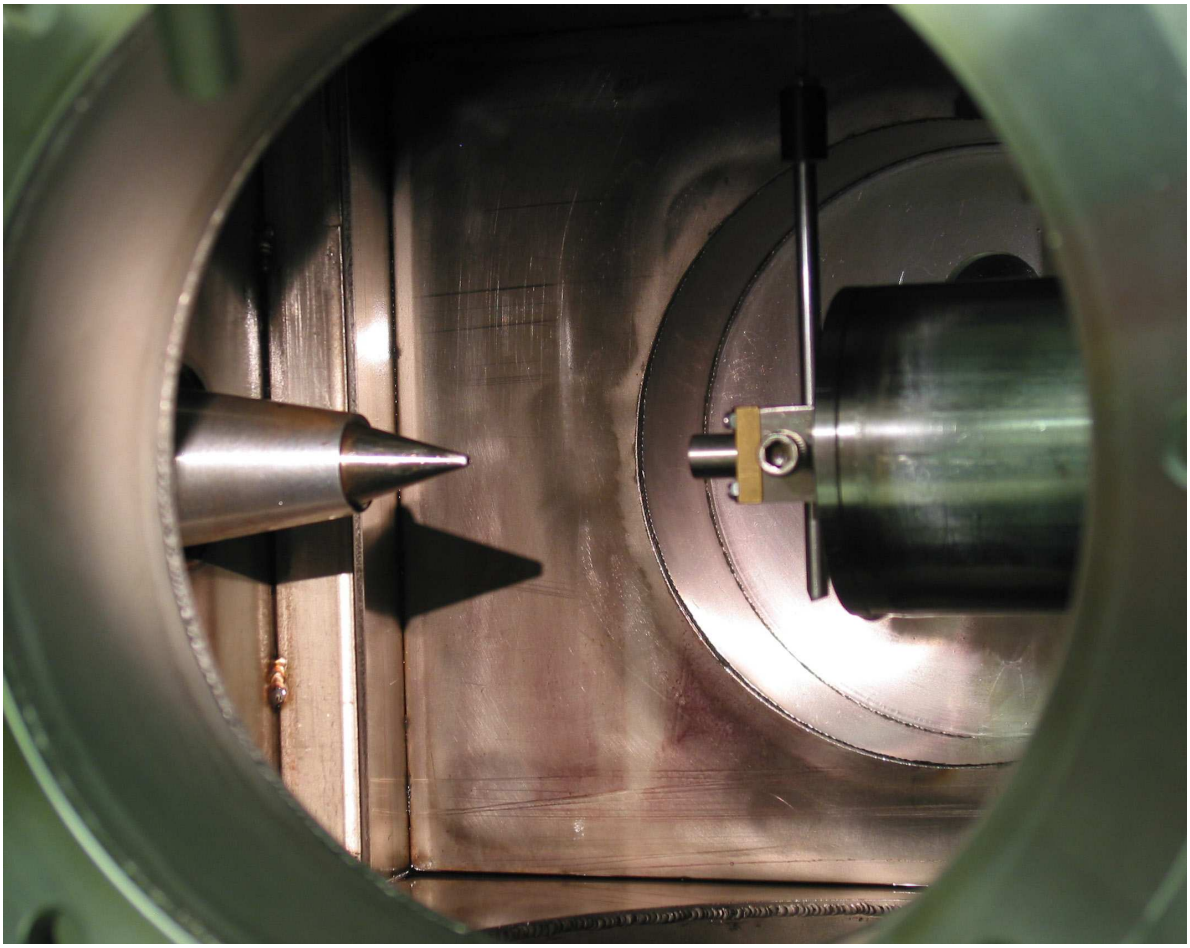

Figure 2.3: Photograph of the cluster source in the vacuum chamber. The metal sample rod is seen going through the rod holder. The vaporization laser enters from the opposite side. The skimmer cone, left, separates the source chamber from the mass spectrometer.

At the end of the first flight tube the clusters ions enter the reflectron assembly, commonly referred to as the "turning region". In this region, the ions pass through a set of grids which are used to slow the ions down to near zero velocity. The ions are in the turning region for approximately 2-3 μs. They are then re-accelerated down the second flight tube by the reflectron field. When a mass spectrum is being taken all of the clusters enter the turning region and all are re-accelerated down the second flight tube. However, the turning region also allows us to intersect mass-selected clusters ions with a high power pulsed laser used to initiate photodissociation. The second (532 nm) or third (355 nm) harmonic of a pulsed Nd: YAG laser (Spectra Physics DCR-3) are used for photodissociation. Once photodissociation has occurred, the parent and fragment ions are reaccelerated down the second flight tube. Whether taking a full mass spectrum or a photodissociation mass spectrum, at the end of the second tube the cluster ions are detected using a Hamamatsu (Model R595) electron multiplier tube detector, EMT, which amplifies the signal by a factor of 10^6. The signal then gains an extra factor of 5 amplification by a Stanford Research Systems pre-amplifier (SRS 445A). The signal is collected using a digital oscilloscope (LeCroy 9310). The data are then transferred to a computer via an IEEE-488 interface where it is analyzed and assigned. Figure 2.4 shows a schematic of the reflectron TOF-MS.

The following equation (2.1) is used to determine the precise mass of each cluster ion as it is detected in time.

$$KE = \frac{1}{2}mv^2 \tag{2.1}$$

The kinetic energy, KE, is the same for all ions since they all pass through the same electric field, m is the mass of the ion, and v is its corresponding velocity. The velocity equation (2.2) can then be substituted into the KE equation (2.1) to obtain a new KE equation (2.3).

$$v = \frac{d}{t} \tag{2.2}$$

$$KE = \frac{1}{2}m\left(\frac{d}{t}\right)^2 \tag{2.3}$$

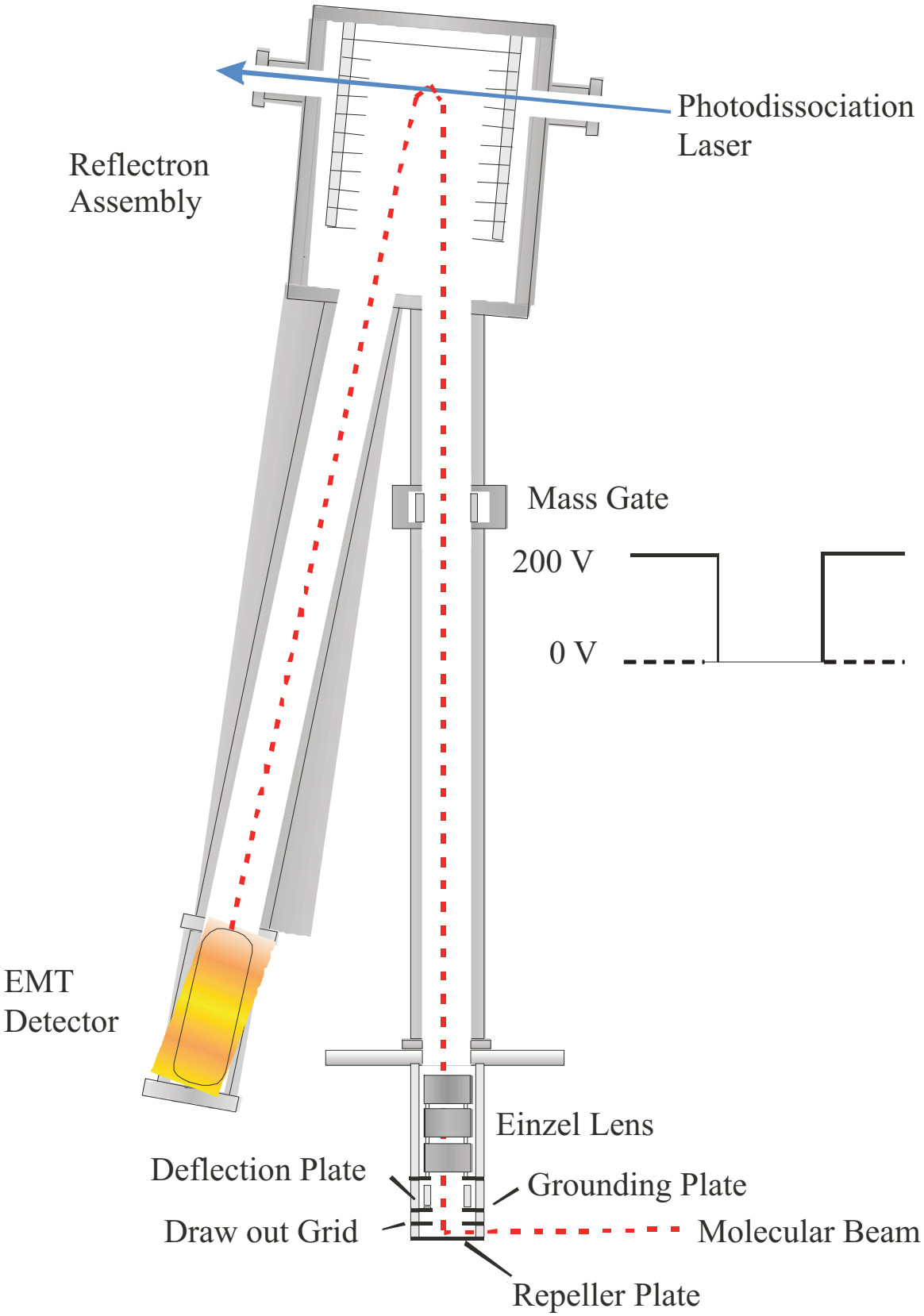

Figure 2.4: The Reflectron Time-of-Flight Mass Spectrometer

Equation 2.3 can be rearranged to show the relationship between mass and time, equation 2.4.

$$m = 2\,(KE)\left(\frac{t}{d}\right)^2 \tag{2.4}$$

Since all ions have the same initial KE, the KE of an ion with mass m_1 equals the KE of an ion with mass m_2. Therefore the following equations (2.5 & 2.6) can be written

$$KE_1 = KE_2 \tag{2.5}$$

$$m_1\left(\frac{d}{t_1}\right)^2 = m_2\left(\frac{d}{t_2}\right)^2 \tag{2.6}$$

Since the repeller and DOG are pulsed, the time when the voltage is applied is time zero. Additionally, all ions drift down the same flight tube making d constant. This allows equation 2.7 to be written which is used to assign each mass peak within the mass spectrum.

$$m_2 = m_1\left(\frac{t_2}{t_1}\right)^2 \tag{2.7}$$

Thus a mass spectrum is assigned by first assigning a known ion, m_1, which is recognized by its known TOF or isotope pattern. Using equation 2.7, the time of arrival of both ions in combination with m_1 is used to determine m_2. The entire mass spectrum can be assigned using this approach. Figure 2.5 shows a mass spectrum of $Nb_nO_m^+$ clusters obtained using our cluster source and reflectron TOF-MS.

In order to obtain large clusters with the highest intensity, various concentrations of oxygen and backing pressures have been investigated. The concentrations of oxygen range from 1 - 20% and the backing pressures range from 20 to 200 psi. For the vanadium group and chromium oxides the optimal concentration of oxygen was determined to be 1-3% with a backing pressure of 60 psi. For these systems, changing the oxygen concentration from 1 to 20% or the backing pressure from 60 to 150 psi did not change the cluster distributions. In addition the detected signal levels for the cluster produced only varied slightly. However, the iron oxide clusters produced were dependent on both the concentration of oxygen and

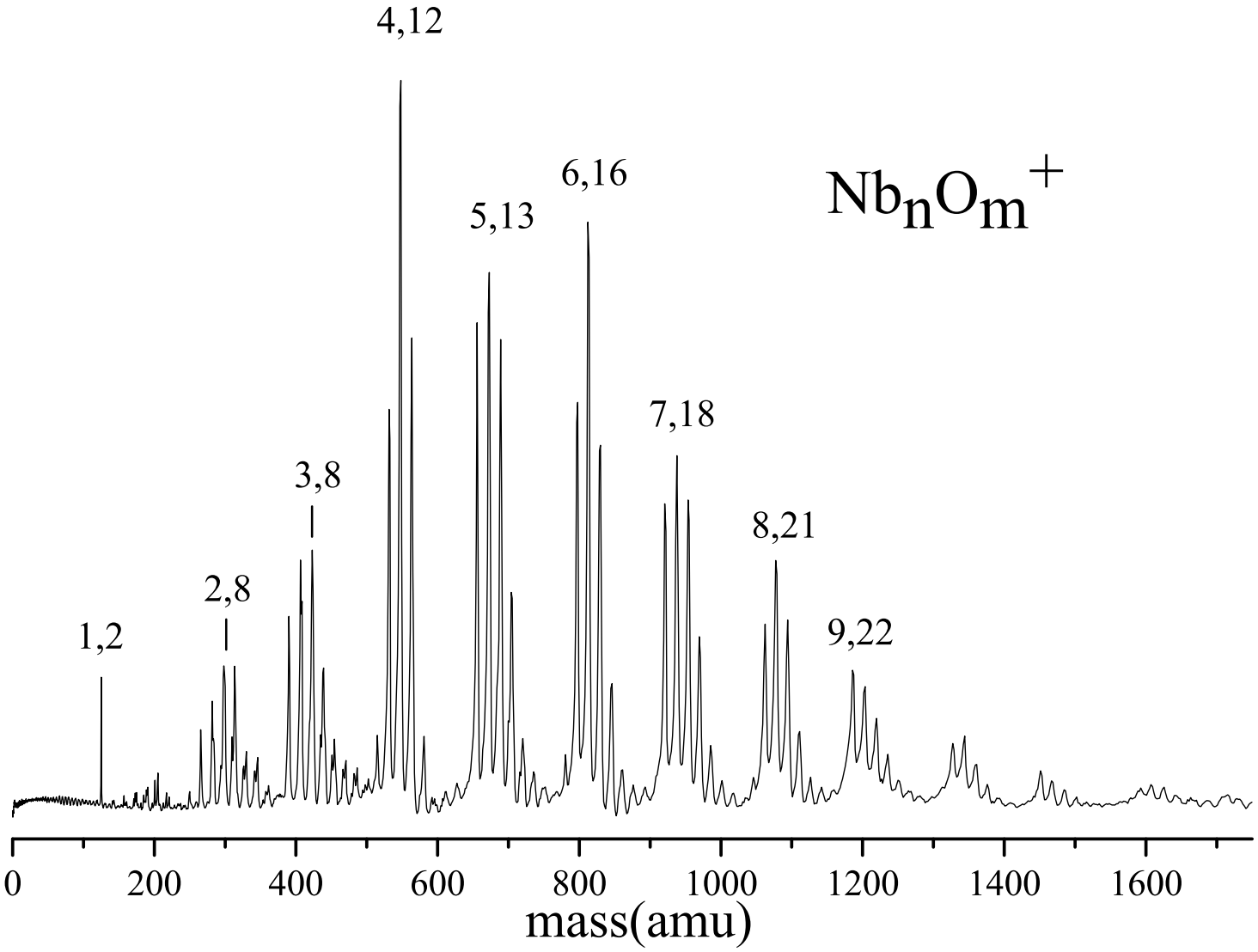

Figure 2.5: The $Nb_nO_m^+$ mass spectrum produced by laser vaporization in a helium mixture seeded with oxygen.

backing pressure. A comparison of the cluster distributions using 150 psi backing pressure is shown for 1% and 20% oxygen in Figure 2.6. Figure 2.7 shows the cluster distributions for 20% oxygen with 70 psi and 150 psi backing pressures. For this system, the optimal oxygen concentration was determined to be 20% with a backing pressure of 150 psi.

Photodissociation mass spectra are also measured for the individual clusters. The same methodology used to assign mass spectra is used to assign photodissociation mass spectra. However, since photodissociation occurs in the turning region, the time zero corresponds to the time when the photodissociation laser is fired. As long as the dissociation occurs while the parent cluster ions are in the acceleration region of the reflectron, the parent and fragment ions will all receive the same initial KE allowing them to be mass resolved in the second flight tube and detected. The photodissociation mass spectra are collected in a difference mode of operation where spectra collected with the photodissociation laser off (only the selected parent ion present) are subtracted from the spectra collected with the photodissociation laser on (which contains fragment peaks and residual parent ion). This method produces a negative parent ion peak, showing depletion, and positive fragment ion peaks, as shown for $Fe_4O_5^+$ in Figure 2.8. Ideally the integrated intensities of the fragment ion peaks would equal the integrated intensity of the parent ion, displaying charge conservation. However, mass discrimination effects within our instrument make it impossible to focus on both the parent and fragment ions with equal detection sensitivity and resolution.[1] Therefore, we focus on the fragment ions and use several focusing conditions to ensure that no fragment ions are missed and that no strong bias occurs for any mass peaks. However, for these reasons, we do not report branching ratios for the various fragment ions. Instead, we distinguish between strong and weak fragment mass peaks. Additionally, in our spectra the fragment ion peaks are amplified which may result in an off scale parent ion peak. This is illustrated in Figure 2.8 for the $Fe_4O_5^+$ cluster.

A general assumption of unimolecular kinetics, according to RRKM, is that the weakest bond in a cluster will break first.[4] The rate of dissociation depends on the amount of excess

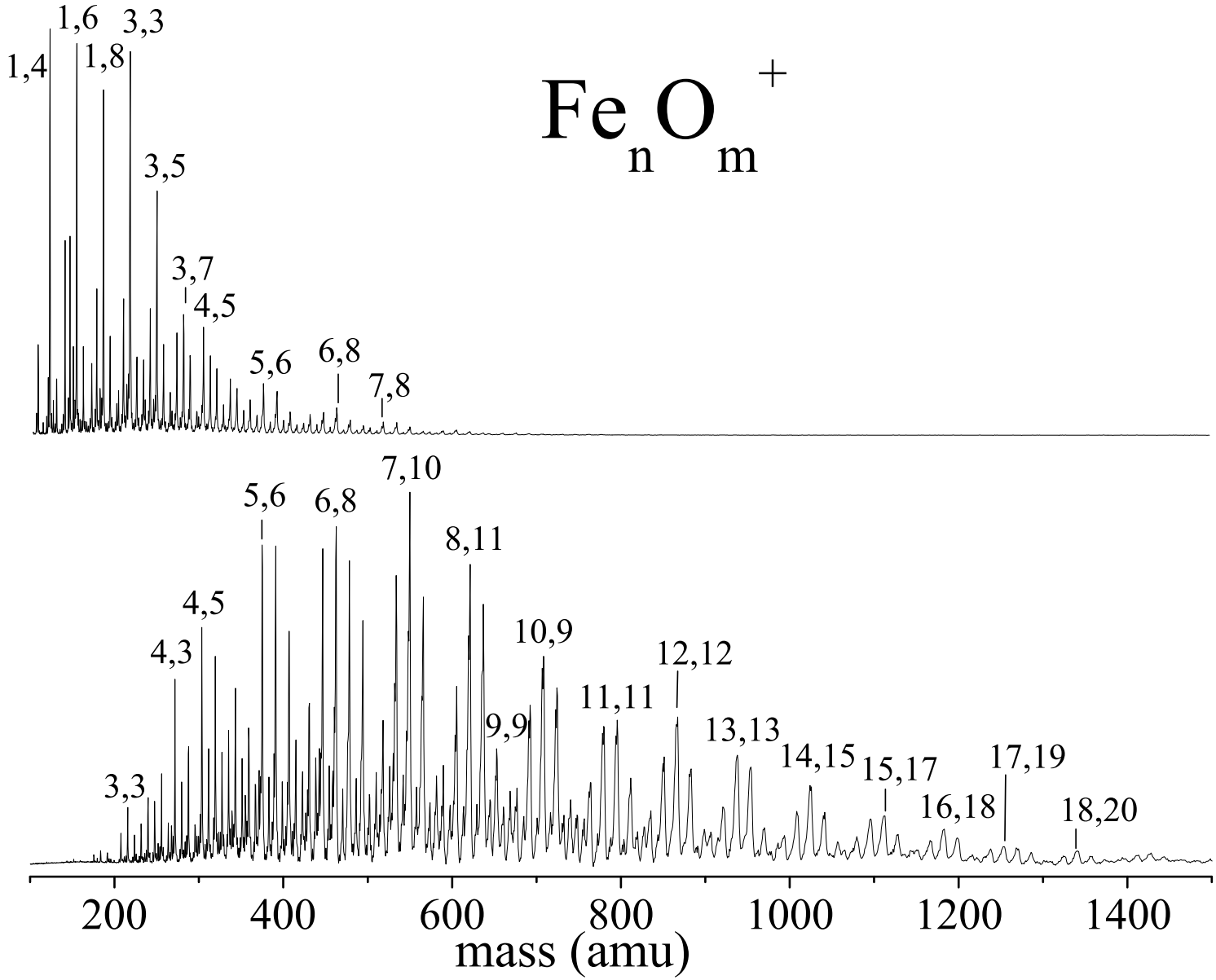

Figure 2.6: The $Fe_nO_m^+$ mass spectrum produced by laser vaporization in a helium mixture seeded with 1% (top) and 20% (bottom) oxygen. The backing pressure for the *General Valve* was 150 psi for both mixtures.

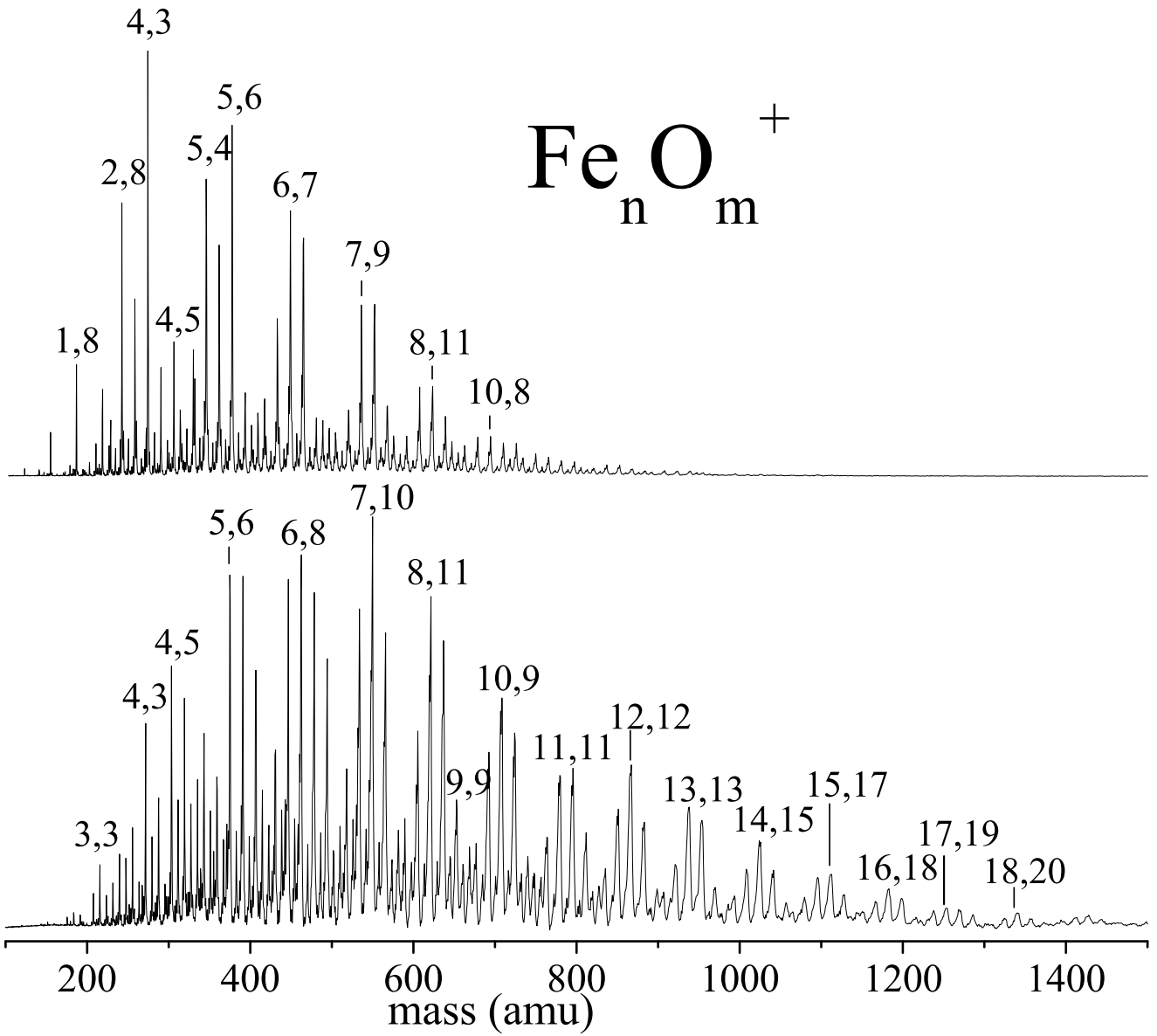

Figure 2.7: The $Fe_nO_m^+$ mass spectrum produced by laser vaporization in a helium mixture seeded with 20% oxygen and backing pressures for the *General Valve* of 70 psi (top) and 150 psi (bottom).

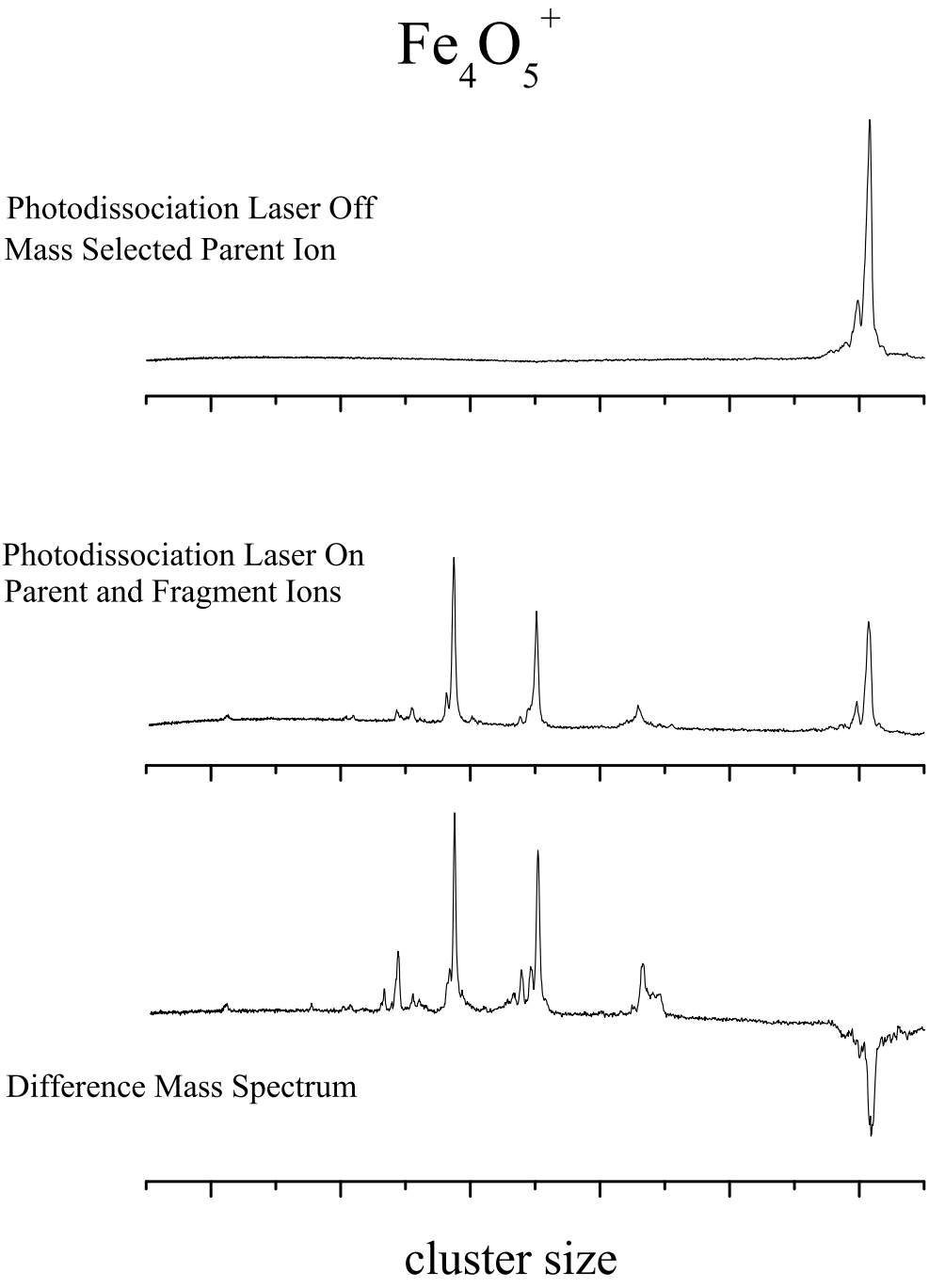

Figure 2.8: Photodissociation mass spectrum of $Fe_4O_5^+$. A mass spectrum is taken of the mass-selected parent cluster with the photodissociation laser off. The photodissociation laser is then turned on to measure a mass spectrum of the parent and fragment ions. The mass spectrum with the laser off is subtracted from the mass spectrum with the laser on to acquire the difference mass spectrum.

energy deposited above the dissociation threshold as well as the density of states near the level where excitation occurs. There are additional factors which affect the observed fragmentation products of clusters in our experiment. Oxide clusters are very strongly bound networks with calculated bond energies of 3-7 eV/bond.[5–11] Therefore, they require high laser fluences to dissociate. The photodissocation laser provides 2.3 eV at 532 nm and 3.5 eV at 355 nm, and one photon from either of these is not enough energy to break a metal oxide bond. Therefore, we use multiphoton conditions for dissociation of these systems. An additional reason for using multiphoton conditions is that the rate of unimolecular dissociation increases with excess energy. Using high laser fluences increases the chances that fragments can absorb light and subsequently fragment again, resulting in sequential dissociative processes. We use laser-power-dependence studies to determine if these sequential dissociative processes occur. If fragmentation is sequential we should observe a decrease and eventual loss of mass peaks resulting from additional fragmentation. The power of the dissociation laser is varied from 5 mJ/pulse to 50 mJ/pulse. These studies do not show such sequential process for the vanadium group and chromium oxides, however these processes are shown for iron oxides. Figure 2.9 shows the power-dependence photodissociation mass spectra for the $Cr_4O_{10}^+$ where the sequential processes are not observed. Figure 2.10 shows the power-dependence photodissociation mass spectra for the $Fe_{15}O_{17}^+$. For the vanadium group and chromium oxides, they might be happening on a timescale that is too fast to be resolved. However, the best interpretation is that several dissociation channels all happen simultaneously in these systems.

The experimental set-up described in this chapter has been used to study the photodissociation of various "met-car" systems,[2,11] Sb_nO_m and Bi_nO_m,[12] $Si_nC_m^+$,[13] metal silicon,[14] V, Nb, and Ta oxides,[15] $Cr_nO_m^+$,[16] and $Fe_nO_m^+$.[17]

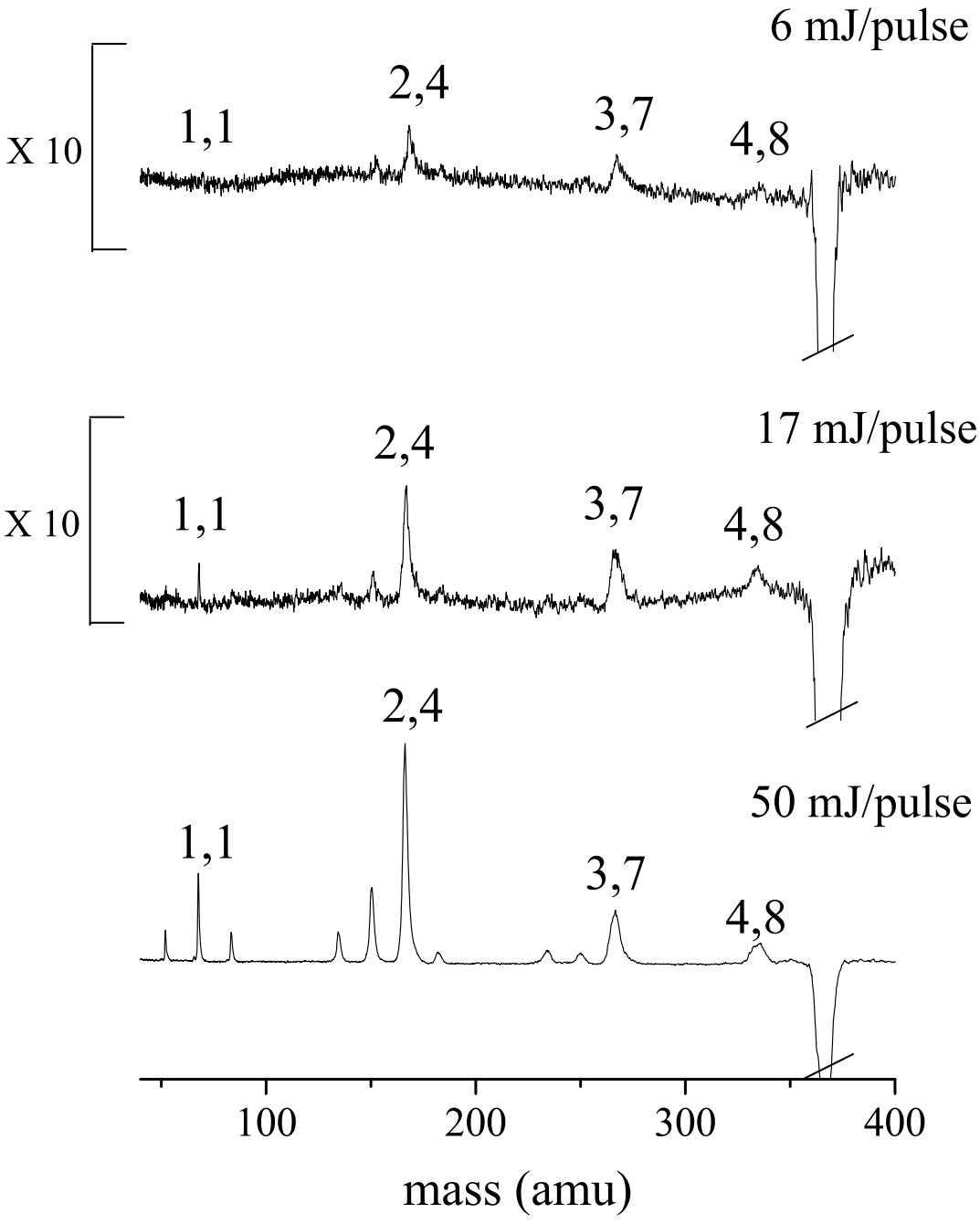

Figure 2.9: Photodissociation mass spectrum of $Cr_4O_{10}^+$ cluster at various fluences of 355 nm.

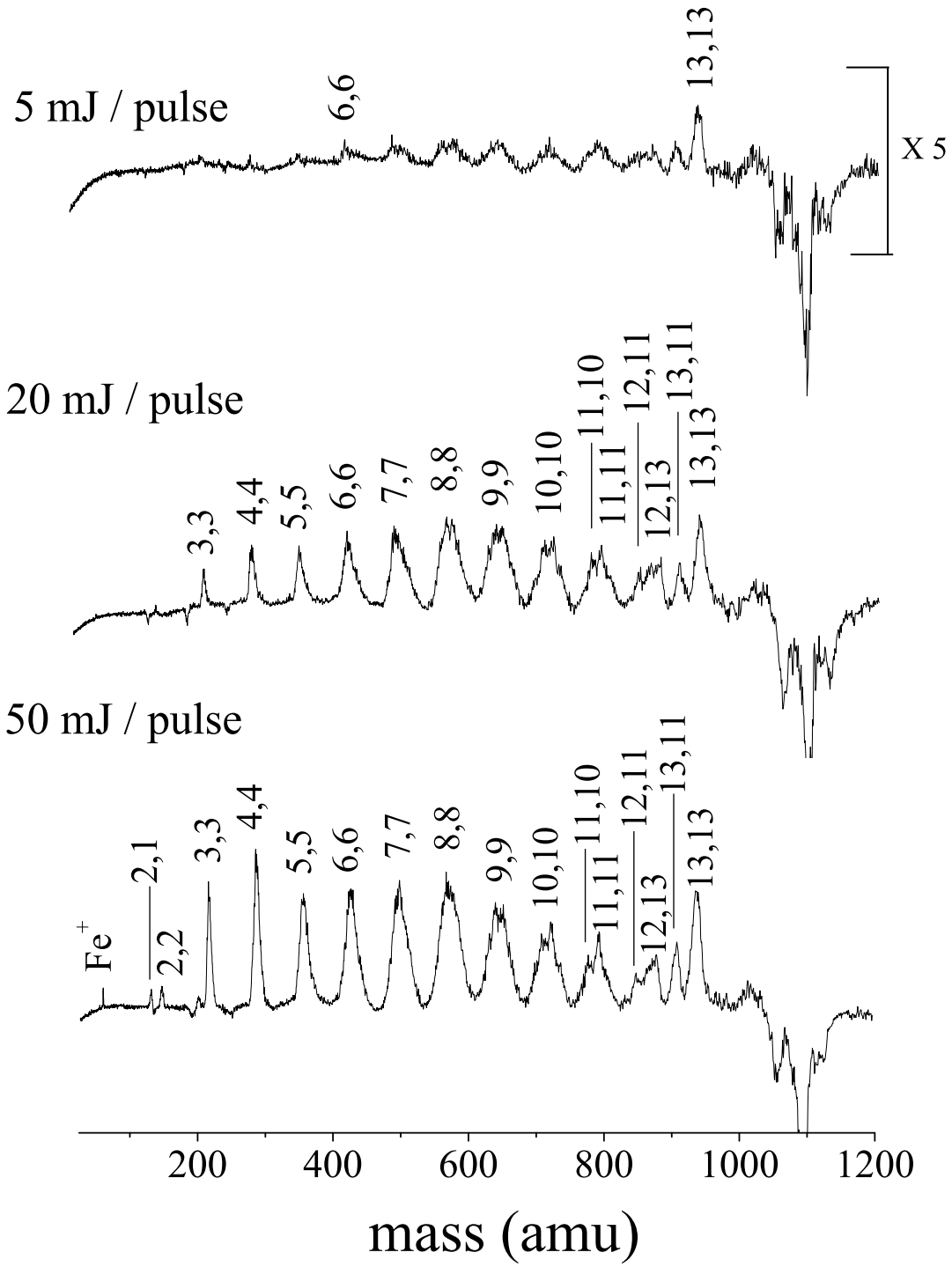

Figure 2.10: Photodissociation mass spectrum of $Fe_{15}O_{17}^{+}$ cluster at various fluences of 355 nm.

2.1 References

[1] Cornett, D. S.; Peschke, M.; Laihing, K.; Cheng, P. Y.; Willey, K. F.; Duncan, M. A. "Reflectron Time-of-Flight Mass-Spectrometer for Laser Photodissociation," *Rev. Sci. Instrum.* **1992**, *63*, 2177.

[2] a) Pilgrim, J. S.; Duncan, M. A. "Beyond metallo-carbohedrenes: growth and decomposition of metal-carbon nanocrystals," *J. Am. Chem. Soc.* **1993**, *115*, 9724; b) Pilgrim, J. S.; Duncan, M. A. "Metallo-carbohedrenes: chromium, iron, and molybdenum analogs," *J. Am. Chem. Soc.* **1993**, *115*, 6958; c) Duncan, M. A. "Synthesis and characterization of metal-carbide clusters in the gas phase," *J. Cluster Sci.* **1997**, *8*, 239.

[3] Wiley, W. C. M., I. H. "Time-of-Flight Mass Spectrometer with Improved Resolution" *Rev. Sci. Instrum.* **1955**, *26.*

[4] Baer, T., Hase, W. *Unimolecular Reaction Dynamics*; Oxford University Press: New York, 1996.

[5] a) Deng, H. T.; Kerns, K. P.; Castleman, A. W. "Formation, structures, and reactivities of niobium oxide cluster ions," *J. Phys. Chem.* **1996**, *100*, 13386. b) Bell, R. C.; Zemski, K. A.; Kerns, K. P.; Deng, H. T.; Castleman, A. W. "Reactivities and collision-induced dissociation of vanadium oxide cluster cations," *J. Phys. Chem. A* **1998**, *102*, 1733. c) Bell, R. C.; Zemski, K. A.; Castleman, A. W. "Size-specific reactivities of vanadium oxide cluster cations," *J. Cluster Sci.* **1999**, *10*, 509. d) Zemski, K. A.; Bell, R. C.; Castleman, A. W. "Reactivities of tantalum oxide cluster cations with unsaturated hydrocarbons," *Int. J. Mass. Spectrom.* **1999**, *184*, 119. e) Zemski, K. A.; Bell, R. C.; Castleman, A. W. "Reactions of tantalum oxide cluster cations with 1-butene, 1,3-butadiene, and benzene (vol 104A, pg 5733, 2000)," *J. Phys. Chem. A* **2000**, *104*, 7408. f) Zemski, K. A.; Justes, D. R.; Bell, R. C.; Castleman, A. W. "Reactions of niobium and tantalum oxide cluster cations and anions with n-butane," *J. Phys. Chem. A* **2001**, *105*, 4410. g) Zemski, K. A.;

Justes, D. R.; Castleman, A. W. "Reactions of group V transition metal oxide cluster ions with ethane and ethylene," *J. Phys. Chem. A* **2001**, *105*, 10237. h) Zemski, K. A.; Justes, D. R.; Castleman, A. W. "Studies of metal oxide clusters: Elucidating reactive sites responsible for the activity of transition metal oxide catalysts," *J. Phys. Chem. B* **2002**, *106*, 6136. i) Justes, D. R.; Mitric, R.; Moore, N. A.; Bonacic-Koutecky, V.; Castleman, A. W. "Theoretical and experimental consideration of the reactions between VxOy+ and ethylene," *J. Am. Chem. Soc.* **2003**, *125*, 6289. j) Justes, D. R.; Moore, N. A.; Castleman, A. W. "Reactions of vanadium and niobium oxides with methanol," *J. Phys. Chem. B* **2004**, *108*, 3855. k) Bergeron, D. E.; Castleman, A. W., Jr.; Jones, N. O.; Khanna, S. N. "Stable Cluster Motifs for Nanoscale Chromium Oxide Materials," *Nano Lett.* **2004**, *4*, 261. l) Kimble, M. L.; Castleman, A. W. "Gas-phase studies of AunOm+ interacting with carbon monoxide," *Int. J. Mass. Spectrom.* **2004**, *233*, 99. m) Kimble, M. L.; Castleman, A. W., Jr.; Mitric, R.; Buergel, C.; Bonacic-Koutecky, V. "Reactivity of Atomic Gold Anions toward Oxygen and the Oxidation of CO: Experiment and Theory," *J. Am. Chem. Soc.* **2004**, *126*, 2526. n) Sun, Q.; Rao, B. K.; Jena, P.; Stolcic, D.; Kim, Y. D.; Gantefor, G.; Castleman, A. W. "Appearance of bulk properties in small tungsten oxide clusters," *J. Chem. Phys.* **2004**, *121*, 9417. o) Sun, Q.; Rao, B. K.; Jena, P.; Stolcic, D.; Kim, Y. D.; Gantefor, G.; Castleman, A. W. "Appearance of bulk properties in small tungsten oxide clusters (vol 121, pg 9417, 2004)," *J. Chem. Phys.* **2005**, *122*. p) Kimble, M. L.; Castleman, A. W.; Burgel, C.; Bonacic-Koutecky, V. "Interactions of CO with AunOm- (n $\leq$ 4)," *Int. J. Mass. Spectrom.* **2006**, *254*, 163. q) Kimble, M. L.; Moore, N. A.; Johnson, G. E.; Castleman, A. W.; Burgel, C.; Mitric, R.; Bonacic-Koutecky, V. "Joint experimental and theoretical investigations of the reactivity of Au2On- and Au3On- (n=1-5) with carbon monoxide," *J. Chem. Phys.* **2006**, *125*. r) Moore, N. A.; Mitric, R.; Justes, D. R.; Bonacic-Koutecky, V.; Castleman, A. W., Jr. "Kinetic Analysis of the Reaction between (V2O5)n=1,2+ and Ethylene," *J. Phys. Chem. B* **2006**, *110*, 3015. s) Reilly, N. M., Reveles, J. U., Johnson, G. E., Khanna,

S. N., Castleman, A.W. Jr. "Influence of charge state on the reaction of $FeO_3^{+/-}$ with carbon monoxide," *Chem. Phys, Lett.* **2007**, *435*, 295. t) Reilly, N. M., Reveles, J. U., Johnson, G. E., Khanna, S. N., Castleman, A.W. Jr. "Experimental and Theoretical Study of the Structures and Reactivity of $Fe_{1-2}O_{\leq 6}^{-}$ Clusters with CO," *J. Phys. Chem. A*. **2007**, *111*, 4158.

[6] a) Harvey, J. N.; Diefenbach, M.; Schroder, D.; Schwarz, H. "Oxidation properties of the early transition-metal dioxide cations MO2+ (M = Ti, V, Zr, Nb) in the gas-phase," *Int. J. Mass. Spectrom.* **1999**, *183*, 85. b) Schrder, D.; Schwarz, H.; Shaik, S. "Characterization, orbital description, and reactivity patterns of transition-metal oxo species in the gas phase," *Struct. Bonding* **2000**, *97*, 91. c) Jackson, P.; Fisher, K. J.; Willett, G. D. "The catalytic activation of primary alcohols on niobium oxide surfaces unraveled: the gas phase reactions of NbxOy- clusters with methanol and ethanol," *Chem. Phys.* **2000**, *262*, 179. d) Schrder, D.; Jackson, P.; Schwarz, H. "Dissociation patterns of small FemOn+ (m=1-4, n ¡= 6) cluster cations formed upon chemical ionization of Fe(CO)(5)/O-2 mixtures," *Eur. J. Inorg. Chem.* **2000**, 1171. e) Jackson, P.; Harvey, J. N.; Schrder, D.; Schwarz, H. "Structure and reactivity of the prototype iron-oxide cluster Fe2O2+," *Int. J. Mass. Spectrom.* **2001**, *204*, 233. f) Schroder, D.; Engeser, M.; Schwarz, H.; Harvey, J. N. "Energetics of the ligated vanadium dications VO2+, VOH2+, and [V,O,H-2](2+)," *Chemphyschem* **2002**, *3*, 584. g) Engeser, M.; Schlangen, M.; Schroder, D.; Schwarz, H.; Yumura, T.; Yoshizawa, K. "Alkane oxidation by VO2+ in the gas phase: A unique dependence of reactivity on the chain length," *Organometallics* **2003**, *22*, 3933. h) Engeser, M.; Schroder, D.; Schwarz, H. "Gas-phase dehydrogenation of methanol with mononuclear vanadium-oxide cations," *Chemistry-a European Journal* **2005**, *11*, 5975. i) Koszinowski, K.; Schlangen, M.; Schroder, D.; Schwarz, H. "Formation, structure, and reactivity of gaseous Ni2O2+," *Eur. J. Inorg. Chem.* **2005**, 2464. j) Feyel, S.; Dobler, J.; Schroder, D.; Sauer, J.; Schwarz, H. "Thermal activation of methane by tetranuclear [V4O10](+)," *Angewandte Chemie-International*

Edition **2006**, *45*, 4681. k) Feyel, S.; Schroder, D.; Rozanska, X.; Sauer, J.; Schwarz, H. "Gas-phase oxidation of propane and 1-butene with [V3O7](+): Experiment and theory in concert," *Angewandte Chemie-International Edition* **2006**, *45*, 4677. l) Feyel, S.; Schroder, D.; Schwarz, H. "Gas-phase oxidation of isomeric butenes and small alkanes by vanadium-oxide and -hydroxide cluster cations," *J. Phys. Chem. A* **2006**, *110*, 2647.

[7] a) Griffin, J. B.; Armentrout, P. B., "Guided ion beam studies of the reactions of Fe-n(+) (n=2-18) with O-2: Iron cluster oxide and dioxide bond energies," *J. Chem. Phys.* **1997**, *106*, 4448. b) Xu, J.; Rodgers, M. T.; Griffin, J. B.; Armentrout, P. B., "Guided ion beam studies of the reactions of V-n(+) (n=2-17) with O-2: Bond energies and dissociation pathways," *J. Chem. Phys.* **1998**, *108*, 9339. c) Griffin, J. B.; Armentrout, P. B., "Guided ion beam studies of the reactions of Cr-n(+) (n=2-18) with O-2: Chromium cluster oxide and dioxide bond energies," *J. Chem. Phys.* **1998**, *108*, 8062. d) Vardhan, D.; Liyanage, R.; Armentrout, P. B., "Guided ion beam studies of the reactions of Ni-n(+) (n=2-18) with O-2: Nickel cluster oxide and dioxide bond energies," *J. Chem. Phys.* **2003**, *119*, 4166. e) Liu, F. Y.; Li, F. X.; Armentrout, P. B., "Guided ion-beam studies of the reactions of Co-n(+) (n=2-20) with O-2: Cobalt cluster-oxide and -dioxide bond energies," *J. Chem. Phys.* **2005**, *123*.

[8] a) Reddy, B. V.; Khanna, S. N., "Chemically induced oscillatory exchange coupling in chromium oxide clusters," *Phys. Rev. Lett.* **1999**, *83*, 3170. b) Morisato, T.; Jones, N. O.; Khanna, S. N.; Kawazoe, Y., "Stable aluminum and chromium oxide clusters as precursors to nanoscale materials," *Comp. Mater. Sci.* **2006**, *35*, 366.

[9] a) Fan, J. W.; Wang, L. S. "Photoelectron-Spectroscopy of Feo- and Feo2- - Observation of Low-Spin Excited-States of Feo and Determination of the Electron-Affinity of Feo2," *J. Chem. Phys.* **1995**, *102*, 8714. b) Wang, L. S.; Wu, H. B.; Desai, S. R. "Sequential oxygen atom chemisorption on surfaces of small iron clusters," *Phys. Rev. Lett.* **1996**, *76*, 4853. c) Wu, H. B.; Desai, S. R.; Wang, L. S. "Observation and photoelectron

spectroscopic study of novel mono- and diiron oxide molecules: FeO_y^- (y=1-4) and $Fe_2O_y^-$ (y=1-5)," *J. Am. Chem. Soc.* **1996**, *118*, 7434. d) Wang, L.-S.; Wu, H.; Desai, S. R.; Lou, L. "Electronic structure of small copper oxide clusters: from Cu2O to Cu2O4," *Phys. Rev. B: Condens. Matter* **1996**, *53*, 8028. e) Gutsev, G. L.; Rao, B. K.; Jena, P.; Li, X.; Wang, L.-S. "Experimental and theoretical study of the photoelectron spectra of MnOx- (x=1-3) clusters," *J. Chem. Phys.* **2000**, *113*, 1473. f) Sun, Q.; Sakurai, M.; Wang, Q.; Yu, J. Z.; Wang, G. H.; Sumiyama, K.; Kawazoe, Y. "Geometry and electronic structures of magic transition-metal oxide clusters M9O6 (M = Fe, Co, and Ni)," *Phys. Rev. B* **2000**, *62*, 8500. g) Gutsev, G. L.; Jena, P.; Zhai, H.-J.; Wang, L.-S. "Electronic structure of chromium oxides, CrOn- and CrOn (n = 1-5) from photoelectron spectroscopy and density functional theory calculations," *J. Chem. Phys.* **2001**, *115*, 7935. h) Zhai, H.-J.; Wang, L.-S. "Electronic structure and chemical bonding of divanadium-oxide clusters (V2Ox, x=3-7) from anion photoelectron spectroscopy," *J. Chem. Phys.* **2002**, *117*, 7882. i) Gutsev, G. L.; Bauschlicher, C. W., Jr.; Zhai, H.-J.; Wang, L.-S. "Structural and electronic properties of iron monoxide clusters FenO and FenO- (n = 2-6): a combined photoelectron spectroscopy and density functional theory study," *J. Chem. Phys.* **2003**, *119*, 11135. j) Zhai, H.-J.; Kiran, B.; Cui, L.-F.; Li, X.; Dixon, D. A.; Wang, L.-S. "Electronic Structure and Chemical Bonding in MOn- and MOn Clusters (M = Mo, W; n = 3-5): A Photoelectron Spectroscopy and ab Initio Study," *J. Am. Chem. Soc.* **2004**, *126*, 16134. k) Yang, X.; Waters, T.; Wang, X.-B.; O'Hair, R. A. J.; Wedd, A. G.; Li, J.; Dixon, D. A.; Wang, L.-S. "Photoelectron Spectroscopy of Free Polyoxoanions Mo6O192- and W6O192- in the Gas Phase," *J. Phys. Chem. A* **2004**, *108*, 10089. l) Zhai, H. J.; Huang, X.; Waters, T.; Wang, X. B.; O'Hair, R. A. J.; Wedd, A. G.; Wang, L. S. "Photoelectron spectroscopy of doubly and singly charged group VIB dimetalate anions: M2O72-, MM ' O-7(2-), and M2O7- (M, M ' = Cr, Mo, W)," *J. Phys. Chem. A* **2005**, *109*, 10512. m) Zhai, H.-J.; Huang, X.; Cui, L.-F.; Li, X.; Li, J.; Wang, L.-S. "Electronic and Structural Evolution and Chemical Bonding in Ditungsten Oxide

Clusters: W2On- and W2On (n = 1-6)," *J. Phys. Chem. A* **2005**, *109*, 6019. n) Huang, X.; Zhai, H. J.; Li, J.; Wang, L. S. "On the structure and chemical bonding of tri-tungsten oxide clusters W3On- and W3On (n=7-10): W3O8 as a potential molecular model for O-deficient defect sites in tungsten oxides," *J. Phys. Chem. A* **2006**, *110*, 85. o) Zhai, H. J.; Wang, L. S. "Probing the electronic properties of dichromium oxide clusters Cr2On- (n=1-7) using photoelectron spectroscopy," *J. Chem. Phys.* **2006**, *125*.

[10] Jones, N. O.; Reddy, B. V.; Rasouli, F.; Khanna, S. N. "Structural growth in iron oxide clusters: Rings, towers, and hollow drums," *Phys. Rev. B* **2005**, *72*; Jones, N. O.; Reddy, B. V.; Rasouli, F.; Khanna, S. N. "Structural growth in iron oxide clusters: Rings, towers, and hollow drums (vol 72, pg 165411, 2005)," *Phys. Rev. B* **2006**, *73*.

[11] a) Pilgrim, J. S.; Duncan, M. A. "Photodissociation of metallo-carbohedrene ($\ddot{\text{M}}$et-Cars$\ddot{}$) cluster cations," *J. Am. Chem. Soc.* **1993**, *115*, 4395; b) Pilgrim, J. S.; Duncan, M. A. "Metal-carbon clusters: The construction of cages and crystals," *Adv. Met. Semicond. Clusters* **1995**, *3*, 181.

[12] France, M. R.; Buchanan, J. W.; Robinson, J. C.; Pullins, S. H.; Tucker, J. L.; King, R. B.; Duncan, M. A. "Antimony and Bismuth Oxide Clusters: Growth and Decomposition of New Magic Number Clusters," *J. Phys. Chem. A* **1997**, *101*, 6214.

[13] Ticknor, B. W.; Duncan, M. A. "Photodissociation of size-selected silicon carbide cluster cations," *Chem. Phys. Lett* **2005**, *405*, 214.

[14] Jaeger, J. B. J., T. D.; Duncan, M. A. " Photodissociation of Metal-Silicon Clusters: Encapsulated versus Surface-Bound Metal," *J. Phys. Chem. A* **2006**, *110*, 9310.

[15] Molek, K. S.; Jaeger, T. D.; Duncan, M. A. "Photodissociation of vanadium, niobium, and tantalum oxide cluster cations," *J. Chem. Phys.* **2005**, *123*, 144313.

[16] Molek, K. S.; Reed, Z. D.; Ricks, A.M.; Duncan, M.A. "Photodissociation of Chromium Oxide Cluster Cations," *J. Phys. Chem. A* **2007**, *in press*.

[17] Molek, K. S.; Anfuso-Cleary, C.; Duncan, M.A. "Photodissociation of Iron Oxide Cluster Cations" *J. Phys. Chem. A* **2007**, *to be submitted.*

Chapter 3

Photodissociation of Vanadium, Niobium, and Tantalum Oxide Cluster Cations[1]

[1]Molek, K. S.; Jaeger, T. D.; Duncan, M. A. "Photodissociation of vanadium, niobium, and tantalum oxide cluster cations," *J. Chem. Phys.* 2005, 123, 144313. Reprinted here with permission of publisher.

3.1 Abstract

Transition metal oxide clusters of the form $M_nO_m^+$ (M=V, Nb, Ta), are produced by laser vaporization in a pulsed nozzle cluster source and detected with time-of-flight mass spectrometry. Consistent with earlier work, cluster oxides for each value of n produce only a limited number of stoichiometries, where m>n. The cluster cations are mass selected and photodissociated using the second (532 nm) or third (355 nm) harmonic of a Nd:YAG laser. All of these clusters require multiphoton conditions for dissociation, consistent with their expected strong bonding. Dissociation occurs by either elimination of oxygen or by fission, repeatedly producing clusters having the same specific stoichiometries. In oxygen elimination, vanadium species tend to lose units of O_2, whereas niobium and tantalum lose O atoms. For each metal increment n, oxygen elimination proceeds until a terminal stoichiometry is reached. Clusters having this stoichiometry do not eliminate more oxygen, but rather undergo fission, producing smaller $M_nO_m^+$ species. The smaller clusters produced as fission products represent the corresponding terminal stoichiometries for those smaller n values. The terminal stoichiometries identified are the same for V, Nb and Ta oxide cluster cations. This behavior suggests that these clusters have stable bonding networks at their core, but additional excess oxygen at their periphery. These combined results determine that $M_2O_4^+$, $M_3O_7^+$, $M_4O_9^+$, $M_5O_{12}^+$ $M_6O_{14}^+$ and $M_7O_{17}^+$ have the greatest stability for V, Nb and Ta oxide clusters.

3.2 Introduction

Transition metal oxides have been studied for over 50 years in the condensed and gas phases and have an array of applications in electronics,[1–3] catalysis,[3–7] ceramics,[1–3] magnetic materials,[1–4] and pharmaceutical agents.[8,9] Despite the numerous uses, the chemical and physical properties of the condensed phase species have puzzled scientists for decades. Recently, oxide nanoparticles have been studied revealing their use as possible building blocks for

magnetic materials as well as solid-state nanoscale structures.[3,8–14] Although nanoparticles and clusters differ in size they may have analogous properties, which differ from those of the bulk materials. This correlation might possibly allow the investigation of clusters to contribute fundamental information for nanoparticle fabrication. Studying gas-phase clusters has allowed the structure, bonding, and reactivity to be probed at the molecular level.[15–37] Theory has also been used to explore structures of these clusters.[38–44] While many experiments have focused on transitional metal oxides, a thorough investigation of cluster stability has not been performed. We address this issue of stability using laser photodissociation of mass-selcted vanadium, niobium, and tantalum oxide cluster cations.

Mass spectrometry is by far the most commonly used technique in studying metal oxide clusters. Perhaps the first experiment to observe the presence of gaseous transition metal oxide molecules was in 1957 by Berkowitz, Chupka and Inghram where they observed $V_4O_9^+$, $V_3O_6^+$, and $V_2O_4^+$.[15] Additional mass spectrometry experiments have provided evidence for non-statistical ratios, rather than single magic numbers like those seen for metal carbide clusters,[45–48] while also revealing several specific oxide stiochiometries, regardless of conditions.[15–28] Castleman and co-workers have reported extensive studies for vanadium, niobium and tantalum oxides clusters showing that at each metal increment specific oxide stoichiometries are formed.[15–17] In addition, they have investigated the reactivity of these metals with small hydrocarbons.[18,19] Bernstein and co-workers have investigated neutral cluster mass distributions using various wavelengths of ultraviolet laser photoionization.[22] Both Castleman and Bernstein have used the intensity patterns of clusters to infer cluster stability information. These clusters have also been studied with rare gas matrix isolation[29] and photoelectron spectroscopy of mass-selected anions.[30–34] Most recently IR spectroscopy has been used to probe the geometric structures of these systems.[35–37,48] Our group, in collaboration with Meijer and coworkers, used IR-resonance enhanced multiphoton ionization (IR-REMPI) to obtain the IR spectra for several metal carbide[48] and oxide[35] cluster systems. Further IR studies have been performed by Fielicke, Meijer, and Asmis using IR-resonance enhanced

multiphoton photodissociation (IR-REPD).[36,37] While still limited in its capability, theory of transition metal oxide clusters has investigated their structures.[38–44]

A variety of experiments have been performed over the years attempting to determine the stability of gas phase clusters such as these metal oxides. However, as shown by numerous investigators many of these previous measurements are problematic.[50,51] The earliest mass spectrometers probed the vapor concentrations of species in equilibrium in metal ovens, which should allow stability to be determined. However, electron impact ionization was used possibly causing fragmentation during ionization. Additionally, size-dependent ionization cross sections may create a bias in the observed concentrations, causing concern over the accuracy of these measurements. Similar issues are also present in more recent mass spectrometry measurements. Photoionization, like electron impact, may suffer from fragmentation and size-dependent cross sections, making it virtually impossible to measure the concentrations of neutral clusters. Energy-variable collision induced dissociation and photodissociation have been used to determine thresholds for bond breaking for the cations of these oxides, however, these methods also have limitations. Photodissociation relies on the absorption of light, which may not be efficient in the threshold region. Collisional measurements may suffer from significant kinetic shift effects, especially for strongly bound clusters. Equilibrium measurements have been performed on the small clusters of the vanadium-group oxides.[15] Additionally, photoionization has probed the neutral clusters[22] while collision induced dissociation has probed vanadium and niobium oxides.[18,19] Despite the plethora of data available, the most stable clusters remain unidentified.

Photodissociation has the capability to determine the relative stability of such clusters and to date very few studies have utilized this method. We have shown in previous work how photodissociation patterns can be used to determine relative cluster stabilites.[23,46] Stable clusters are difficult to dissociate. However, when larger cluster dissociate these species are produced more often as product fragments. While any single fragmentation spectrum can not reveal the stability of cluster fragments due to absorption efficiencies, cross sections and

dynamics, the fragmentation spectra of many clusters will eventually reveal the stable clusters. These stable cations are produced as charged products when larger clusters dissociate while the stable neutrals can be inferred by mass conservation. Our group has used these methods to study metal and silicon carbide clusters,[46] metal silicon clusters,[49] and main group metal oxide clusters.[23] In this study we apply this photodissociation methodology to transition metal oxides of the vanadium group. Castleman and coworkers have reported some photodissociation measurements on vanadium oxide cations,[18b] however, those measurements were not for large clusters with more than six metal atoms. We have investigated the stability patterns for vanadium, niobium, and tantalum oxide clusters.

3.3 Experimental

Clusters were produced via laser vaporization in a pulsed nozzle cluster source and mass analyzed in a reflectron time-of-flight mass-spectrometer (TOF-MS) as described previously.[23, 46] The second (532 nm) or third (355 nm) harmonic of a Nd: YAG laser (Spectra Physics DCR-11) is used to vaporize a rotating and translating metal rod held in a standard rod holder, thereby producing metal atoms. A He mixture seeded with 1-5% oxygen is pulsed through a General Valve (1 mm orifice) nozzle with a 270 μsec pulse duration and 60 psi backing pressure. The gas is pulsed through the rod holder producing a molecular beam of clusters, which is expanded into a differentially pumped chamber then skimmed into the mass spectrometer chamber. Cluster cations grown directly from the laser plasma are sampled into the reflectron time-of-flight mass spectrometer with pulsed acceleration plates. Pulsed deflection plates in the first flight tube are used to select the clusters of interest before they enter the reflectron region. Photoexcitation occurs using 532 nm or 355 nm from a Nd: YAG (Continuum Surelite I), timed to intersect the clusters at the turning point in the reflectron field. Subsequently the parent and fragment ions are mass analyzed in the second drift tube and detected using an electron multiplier tube and a digital oscilloscope (LeCroy 9310A).

Photodissociation spectra are collected with a computer difference technique which simultaneously monitors the depletion of the parent ion and the appearance of the fragment ion. Different studies were performed as a function of laser wavelength and pulse energy for each cluster size. Photodissociation used 20-50 mL/pulse of unfocused laser beam in a spot size of roughly 1 cm^2. Data are transferred from a digital scope to a PC via an IEEE-488 interface.

3.4 Results and Discussion

The mass spectrum of $Ta_nO_m^+$ cation clusters produced in our experiment is shown in Figure 3.1. Clusters are produced containing up to about 10 metal atoms. There are several oxide stoichiometries, m, for each metal increment, n. For example, the mass multiplet at n=3 contains peaks corresponding to $Ta_3O_7^+$, $Ta_3O_8^+$, $Ta_3O_9^+$, $Ta_3O_{10}^+$, and $Ta_3O_{11}^+$. There is a similar multiplet of oxide stoichiometries for each metal increment, n. Other than the number of oxygen atoms always being greater than the number of metal atoms, there are no clear patterns in the stoichiometries apparent. The most intense peak within the multiplets corresponds approximately to m=2n+x, where x=2-4. The value of m can be shifted slightly as the oxygen concentration is increased or decreased in the gas mixture. The cluster distributions are measure for vanadium and niobium oxides are similar to those measured for niobium and tantalum oxides, however, the most abundant peaks within each multiplet are not exactly the same for all three metals. These distributions are very similar to the cation mass spectra measured previously for these metal oxide systems.[18,19,21,22,36,37]

We have attempted to mass select each cluster size individually and dissociate it with laser excitation at 532 nm and 355 nm in order to determine relative stabilities of these oxides. In general, the efficiency of dissociation is not high under any conditions. Both 532 nm and 355 nm require high laser fluences in order to attain measurable dissociation signals. These high pulse energies of 20-50 mJ/cm^2 pulse indicate that multiphoton processes are required. This is understandable since bond energies for these systems have been calculated to be 3-6 eV/bond.[19,24] In addition, the absorption spectra of these clusters are unknown

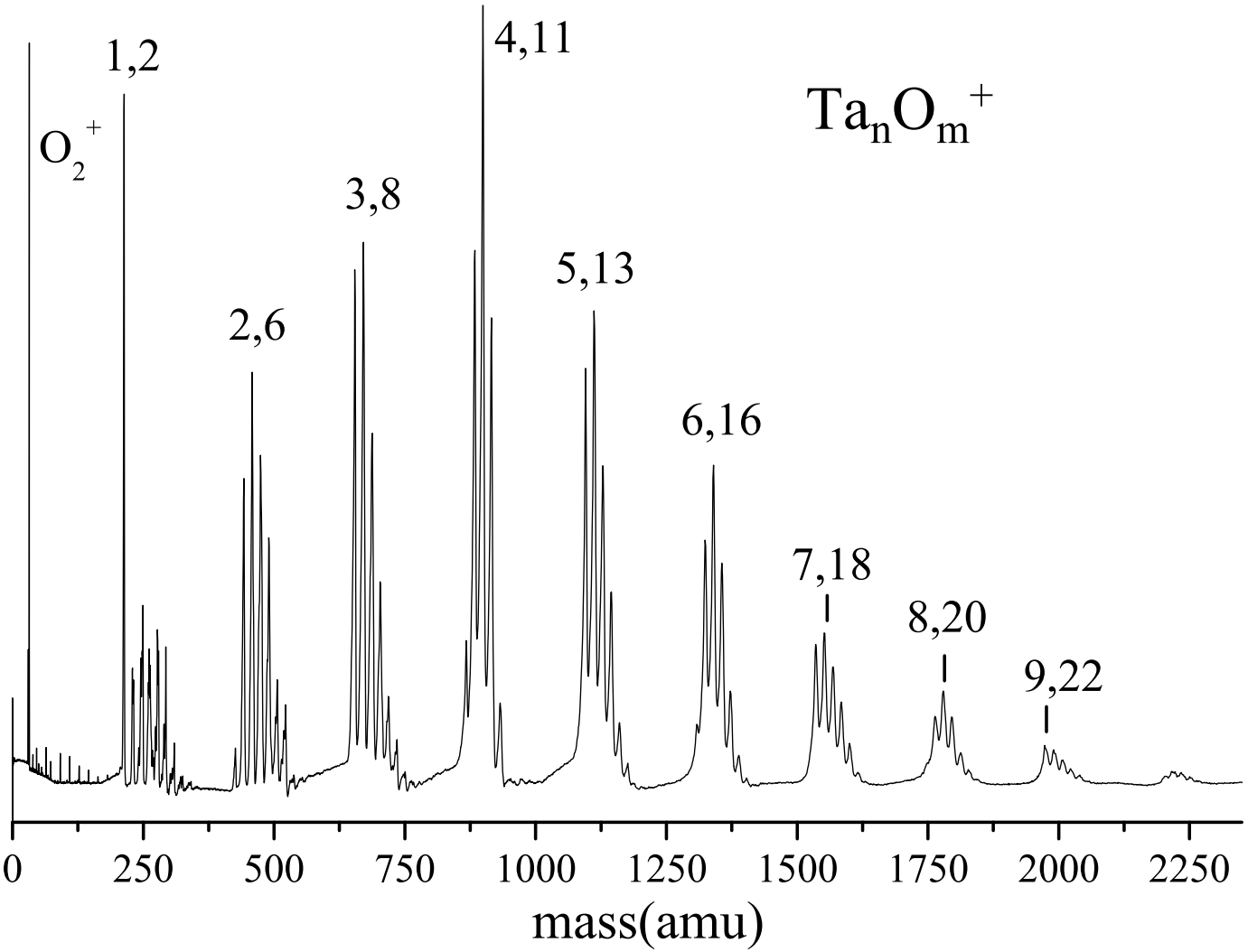

Figure 3.1: Time-of-flight mass spectrum for $Ta_nO_m^+$ clusters formed in a helium expansion. This mass spectrum is representative of similar ones obtained for V and Nb.

making it possible that high fluences are required in order to overcome weak absorption at the wavelengths employed for dissociation. While the efficiency of dissociation is dependent on wavelength for some clusters, the prominent fragments remain the same at both wavelengths. Selected examples of the photofragmentation mass spectra measured for these clusters are shown throughout this chapter. All of these spectra are collected in the difference mode of operation as described earlier. Table 3.1 lists all the cluster ions that we were able to photodissociate and the detected photofragments. For some clusters there were fragments which were noticeably more intense. These are listed in bold in the table.

The photodissociation mass spectrum for the complexes $Ta_2O_5^+$, $Ta_2O_6^+$, and $Ta_2O_7^+$ is shown in Figure 3.2. These clusters eliminated one or more oxygen atoms. The $Ta_2O_7^+$ parent ion produces the $Ta_2O_5^+$ and $Ta_2O_4^+$ fragment ions (indicated by the 2,5 and 2,4 stoichiometries). This cluster dissociates primarily by losing either two oxygen atoms or molecular oxygen to form the $Ta_2O_5^+$. Because neutral fragments are not detected, we can only be sure of the mass conservation and not whether the fragments are atomic or molecular. However, since the elimination of molecular fragments represents the lower energy process, it is assumed that when possible this is the method of elimination, as opposed to atomic elimination. The $Ta_2O_4^+$ fragment ion could occur via elimination of an additional O atom (together with or after the loss of molecular oxygen). However, as noted previously, we cannot distinguish between sequential and concerted dissociation processes and laser power studies are inconclusive as all fragments appear and disappear together as we vary the pulse energy. Because of this we indicate the inferred neutral mass loss in brackets from now on to indicate our uncertainty about the exact fragment.

The middle frame of Figure 3.2 shows that $Ta_2O_6^+$ dissociates by the loss of one or two atoms or molecular oxygen, producing mostly the 2,4 fragment ion. As seen for $Ta_2O_7^+$, no fragments smaller than 2,4 are detected. This same behavior is seen for $Ta_2O_5^+$ and while the extent of fragmentation is less, no fragments smaller than the 2,4 are detected. A broadening of the $Ta_2O_4^+$ mass peak is shown in this spectrum which is greater than our instrument

Table 3.1: The metal oxide photofragments ($M_nO_m^+$ = n,m) detected using 355 nm and 532 nm. The stoichiometries indicated in bold were most prominent fragment ions detected.

Parent Cation Cluster	V	Nb	Ta
2,4	2,3; **1,2**; 1,1	**1,2**	
2,5	**2,4**; 2,3; **1,2;**1,1	**2,4**; 1,2	**2,4**
2,6	**2,4**; 1,2	**2,5**	2,5; **2,4**
2,7	**2,5**; 2,4; 2,3; **1,2**; 1,1	**2,5**; 2,4; 1,2	**2,5**; 2,4
2,8	**2,4**; 2,3	**2,6**; 2,5; 1,3	**2,6**; 2,4
2,9	**2,5**; 2,4; 2,3	**2,7**; **2,6**	
3,6	**2,4**; 2,3		
3,7	**3,6**; 3,5; **2,4**; 1,2		
3,8	3,7; **3,6**; 2,4	**3,7**	**3,7**; 3,6
3,9	**3,7**; 2,5	**3,7**	
3,10	3,8; **3,7**; 2,4	**3,8**; **3,7**	
4,9	**2,4**; 1,2	**3,7**	**3,7**; 3,6; 2,4
4,10	4,9; **4,8**; 3,7; 3,6; 2,4	**4,9**	
4,11	**4,9**; 2,4; 1,2	**4,10**; 4,9	**4,10**; **4,9**
4,12	**4,10**; 4,8	4,11; **4,10**; 4,9	4,11; **4,10**; 4,9
5,12			**4,9**
5,13	**5,11**; 3,7; 2,4	**5,12**	**5,12**
5,14		5,13; **5,12**	**5,13**; **5,12**
6,15	**6,13**		
6,16	**6,14**; 2,4	6,15; **6,14**	6,15
6,17	**6,15**; 6,13	**6,15**	**6,15**
7,17	5,12; **3,7**; 2,4		
7,18	**7,16**	**7,17**	**7,17**
7,19			7,18; **7,17**
8,19	5,12; **4,9**; 3,7; 2,4		
8,20	**8,18**	**8,19**; 7,17	
9,22	5,12; 4,9; 4,8; 3,7; 3,6; **2,4**; 1,2; 1,1		

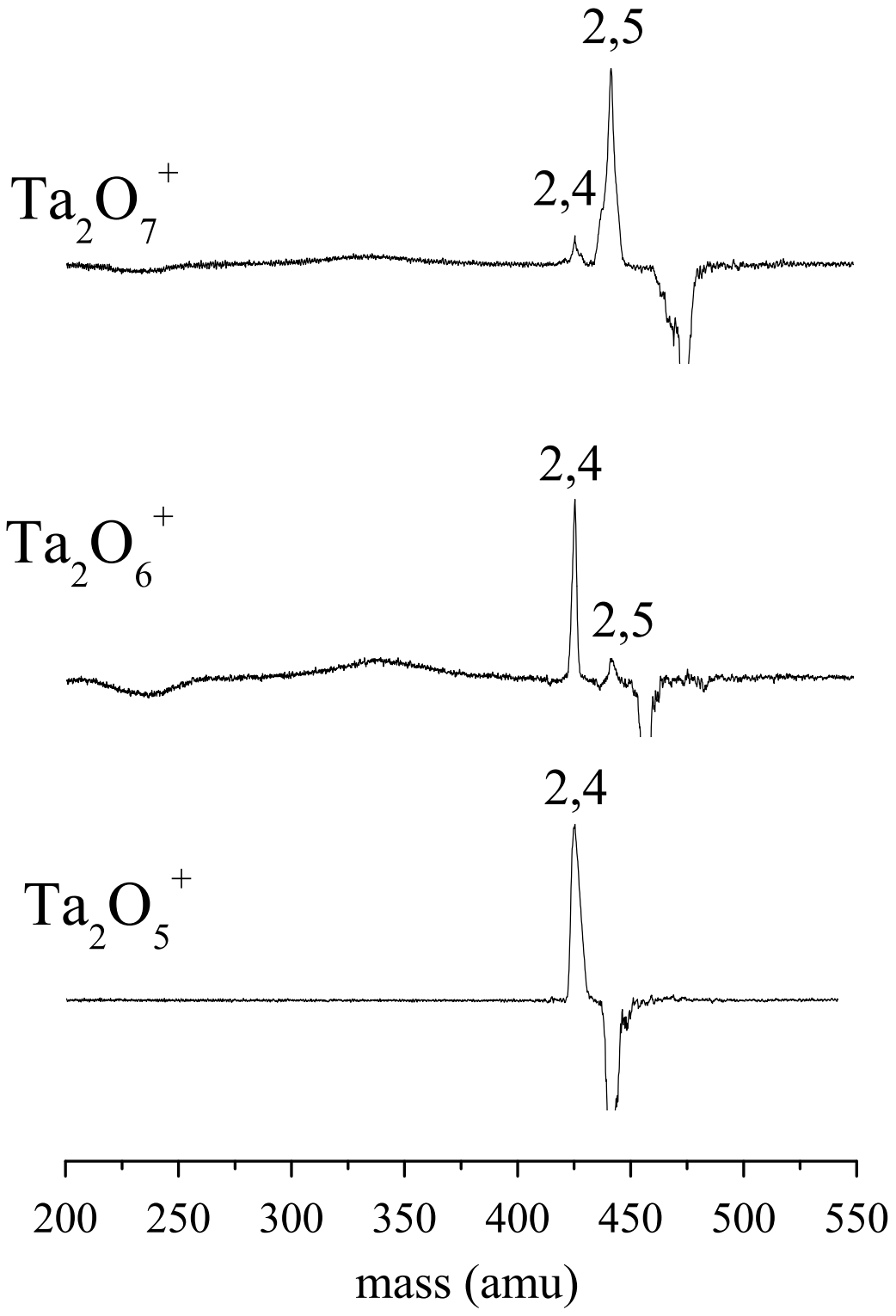

Figure 3.2: Photodissociation mass spectra of $Ta_2O_m^+$ clusters at 355 nm.

resolution. This points to a slow fragmentation process in comparison to our instrument timescale, indicating a metastable behavior for this ion. The 2,4 ion is the smallest fragment produced with high intensity for the $M_2O_m^+$ complexes of all three metals, as shown in Table 3.1. While some $M_2O_m^+$ ions fragment beyond the $M_2O_4^+$ and not all fragment down to this, the $M_2O_4^+$ is prominent for all $M_2O_m^+$ ions fragments and it is the so-called "terminal" ion. The repeated appearance of the $M_2O_4^+$ ions as a fragment from $M_2O_m^+$ where m >4 indicates that it is relatively more stable that other clusters within the $M_2O_m^+$ family of clusters. We therefore designate the 2,4 species as the "core" cluster of the n=2 group.

The same kind of fragmentation behavior can be seen in Figure 3.3 for the n=3 group of vanadium oxide clusters. $V_3O_8^+$ fragments by the loss of $[O_2]$ to produce $V_3O_6^+$. $V_3O_7^+$ produces $V_3O_6^+$ by the loss of two oxygen atoms and $V_3O_5^+$ by the loss of $[O_2]$. Again $V_2O_4^+$ is detected as a fragment as is the VO_2^+ ion. In data not shown, VO_2^+ is the main fragment produced when $V_2O_4^+$ is dissociated, which suggests that it is a sequential product. $V_3O_6^+$ and $V_2O_4^+$ are both prominent fragment ions in the dissociation of $V_3O_7^+$ and $V_3O_8^+$. However, when $V_3O_6^+$ is dissociated the one main fragment is $V_2O_4^+$, which occurs by the loss of $[VO_2]$. This direct channel agrees with the sequential path suggest above for the fragmentation of $V_3O_6^+$ derived from $V_3O_8^+$. From the $V_3O_m^+$ family we see that $V_3O_6^+$ and $V_2O_4^+$ are produced as fragments from several different parents. In addition species where m>6 tend to lose oxygen. This behavior indicates that the 3,6 cluster is the terminal ion for this family. Interestingly, a slightly different patterns if found for the n=3 group of niobium and tantalum clusters. In those experiments, the 3,7 is clearly the terminal ion.

Figure 3.4 shows the dissociation for the $V_4O_m^+$ group, where m=9-12. Where m=10, 11, 12 the prominent fragment ions formed correspond to the loss of $[O_2]$. However, the $V_4O_9^+$ species does not lose oxygen, but rather it eliminates $[V_2O_5]$ to form the $V_2O_4^+$ species or $[V_3O_7]$ to form VO_2^+. The VO_2^+ could also come as a sequential produt from further fragmentation of $V_2O_4^+$. The elimination of $[V_2O_5]$ as an inferred neutral is important since this is the stoichiometry of the most common bulk vanadium oxide phase.[52] All of these

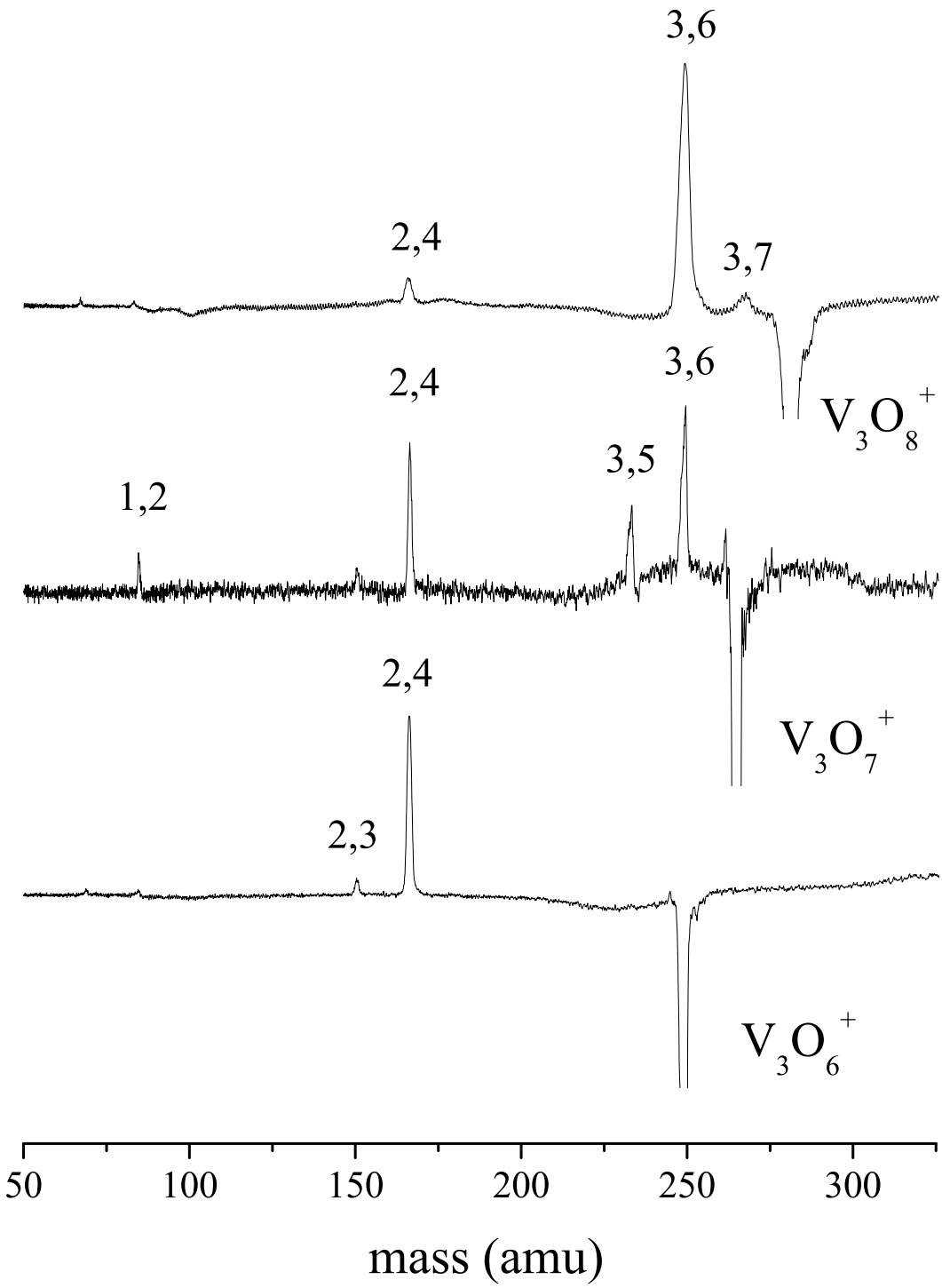

Figure 3.3: Photodissociation mass spectra of $V_3O_m^+$ clusters at 532 nm.

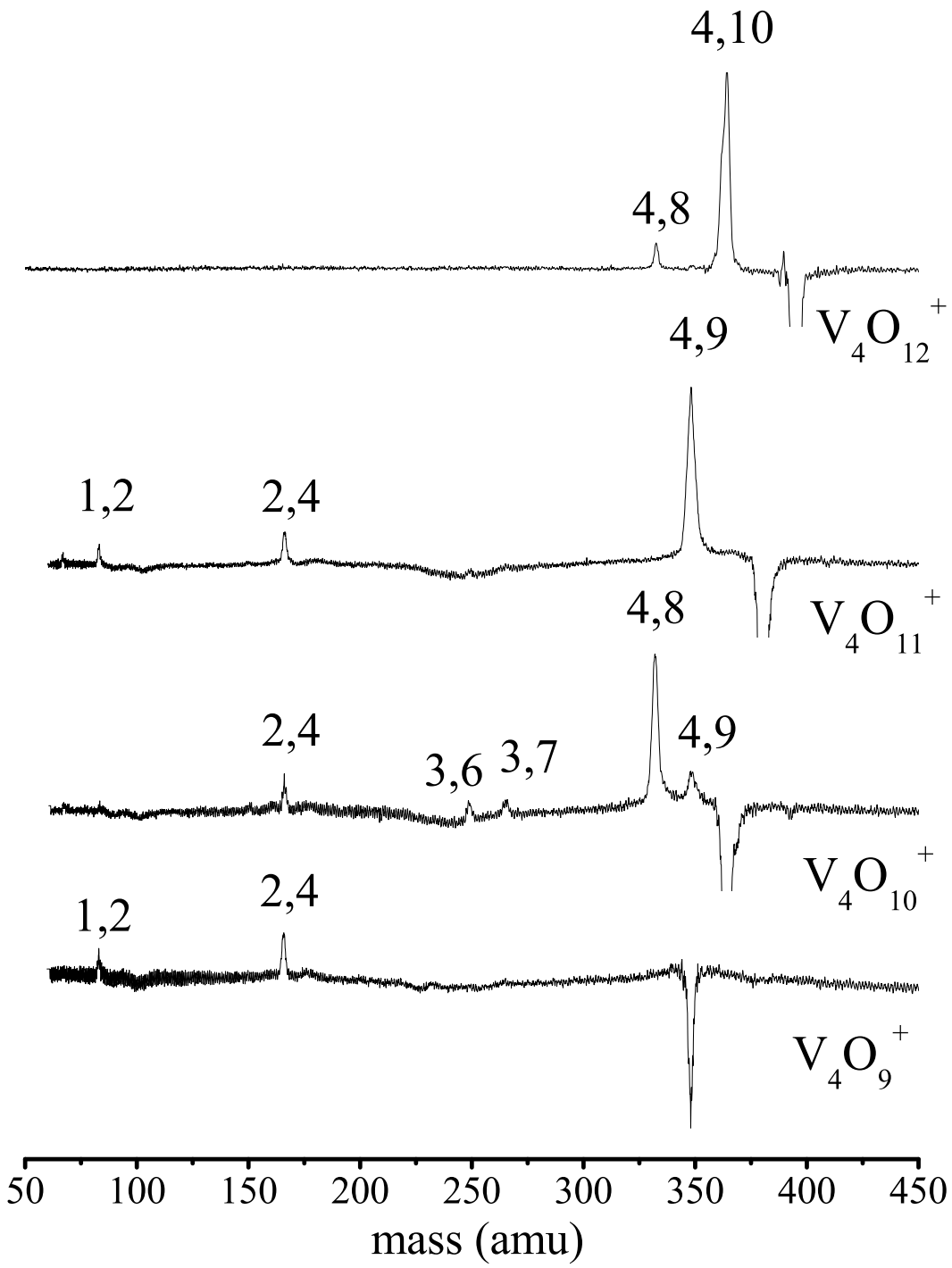

Figure 3.4: Photodissociation mass spectra of $V_4O_m^+$ clusters at 355 nm.

species produce a small amount of $V_2O_4^+$ and VO_2^+, presumably as sequential fragments. In addition, small amounts of $V_3O_6^+$ and $V_3O_7^+$ are detected from the $V_4O_{10}^+$ parent ion. The 4,9 is apparently the terminal ion for this family, although this conclusion is somewhat skewed by the tendency of vanadium oxide clusters to lose $[O_2]$. However, the only time any $V_4O_m^+$ ion is produced for m<9 is by the loss of $[O_2]$, as in $V_4O_{10}^+$.

The dissociation behavior of $Ta_4O_m^+$ is somewhat similar to that of the $V_4O_m^+$ family, as shown in Figure 3.5. There are several noteworthy differences between tantalum and vanadium. First, the dissociation efficiency of the Ta oxide clusters is much less than it is for the corresponding V clusters. This is verified by the smaller signal levels for the tantalum oxides. An additional difference between Ta and V is the tendency for both $Ta_4O_{12}^+$ and $Ta_4O_{11}^+$ to lose a series of O atoms as opposed to $[O_2]$. However, the loss of O atoms ceases with the formation of the $Ta_4O_9^+$ fragment ion. No n=4 fragment ions with less than nine oxygens are detected under any conditions from these parents. There are also some similarities between Ta and V. $Ta_4O_9^+$ behaves somewhat like $V_4O_9^+$ in that it fragments by losing metal oxides, as opposed to O or O_2 increments. $Ta_4O_9^+$ loses $[TaO_2]$ and $[Ta_2O_5]$ to produce $Ta_3O_7^+$ and $Ta_2O_4^+$ respectively. The $M_3O_7^+$ fragment was not detected from $V_4O_9^+$, but the $M_2O_4^+$ fragments was seen for both. Formation of the intermediate fragment for tantalum suggests that the extent of fragmentation in this system is less than it was for the corresponding vanadium cluster. Again, as noted above for the vanadium family, the MO_2 and M_2O_5 stoichiometries of the bulk are evident in the neutral mass losses.

We have obtained data like that shown in Figures 3.2-3.5 for many of these clusters, as indicated in Table 3.1. From this data we can start to recognize patterns in the dissociation behavior of these various $M_nO_m^+$ clusters. The clusters having more oxygens, m, than metals, n, tend to lose oxygen as the primary photofragment. Oxygen is most often eliminated in units of two for vanadium, implying the loss of molecular O_2. However, niobium and tantalum usually lose units of atomic oxygen. The loss of oxygen, in either atomic or molecular form, ceases at a so-called terminal stoichiometry, after which the loss of both metal and oxygen

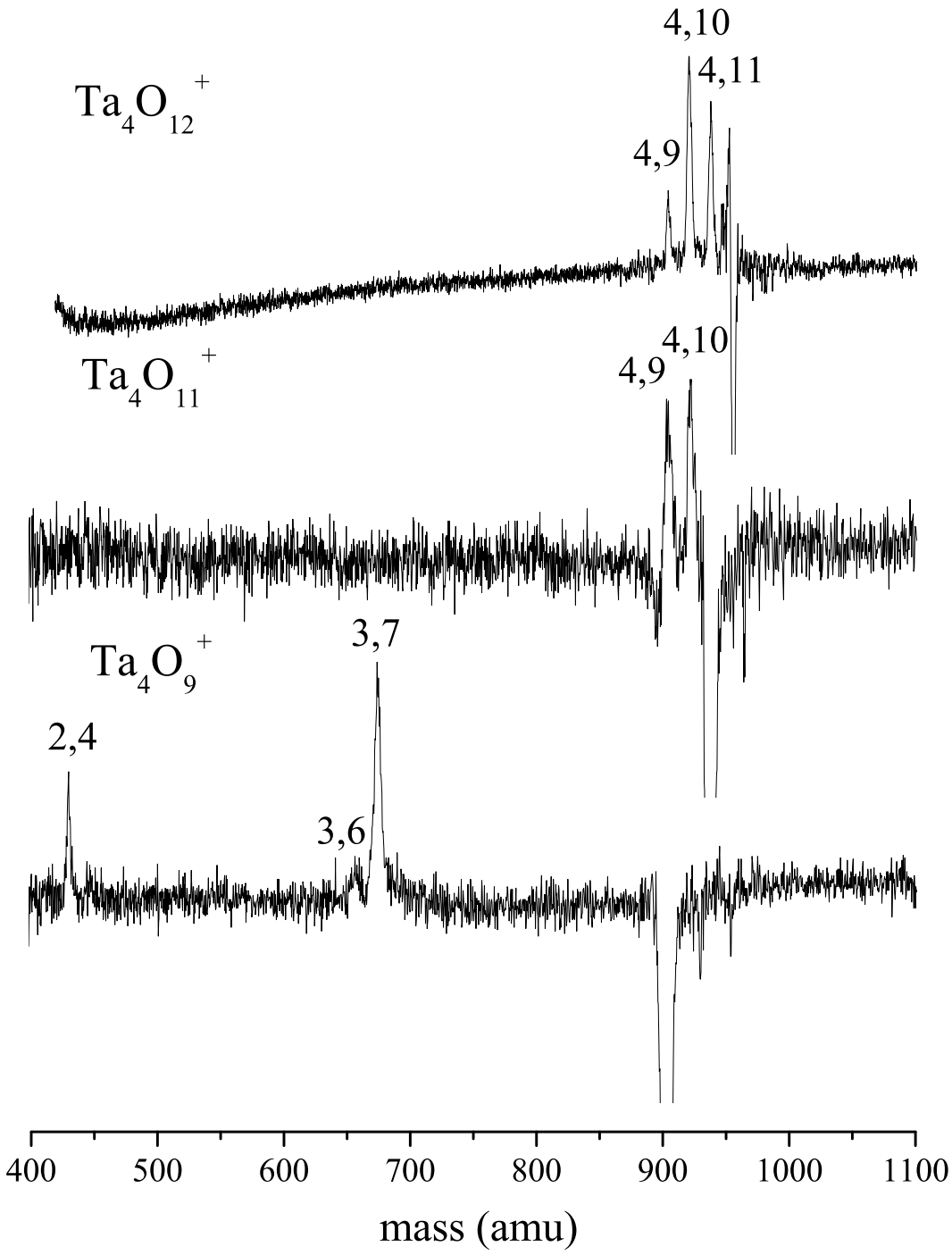

Figure 3.5: Photodissociation mass spectra of $Ta_4O_m^+$ clusters at 355 nm.

proceeds together in units of $[M_2O_5]$ and $[MO_2]$. The terminal stoichiometry for the n=2 families is $M_2O_4^+$ for V, Nb, and Ta. For the n=3 families, this stoichiometry is clearly $M_3O_7^+$ for Nb and Ta, though both $V_3O_6^+$and $V_3O_7^+$ are formed as a terminal ion in different experiments. For the n=4 families, $M_4O_9^+$ is the terminal ion for all three metals.

Selected examples of the dissociation of n=5 clusters are shown in Figure 3.6. Again, the behavior of vanadium is slightly different than that of niobium and tantalum. $V_5O_{13}^+$ dissociates by losing $[O_2]$, yielding primarily $V_5O_{11}^+$, whereas the terminal stoichiometry for various $Nb_5O_m^+$ and $Ta_5O_m^+$ parent ions is 5,12. As shown in Table 3.1 or Figure 3.6, one of more O atoms are eliminated terminating at the 5,12. The only vanadium cluster we were able to dissociate from this group was the $V_5O_{13}^+$, which produces the 5,11 fragment and not 5,12. However as noted above vanadium prefers the lose $[O_2]$ which may explain the difference in the terminal ion.

Figure 3.7 shows two examples of clusters from the n=6 group, $V_6O_{16}^+$ and $Nb_6O_{16}^+$. Both of these clusters lose what appears to be $[O_2]$ or two O atoms, respectively and both produced the terminal ion 6,14. This ion is also seen from several other parents in the n=6 group. Similar selected examples are shown for the n=7 group in Figure 3.8. Both $Nb_7O_{18}^+$ and $Ta_8O_{18}^+$ produce the 7,17 ions without further fragmentation. This ions is also a prominent fragment from other clusters in the n=7 group. We therefore, conclude that 6,14 and 7,17 are the respective terminal ions for their families of clusters.

When a terminal ion is selected and photodissociated metal oxide fragments are eliminated rather than just oxygen. Figure 3.9 shows an example of this behavior for the three $M_4O_9^+$ ions. All three produce the $M_3O_7^+$ ion via the loss of $[MO_2]$. Vanadium and tantalum also produce small amounts o f the $M_2O_4^+$ by loss of $[M_2O_5]$. These fission fragments correspond primarily to the terminal ions found above for the cluster families with smaller n values. The exception to this is the $V_3O_7^+$ where $V_3O_6^+$ was the most prominent ion in the elimination of excess oxygen from larger members of the n=3 family. However both of these ions seem to have comparable stability as a small amount of both are produced in the sequen-

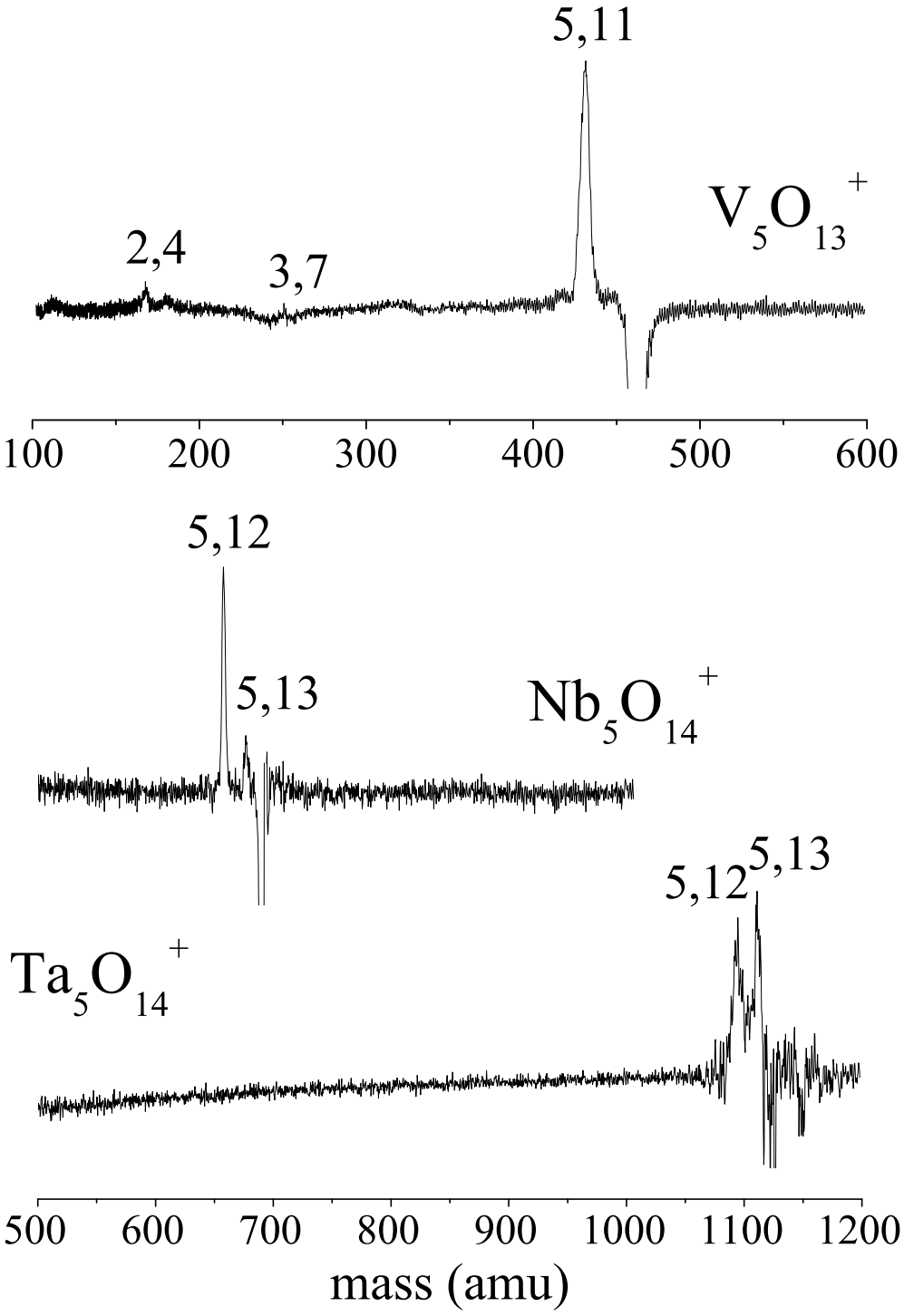

Figure 3.6: Photodissociation mass spectra of $M_5O_{13}^+$ (M=V) and $M_5O_{14}^+$ (M=Nb and Ta) at 532 nm (V) and 355 nm (Nb, Ta).

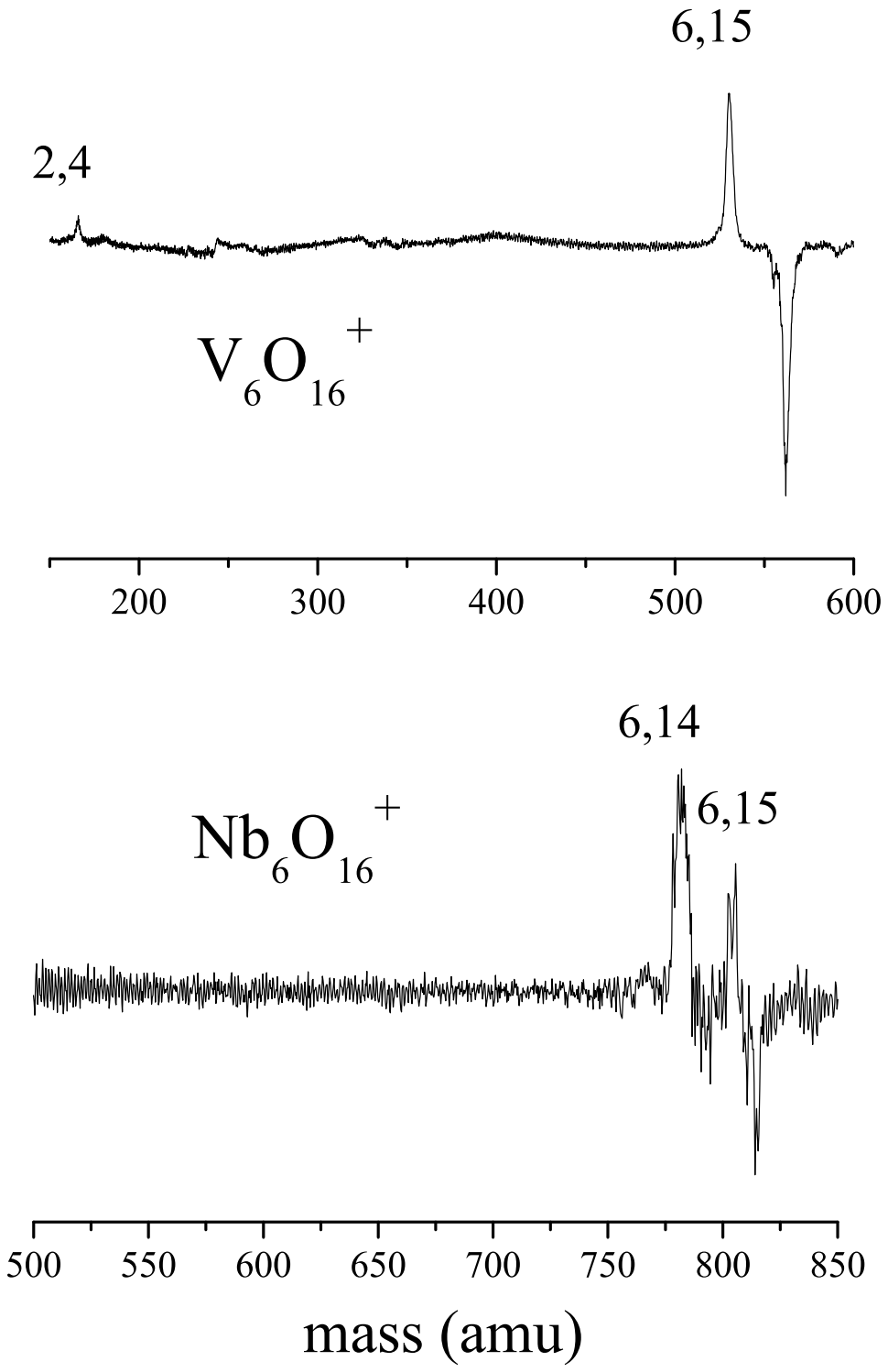

Figure 3.7: Photodissociation mass spectra of $M_6O_{16}^+$ (M=V and Nb) at 532 nm (V) and 355 nm (Nb).

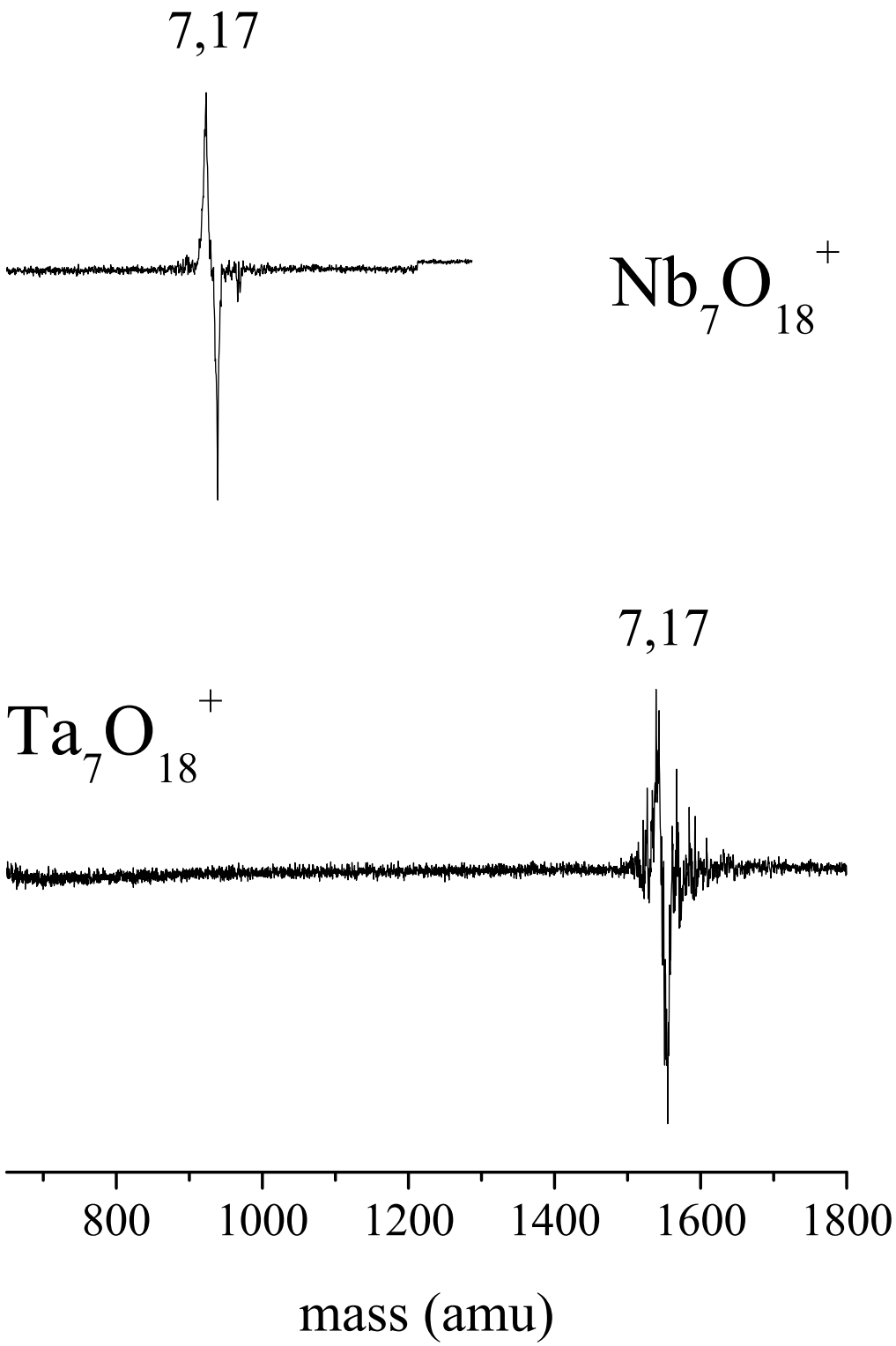

Figure 3.8: Photodissociation mass spectra of $M_7O_{18}^+$ (M=Nb and Ta) at 355 nm.

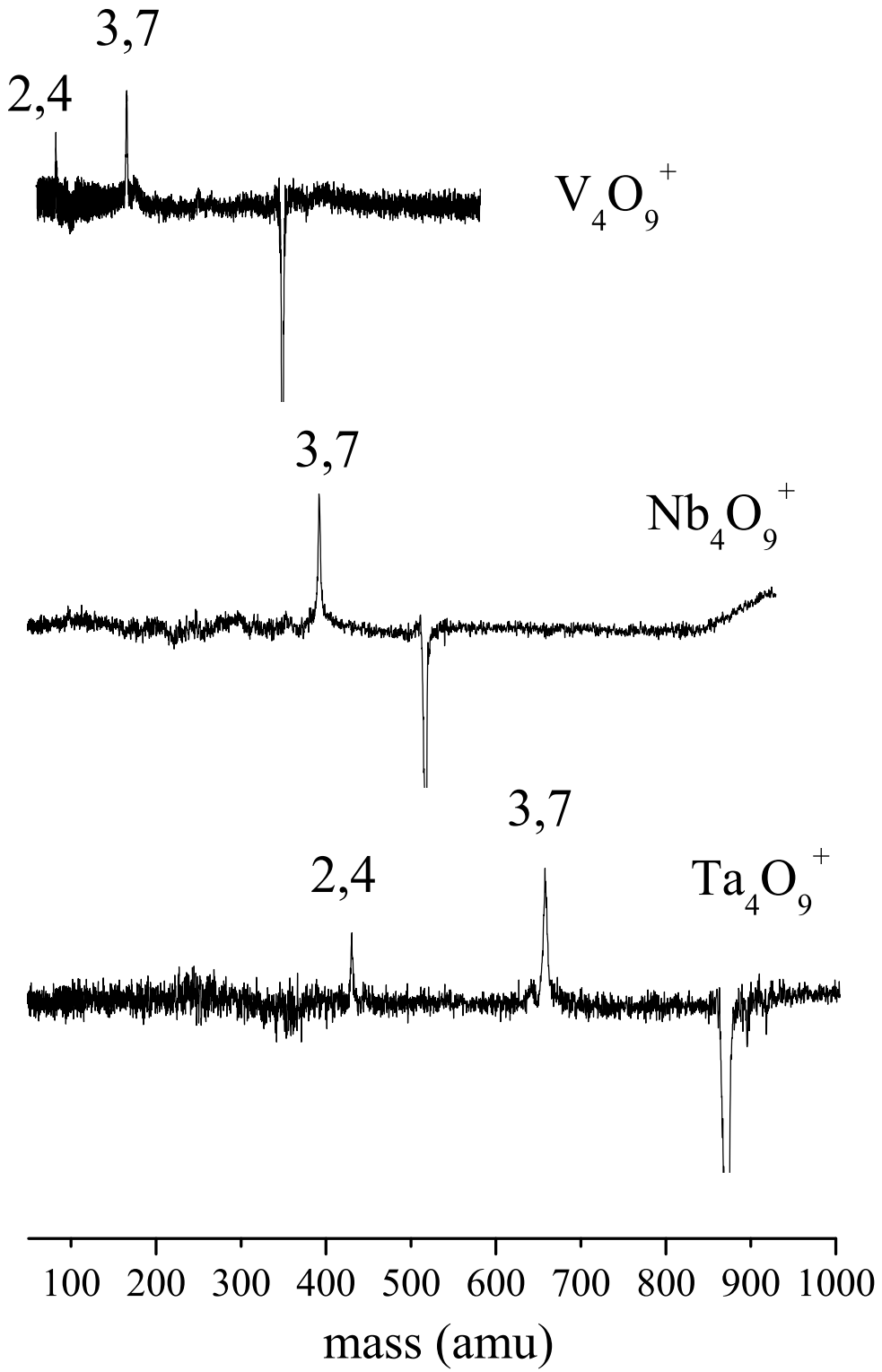

Figure 3.9: Photodissociation mass spectra of $M_4O_9^+$ (M=V, Nb and Ta) at 355 nm.

tial fragmentation of $V_4O_{10}^+$, as shown in Figure 3.4. The fission products resulting from the fragmentation of terminal ions are also evident as minor fragment ions in other clusters shown in previous figures. Apparently when there is excess energy present, oxygen eliminations occurs first and subsequently fission. The same stable core ions can be produced either directly from the fission of larger terminal ions, or by sequential "oxygen loss-then-fission" of non-terminal ions.

We have rather complete sets of data for the fragmentation of parent ions up through n=4. This data makes it very clear that the most stable ions are the MO_2^+, $M_2O_4^+$ and $M_3O_7^+$ species for all three metals (and $V_3O_6^+$). Our data is less complete for the larger clusters. These clusters are produced with lower densities from the source and their photodissociation is less efficient. The lower fragmentation efficiency could result from stronger oxide bonding, lower absorption at the available wavelengths or from longer unimolecular lifetimes in the energized ions. None the less, the result was small signals for the larger clusters, and in some cases fragmentation could not be detected even with significant signal averaging. We therefore show only a few selected fragmentation spectra for the larger clusters.

Figure 3.10 shows the photodissociation of $Ta_5O_{12}^+$ and $V_7O_{17}^+$. Both of these were found to be terminal ions from oxygen elimination patterns presented earlier. Figure 3.10 provides additional proof for this as there is no oxygen fragmentation for either ion, but rather products of fission. $Ta_5O_{12}^+$ dissociates to a small amount of the 4,9 with the inferred neutral loss being $[VO_3]$. $V_7O_{17}^+$ yields mostly the 3,7 ion (no 3,6) and minor amounts of 5,12 and 2,4. In this case, the 3,7 fragment corresponds to the neutral loss of $[V_4O_{10}]$, which is twice the $[V_2O_5]$ bulk stoichiometry. Although we could produce about the same amount of parent clusters where n>7, we mainly have data for the vanadium species, as it was easier to dissociate. Figure 3.11 shows the dissociation measured for $V_8O_{19}^+$ and $V_9O_{22}^+$. In both cases fission products are observed, producing prominent terminal ions identified earlier (5,12; 4,9; 3,7; 2,4, etc.). The 9,22 produces about equal amounts of the 3,6 and 3,7 fragments, thus providing further evidence of their comparable stability. Both of these parent clusters provide

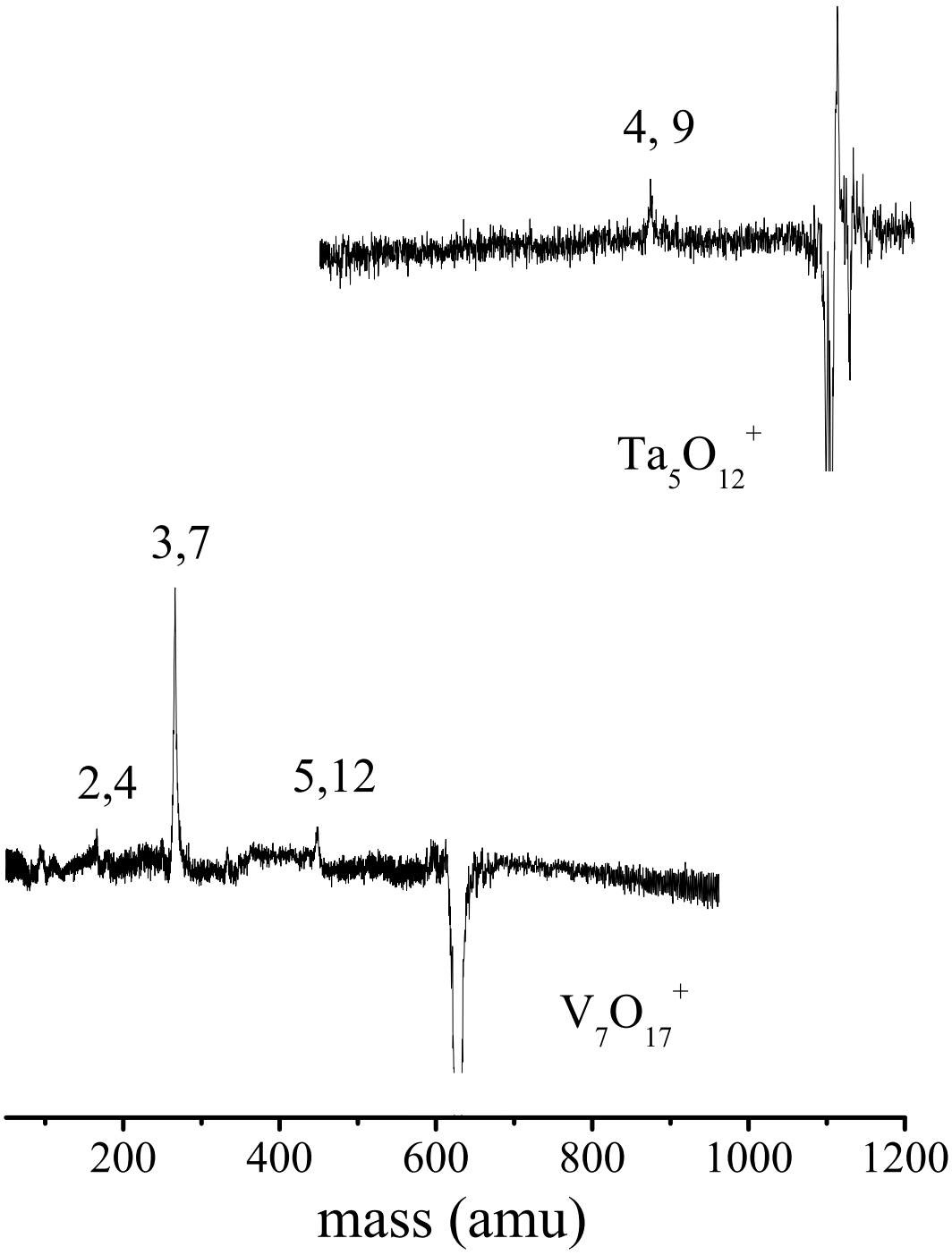

Figure 3.10: Photodissociation mass spectra of $Ta_5O_{12}^+$ (top) and $V_7O_{17}^+$ (bottom) at 355 nm.

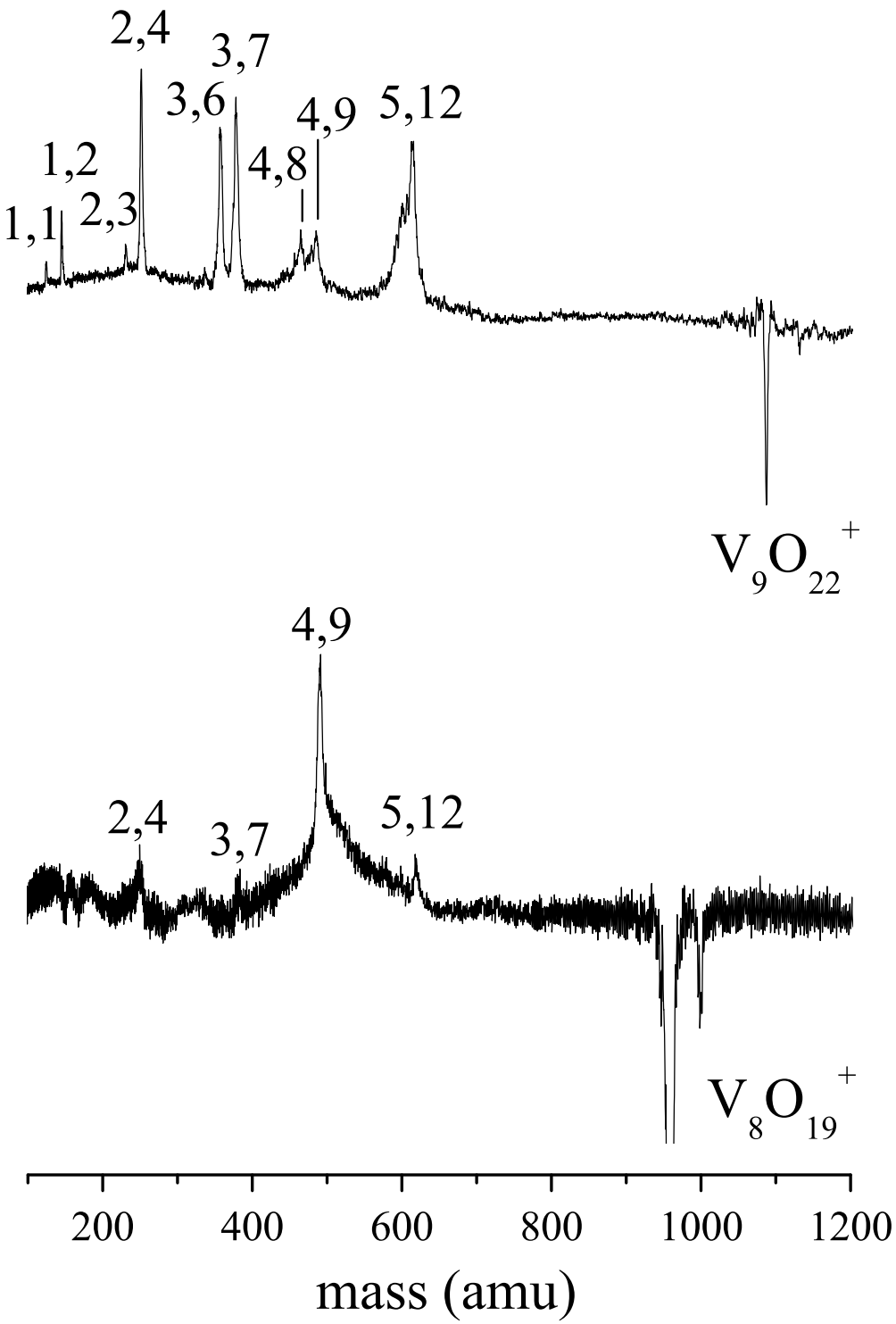

Figure 3.11: Photodissociation mass spectra of $V_9O_{22}^+$ (top) and $V_8O_{19}^+$ (bottom) using 355 nm.

additional evidence for loss of multiples of the neutral V_2O_5 species. $V_9O_{22}^+$ fragments to 5,12 whereas $V_8O_{19}^+$ fragments to 4,9. An additional loss of V_2O_5 accounts for the prominent 2,4 fragment from $V_9O_{22}^+$. While the data is less complete for the larger clusters, the same stable cations and neutral mass differences are produced repeatedly from these cluster parents as seen for the small ones.

Many of the larger clusters produce $M_4O_9^+$, $M_5O_{12}^+$ and $M_7O_{17}^+$ as fragment ions. This is shown in the aforementioned figures as well as the Table 3.1. These species can be identified as stable clusters from both oxygen elimination and fission products of larger species. However, the $M_6O_{14}^+$ is only produced from oxygen elimination rather than fission. While this cluster is the most stable within the n=6 family, it cannot be considered as stable as the other cations identified through both oxygen elimination and fission products.

The most stable cations seen throughout these experiments are therefore MO_2^+, $M_2O_4^+$, $M_3O_7^+$, $M_4O_9^+$, $M_5O_{12}^+$, $M_6O_{14}^+$ and $M_7O_{17}^+$. These cluster stability patterns can be compared to previous work. Castleman and coworkers have reported the photodissociation of $V_nO_m^+$ clusters where n<6, though only a few selected oxides were studied for each metal increment, n.[18a] Our data on these same clusters is very similar to what Castleman reported, although our data on these smaller clusters is more complete and we are able to extend the work to larger clusters which allows patterns not seen previously to emerge. However, there are differences in the exact branching ratios between our experiments and those performed by Castleman and coworkers. These are dependent on cluster temperature and the amount of excitation energy used, both of which are understandably different in different labs. However, nothing reported by Castleman disagrees with our main conclusions. In addition, Castleman and coworkers have investigated collision induced dissociation of both vanadium oxide cluster cations[18b] and anions,[19b] as well as niobium oxide cations.[19a] The fragments reported for the cations are for the most part the same as those we have reported. In addition, the same neutral leaving groups were reported for both cation and anion systems as we have reported here (MO_2, MO_3, M_2O_5). There is no previous photodissociation or collision induced

dissociation of tantalum oxide clusters. However, as shown here, these systems are very similar to vanadium and niobium oxides. Castleman and coworkers concluded that the overall oxide cluster stabilities are as follows, V<Nb<Ta. Our work is qualitatively consistent with this as all of our clusters require multiphoton conditions for dissociation, but the vanadium system is certainly easier to dissociate than the niobium and tantalum systems.

Castleman has also investigated the *reactivity* of all three metal oxide clusters with many small hydrocarbon molecules.[19] The stable cations that we have suggested are for the most part less reactive than their more oxygen-rich counterparts. The reaction products documented for these species correspond to association products, where an adsorbate adds to the intact cation. In the oxygen-rich clusters, reactions often lead to the loss of oxygen and the formation of a small oxide cluster, which typically corresponds to those we have reported as having the largest relative stability. Thus, the previous work agrees with our conclusions that the stable cations here are produced often as dissociation products and that the same clusters are relatively less reactive.

While there is less previous work on the neutral clusters, we can compare our results with those clusters detected using vacuum ultraviolet photoionization by Bernstein and coworkers.[22g] Although ionization potentials and cross sections are not known for any of these species, VUV photoionization is the best way to ionize clusters without fragmentation, allowing the detection of the most abundant neutral clusters formed. The most abundant clusters detected with 118 nm photoionization studies were V_2O_5, V_3O_7, V_4O_9, V_5O_{12}, V_6O_{14}, and V_7O_{17} with small amounts of V_8O_{19}. Again the V_2O_5 cluster corresponds to the bulk stoichiometry and this is the species inferred as a stable neutral leaving group in many of our fragmentation spectra. While the $V_2O_4^+$ was not detected as a neutral in the photoionization studies, essentially all the other clusters which we have identified as stable cations were detected. There are two possible explanations for the consistency between the neutral and cation clusters detected. One explanation is in the larger clusters, n>2, the difference in charge does not affect the stability of the cluster. For example in the metal-carbide

systems,[45–48] stability is fairly independent of the charge. This can be explained because the bonds in these clusters are strong and favorable bonding might outweigh stability differences created by the last electron, thus the charge does not matter as much as the stable bonding network. The bond energies in these oxide clusters are even stronger than those suggested for the carbide clusters, therefore, this might be a plausible explanation. This idea would also explain why the difference in cations and neutrals would be most apparent in the small clusters with fewer bonds, for example V_2O_5 versus $V_2O_4^+$. Conversely, another explanation for the lack of difference between cations and neutrals is that the VUV ionization detects clusters which are easier to ionize as opposed to those that are the most stable. Clusters that are the most stable as cations often have low ionization potentials, making it conceivable that the VUV ionization detects low IP clusters more easily than stable neutral clusters. In both our work and previous work by Castleman, the dissociation measurements directly establish the stability of the cluster cations. Certain small neutrals are identified as stable (VO_2 and V_2O_5) because they are leaving groups from many cluster fragmentation events. However, the photoionization results are not as definitive because ionization potentials cannot be measured for all clusters in question. Calculated ionization potentials are close to the photon energy (10.5 eV) employed at 118 nm,[22g] however, there is considerable uncertainty in those calculations. This possible bias in the photoionization measurements makes it impossible at present to resolve the issue of cation versus neutral stabilities.

Structures of the most stable cation clusters we have identified should certainly be considered. Several groups have performed theoretical calculations on these species.[18,19,22,24,36–44] The most stable geometric configurations determined for the n=1-4 clusters are shown in Figure 3.12. Theory has not been used to determine structures for the n=5 group, however, we have proposed a structure for the $M_5O_{12}^+$, in Figure 3.12, based on structural patterns in small clusters as well as model building. Unfortunately, experiments have not yet been able to test all the proposed structures. The most applicable work in this area are the new infrared photodissociation experiments using the FELIX free electron laser.[36,37] FELIX has been used

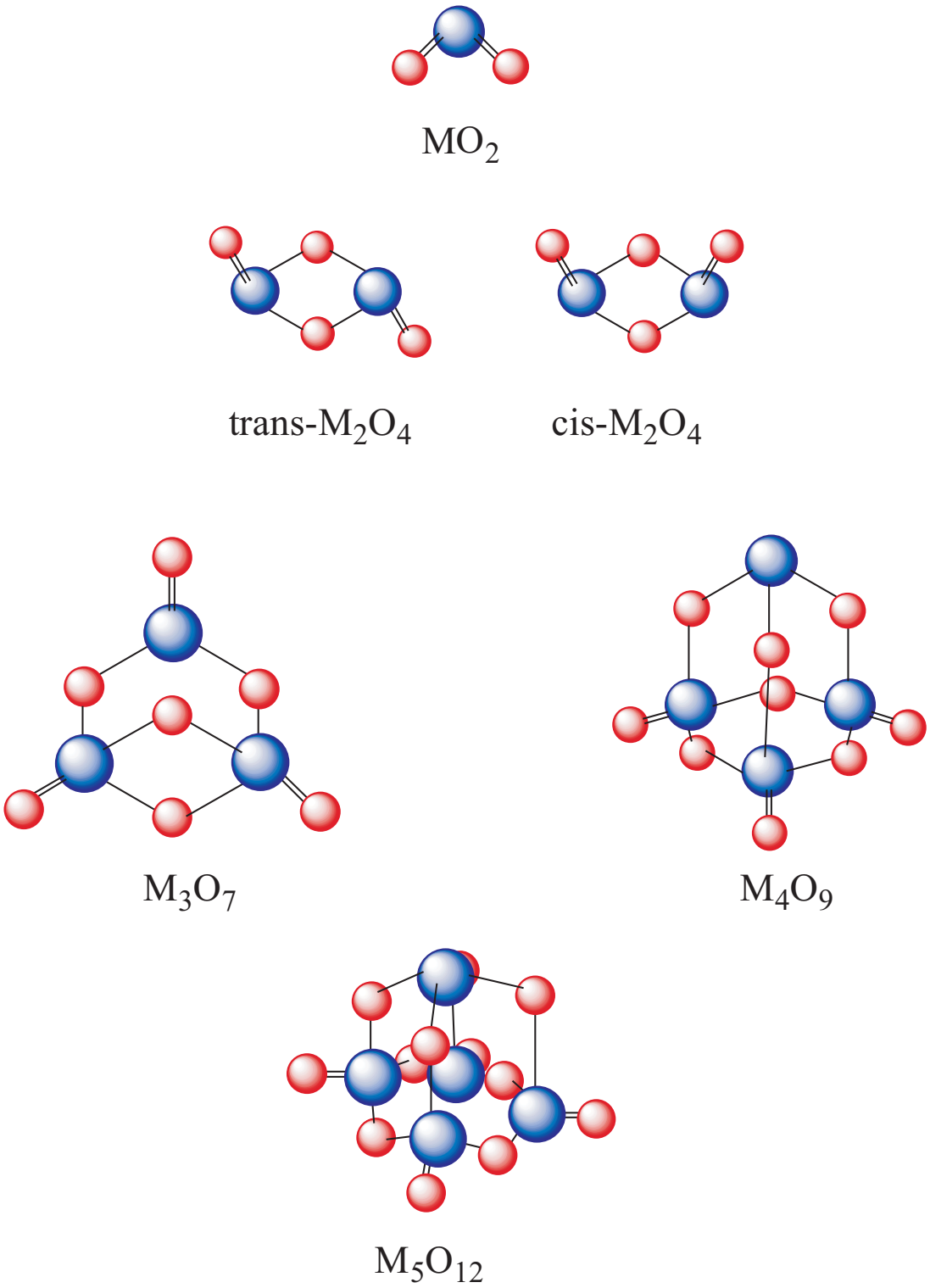

Figure 3.12: Proposed structures for the most stable $M_nO_m^+$ clusters. The structures for MO_2, M_2O_4, M_3O_7 and M_4O_9 clusters have been calculated with density functional theory by previous workers. The structures for the M_5O_{12} clusters are proposed here just on the basis of model building.

to measure vibrational patterns which are compared to the patterns predicted for different cluster geometries. Since these clusters require multiphoton conditions to dissociate, these experiments work the best, yet they have not been able to obtain spectra for the most stable cations identified here. However, the small clusters have been probed using rare gas tagging experiments which rely on the elimination of the tag atoms rather than fragmentation of the oxide cluster itself. Asmis and coworkers have used this method to study the VO_2^+ and $V_2O_4^+$ cations identified here.[37b] There is excellent agreement between the calculated structures in Figure 3.12 and those measured via tagging. However, the experiments have not been able to identify which of the isomers, cis or trans, is present in their spectra and both are predicted by theory to be very close in stability.

These stable cation stoichiometries and structures can also be compared to the known inorganic chemistry of these metals where oxidations states are typically +5 and/or +4. The bulk oxide stoichiometry for these three metals is M_2O_5, where the metal has an effective oxidation state of +5, whereas +4 oxidation state is found in the VO_2 bulk oxide or polyoxoxmetallate anions such as $V_{18}O_{42}^{12-}$.[52] If we then look at the stable cation clusters, we see that $M_4O_9^+$ and $M_6O_{14}^+$ require one metal with a +5 oxidation and one with a +4 oxidation state, whereas the metal in the $M_3O_7^+$, $M_5O_{12}^+$, and $M_7O_{17}^+$ clusters all have a +5 oxidation state. The metal in the $M_2O_4^+$ cluster must have a +4.5 oxidation state since the structure is symmetrical indicating that the two metal atoms are equal. The $M_3O_6^+$ seen only for vanadium corresponds to an oxidation state of +4 for all the metal. Thus, the oxides seen conform for the most part to the species having +4 and +5 oxidation states for these metals, although, slight deviations from all metals having the +5 state are necessary because of the numerology of singly charged cations at different cluster sizes.

The consistency between those clusters which we have identified as being the most stable and the known inorganic chemistry is interesting. In addition our results are qualitatively consistent the results from previous measurements. These measurements have been compared to the structures predicted by density functional theory. However, additional experiments are

needed to determine structures for the larger cluster cations proposed here just as additional theoretical work is required to explain the enhanced stabilities of the clusters identified here.

3.5 Conclusions

We have produced vanadium, niobium, and tantalum oxide cation clusters and studied these species with mass-selected photodissociation. All of these clusters are difficult to dissociate which is consistent with their expected strong bonding. The cluster cation distributions are similar, as has also been noted by previous workers. We have determined two general types of dissociation. Some clusters eliminate excess oxygen in unit of O_2 such as vanadium, whereas niobium and tantalum lose atomic oxygen. Clusters with excess oxygen eliminate oxygen until a terminal oxide stoichiometry is reached at which point further fragmentation occurs via fission. Fission occurs by loss of stable metal oxide fragments. All three metals eliminate MO_2, MO_3 and M_2O_5 as stable neutrals. The terminal cations identified at each metal size increment, n, also repeatedly appear as abundant photofragments from larger clusters for different metals. The most stable cation stoichoimetries established are MO_2^+, $M_2O_4^+$, $M_3O_7^+$, $M_4O_9^+$, $M_5O_{12}^+$, $M_6O_{14}^+$ and $M_7O_{17}^+$. However, vanadium is an anomaly as $V_3O_6^+$ has a comparable stability to $V_3O_7^+$. Where applicable, these conclusions agree with other data on the same oxide cluster cations. There is evidence that neutral clusters of these same metals follow the same stability, further work is needed to confirm this. Despite the new data on structures of the small clusters, additional work from both theory and experiment is needed to establish the structures that correspond to these stable clusters and to explain the source of their stability.

3.6 References

[1] Cox, P. A. *Transition Metal Oxides*; Clarendon: Oxfrod, 1992.

[2] Rao, C. N.; Raveau, B. *Transition Metal Oxides*; Wiley: New York, 1998.

[3] Hayashi, C.; Uyeda, R.; Tasaki, A. *Ultra-Fine Particles*; Noyes: Westwood, 1997.

[4] Henrich, V. E.; Cox, P. A. *The Surface Science of Metal Oxides*; Cambridge University Press: Cambridge, 1994.

[5] Somorjai, G. A. *Introduction to Surface Chemistry and Catalysis*; Wiley-Interscience: New York, 1994.

[6] Gates, B. C. "Supported Metal-Clusters - Synthesis, Structure, and Catalysis," *Chem. Rev. (Washington D.C.)* **1995**, *95*, 511.

[7] a) Street, S. C.; Xu, C.; Goodman, D. W. "The physical and chemical properties of ultrathin oxide films," *Annu. Rev. Phys. Chem.* **1997**, *48*, 43; b) Rainer, D. R.; Goodman, D. W. "Metal clusters on ultrathin oxide films: model catalysts for surface science studies," *J. Mol. Catal. A: Chem.* **1998**, *131*, 259; c) St. Clair, T. P.; Goodman, D. W. "Metal nanoclusters supported on metal oxide thin films: bridging the materials gap," *Top. Catal.* **2000**, *13*, 5; d) Wallace, W. T.; Min, B. K.; Goodman, D. W. "The nucleation, growth, and stability of oxide-supported metal clusters," *Top. Catal.* **2005**, *34*, 17.

[8] Pope, M. T.; Mller, A. *Poloyoxometalate Chemistry From Topology via Self-Assembly to Applications*; Kluwer: Boston, 2001.

[9] Crans, D. C.; Smee, J. J.; Gaidamauskas, E.; Yang, L. Q. "The chemistry and biochemistry of vanadium and the biological activities exerted by vanadium compounds," *Chem. Rev. (Washington D.C.)* **2004**, *104*, 849.

[10] a) Rockenberger, J.; Scher, E. C.; Alivisatos, A. P. "A new nonhydrolytic single-precursor approach to surfactant-capped nanocrystals of transition metal oxides," *J.*

Am. Chem. Soc. **1999**, *121*, 11595; b) Nolting, F.; Luning, J.; Rockenberger, J.; Hu, J.; Alivisatos, A. P. "A PEEM study of small agglomerates of colloidal iron oxide nanocrystals," *Surf. Rev. Lett.* **2002**, *9*, 437; c) Jun, Y. W.; Casula, M. F.; Sim, J. H.; Kim, S. Y.; Cheon, J.; Alivisatos, A. P. "Surfactant-assisted elimination of a high energy facet as a means of controlling the shapes of TiO2 nanocrystals," *J. Am. Chem. Soc.* **2003**, *125*, 15981.

[11] Ayers, T. M.; Fye, J. L.; Li, Q.; Duncan, M. A. "Synthesis and isolation of titanium metal cluster complexes and ligand-coated nanoparticles with a laser vaporization flowtube reactor," *J. Cluster Sci.* **2003**, *14*, 97.

[12] Cushing, B. L.; Kolesnichenko, V. L.; O'Connor, C. J. "Recent advances in the liquid-phase syntheses of inorganic nanoparticles," *Chem. Rev. (Washington D.C.)* **2004**, *104*, 3893.

[13] Kang, E.; Park, J.; Hwang, Y.; Kang, M.; Park, J. G.; Hyeon, T. "Direct synthesis of highly crystalline and monodisperse manganese ferrite nanocrystals," *J. Phys. Chem. B* **2004**, *108*, 13932.

[14] Fernandez-Garcia, M.; Martinez-Arias, A.; Hanson, J. C.; Rodriguez, J. A. "Nanostructured oxides in chemistry: Characterization and properties," *Chem. Rev. (Washington D.C.)* **2004**, *104*, 4063.

[15] a) Berkowitz, J.; Chupka, W. A.; Inghram, M. G. "Thermodynamics of the V-O System - Dissociation Energies of Vo and Vo2," *J. Chem. Phys.* **1957**, *27*, 87; b) Inghram, M. G.; Chupka, W. A.; Berkowitz, J. "Thermodynamics of the Ta-O System - Dissociation Energies of Tao and Tao2," *J. Chem. Phys.* **1957**, *27*, 569.

[16] Farber, M.; Uy, O. M.; Srivastava, R. D. "Effusion-mass spectrometric determination of the heats of formation of the gaseous molecules V4O10, V4O8, VO2, and VO," *J. Chem. Phys.* **1972**, *56*, 512.

[17] Bennett, S. L.; Lin, S. S.; Gilles, P. W. "High-Temperature Vaporization of Ternary-Systems .1. Mass-Spectrometry of Oxygen-Rich Vanadium-Tungsten-Oxygen Species," *J. Phys. Chem.* **1974**, *78*, 266.

[18] a) Kooi, S. E.; Castleman, A. W. "Photofragmentation of vanadium oxide cations," *J. Phys. Chem. A* **1999**, *103*, 5671; b) Bell, R. C.; Zemski, K. A.; Justes, D. R.; Castleman, A. W. "Formation, structure and bond dissociation thresholds of gas-phase vanadium oxide cluster ions," *J. Chem. Phys.* **2001**, *114*, 798.

[19] a) Deng, H. T.; Kerns, K. P.; Castleman, A. W. "Formation, structures, and reactivities of niobium oxide cluster ions," *J. Phys. Chem.* **1996**, *100*, 13386; b) Bell, R. C.; Zemski, K. A.; Kerns, K. P.; Deng, H. T.; Castleman, A. W. "Reactivities and collision-induced dissociation of vanadium oxide cluster cations," *J. Phys. Chem. A* **1998**, *102*, 1733; c) Bell, R. C.; Zemski, K. A.; Castleman, A. W. "Size-specific reactivities of vanadium oxide cluster cations," *J. Cluster Sci.* **1999**, *10*, 509; d) Zemski, K. A.; Bell, R. C.; Castleman, A. W. "Reactivities of tantalum oxide cluster cations with unsaturated hydrocarbons," *Int. J. Mass. Spectrom.* **1999**, *184*, 119; e) Zemski, K. A.; Bell, R. C.; Castleman, A. W. "Reactions of tantalum oxide cluster cations with 1-butene, 1,3-butadiene, and benzene (vol 104A, pg 5733, 2000)," *J. Phys. Chem. A* **2000**, *104*, 7408; f) Zemski, K. A.; Justes, D. R.; Bell, R. C.; Castleman, A. W. "Reactions of niobium and tantalum oxide cluster cations and anions with n-butane," *J. Phys. Chem. A* **2001**, *105*, 4410; g) Zemski, K. A.; Justes, D. R.; Castleman, A. W. "Reactions of group V transition metal oxide cluster ions with ethane and ethylene," *J. Phys. Chem. A* **2001**, *105*, 10237; h) Zemski, K. A.; Justes, D. R.; Castleman, A. W. "Studies of metal oxide clusters: Elucidating reactive sites responsible for the activity of transition metal oxide catalysts," *J. Phys. Chem. B* **2002**, *106*, 6136; i) Justes, D. R.; Mitric, R.; Moore, N. A.; Bonacic-Koutecky, V.; Castleman, A. W. "Theoretical and experimental consideration of the reactions between VxOy+ and ethylene," *J. Am. Chem. Soc.* **2003**, *125*, 6289; j) Justes, D. R.; Moore, N. A.; Castleman, A. W. "Reactions of vanadium and niobium oxides with methanol," *J.*

Phys. Chem. B **2004**, *108*, 3855; k) Bergeron, D. E.; Castleman, A. W., Jr.; Jones, N. O.; Khanna, S. N. "Stable Cluster Motifs for Nanoscale Chromium Oxide Materials," *Nano Lett.* **2004**, *4*, 261; l) Sun, Q.; Rao, B. K.; Jena, P.; Stolcic, D.; Kim, Y. D.; Gantefor, G.; Castleman, A. W. "Appearance of bulk properties in small tungsten oxide clusters," *J. Chem. Phys.* **2004**, *121*, 9417.

[20] Fialko, E. F., Kikhtenko, A.V., Goncharvo, V.B., and Zamaraev, K.I. "Molybdenum Oxide Cluster Ions in the Gas Phase: Strucutre and Reactivity with Small Molecules," *J. Phys. Chem. A* **1997**, *101*, 8607.

[21] Wang, X., Gu, Z., Qin, Q. "A mass spectrometric study on the formation of ionic Ta-containing oxide for laser ablation of Ta and Ta2O5 in O2 ambient," *Int. J. Mass. Spectrom.* **1999**, *188*, 205.

[22] a) Foltin, M.; Stueber, G. J.; Bernstein, E. R. "On the growth dynamics of neutral vanadium oxide and titanium oxide clusters," *J. Chem. Phys.* **1999**, *111*, 9577; b) Foltin, M.; Stueber, G. J.; Bernstein, E. R. "Investigation of the structure, stability, and ionization dynamics of zirconium oxide clusters," *J. Chem. Phys.* **2001**, *114*, 8971; c) Shin, D. N.; Matsuda, Y.; Bernstein, E. R. "On the iron oxide neutral cluster distribution in the gas phase. I. Detection through 193 nm multiphoton ionization," *J. Chem. Phys.* **2004**, *120*, 4150; d) Shin, D. N.; Matsuda, Y.; Bernstein, E. R. "On the iron oxide neutral cluster distribution in the gas phase. II. Detection through 118 nm single photon ionization," *J. Chem. Phys.* **2004**, *120*, 4157; e) Matsuda, Y.; Shin, D. N.; Bernstein, E. R. "On the zirconium oxide neutral cluster distribution in the gas phase: Detection through 118 nm single photon, and 193 and 355 nm multiphoton, ionization," *J. Chem. Phys.* **2004**, *120*, 4142; f) Matsuda, Y.; Shin, D. N.; Bernstein, E. R. "On the copper oxide neutral cluster distribution in the gas phase: Detection through 355 nm and 193 nm multiphoton and 118 nm single photon ionization," *J. Chem. Phys.* **2004**, *120*, 4165; g) Matsuda, Y.; Bernstein, E. R. "On the titanium oxide neutral cluster distribution in the

gas phase: Detection through 118 nm single-photon and 193 mn multiphoton ionization," *J. Phys. Chem. A* **2005**, *109*, 314; h) Matsuda, Y.; Bernstein, E. R. "Identification, structure, and spectroscopy of neutral vanadium oxide clusters," *J. Phys. Chem. A* **2005**, *109*, 3803.

[23] France, M. R.; Buchanan, J. W.; Robinson, J. C.; Pullins, S. H.; Tucker, J. L.; King, R. B.; Duncan, M. A. "Antimony and Bismuth Oxide Clusters: Growth and Decomposition of New Magic Number Clusters," *J. Phys. Chem. A* **1997**, *101*, 6214.

[24] a) Harvey, J. N.; Diefenbach, M.; Schroder, D.; Schwarz, H. "Oxidation properties of the early transition-metal dioxide cations MO2+ (M = Ti, V, Zr, Nb) in the gas-phase," *Int. J. Mass. Spectrom.* **1999**, *183*, 85; b) Schrder, D.; Schwarz, H.; Shaik, S. "Characterization, orbital description, and reactivity patterns of transition-metal oxo species in the gas phase," *Struct. Bonding* **2000**, *97*, 91.

[25] Jackson, P.; Fisher, K. J.; Willett, G. D. "The catalytic activation of primary alcohols on niobium oxide surfaces unraveled: the gas phase reactions of NbxOy- clusters with methanol and ethanol," *Chem. Phys.* **2000**, *262*, 179.

[26] Wang, X.; Neukermans, S.; Vanhoutte, F.; Janssens, E.; Verschoren, G.; Silverans, R. E.; Lievens, P. "Stability patterns and ionization potentials of CrnOm clusters (n=3-50, m=0, 1, 2)," *Appl. Phys. B: Lasers Opt.* **2001**, *73*, 417.

[27] Fielicke, A.; Rademann, K. "Stability and reactivity patterns of medium-sized vanadium oxide cluster cations VxOy+ ($4 \leq x \leq 14$)," *Phys. Chem. Chem. Phys.* **2002**, *4*, 2621.

[28] Vardhan, D.; Liyanage, R.; Armentrout, P. B. "Guided ion beam studies of the reactions of Ni-n(+) (n=2-18) with O-2: Nickel cluster oxide and dioxide bond energies," *J. Chem. Phys.* **2003**, *119*, 4166.

[29] a) Zhou, M. F.; Andrews, L. "Infrared spectra and density functional calculations of the CrO2-, MoO2-, and WO2- molecular anions in solid neon," *J. Chem. Phys.* **1999**, *111*,

4230; b) Andrews, L.; Rohrbacher, A.; Laperle, C. M.; Continetti, R. E. "Laser desorption/ionization of transition metal atoms and oxides from solid argon," *J. Phys. Chem. A* **2000**, *104*, 8173; c) Wang, X.; Andrews, L. "Precious Metal-Molecular Oxygen Complexes: Neon Matrix Infrared Spectra and Density Functional Calculations for M(O2), M(O2)2 (M = Pd, Pt, Ag, Au)," *J. Phys. Chem. A* **2001**, *105*, 5812; d) Danset, D.; Manceron, L.; Andrews, L. "Vibrational Spectra of Nickel and Platinum Dioxide Molecules Isolated in Solid Argon," *J. Phys. Chem. A* **2001**, *105*, 7205.

[30] a) Wang, L.-S.; Wu, H.; Desai, S. R.; Lou, L. "Electronic structure of small copper oxide clusters: from Cu2O to Cu2O4," *Phys. Rev. B: Condens. Matter* **1996**, *53*, 8028; b) Gutsev, G. L.; Rao, B. K.; Jena, P.; Li, X.; Wang, L.-S. "Experimental and theoretical study of the photoelectron spectra of MnOx-(x=1-3) clusters," *J. Chem. Phys.* **2000**, *113*, 1473; c) Gutsev, G. L.; Jena, P.; Zhai, H.-J.; Wang, L.-S. "Electronic structure of chromium oxides, CrOn- and CrOn (n = 1-5) from photoelectron spectroscopy and density functional theory calculations," *J. Chem. Phys.* **2001**, *115*, 7935; d) Zhai, H.-J.; Wang, L.-S. "Electronic structure and chemical bonding of divanadium-oxide clusters (V2Ox, x=3-7) from anion photoelectron spectroscopy," *J. Chem. Phys.* **2002**, *117*, 7882; e) Gutsev, G. L.; Bauschlicher, C. W., Jr.; Zhai, H.-J.; Wang, L.-S. "Structural and electronic properties of iron monoxide clusters FenO and FenO- (n = 2-6): a combined photoelectron spectroscopy and density functional theory study," *J. Chem. Phys.* **2003**, *119*, 11135; f) Zhai, H.-J.; Kiran, B.; Cui, L.-F.; Li, X.; Dixon, D. A.; Wang, L.-S. "Electronic Structure and Chemical Bonding in MOn- and MOn Clusters (M = Mo, W; n = 3-5): A Photoelectron Spectroscopy and ab Initio Study," *J. Am. Chem. Soc.* **2004**, *126*, 16134; g) Yang, X.; Waters, T.; Wang, X.-B.; O'Hair, R. A. J.; Wedd, A. G.; Li, J.; Dixon, D. A.; Wang, L.-S. "Photoelectron Spectroscopy of Free Polyoxoanions Mo6O192- and W6O192- in the Gas Phase," *J. Phys. Chem. A* **2004**, *108*, 10089; h) Zhai, H.-J.; Huang, X.; Cui, L.-F.; Li, X.; Li, J.; Wang, L.-S. "Electronic and Structural Evolution and Chemical Bonding in Ditungsten Oxide Clusters: W2On- and W2On (n

= 1-6)," *J. Phys. Chem. A* **2005**, *109*, 6019.

[31] a) Yang, D. S.; Hackett, P. A. "ZEKE spectroscopy of free transition metal clusters," *J. Electron Spectrosc. Relat. Phenom.* **2000**, *106*, 153; b) Yang, D. S. "Photoelectron spectra of metal-containing molecules with resolutions better than 1 meV," *Coord. Chem. Rev.* **2001**, *214*, 187.

[32] Green, S. M. E.; Alex, S.; Fleischer, N. L.; Millam, E. L.; Marcy, T. P.; Leopold, D. G. "Negative ion photoelectron spectroscopy of the group 5 metal trimer monoxides V3O, Nb3O, and Ta3O," *J. Chem. Phys.* **2001**, *114*, 2653.

[33] a) Pramann, A.; Nakamura, Y.; Nakajima, A.; Kaya, K. "Photoelectron Spectroscopy of Yttrium Oxide Cluster Anions: Effects of Oxygen and Metal Atom Addition," *J. Phys. Chem. A* **2001**, *105*, 7534; b) Pramann, A.; Koyasu, K.; Nakajima, A.; Kaya, K. "Photoelectron spectroscopy of cobalt oxide cluster anions," *J. Phys. Chem. A* **2002**, *106*, 4891; c) Pramann, A.; Koyasu, K.; Nakajima, A.; Kaya, K. "Anion photoelectron spectroscopy of VnOm- (n=4-15; m=0-2)," *J. Chem. Phys.* **2002**, *116*, 6521.

[34] Yoder, B. L.; Maze, J. T.; Raghavachari, K.; Jarrold, C. C. "Structures of Mo2Oy- and Mo2Oy (y=2, 3, and 4) studied by anion photoelectron spectroscopy and density functional theory calculations," *J. Chem. Phys.* **2005**, *122*, 094313/1.

[35] a) von Helden, G.; Kirilyuk, A.; van Heijnsbergen, D.; Sartakov, B.; Duncan, M. A.; Meijer, G. "Infrared spectroscopy of gas-phase zirconium oxide clusters," *Chem. Phys.* **2000**, *262*, 31; b) van Heijnsbergen, D.; von Helden, G.; Meijer, G.; Duncan, M. A. "Infrared resonance-enhanced multiphoton ionization spectroscopy of magnesium oxide clusters," *J. Chem. Phys.* **2002**, *116*, 2400; c) van Heijnsbergen, D.; Demyk, K.; Duncan, M. A.; Meijer, G.; von Helden, G. "Structure determination of gas phase aluminum oxide clusters," *Phys. Chem. Chem. Phys.* **2003**, *5*, 2515.

[36] a) Fielicke, A.; Meijer, G.; von Helden, G. "Infrared spectroscopy of niobium oxide cluster cations in a molecular beam: Identifying the cluster structures," *J. Am. Chem. Soc.* **2003**, *125*, 3659; b) Fielicke, A.; Meijer, G.; von Helden, G. "Infrared multiple photon dissociation spectroscopy of transition metal oxide cluster cations - Comparison of group Vb (V, Nb, Ta) metal oxide clusters," *European Physical Journal D* **2003**, *24*, 69.

[37] a) Asmis, K. R.; Bruemmer, M.; Kaposta, C.; Santambrogio, G.; von Helden, G.; Meijer, G.; Rademann, K.; Woeste, L. "Mass-selected infrared photodissociation spectroscopy of V4O10+," *Phys. Chem. Chem. Phys.* **2002**, *4*, 1101; b) Bruemmer, M.; Kaposta, C.; Santambrogio, G.; Asmis, K. R. "Formation and photodepletion of cluster ion-messenger atom complexes in a cold ion trap: Infrared spectroscopy of VO+, VO+2, and VO+3," *J. Chem. Phys.* **2003**, *119*, 12700; c) Asmis, K. R.; Meijer, G.; Bruemmer, M.; Kaposta, C.; Santambrogio, G.; Woeste, L.; Sauer, J. "Gas phase infrared spectroscopy of mono- and divanadium oxide cluster cations," *J. Chem. Phys.* **2004**, *120*, 6461.

[38] Sambrano, J. R.; Gracia, L.; Andres, J.; Berski, S.; Beltran, A. "A theoretical study on the gas phase reactions of the anions NbO3-, NbO5-, and NbO2(0H)(2)(-) with H2O and O-2," *J. Phys. Chem. A* **2004**, *108*, 10850.

[39] Chakrabarti, A.; Hermann, K.; Druzinic, R.; Witko, M.; Wagner, F.; Petersen, M. "Geometric and electronic structure of vanadium pentoxide: A density functional bulk and surface study," *Phys. Rev. B* **1999**, *59*, 10583.

[40] Zimmermann, R.; Steiner, P.; Claessen, R.; Reinert, F.; Hufner, S.; Blaha, P.; Dufek, P. "Electronic structure of 3d-transition-metal oxides: on-site Coulomb repulsion versus covalency," *J. Phys.: Condens. Matter* **1999**, *11*, 1657.

[41] Wachs, I. E.; Briand, L. E.; Jehng, J. M.; Burcham, L.; Gao, X. T. "Molecular structure and reactivity of the group V metal oxides," *Catal. Today* **2000**, *57*, 323.

[42] Vyboishchikov, S. F.; Sauer, J. "Gas-phase vanadium oxide anions: Structure and detachment energies from density functional calculations," *J. Phys. Chem. A* **2000**, *104*, 10913; Vyboishchikov, S. F.; Sauer, J. "(V2O5)(n) gas-phase clusters (n=1-12) compared to V2O5 crystal: DFT calculations," *J. Phys. Chem. A* **2001**, *105*, 8588.

[43] Albaret, T.; Finocchi, F.; Noguera, C. "Density functional study of stoichiometric and O-rich titanium oxygen clusters," *J. Chem. Phys.* **2000**, *113*, 2238.

[44] a) Calatayud, M.; Silvi, B.; Andres, J.; Beltran, A. "A theoretical study on the structure, energetics and bonding of VOx+ and VOx (x=1-4) systems," *Chem. Phys. Lett.* **2001**, *333*, 493; b) Calatayud, M.; Andres, J.; Beltran, A. "A systematic density functional. theory study of VxOy+ and VxOY (X=2-4, Y=2-10) systems," *J. Phys. Chem. A* **2001**, *105*, 9760.

[45] a) Guo, B. C.; Kerns, K. P.; Castleman, A. W., Jr. "Ti8C12+-metallo-carbohedrenes: a new class of molecular clusters?," *Science (Washington, DC, United States)* **1992**, *255*, 1411; b) Guo, B. C.; Wei, S.; Purnell, J.; Buzza, S.; Castleman, A. W., Jr. "Metallo-carbohedrenes [M8C12+ (M = vanadium, zirconium, hafnium, and titanium)]: a class of stable molecular cluster ions," *Science (Washington, DC, United States)* **1992**, *256*, 515; c) Guo, B. C.; Castleman, A. W., Jr. "Metallo-carbohedrenes: a new class of molecular clusters," *Adv. Met. Semicond. Clusters* **1994**, *2*, 137; d) Cartier, S. F.; May, B. D.; Castleman, A. W., Jr. "Formation, Structure, and Stabilities of Metallocarbohedrenes," *J. Phys. Chem.* **1996**, *100*, 8175.

[46] a) Pilgrim, J. S.; Duncan, M. A. "Beyond Metallo-Carbohedrene: Growth and Decomposition of Metal-Carbon Nanocrystals," *J. Am. Chem. Soc.* **1993**, *115*, 9724; b) Pilgrim, J. S.; Duncan, M. A. "Metallo-carbohedrenes: chromium, iron, and molybdenum analogs," *J. Am. Chem. Soc.* **1993**, *115*, 6958; c) Pilgrim, J. S.; Duncan, M. A. "Metal-carbon clusters: The construction of cages and crystals," *Adv. Met. Semicond. Clusters* **1995**, *3*, 181; d) Duncan, M. A. "Synthesis and characterization of metal-carbide clusters in

the gas phase," *J. Cluster Sci.* **1997**, *8*, 239; e) Ticknor, B. W. D.; M. A. "Photodissociation of size-selected silicon carbide cluster cations," *Chem. Phys. Lett* **2005**, *405*, 214.

[47] Rohmer, M.-M.; Benard, M.; Poblet, J.-M. "Structure, Reactivity, and Growth Pathways of Metallocarbohedrenes M8C12 and Transition Metal/Carbon Clusters and Nanocrystals: A Challenge to Computational Chemistry," *Chem. Rev. (Washington D.C.)* **2000**, *100*, 495.

[48] a) van Heijnsbergen, D.; von Helden, G.; Duncan, M. A.; van Roij, A. J. A.; Meijer, G. "Vibrational spectroscopy of gas-phase metal-carbide clusters and nanocrystals," *Phys. Rev. Lett.* **1999**, *83*, 4983; b) von Helden, G.; van Heijnsbergen, D.; Meijer, G. "Resonant ionization using IR light: A new tool to study the spectroscopy and dynamics of gas-phase molecules and clusters," *J. Phys. Chem. A* **2003**, *107*, 1671.

[49] Jaeger, J. B. J., T. D.; Duncan, M. A. " Photodissociation of Metal-Silicon Clusters: Encapsulated versus Surface-Bound Metal," *J. Phys. Chem. A* **2006**, *110*, 9310.

[50] *Clusters of Atoms and Molecules Vol. I*; Haberland, H., Ed.; Springer: Berlin, 1995; Vol. 52; *Clusters of Atoms and Molecules Vol. II*; Haberland, H., Ed.; Springer: Berlin, 1995; Vol. 52.

[51] Johnston, R. L. *Atomic and Molecular Clusters*; Taylor & Francis: London, 2002.

[52] Cotton, F. A.; Wilkinson, G.; Murillo, C. A.; Bochmann, M. *Advanced Inorganic Chemistry*, Sixth ed.; John Wiley and Sons: New York, 1999.

Chapter 4

Photodissociation of Chromium Oxide Cluster Cations[1]

[1]Molek, K. S.; Reed, Z. D.; Ricks, A.M.; Duncan, M.A. "Photodissociation of Chromium Oxide Cluster Cations," *J. Phys. Chem. A* 2007, in press. Reprinted here with permission of publisher.

4.1 Abstract

Chromium oxide cluster cations, $Cr_nO_m^+$, are produced by laser vaporization in a pulsed nozzle cluster source and detected with time-of-flight mass spectrometry. Cluster distributions are consistent with earlier work, with only a limited number of stoichiometries produced for each value of n, where $m > n$. The cluster cations are mass selected and photodissociated using the second (532 nm) or third (355 nm) harmonic of a Nd:YAG (yttrium aluminum garnet) laser. At either wavelength, multiple photon absorption is required to dissociate these clusters, which is consistent with their expected strong bonding. Cluster dissociation occurs via elimination of molecular oxygen, or by fission processes producing stable cation species and/or eliminating stable *neutrals* such as CrO_3, Cr_2O_5, or Cr_4O_{10}. Specific *cation* clusters are identified to be stable because they are produced repeatedly in the decomposition of larger clusters include $Cr_2O_4^+$, $Cr_3O_6^+$, $Cr_3O_7^+$, $Cr_4O_9^+$, and $Cr_4O_{10}^+$.

4.2 Introduction

Transition metal oxides are used extensively for applications in electronics, catalysis, and magnetic materials.[1–9] The properties of the bulk materials as well as the corresponding nanoparticle and gas phase cluster oxides have been the subjects of many recent studies. Oxide nanoparticles synthesized by a variety of methods are found in applications such as solar energy, magnetism, and medicine.[4,10–17] Gas phase metal oxide experiments have contributed fundamental information needed to understand properties such as bonding, reactivity, and structure.[18–39] Theory has been combined with such experiments to provide the structures and stabilities of the small clusters.[40–47] While, there are many studies of the mass spectrometry of cluster oxides,[18–29] and some investigations of their spectroscopy,[30–39] determining the relative stability of these systems remains problematic. In this study of chromium oxide clusters, we address this issue of cluster stability using laser photodissociation of mass-selected chromium oxide cluster cations.

Mass spectrometry has been used extensively to study metal oxide clusters, documenting the stoichiometries formed and relative abundances.[18–29] Unlike the singular "magic numbers" seen for metal carbides,[48–54] metal oxides exhibit several stoichiometries for each metal increment. Extensive studies of the reactivities of transition metal oxides with small hydrocarbons have been reported by Castleman and coworkers.[22] Additional experiments by Bernstein and coworkers have investigated mass distributions using laser photoionization at vacuum ultraviolet wavelengths.[24] In these previous experiments, the patterns of unreactive clusters or those with high abundance were used to infer relative stability. Rare gas matrix isolation[30] and photoelectron spectroscopy of mass selected-anions[31–36] have been used to study the spectroscopy of small oxide species. Additional experiments have probed the vibrational spectroscopy of these systems in the far-infrared region using a free electron laser.[37–39] IR-resonance enhanced multiphoton ionization (IR-REMPI) was demonstrated by our group in collaboration with Meijer and coworkers to obtain spectra for several metal carbide[51] and oxide[37] cluster systems. Other work by Fielicke, von Helden, Meijer, and Asmis employed infrared resonance enhanced multiphoton photodissociation (IR-REPD) of mass-selected oxide cation and anion species.[38,39] Theory has also been used to determine structures and spectra of various transition metal oxide clusters.[40–47]

Numerous attempts have been made to experimentally determine the relative stabilities of gas phase cluster such as metal oxides.[55,56] However, most of these experiments involve some form of mass spectrometry, and problems arise from unknown ionization potentials, fragmentation processes and size-dependent cross sections. These same issues always make it difficult to measure the relative concentrations of neutral clusters detected by mass spectrometry, regardless of the ionization method employed. Additional problems arise in cation experiments using energy-variable collision induced dissociation or photodissociation to determine the thresholds for bond breaking. Photoabsorption may not be efficient in the threshold region, and collisional measurements may suffer from significant kinetic shifts, especially for strongly bound clusters. Equilibrium measurements have been performed on the small vana-

dium oxide clusters,[17] photoionization has been employed on the neutral clusters,[24] collision induced dissociation has investigated various transition metal oxides,[22] and photodissociation has been applied to vanadium, niobium and tantalum oxides.[21,23] The combined results from these experiments provide evidence for the relative stabilities of some oxide species. Although numerous experiments have studied the vanadium-group oxides, only a few such experiments have considered other transition metal oxide systems.[22]

We have shown repeatedly that mass-selected photofragmentation studies of cluster cations is an effective method in determining relative cluster stabilities.[23,49,57] Stable clusters cations are difficult to dissociate and they are produced often as product ions upon the dissociation of larger clusters. Although stable neutral leaving groups are not detected in photodissociation experiments, they can be deduced from the ions which are detected via mass conservation. These methods have been used previously in our lab to study metal carbide clusters[49] and metal-silicon clusters.[57] Recently we have studied the vanadium group oxide cluster cations,[23] where we demonstrated that certain cluster stoichiometries are indeed much more stable than others and that other forms of mass spectrometry measurements did not provide a clear picture of these stability patterns. In the present work, we apply this same photodissociation technique to investigate chromium oxide clusters.

4.3 Experimental

Clusters are produced by laser vaporization in a pulsed nozzle source and mass analyzed in a reflectron time-of-flight spectrometer, as described previously.[23,49,57] The second harmonic (532 nm) of a Nd:YAG laser (Spectra Physics GCR-11) is employed to vaporize material from the surface of a rotating and translating chromium rod. A helium mixture seeded with 1-3% oxygen is pulsed with a General Valve (60 psi backing pressure; 1 mm orifice) through the sample rod holder, and oxide cluster cations grow directly from the laser-generated plasma. This molecular beam mixture is expanded in a differentially pumped source chamber and skimmed from there into the detection chamber, where cluster cations are sampled

with a reflectron time-of-flight mass spectrometer using pulsed acceleration fields. Pulsed deflection plates in the first flight tube section are used to size-select the clusters of interest before they enter the reflectron. Photoexcitation employs a Nd:YAG laser (DCR-3) at 355 nm, which is timed to intersect the clusters at their turning point in the reflectron field. Subsequently, the parent and fragment ions are mass analyzed in the second drift tube section and detected using an electron multiplier tube and a digital oscilloscope (LeCroy 9310A). Data are transferred from the digital scope to a computer via an IEEE-488 interface. Different studies were performed as a function of laser wavelength and pulse energy for each cluster size. Photodissociation used 20-45 mJ/pulse of unfocused laser beam in a spot size of roughly 1 cm^2.

To investigate the structures and energetics of these metal oxide clusters, geometry optimizations were performed, by Zach Reed in our group, using density functional theory (DFT) computations with the Gaussian 03W program.[58] The Becke-3 Lee-Yang-Parr (B3LYP)[59,60] and Becke-3-Perdew-Wang '91 (B3PW91)[61] functionals were used with the LANL2DZ effective core potential basis set.[62,63] Atomization energies and energies per atom are reported for the minimum energy structures. No symmetry restrictions were placed on the clusters. Minimum energy structures, energies, and vibrations were computed for CrO_3, CrO_3^+, Cr_2O_4, $Cr_2O_4^+$, Cr_2O_5, $Cr_2O_5^+$, Cr_3O_6, $Cr_3O_6^+$, Cr_3O_7, $Cr_3O_7^+$, Cr_4O_{10}, and $Cr_4O_{10}^+$ and these data are reported in the Supporting Information of the paper.[67]

4.4 Results and Discussion

The mass spectrum of $Cr_nO_m^+$ cation clusters produced is shown in Figure 4.1. Clusters containing up to about 14 metal atoms and varying numbers of oxygen atoms are produced with measurable intensity. Each metal size, n, corresponds to a limited number of stoichiometries, where the number of oxygens, m, are always greater than n. For example for n = 4 the only masses seen are those corresponding to $Cr_4O_9^+$, $Cr_4O_{10}^+$, $Cr_4O_{11}^+$, $Cr_4O_{12}^+$. A similar trend is seen for all the metal cluster sizes here, giving rise to groups of peaks in the mass spectrum

corresponding to the oxides for each metal increment. $Cr_4O_{10}^+$ appears to be anomalous in this spectrum, and indeed this species is found under all conditions to have roughly twice the intensity of any other peak. The cluster mass distribution shown here agrees for the most part with the previous one reported by Castleman and coworkers,[22h] although in their data $Cr_4O_{10}^+$ does not have such an enhanced intensity. Mass spectra of partially oxidized $Cr_nO_{1,2}$ clusters were reported by Lievens and coworkers,[26] but these cannot be compared to our data on fully oxidized species.

To investigate the relative stabilities of these various chromium oxide species, we employ mass-selected photodissociation experiments. We select each cluster mass having enough intensity and excite it at 532 and 355 nm to initiate photodecomposition. We find that both wavelengths can induce fragmentation, but that each requires high laser fluences of 35-80 mJ/cm^2 pulse to obtain significant amounts of dissociation. This is consistent with the conditions that we have applied previously to study oxide clusters of the vanadium group,[23] and it indicates that multiphoton excitation is required to break the bonds. The chromium oxide cluster bond energies have been measured with thresholds for energetic oxidation reactions[29] and they have been calculated with density functional theory.[42]

These methods suggest that these bond energies are in the range of 5-7 eV, which validates the requirement of multiphoton excitation. While dissociation is not efficient under any conditions, 355 nm gives the best signals, perhaps because of the greater photon energy or better absorption efficiency at this wavelength. Therefore the data shown throughout this paper are those obtained at 355 nm. Selected examples of the photofragmentation mass spectra measured for these clusters are shown throughout this chapter. All of these spectra are collected in the difference mode of operation as described earlier. Table 4.1 lists all the cluster ions that we were able to photodissociate and the detected photofragments. For some clusters there were fragments which were noticeably more intense. These are listed in bold in the table.

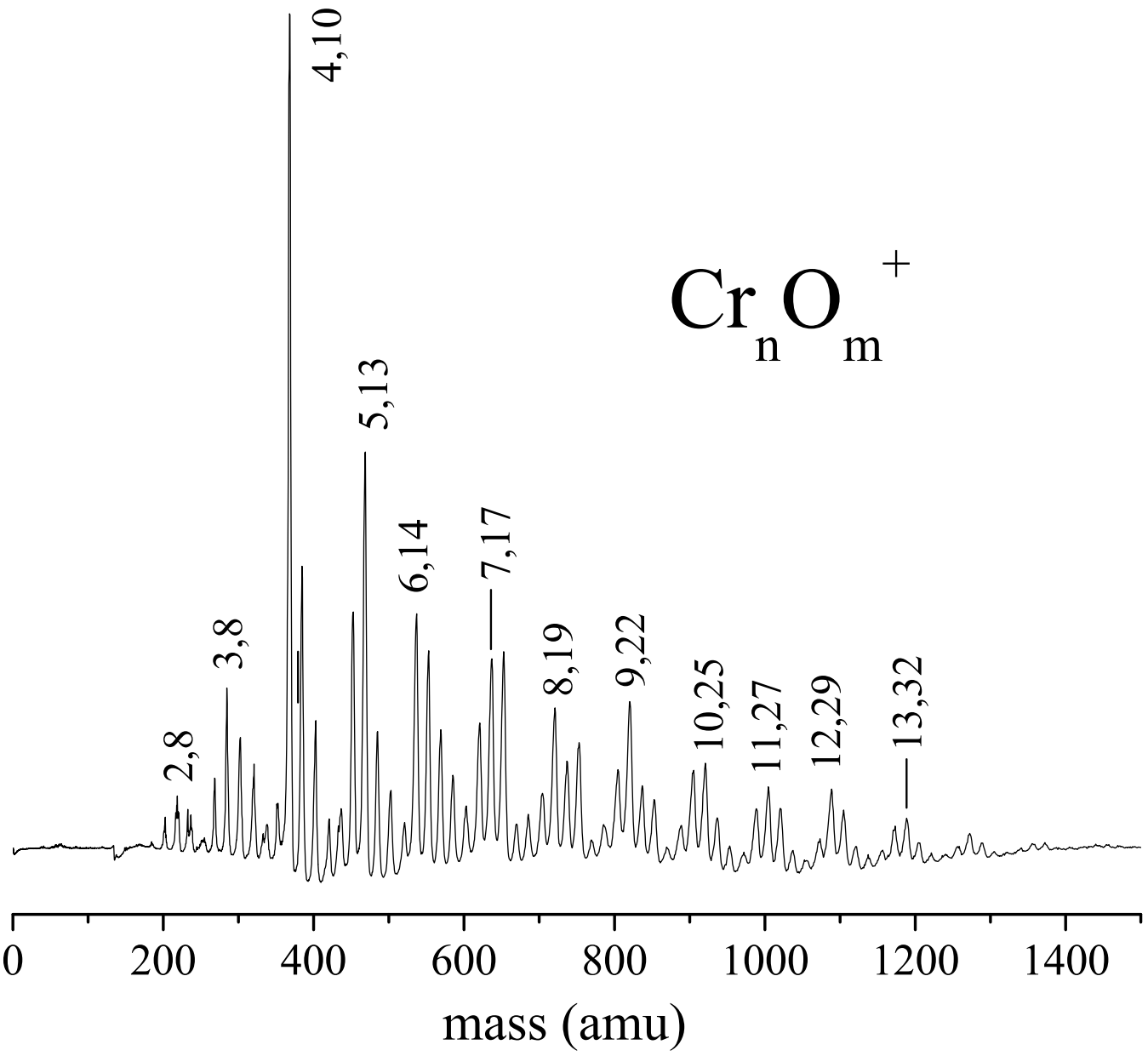

Figure 4.1: Time of flight mass spectrum for $Cr_nO_m^+$ clusters formed in a He expansion.

Table 4.1: The chromium oxide photofragments ($M_nO_m^+$ = n,m) detected using 355 nm. The stoichiometries indicated in bold were most prominent fragment ions detected.

Parent Cation Cluster	Fragment Clusters
2,4	2,3; **2,2**; 1,2; **1,1**, Cr^+
2,5	2,4; **2,3**; 1,2; 1,1, Cr^+
2,6	2,5; **2,4**; 2,3; 2,2; 1,2; 1,1, Cr^+
2,7	**2,5**; 2,4; 2,3; 1,2; 1,1, Cr^+
3,5	3,3; 2,6; **2,4**; 2,3; 2,2; 1,2; 1,1; Cr^+
3,6	3,4; 2,4; **2,3**; 2,2; 1,2; **1,1**, Cr^+
3,7	3,5; **2,4**; 2,3; 2,2; 1,2; 1,1, Cr^+
3,8	**3,6**; 2,5; 2,4; **2,3**; 2,2; 1,2; **1,1**, Cr^+
3,9	3,8; 3,7; 3,6; 2,5; **2,4**; 2,3; 2,2; 1,3; 1,2; **1,1**, Cr^+
4,8	2,4; **2,3**; 2,2; 1,2; **1,1**, Cr^+
4,9	3,6; **2,4**; 2,3; 2,2; 1,2; 1,1, Cr^+
4,10	4,8; 3,7; 3,6; 3,5; 2,5; **2,4**; 2,3; 2,2; 1,2; 1,1, Cr^+
4,11	4,10; **4,9**; **3,6**; 2,5; 2,4; 2,3; 1,1
5,12	4,9; 3,7; 3,6; 3,5; **2,4**; 2,3; 2,2; 1,2; 1,1; Cr^+
5,13	4,10; 3,7; 3,6; 3,5; 2,5; **2,4**; 2,3; 2,2; 1,1
6,14	4,9; 4,8; 3,7; 3,6; 3,5; **2,4**; 2,3; 2,2; 1,1
6,15	4,10; 4,9; 3,7; 3,6; 3,5; 2,5; **2,4**; 2,3; 2,2; 1,2; 1,1; Cr^+
6,16	**4,10**; 3,7; 3,6; 3,5; 2,5; **2,4**; 2,3; 1,1; Cr^+
7,16	4,8; **3,6**; 3,5; **2,4**; **2,3**; 2,2; 1,2; 1,1; Cr^+; O^+
8,20	**4,10**; 4,9; 4,8; 3,7; 3,6; 3,5; 2,4; 2,3; 2,2; 1,1; Cr^+; O^+
8,21	5,12; 4,11; **4,10**; 4,9; 4,8; 3,7; 3,6; 2,4; 2,3
9,21	6,13; **5,11**; 4,9; 4,8; 4,7; **3,6**; 3,5; 2,4; 2,3
9,22	**5,12**; 4,10; 4,9; 4,8; 3,7; **3,6**; 3,5; **2,4**; 2,3; 2,2
9,23	5,12; **4,9**; 4,8; 3,7; 3,6; 3,5; **2,4**; 2,3
9,24	5,13; 5,12; 5,11; **4,10**; 4,9; 4,8; 3,8; 3,7, 3,6; 3,5; 2,5; 2,4; 2,3; 2,2
10,25	6,15; 6,14; 6,13; 5,12; 5,11; **4,10**; 4,9; 4,8; 3,7; **3,6**; 3,5; **2,4**; 2,3
10,26	7,17; 6,15; 6,14; **4,10**; 4,9; 4,8; 3,7; 3,6; 2,4; 2,3
11,27	7,17; 6,14; 6,13; 5,12; 5,11; 4,10; **4,9**; 4,8; 3,7; **3,6**; 3,5; **2,4**; 2,3
12,29	8,18; 7,16; 6,13; 5,12; 5,11; 4,10; **4,9**; 4,8; 3,7; 3,6; 3,5; 2,4; 2,3
13,32	9,22; 7,16; 6,14; 6,13; **5,12**; 5,11; 4,10; **4,9**; 4,8; 3,7; 3,6

Figure 4.2 shows the photodissociation mass spectra for the clusters $Cr_3O_5^+$, $Cr_3O_7^+$, and $Cr_3O_8^+$, hereafter designated as the 3,5; 3,7; and 3,8 species, respectively. Extensive fragmentation occurs with formation of product ions containing one, two, or three metal atoms. The 2,4 fragment ion is prominent in all three spectra. The 1,1 is also seen in all three, but with a lower intensity. There are several other mass peaks seen which are not repeated in different spectra. For example the 3,8 spectrum contains fragment mass peaks corresponding to the 3,6 and 2,3. An additional trend is observed in these spectra. The 3,5 parent produces the 3,3 fragment, the 3,7 parent produces the 3,5 fragment, and the 3,8 parent produces the 3,6 fragment. All of these fragment ions are produced from the elimination of two oxygen atoms or molecular oxygen. The loss of O_2 is the lower energy channel, and since there is little or no signal corresponding to the loss of one oxygen atom, it is perhaps safe to assume that the fragment ions indicated were produced by the elimination of molecular oxygen. This same trend occurs for additional $Cr_3O_m^+$ clusters not shown in this figure. Hereafter, we indicate neutral leaving groups inferred by mass conservation in brackets, e.g. [O_2], to indicate our uncertainty about atomic versus molecular elimination processes.

All of the lower mass fragments shown in Figure 4.2 from all three $Cr_3O_m^+$ clusters could occur through either direct or sequential dissociation processes. In a direct process, the parent ion eliminates the neutral atoms or molecules necessary to conserve mass in one concerted event, whereas in a sequential process the stepwise elimination passes through intermediate fragment ions. For example, the 2,4 fragment from 3,7 could occur directly by the elimination of [1,3] or through the sequence 3,7 $\rightarrow$ 3,5 $\rightarrow$ 2,4. On the other hand, the 2,4 ion produced by the fragmentation of 3,5 likely represents a direct process because no intermediate ions are seen that have four oxygens. Sequential processes most likely would go through intermediate ions that 2,4. On the other hand, the 2,4 ion produced by the fragmentation of 3,5 likely represents a direct process because no intermediate ions are seen that have four oxygens. Sequential processes most likely would go through intermediate ions that Figure 4.2 Pho-

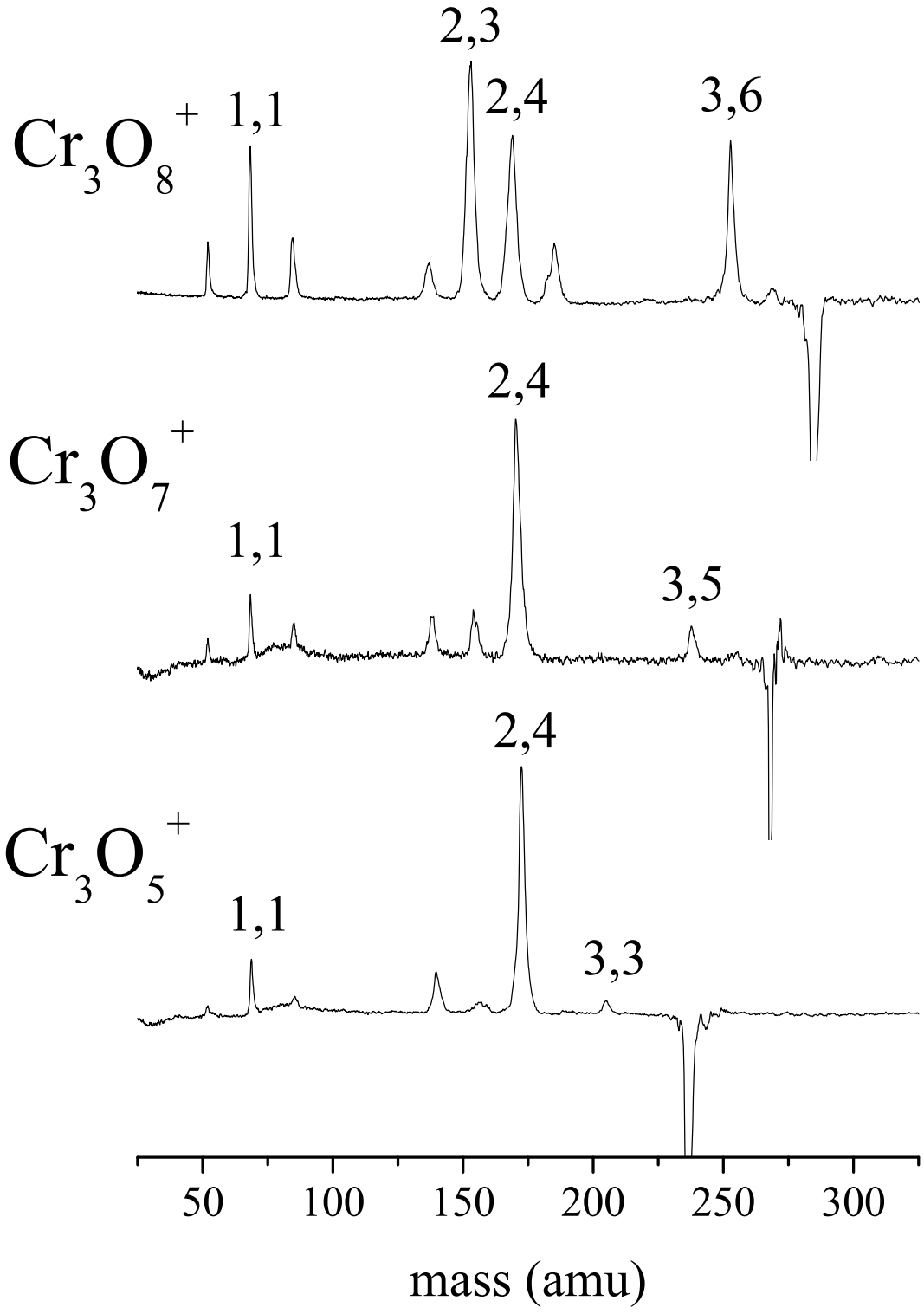

Figure 4.2: Photodissociation mass spectra of $Cr_3O_m^+$ clusters at 355 nm.

todissociation mass spectra of $Cr_3O_m^+$ clusters at 355 nm. also appear in the fragmentation spectrum. However, it is not possible to exclude intermediates that are not detected. These might not appear in the mass spectrum if they have rapid decomposition rates compared to the instrument acceleration timescale (1-2 μsec). Laser power or wavelength studies can sometime reveal the nature of these dissociation mechanisms. However, we find that the dissociation channels seen here are independent of the dissociation laser wavelength (532 vs. 355 nm) or laser power (over the range of 1-10 mJ/cm^2 pulse). It therefore remains impossible to distinguish between the possible concerted and sequential processes that might occur here, and this same problem is found throughout this study for all the different cluster sizes. This uncertainty makes it difficult to draw detailed conclusions from the fragmentation spectrum for any one individual cluster. However, as shown in our previous work,[23,49,57] comparing the dissociation spectra for many different cluster sizes makes it possible to detect *patterns* of behavior that do provide new insights. From this point onward, we discuss each cluster size and mention only those dissociation routes that appear to be common to more than one cluster system.

With these considerations in mind, we can identify three patterns in the $Cr_3O_m^+$ data. The ions 1,1 and 2,4 appear in essentially all of these spectra, and are therefore suggested to be relatively stable cation clusters. The elimination of [O_2] is determined to occur for the n = 3 group, via neutral mass differences. Finally, the elimination of the neutral [1,3] unit also seems to be important. This is the neutral difference between the strong 2,4 peak and the 3,7 parent. Likewise, if [1,3] is lost from the 3,6 intermediate in the 3,8 spectrum this would explain the appearance of the 2,3 fragment. The only other time the 2,3 fragment appears in the $Cr_3O_m^+$ data is also by elimination of [1,3] from 3,6 when this species is selected directly as a parent ion (data not shown).

The $Cr_4O_m^+$ clusters exhibit similar behavior, as shown in Figure 4.3 and Table 4.1. The fragmentation of $Cr_4O_{10}^+$ in this figure has a much better signal to noise level than other clusters which is attributed to considerably larger signals in the mass spectrum compared

to the other clusters. As shown in the figure, the 2,4 fragment ion is the most intense one in the 4,9 and 4,10 fragmentation spectra. This fragment ion also appears prominently in all the n = 4 spectra, as does the small ion 1,1. We also see the neutral loss of [O_2] for some of these clusters. Likewise, the neutral loss of [CrO_3] is also common throughout these data. This could explains the sequence of 4,9 → 3,6 → 2,3 as well as the sequence of 4,10 → 3,7 → 2,4. It is interesting to note that each parent ion produces a different $Cr_3O_m^+$ fragment. Both parents prefer the elimination of [1,3] which produces the corresponding $Cr_3O_m^+$ fragments. Apparently, the [1,3] loss is more important that the cation stability. However the $Cr_4O_8^+$ parent (data not shown) does not produce a $Cr_3O_m^+$ fragment at all, demonstrating that this argument only applies for $Cr_3O_m^+$ fragments above a certain size.

The $Cr_5O_m^+$ clusters (m=12,13), shown in Figure 4.4, exhibit some of the same patterns seen in the small cluster, except there is no evidence for [O_2] loss. The 2,4 species is again by far the most intense fragment ion observed. The smaller 1,1 species is also seen. The loss of neutral [1,3] is also apparent through this data. As shown in the figure, this could explain the sequence of 5,12 → 4,9 → 3,6 → 2,3 as well as the sequence of 5,13 → 4,10 → 3,7 → 2,4. Again we see that the prominent 3,m and 4,m fragment ions vary according to the parent ion. As shown in the figure, we only see the fragments 3,6 and 4,9 versus 3,7 and 4,10 when they fall in a sequence of [1,3] losses from the parent. The [1,3] leaving group appears to take precedence over the formation of preferred cation fragments in this size range. While the 2,4 ion is seen where if could be formed via a loss of [1,3], it is also seen when the elimination of [1,3] is not possible, indicating its intrinsic stability as a cation.

The fragmentation of the $Cr_6O_m^+$ clusters (m=14,16) is shown in Figure 4.5. As in all the data seen before, the 2,4 fragment ion is among the most prominent. As in the $Cr_5O_m^+$ data, there are 3,7 and 4,10 as well as 3,6 and 4,9 fragments found together from different parents; in both cases the [1,3] difference is apparent. Surprisingly, there are no $Cr_5O_m^+$ fragments detected at all; the fragments closest to the parent ion in mass are the n=4 species. This is interesting because the closest fragment ion, $Cr_4O_9^+$, to the parent ion, $Cr_6O_{14}^+$ occurs by

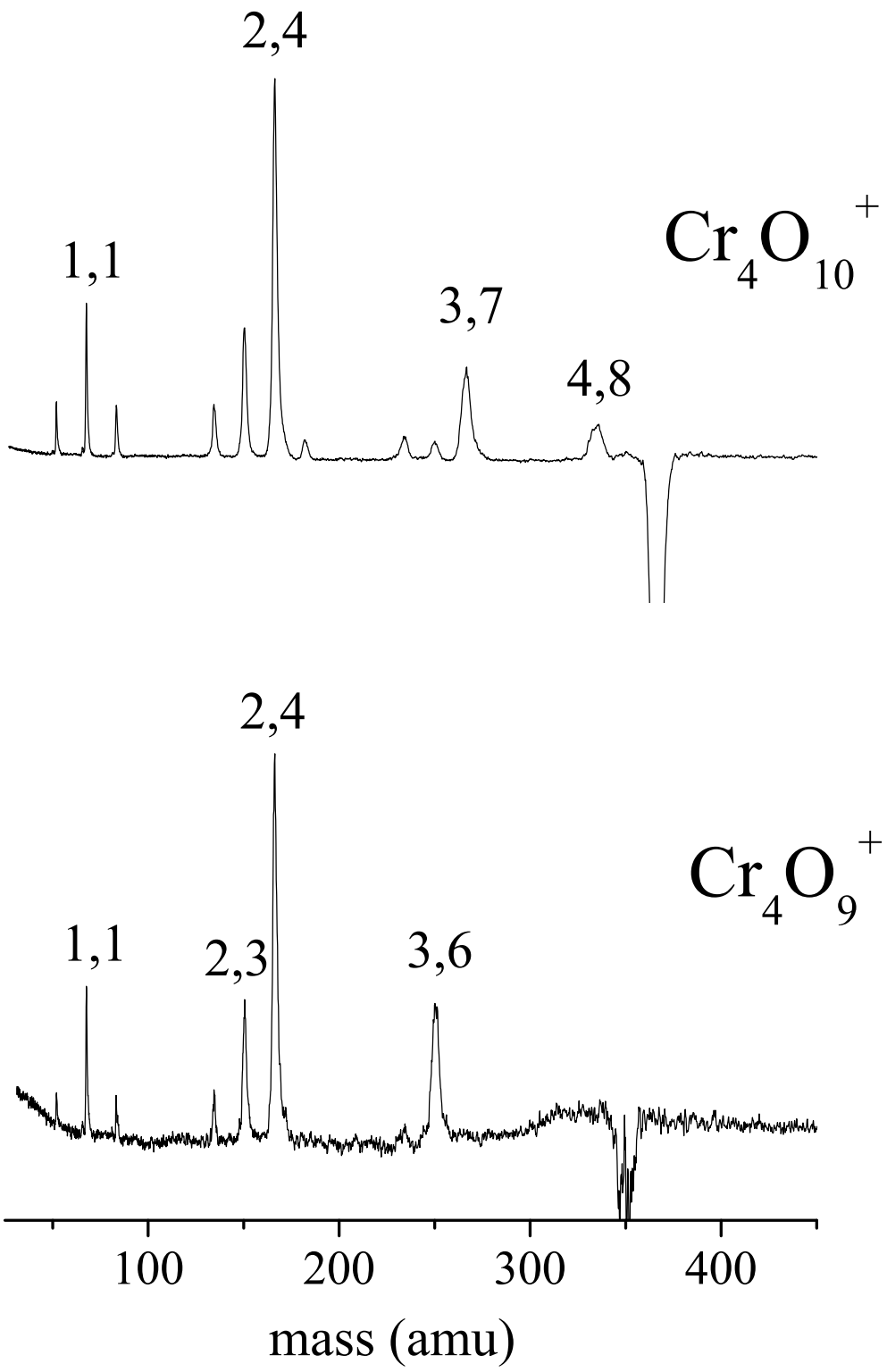

Figure 4.3: Photodissociation mass spectra of $Cr_4O_m^+$ clusters at 355 nm.

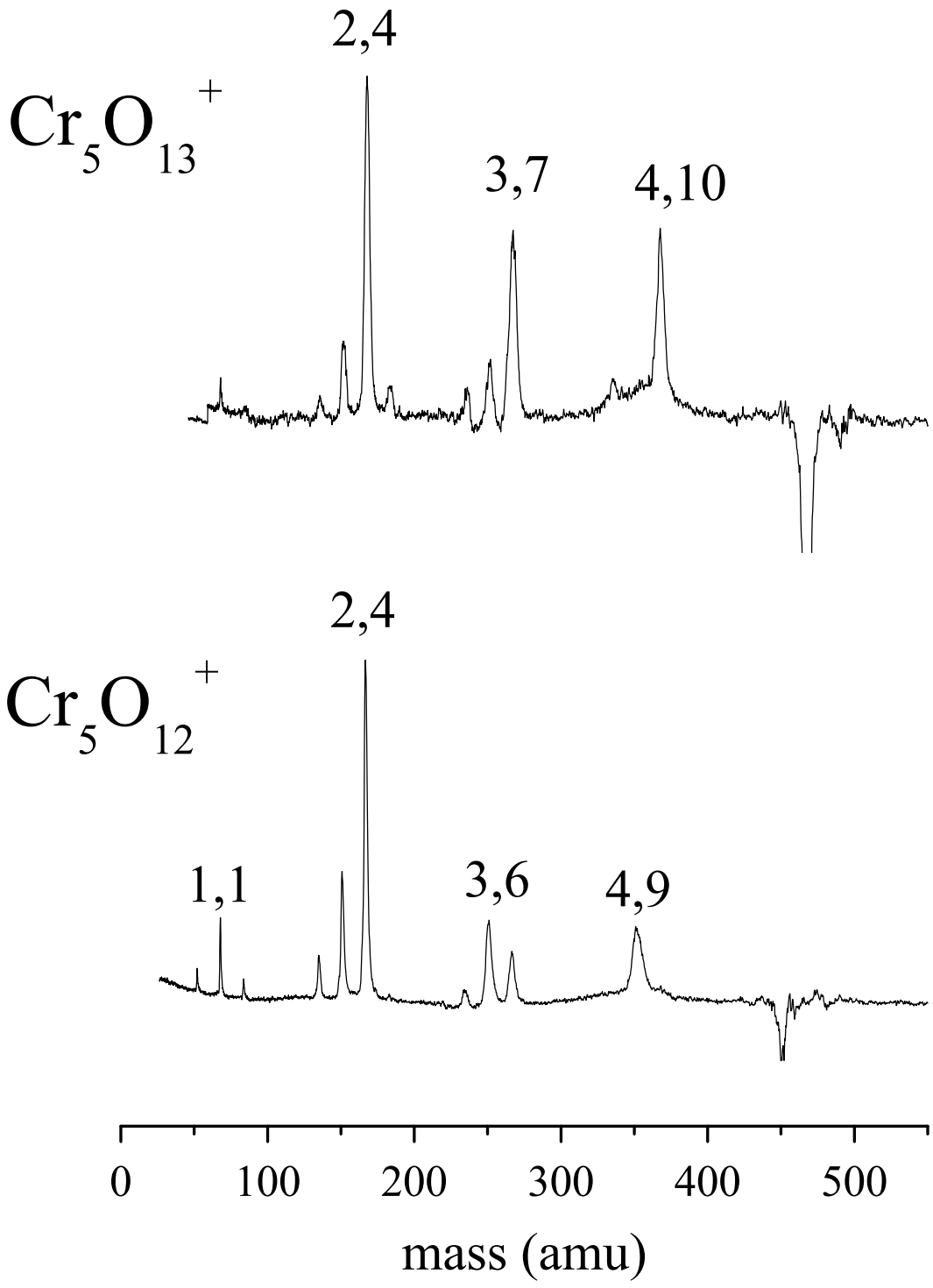

Figure 4.4: Photodissociation mass spectra of $Cr_5O_m^+$ clusters at 355 nm.

neutral loss of [2,5]. This is the first evidence for the [2,5] as a possible neutral leaving group, but, as shown later, it also occurs in some of the larger cluster fragmentation channels. The interval between the $Cr_6O_{16}^+$ parent and its highest mass fragment ion, $Cr_4O_{10}^+$ is [2,6], which could of course represent two units of [1,3]. Again, the 4,10 species, which was so prominent in the original cluster distribution grown from the source, is particularly abundant here as a fragment.

Figure 4.6 shows the fragmentation of the $Cr_7O_{16}^+$, $Cr_7O_{17}^+$ and $Cr_7O_{18}^+$ clusters. As in the data before, the 2,4 cluster is prominent among the low-mass fragments, as are 3,6 and 3,7. Like the n=6 family of clusters, neither the 7,17 or 7,18 parents produce fragments in the n=5 or 6 range. The 7,16 parent has several fragments in this range, including 6,13 and 5,11. These fragments represent the familiar neutral leaving groups [1,3] and [2,5], respectively, from the 7,16 parent ion. In contrast to previously mentioned groups where the 4,10 was a prominent fragment ion, the only n=7 species where the 4,10 is observed as a fragment ion is in the decomposition of the 7,18 species. Rather, we find the first evidence for the *neutral* loss of [4,10] species. The dissociation of 7,16 directly to the 3,6 fragment could occur via the direct elimination of [4,10]. However, it could also involve the elimination of two units of [2,5] via the sequence 7,16 → 5,11 → 3,6. Additionally, the 3,7 fragment ion could also be produced via the loss of [4,10] from the 7,17 parent ion. In the 7,18 fragmentation, the 4,10 cation could come from the elimination of a [3,8] unit, or more likely from the sequential loss of [1,3] and [2,5].

The fragmentation patterns of the n=8 group of clusters, shown in Figure 4.7, are all similar, with no formation of any n=5,6,7 fragment ions. The highest mass fragments detected are the $Cr_4O_{10}^+$ and $Cr_4O_9^+$ species, which represent about half the mass of each of these parents. It is plausible to imagine a fission process occurring where these clusters are split into two roughly equal pieces. The highest mass fragmentation from the $Cr_8O_{19}^+$ is the $Cr_4O_9^+$ fragment, which is consistent with this idea of fission. The 4,9 fragment, from the 8,19, could also be formed by the elimination of a single [Cr_4O_{10}] or by sequential elimination of

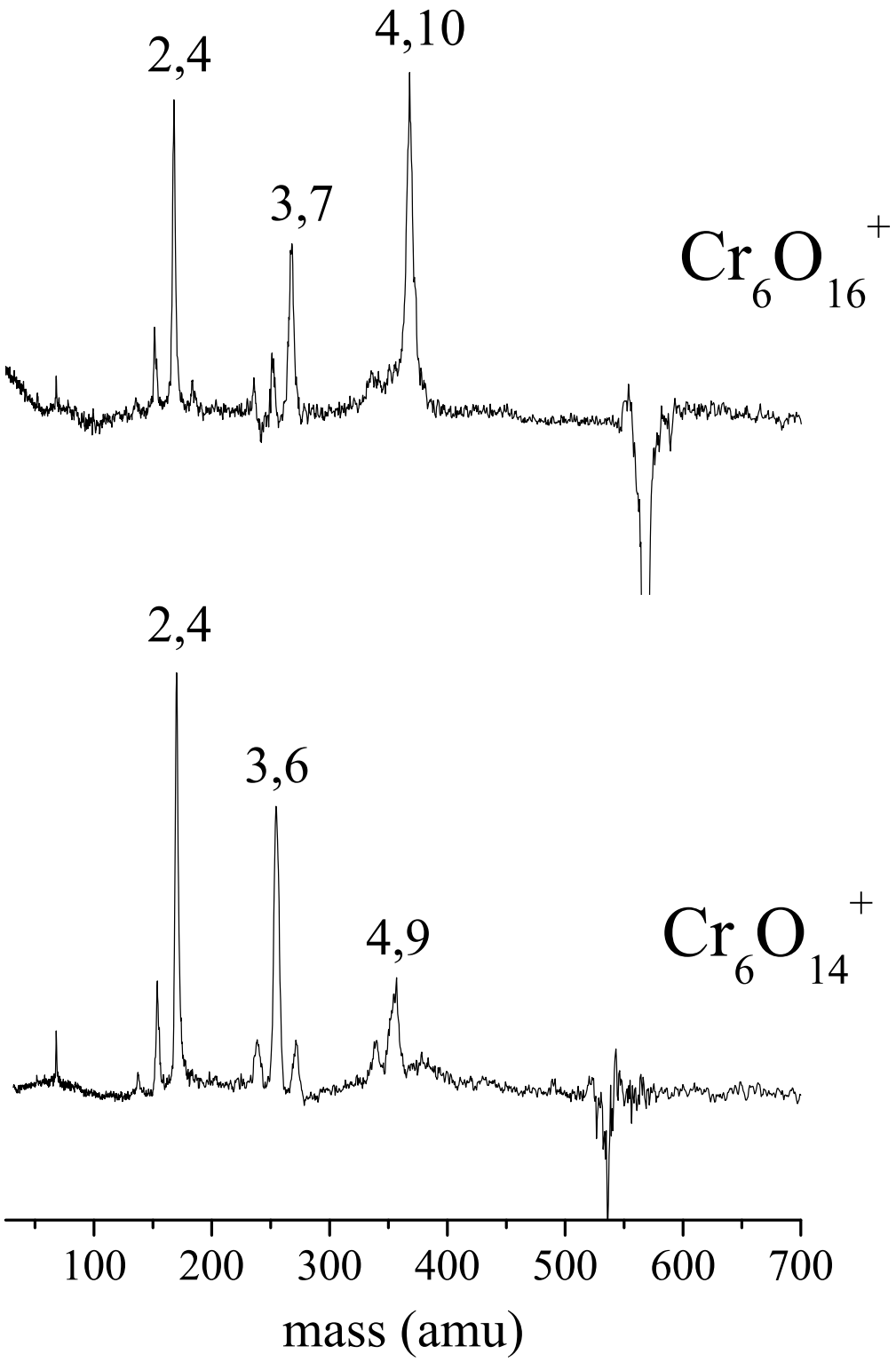

Figure 4.5: Photodissociation mass spectra of $Cr_6O_m^+$ clusters at 355 nm.

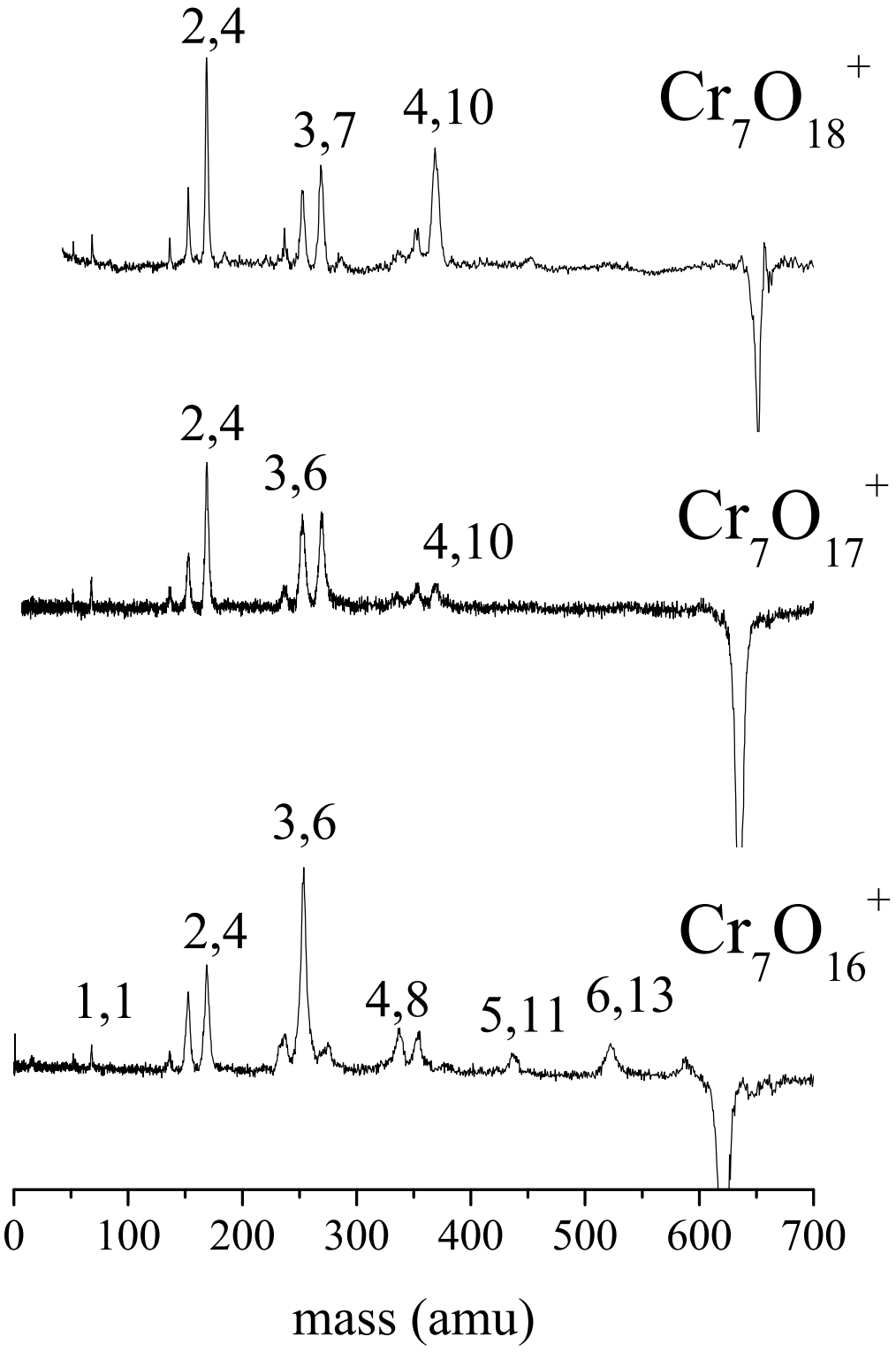

Figure 4.6: Photodissociation mass spectra of $Cr_7O_m^+$ clusters at 355 nm.

two units of [2,5]. However, the lack of intermediate fragment masses indicates that direct elimination of neutral [4,10] does occur. We see this same process occur where the 8,20 parent fragments to 4,10, although the 4,9 fragment is also a prominent fragment ion in this case. The fragmentation of the 8,21 parent does not exhibit the loss of [4,10] rather the 4,10 is the most prominent fragment ion seen. There is no simple loss of neutrals seen previously that can explain the formation of the 4,10 fragment ion. This data, and those discussed previously, indicates that both the 4,9 and 4,10 species are relatively stable as cation. Like the n = 7 data, there also suggest that the 4,10 species is a stable neutral leaving group. Selected examples of data for the $Cr_nO_m^+$ (n=9-12) cluster species are shown in Figures 4.8-4.10. These data continue to show many of the same patterns seen already, and can be summarized together. The fragment ions in the small mass range for all of these continue to be the same species seen already (2,4; 3,6 and 3,7; 4,9 and 4,10). In some cases, such as the fragmentation of the 9,24; 10,26 and 12,29 parents, the 4,9 and 4,10 fragment ions are particularly abundant. However, as the size of the parent ion increases, new cation fragments begin to be observed in the higher mass range.

It is understandable that larger pieces would remain when the fragmentation begins at larger clusters, but the specific sizes of these fragments continue to be interesting. In essentially every system, there is a large gap between the parent ion and the nearest high mass fragment ion seen. Moreover, the gap often corresponds to the loss of the [4,10] species. This occurs in the formation of 5,11 from 9,21; 5,12 from 9,22; 6,15 from 10,25; 7,17 from 11,27; and 8,19 from 12,29. In each of these systems, the lower masses that are also seen in these fragmentation patterns more often than not differ from the highest mass fragment by the intervals of [1,3] or [2,5] seen before. In the fragmentation of the 9,21 parent, the highest mass fragment is 5,11, and the next in decreasing mass is 4,8. This 4,8 species is not prominent in other fragmentation patterns, but it differs from 5,11 by the [1,3] interval. Another interesting case is the strong production of 4,9 from the 12,29 parent. This difference corresponds to *two* units of [4,10] neutral loss. It is clear that these common trends of the

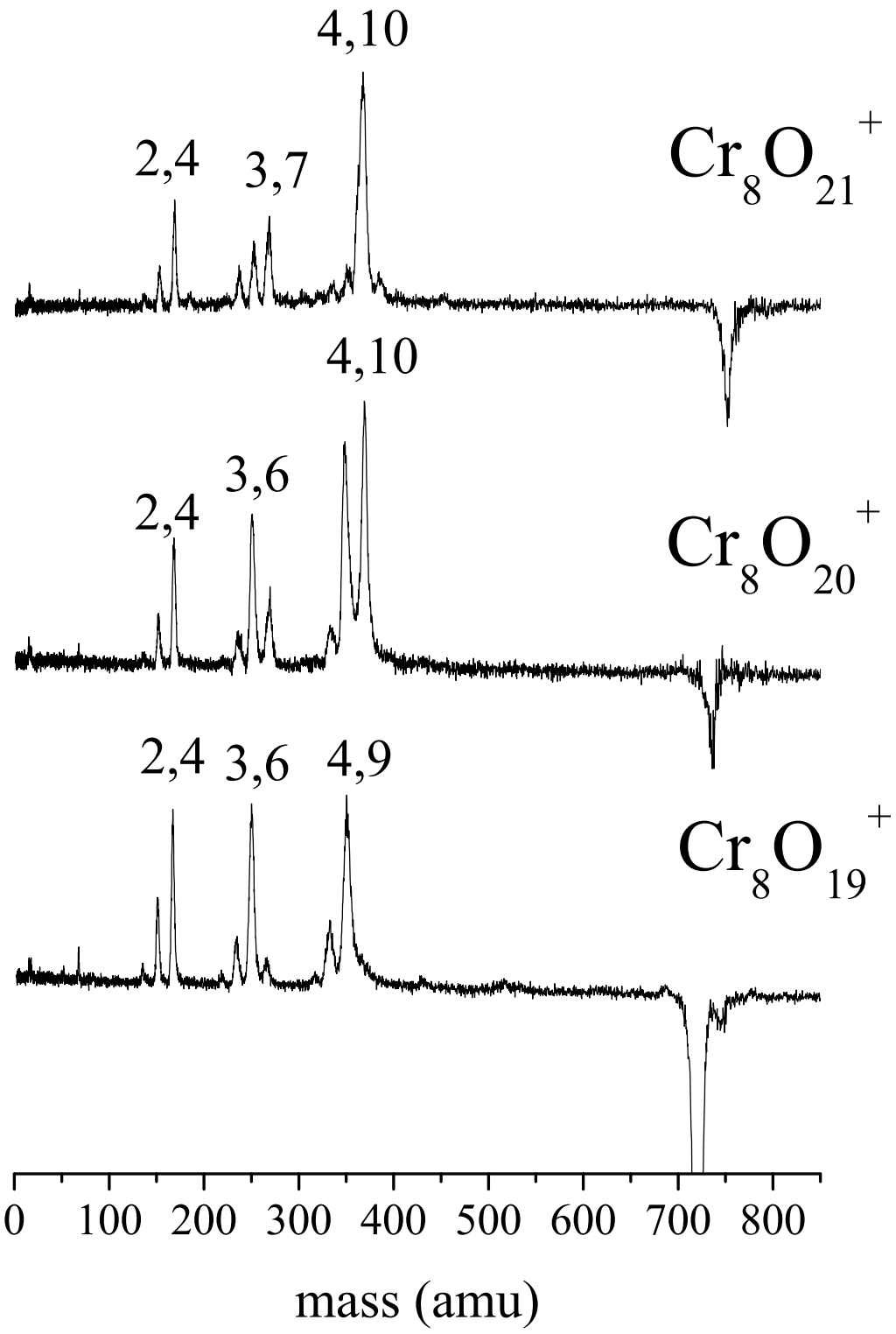

Figure 4.7: Photodissociation mass spectra of $Cr_8O_m^+$ clusters at 355 nm.

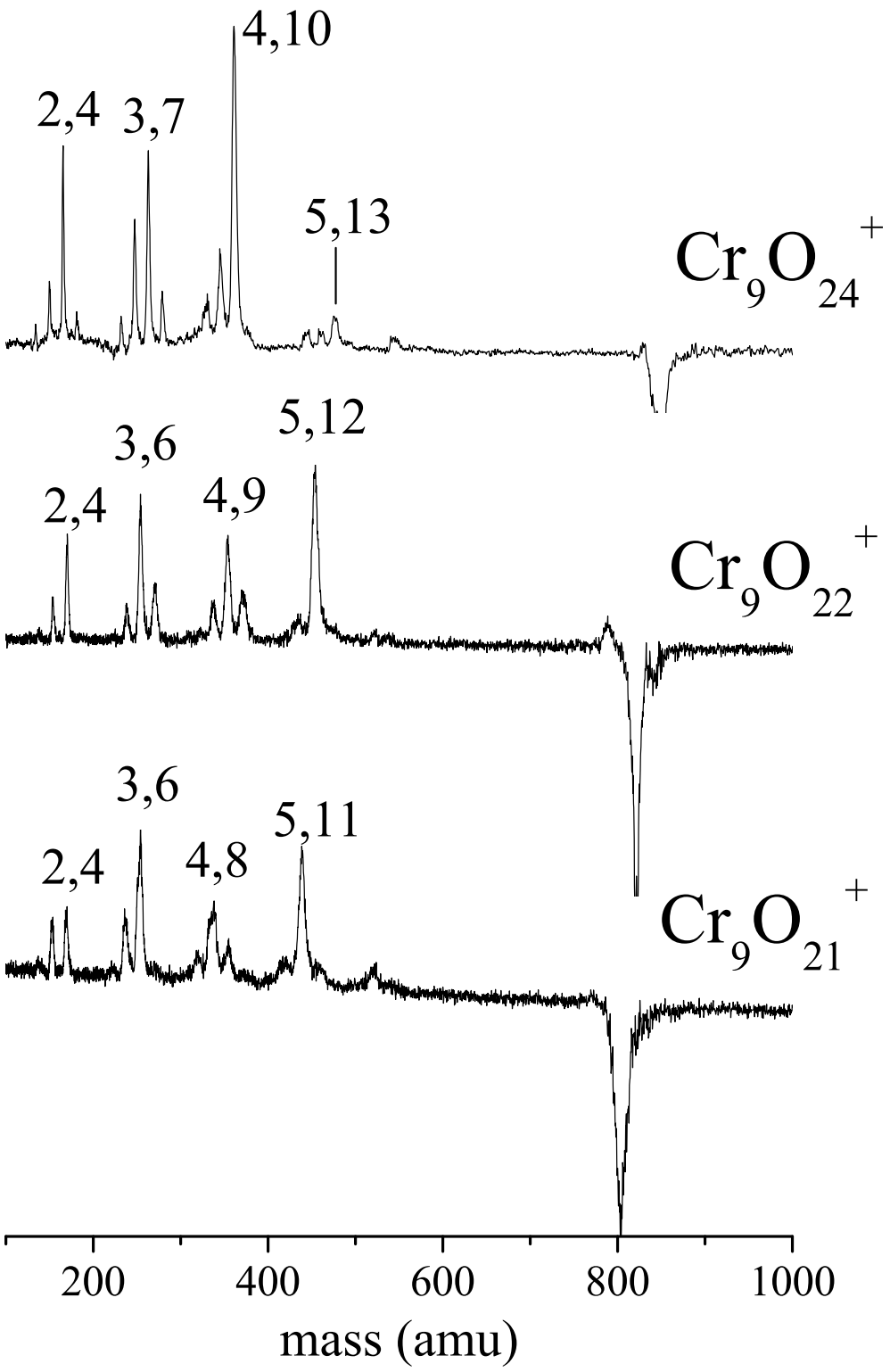

Figure 4.8: Photodissociation mass spectra of $Cr_9O_m^+$ clusters at 355 nm.

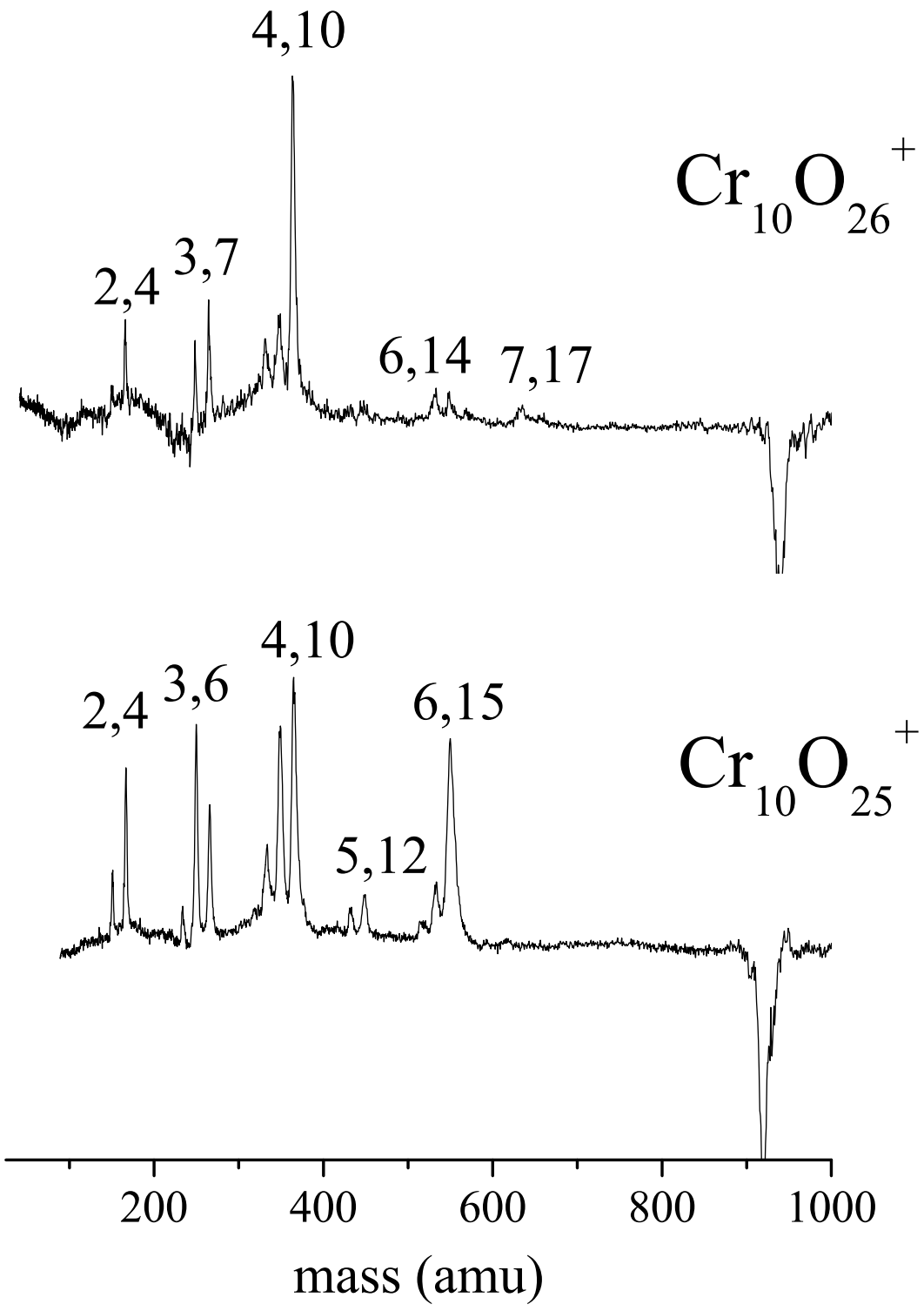

Figure 4.9: Photodissociation mass spectra of $Cr_{10}O_m^+$ clusters at 355 nm.

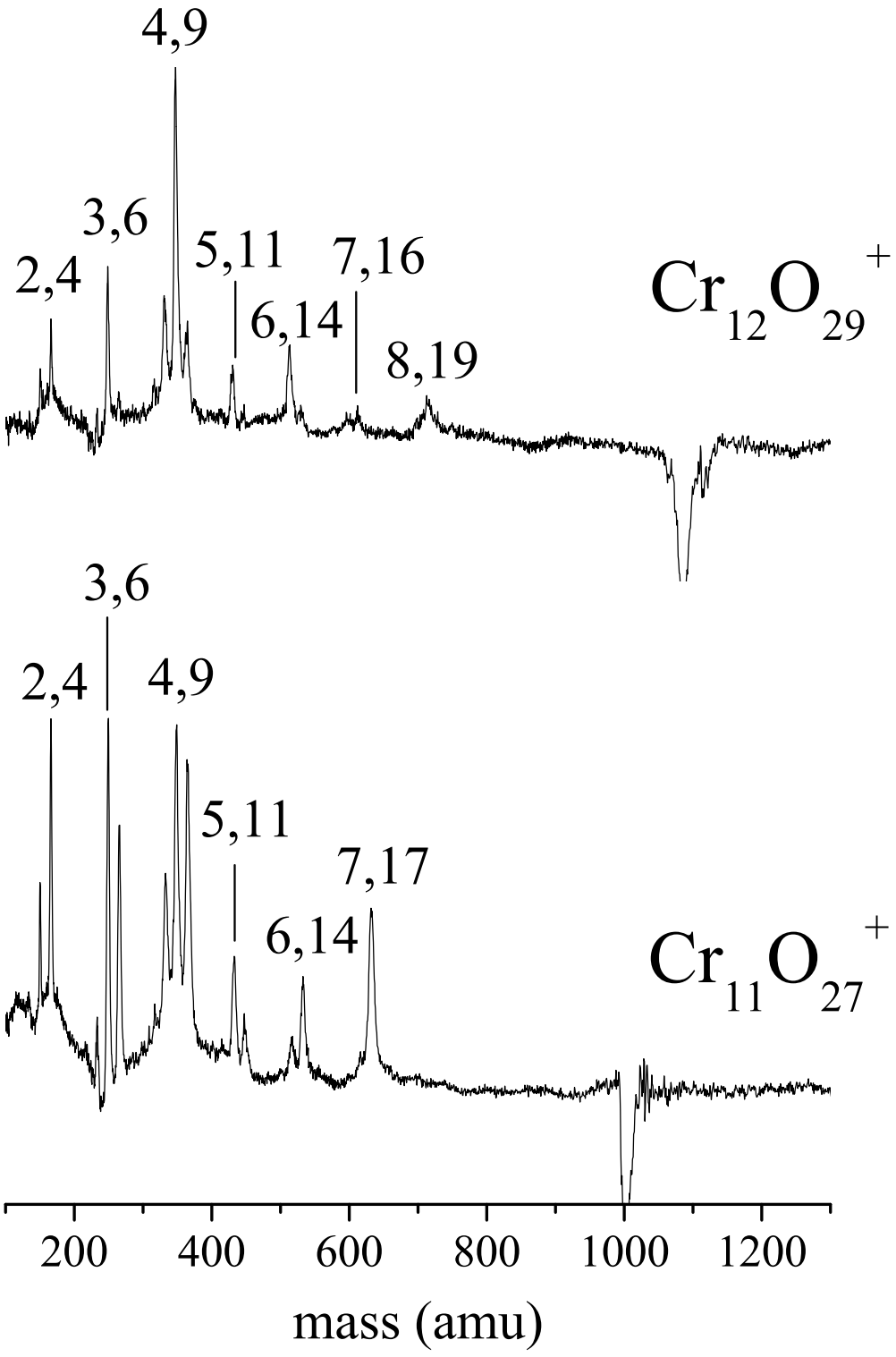

Figure 4.10: Photodissociation mass spectra of $Cr_{11}O_{27}^{+}$ and $Cr_{12}O_{29}^{+}$ clusters at 355 nm.

loss of particular neutral intervals pervade this data. There are no large *cation* species in the size range above n=4 that are produced repeatedly enough to firmly identify them as especially stable.

It is evident from the data presented here that the cation stoichiometries 1,1; 2,4; 3,6; 3,7; 4,9 and 4,10, as well as the neutral stoichiometries 1,3; 2,5 and 4,10 occur repeatedly throughout these fragmentation processes. As in our previous work, we interpret the production of such species from a variety of parent ions and from different dissociation laser conditions (wavelength, power) to indicate the intrinsic relative stability of these clusters. Also consistent with this, some of these same stoichiometries are apparent as abundant species in the distribution of clusters which grew initially from the cluster source (e.g., 4,10). The special cluster neutrals and ions here can be compared to those found earlier for the vanadium group of oxide clusters produced and studied in this same way.[23] For the vanadium, niobium, and tantalum oxides, we found the stable cation stoichiometries to be 1,2; 2,4; 3,7; 4,9; 5,12; 6,14; and 7,17. The neutral species suggested by mass conservation were 1,2 and 2,5. As indicated, many of the stoichiometries seen for the vanadium group of cluster oxides are seen again here. The stable cations and neutral seen here can be contrasted with our recent results for iron oxide clusters, where 1:1 stoichiometries were seen throughout the data, i.e., species such as 3,3; 4,4; 5,5.[65] Thus, the oxide clusters of chromium resemble those of the vanadium group more than they do the oxides of iron.

To investigate the reasons for the stability of the specific ions and neutrals identified here, Zach Reed, in our group, has performed DFT calculations to explore the structures and binding energies for these clusters. The most commonly used functional, B3LYP was employed for these calculations. The B3PW91 functional was also explored. A recent study by Dixon and coworkers showed that the former functional has problems for small chromium oxide clusters, while the latter provide energetic data judged to be more reliable.[66] The stable ions $Cr_2O_4^+$, $Cr_3O_6^+$, $Cr_3O_7^+$, and $Cr_4O_{10}^+$ and the stable neutrals CrO_3, Cr_2O_5 and Cr_4O_{10} were investigated. Figure 4.11 shows the schematic structures determined for these species,

while the specific details of these structures are presented in the Supporting Information for the published paper.[67] For each of these stable ions and neutrals, the corresponding neutrals and ions, respectively, have been investigated the to explore the role of charge in the relative stability. The energetics for these species are summarized in Table 4.2.

As shown in Figure 4.11, the structures for all of these oxides involve alternating metal-oxygen-metal networks. This is expected because the structures of the corresponding bulk oxide solids have similar connectivity. Additionally, to balance the greater effective positive charge on the metal, there are so-called terminal oxygen atoms on most of the chromium atoms. Only in the case of the $Cr_2O_4^+$ species is there evidence of metal-metal bonding. As expected, the bond energies for these species are substantial. Table 4.2 shows that each of these clusters has average per-bond energies in the range of 80-150 kcal/mol (3.5-6.5 eV). DFT is perhaps not the best method with which to calculate exact bond energies and the numbers obtained for each cluster vary noticeably with the functional employed. Likewise, the spin of the ground state is different for several of these clusters with the two functionals. Therefore, these bond energetics must be viewed as rough estimates, but it is clear that these systems have strong bonding stability. The relative numbers for these bond energies are also informative when charged versus neutral species are considered. In the case of CrO_3, the neutral which is seen as a leaving group does indeed have a much greater binding energy than its corresponding ion. The neutral has a closed shell singlet ground state with one of the common bulk stoichiometries and the +6 oxidation state for the metal atom. Because it is closed shell, it is not surprising that this neutral is more stable than its corresponding cation. Most of the larger clusters are also somewhat more stable as neutrals than they are as ions. The only possible exception to this is the $Cr_2O_4^+$, which has a slightly greater bonding energy as a cation when the B3PW91 functional is employed. As noted above, the 2,4 cation could conceivably take on a structure with the metals in two different oxidation states, having two terminal oxygen atoms connected to one chromium atom, one bridging, and one terminal oxygen on the other chromium atom. However, although we investigated

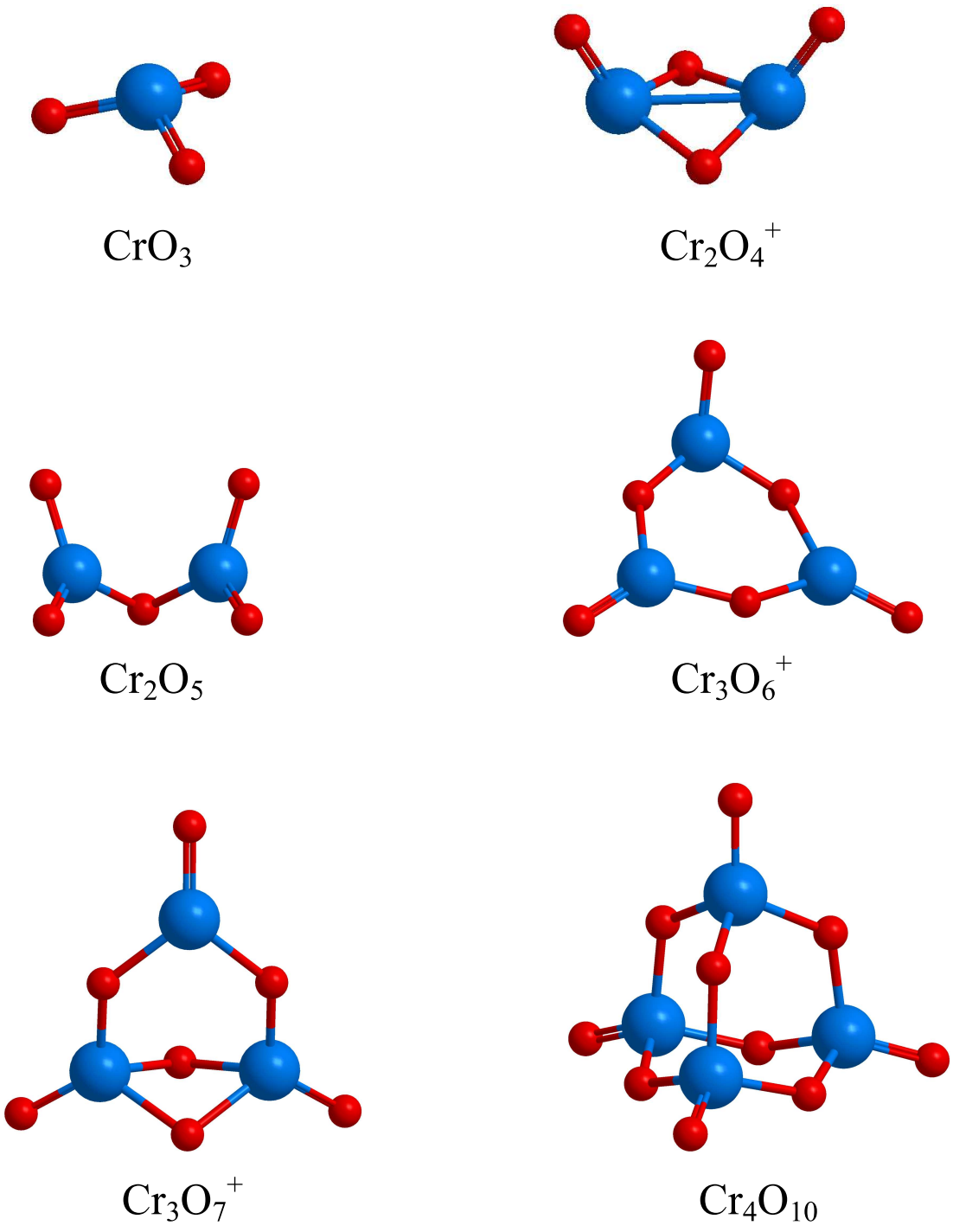

Figure 4.11: Proposed structures of the neutral leaving groups of Cr_nO_m and a few cation clusters, $Cr_nO_m^+$. All of these have been calculated with density-functional theory.

Table 4.2: The energetics for the $Cr_nO_m^{+/0}$ clusters studied here. All units are kcal/mol.

	Atomization energy B3LYP	Atomization energy B3PW91	Energy per bond B3LYP	Energy per bond B3PW91	Spin Multiplicity
CrO_3	455.2	453.1	75.9	75.5	1
CrO_3^+	404.8	314.4	67.5	55.7	2
Cr_2O_4	663.2	652.6	82.9	81.6	1
$Cr_2O_4^+$	613.9	658.9	68.2	73.2	2
Cr_2O_5	813.9	807.6	81.4	80.8	1
$Cr_2O_5^+$	747.2	724.8	74.7	72.5	2
Cr_3O_6	1114.1	1098.8	92.8	91.6	5
$Cr_3O_6^+$	1064.4	1047.9	88.8	87.3	6
Cr_3O_7	1266	1255	90.4	89.6	5
$Cr_3O_7^+$	1174.1	1163.4	83.9	83.1	6
Cr_4O_{10}	1805.3	1805.3	90.3	90.3	1[a]
$Cr_4O_{10}^+$	1591.1	1738.2	79.6	86.9	4

structures such as these, they were not found to be stable minima. Extensive searching and investigation of many other structures led to the species shown here. These are all relatively symmetric structures, in which the metal atoms almost always occupy equivalent sites and thus have the same oxidation states. These effective oxidation state are either +4 or +5 in all the larger clusters. In the case of the 4,10 neutral, which was studied previously with theory, the structure found here is quite close to that reported previously by Castleman, Jena and coworkers.[22k] In all of these systems, the neutral and ion with the same stoichiometry have essentially the same structures, differing only because of slight changes in bond distances and angles. This is presumably because these structures already maximize the number of strong metal-oxygen bonds.

The structures shown here demonstrate that the stable clusters grown for chromium oxides and eliminated by fragmentation represent compact symmetric structures. However, based on our calculated bonding energetics, it is difficult to understand why the experimental data suggests that these species are more stable than other clusters in the same size range. As noted above, essentially all the neutral species are more stable than their corresponding cations, even though only a few of these neutrals are found to be common leaving groups. The 1,3 cluster is understandable, because there is such a larger binding preference for this neutral. However, the larger clusters have somewhat similar energetics for ions versus neutrals and for clusters with similar sizes. For example, we can compare the per-bond energy of $Cr_2O_4^+$, which is prominent throughout these systems with the $Cr_2O_5^+$ ion, which is never detected as a major photofragment from any larger clusters. Surprisingly, the 2,5 ion has a greater per-bond binding energy than the 2,4 species. The 2,4 species has a symmetric compact structure, but the 2,5 cluster, which is more like an open chain, apparently has greater bonding stability. The 3,6 and 3,7 species are both found in the experiment, but the calculations indicate that the 3,6 species should be a good deal more stable per-bond. Therefore, although the experimental trends for cluster stability are quite clear from our dissociation patterns, the computed energetics for these clusters do not provide much insight

to support these trends. This puzzling situation may simply result from the poor energetics provided by DFT treatments. Unfortunately, while higher level treatments could in principle provide better energetics, such computations on the larger clusters here present significant theoretical challenges.

The oxide stoichiometries presented here can be compared to the known bulk-phase chromium oxides. In addition, the oxidation states implied here can be compared to those known for chromium in its various compounds. In the case of the vanadium group oxide clusters, all the prominent stoichiometries could be rationalized in terms of the well-known +4 and +5 oxidation states of those metals. The most common oxidation states of chromium[3] are respectively +3, +6 and +2. Illustrating this, the most common oxide of chromium in the bulk is Cr(III) oxide, Cr_2O_3, which has the corundum structure.[1–3] Cr(IV) oxide (CrO_2) has a rutile structure and is ferromagnetic, whereas Cr(VI) oxide (CrO_3), commonly known as chromic anhydride, is one of the most powerful oxidizers used in organic chemistry.[1–3] The +6 oxidation state for chromium is also found in its well-known chromate (CrO_4^{2-}) and dichromate ($Cr_2O_7^{2-}$) ions.[3] Castleman and co-workers also noted that the +6 oxidation state was favored in the formation of anion clusters, where the stoichiometry pattern Cr_nO_{3n} was observed.[21] In the clusters seen here, there is strong evidence again for the importance of the +6 oxidation state, as seen in the CrO_3 neutral leaving group eliminated from many of the clusters here. However, there is no obvious tendency for chromium to take on the +3 or +2 oxidation states. We see no evidence for neutral Cr_2O_3 or CrO elimination in our data. The most prominent larger clusters here are those with stoichiometries like $Cr_2O_4^+$, $Cr_3O_7^+$ and $Cr_4O_{10}^{+/0}$. These clusters appear to have an intermediate oxidation state in the +4/+5 range. Oxidation states of +4 or +5 are possible for chromium, but much less common. Another possibility for these systems is that they have mixed valence character. For example, the $Cr_2O_4^+$ ion could be rationalized to have one Cr in the +3 state and the other in the +6 state, however the theory does not support this idea. Likewise, the $Cr_3O_7^+$ species could conceivably have two +6 metal atoms and one in the +3 state. In pure metal clusters,

oxidation states are not usually discussed because charge can be highly delocalized. However, in these metal oxide clusters, localized bonding and charges are possible and have been investigated in the previous mentioned calculations. Overall, it is apparent that the most abundant stoichiometries seen here for chromium are more like those of vanadium oxides than they are like those of iron oxides, in direct contradiction to the trends known for oxidation states in the usual compounds of these elements.

4.5 Conclusions

Chromium oxide cluster cations produced by laser vaporization have been investigated with time-of-flight mass spectrometry and mass-selected photodissociation. A limited number of oxide stoichiometries are observed at each cluster size with a specific number of metal atoms. The $Cr_4O_{10}^+$ has especially large abundance in the cluster distribution produced by the source. Photodissociation of these clusters is only possible via multiphoton excitation, consistent with strong metal oxide bonding. Dissociation produces a number of cation clusters repeatedly from many different parent ions, including CrO^+, $Cr_2O_4^+$, $Cr_3O_6^+$, $Cr_3O_7^+$ and $Cr_4O_{10}^+$, and these clusters are concluded to be significantly more stable than others in the same size region. Likewise, the neutral clusters CrO_3, Cr_2O_5 and Cr_4O_{10} are observed repeatedly as leaving groups from a variety of parent cluster ions, and these are concluded to be stable neutrals. The strong stability of the 4,10 cluster as both a neutral and an ion may be in part attributed to the high symmetry of its structure. The cluster stoichiometries seen here resemble those seen previously for the vanadium group oxide clusters and are quite different from those seen for iron oxides. The oxidation states implied by these data are most often +4 and +5 for the chromium, which are not common in its solid oxide materials.

Density functional theory computations on these clusters derive structures that are appealing with alternating metal-oxygen-metal networks that lead to strong bonding stability. However, the detailed comparison of the per-bond energetics for different cluster sizes

does not provide as clear and compelling a picture of the most stable clusters as the experiment does. Future theoretical investigations of these systems would be useful. Because of their high intrinsic stability, these systems might be candidates for isolation as nanocluster materials.

Supporting Information

The Supporting Information for this chapter with the full details for the density functional calculations on the clusters studied here can be found in the paper.[67]

4.6 References

[1] Cox, P. A., *Transition Metal Oxides*, Clarendon Press, Oxford, 1992.

[2] Rao, C. N.; Raveau, B. *Transition Metal Oxides*, John Wiley, New York, 1998.

[3] Cotton, F. A.; Wilkinson, G.; Murillo, C. A.; Bochmann, M., *Advanced Inorganic Chemistry*, 6th edition, John Wiley & Sons, New York, 1999.

[4] Hayashi, C.; Uyeda, R.; Tasaki, A., *Ultra-Fine Particles*; Noyes, Westwood, 1997.

[5] Henrich, V. E.; Cox, P. A., *The Surface Science of Metal Oxides*; Cambridge University Press, Cambridge, 1994.

[6] Somorjai, G. A., *Introduction to Surface Chemistry and Catalysis*; Wiley-Interscience, New York, 1994.

[7] Gates, B. C., "Supported Metal-Clusters - Synthesis, Structure, and Catalysis," *Chem. Rev.* **1995**, *95*, 511.

[8] a) Rainer, D. R.; Goodman, D. W., "Metal clusters on ultrathin oxide films: model catalysts for surface science studies," *J. Mol. Catal. A: Chem.* **1998**, *131*, 259. b) St. Clair, T. P.; Goodman, D. W., "Metal nanoclusters supported on metal oxide thin films: bridging the materials gap," *Top. Catal.* **2000**, *13*, 5. c) Wallace, W. T.; Min, B. K.; Goodman, D. W., "The nucleation, growth, and stability of oxide-supported metal clusters," *Top. Catal.* **2005**, *34*, 17. d) Chen, M. S.; Goodman, D. W., "Catalytically active gold: From nanoparticles to ultrathin films," *Acc. Chem. Res.* **2006**, *39*, 739.

[9] a) Wachs, I. E.; Briand, L. E.; Jehng, J. M.; Burcham, L.; Gao, X. T., "Molecular structure and reactivity of the group V metal oxides," *Catal. Today* **2000**, *57*, 323. b) Chen, Y. S.; Wachs, I. E. "Tantalum oxide-supported metal oxide (Re2O7, CrO3, MoO3, WO3, V2O5, and Nb2O5) catalysts: synthesis, Raman characterization and chemically probed by methanol oxidation," *J. Catal.* **2003**, *217*, 468. c) Wachs, I. E., "Recent

conceptual advances in the catalysis science of mixed metal oxide catalytic materials," *Catal. Today* **2005**, *100*, 79. d) Wachs, I. E.; Jehng, J. M.; Ueda, W., "Determination of the chemical nature of active surface sites present on bulk mixed metal oxide catalysts," *J. Phys. Chem. B* **2005**, *109*, 2275. e) Tian, H. J.; Ross, E. I.; Wachs, I. E., "Quantitative determination of the speciation of surface vanadium oxides and their catalytic activity," *J. Phys. Chem. B* **2006**, *110*, 9593.

[10] Pope, M. T.; Mller, A., *Poloyoxometalate Chemistry From Topology via Self-Assembly to Applications*, Kluwer, Boston, 2001.

[11] Crans, D. C.; Smee, J. J.; Gaidamauskas, E.; Yang, L. Q., "The chemistry and biochemistry of vanadium and the biological activities exerted by vanadium compounds," *Chem. Rev.* **2004**, *104*, 849.

[12] a) Rockenberger, J.; Scher, E. C.; Alivisatos, A. P., "A new nonhydrolytic single-precursor approach to surfactant-capped nanocrystals of transition metal oxides," *J. Am. Chem. Soc.* **1999**, *121*, 11595. b) Puntes, V. F.; Krishnan, K. M.; Alivisatos, A. P., "Colloidal nanocrystal shape and size control: The case of cobalt," *Science* **2001**, *291*, 2115. c) Nolting, F.; Luning, J.; Rockenberger, J.; Hu, J.; Alivisatos, A. P., "A PEEM study of small agglomerates of colloidal iron oxide nanocrystals," *Surf. Rev. Lett.* **2002**, *9*, 437. d) Jun, Y. W.; Casula, M. F.; Sim, J. H.; Kim, S. Y.; Cheon, J.; Alivisatos, A. P., "Surfactant-assisted elimination of a high energy facet as a means of controlling the shapes of TiO2 nanocrystals," *J. Am. Chem. Soc.* **2003**, *125*, 15981. e) Casula, M. F.; Jun, Y. W.; Zaziski, D. J.; Chan, E. M.; Corrias, A.; Alivisatos, A. P., "The concept of delayed nucleation in nanocrystal growth demonstrated for the case of iron oxide nanodisks," *J. Am. Chem. Soc.* **2006**, *128*, 1675.

[13] Ayers, T. M.; Fye, J. L.; Li, Q.; Duncan, M. A., "Synthesis and isolation of titanium metal cluster complexes and ligand-coated nanoparticles with a laser vaporization flow-tube reactor," *J. Cluster Sci.* **2003**, *14*, 97.

[14] Roesky, H. W.; Haiduc, I.; Hosmane, N. S., "Organometallic oxides of main group and transition elements downsizing inorganic solids to small molecular fragments," *Chem. Rev.* **2003**, 103, 2579.

[15] Cushing, B. L.; Kolesnichenko, V. L.; O'Connor, C. J., "Recent advances in the liquid-phase syntheses of inorganic nanoparticles," *Chem. Rev.* **2004**, *104*, 3893.

[16] Kang, E.; Park, J.; Hwang, Y.; Kang, M.; Park, J. G.; Hyeon, T., "Direct synthesis of highly crystalline and monodisperse manganese ferrite nanocrystals," *J. Phys. Chem. B* **2004**, *108*, 13932.

[17] Fernandez-Garcia, M.; Martinez-Arias, A.; Hanson, J. C.; Rodriguez, J. A., "Nanostructured oxides in chemistry: Characterization and properties," *Chem. Rev.* **2004**, *104*, 4063.

[18] a) Berkowitz, J.; Chupka, W. A.; Inghram, M. G., "Thermodynamics of the V-O System - Dissociation Energies of Vo and Vo2," *J. Chem. Phys.* **1957**, 27, 87. b) Inghram, M. G.; Chupka, W. A.; Berkowitz, J., "Thermodynamics of the Ta-O System - Dissociation Energies of Tao and Tao2," *J. Chem. Phys.* **1957**, 27, 569.

[19] Farber, M.; Uy, O. M.; Srivastava, R. D., "Effusion-mass spectrometric determination of the heats of formation of the gaseous molecules V4O10, V4O8, VO2, and VO," *J. Chem. Phys.* **1972**, 56, 512.

[20] Bennett, S. L.; Lin, S. S.; Gilles, P. W., "High-Temperature Vaporization of Ternary-Systems .1. Mass-Spectrometry of Oxygen-Rich Vanadium-Tungsten-Oxygen Species," *J. Phys. Chem.* **1974**, 78, 266.

[21] a) Kooi, S. E.; Castleman, A. W., "Photofragmentation of vanadium oxide cations," *J. Phys. Chem. A* **1999**, 103, 5671. b) Bell, R. C.; Zemski, K. A.; Justes, D. R.; Castleman, A. W., "Formation, structure and bond dissociation thresholds of gas-phase vanadium oxide cluster ions," *J. Chem. Phys.* **2001**, *114*, 798.

[22] a) Deng, H. T.; Kerns, K. P.; Castleman, A. W., "Formation, structures, and reactivities of niobium oxide cluster ions," *J. Phys. Chem.* **1996**, *100*, 13386. b) Bell, R. C.; Zemski, K. A.; Kerns, K. P.; Deng, H. T.; Castleman, A. W., "Reactivities and collision-induced dissociation of vanadium oxide cluster cations," *J. Phys. Chem.* A **1998**, *102*, 1733. c) Bell, R. C.; Zemski, K. A.; Castleman, A. W., "Size-specific reactivities of vanadium oxide cluster cations," *J. Cluster Sci.* **1999**, *10*, 509. d) Zemski, K. A.; Bell, R. C.; Castleman, A. W., "Reactivities of tantalum oxide cluster cations with unsaturated hydrocarbons," *Int. J. Mass. Spectrom.* **1999**, *184*, 119. e) Zemski, K. A.; Bell, R. C.; Castleman, A. W., "Reactions of tantalum oxide cluster cations with 1-butene, 1,3-butadiene, and benzene," *J. Phys. Chem.* A **2000**, *104*, 7408. f) Zemski, K. A.; Justes, D. R.; Bell, R. C.; Castleman, A. W., "Reactions of niobium and tantalum oxide cluster cations and anions with n-butane," *J. Phys. Chem.* A **2001**, *105*, 4410. g) Zemski, K. A.; Justes, D. R.; Castleman, A. W., "Reactions of group V transition metal oxide cluster ions with ethane and ethylene," *J. Phys. Chem. A* **2001**, *105*, 10237. h) Zemski, K. A.; Justes, D. R.; Castleman, A. W., "Studies of metal oxide clusters: Elucidating reactive sites responsible for the activity of transition metal oxide catalysts," *J. Phys. Chem. B* **2002**, *106*, 6136. i) Justes, D. R.; Mitric, R.; Moore, N. A.; Bonacic-Koutecky, V.; Castleman, A. W., "Theoretical and experimental consideration of the reactions between VxOy+ and ethylene," *J. Am. Chem. Soc.* **2003**, *125*, 6289. j) Justes, D. R.; Moore, N. A.; Castleman, A. W., "Reactions of vanadium and niobium oxides with methanol," *J. Phys. Chem. B* **2004**, *108*, 3855. k) Bergeron, D. E.; Castleman, A. W.; Jones, N. O.; Khanna, S. N., "Stable Cluster Motifs for Nanoscale Chromium Oxide Materials," *Nano. Lett.* **2004**, *4*, 261. l) Kimble, M. L.; Castleman, A. W., "Gas-phase studies of AunOm+ interacting with carbon monoxide," *Int. J. Mass. Spectrom.* **2004**, *233*, 99. m) Sun, Q.; Rao, B. K.; Jena, P.; Stolcic, D.; Kim, Y. D.; Gantefor, G.; Castleman, A. W., "Appearance of bulk properties in small tungsten oxide clusters," *J. Chem. Phys.* **2004**, *121*, 9417. n) Kimble, M. L.; Castleman, A. W.; Burgel, C.; Bonacic-Koutecky,

V., "Interactions of CO with AunOm- (n ¿= 4)," *Int. J. Mass. Spectrom.* **2006**, *254*, 163. o) Kimble, M. L.; Moore, N. A.; Johnson, G. E.; Castleman, A. W.; Burgel, C.; Mitric, R.; Bonacic-Koutecky, V., "Joint experimental and theoretical investigations of the reactivity of Au2On- and Au3On- (n=1-5) with carbon monoxide," *J. Chem. Phys.* **2006**, *125*. p) Moore, N. A.; Mitric, R.; Justes, D. R.; Bonacic-Koutecky, V.; Castleman, A. W., "Kinetic Analysis of the Reaction between (V2O5)n=1,2+ and Ethylene," *J. Phys. Chem. B* **2006**, *110*, 3015. q) Reilly, N. M., Reveles, J. U., Johnson, G. E., Khanna, S. N., Castleman, A.W., "Influence of charge state on the reaction of FeO3 with carbon monoxide," *Chem. Phys. Lett.* **2007**, *435*, 295.

[23] a) France, M. R.; Buchanan, J. W.; Robinson, J. C.; Pullins, S. H.; Tucker, J. L.; King, R. B.; Duncan, M. A., "Antimony and Bismuth Oxide Clusters: Growth and Decomposition of New Magic Number Clusters," *J. Phys. Chem. A* **1997**, *101*, 6214. b) Molek, K. S.; Jaeger, T. D.; Duncan, M. A., "Photodissociation of vanadium, niobium, and tantalum oxide cluster cations," *J. Chem. Phys.* **2005**, *123*.

[24] a) Foltin, M.; Stueber, G. J.; Bernstein, E. R., "On the growth dynamics of neutral vanadium oxide and titanium oxide clusters," *J. Chem. Phys.* **1999**, *111*, 9577. b) Foltin, M.; Stueber, G. J.; Bernstein, E. R., "Investigation of the structure, stability, and ionization dynamics of zirconium oxide clusters," *J. Chem. Phys.* **2001**, *114*, 8971. c) Shin, D. N.; Matsuda, Y.; Bernstein, E. R., "On the iron oxide neutral cluster distribution in the gas phase. I. Detection through 193 nm multiphoton ionization," *J. Chem. Phys.* **2004**, *120*, 4150. d) Shin, D. N.; Matsuda, Y.; Bernstein, E. R., "On the iron oxide neutral cluster distribution in the gas phase. II. Detection through 118 nm single photon ionization," *J. Chem. Phys.* **2004**, *120*, 4157. e) Matsuda, Y.; Shin, D. N.; Bernstein, E. R., "On the zirconium oxide neutral cluster distribution in the gas phase: Detection through 118 nm single photon, and 193 and 355 nm multiphoton, ionization," *J. Chem. Phys.* **2004**, *120*, 4142. f) Matsuda, Y.; Shin, D. N.; Bernstein, E. R., "On the copper oxide neutral cluster distribution in the gas phase: Detection through 355 nm and 193 nm multiphoton and

118 nm single photon ionization," *J. Chem. Phys.* **2004**, *120*, 4165. g) Matsuda, Y.; Bernstein, E. R., "On the titanium oxide neutral cluster distribution in the gas phase: Detection through 118 nm single-photon and 193 nm multiphoton ionization," *J. Phys. Chem. A* **2005**, *109*, 314. h) Matsuda, Y.; Bernstein, E. R., "Identification, structure, and spectroscopy of neutral vanadium oxide clusters," *J. Phys. Chem. A* **2005**, *109*, 3803. i) Dong, F.; Heinbuch, S.; He, S. G.; Xie, Y.; Rocca, J. J.; Bernstein, E. R., "Formation and distribution of neutral vanadium, niobium, and tantalum oxide clusters: Single photon ionization at 26.5 eV," *J. Chem. Phys.* **2006**, *125*, 164318.

[25] a) Harvey, J. N.; Diefenbach, M.; Schroder, D.; Schwarz, H., "Oxidation properties of the early transition-metal dioxide cations MO2+ (M = Ti, V, Zr, Nb) in the gas-phase," *Int. J. Mass. Spectrom.* **1999**, *183*, 85. b) Schrder, D.; Schwarz, H.; Shaik, S., "Characterization, orbital description, and reactivity patterns of transition-metal oxo species in the gas phase," *Struct. Bonding* **2000**, *97*, 91. c) Schrder, D.; Jackson, P.; Schwarz, H., "Dissociation patterns of small FemOn+ (m=1-4, n ¡= 6) cluster cations formed upon chemical ionization of Fe(CO)(5)/O-2 mixtures," *Eur. J. Inorg. Chem.* **2000**, 1171. d) Jackson, P.; Fisher, K. J.; Willett, G. D., "The catalytic activation of primary alcohols on niobium oxide surfaces unraveled: the gas phase reactions of NbxOy- clusters with methanol and ethanol," *Chem. Phys.* **2000**, *262*, 179. e) Jackson, P.; Harvey, J. N.; Schrder, D.; Schwarz, H., "Structure and reactivity of the prototype iron-oxide cluster Fe2O2+," *Int. J. Mass. Spectrom.* **2001**, *204*, 233. f) Schroder, D.; Engeser, M.; Schwarz, H.; Harvey, J. N., "Energetics of the ligated vanadium dications VO2+, VOH2+, and [V,O,H-2](2+)," *ChemPhysChem* **2002**, *3*, 584. g) Engeser, M.; Schlangen, M.; Schroder, D.; Schwarz, H.; Yumura, T.; Yoshizawa, K., "Alkane oxidation by VO2+ in the gas phase: A unique dependence of reactivity on the chain length," *Organometallics***2003**, *22*, 3933. h) Engeser, M.; Schroder, D.; Schwarz, H., "Gas-phase dehydrogenation of methanol with mononuclear vanadium-oxide cations," *Chemistry-a European Journal* **2005**, *11*, 5975. i) Koszinowski, K.; Schlangen, M.; Schroder, D.; Schwarz, H., "Forma-

tion, structure, and reactivity of gaseous Ni2O2+," *Eur. J. Inorg. Chem.* **2005**, 2464. j) Feyel, S.; Dobler, J.; Schroder, D.; Sauer, J.; Schwarz, H., "Thermal activation of methane by tetranuclear [V4O10](+)," *Angew. Chem. Int. Ed. Eng.* **2006**, *45*, 4681. k) Feyel, S.; Schroder, D.; Rozanska, X.; Sauer, J.; Schwarz, H., "Gas-phase oxidation of propane and 1-butene with [V3O7](+): Experiment and theory in concert," *Angew. Chem. Int. Ed. Eng.* **2006**, *45*, 4677. l) Feyel, S.; Schroder, D.; Schwarz, H., "Gas-phase oxidation of isomeric butenes and small alkanes by vanadium-oxide and -hydroxide cluster cations," *J. Phys. Chem. A* **2006**, *110*, 2647.

[26] Wang, X.; Neukermans, S.; Vanhoutte, F.; Janssens, E.; Verschoren, G.; Silverans, R. E.; Lievens, P., "Stability patterns and ionization potentials of CrnOm clusters (n=3-50, m=0, 1, 2)," *Appl. Phys. B: Lasers Opt.* **2001**, *73*, 417.

[27] Fielicke, A.; Rademann, K., "Stability and reactivity patterns of medium-sized vanadium oxide cluster cations VxOy+ (4 ¡= x ¡= 14)," *Phys. Chem. Chem. Phys.* **2002**, *4*, 2621.

[28] Aubriet, F.; Muller, J. F., "About the atypical behavior of CrO3, MoO3, and WO3 during their UV laser ablation/ionization," *J. Phys. Chem. A* **2002**, *106*, 6053.

[29] a) Griffin, J. B.; Armentrout, P. B., "Guided ion beam studies of the reactions of Fe-n(+) (n=2-18) with O-2: Iron cluster oxide and dioxide bond energies," *J. Chem. Phys.* **1997**, *106*, 4448. b) Xu, J.; Rodgers, M. T.; Griffin, J. B.; Armentrout, P. B., "Guided ion beam studies of the reactions of V-n(+) (n=2-17) with O-2: Bond energies and dissociation pathways," *J. Chem. Phys.* **1998**, *108*, 9339. c) Griffin, J. B.; Armentrout, P. B., "Guided ion beam studies of the reactions of Cr-n(+) (n=2-18) with O-2: Chromium cluster oxide and dioxide bond energies," *J. Chem. Phys.* **1998**, *108*, 8062. d) Vardhan, D.; Liyanage, R.; Armentrout, P. B., "Guided ion beam studies of the reactions of Ni-n(+) (n=2-18) with O-2: Nickel cluster oxide and dioxide bond energies," *J. Chem. Phys.* **2003**, *119*, 4166. e) Liu, F. Y.; Li, F. X.; Armentrout, P. B., "Guided ion-beam

studies of the reactions of Co-n(+) (n=2-20) with O-2: Cobalt cluster-oxide and -dioxide bond energies," *J. Chem. Phys.* **2005**, *123*.

[30] a) Chertihin, G. V.; Bare, W. D.; Andrews, L., "Reactions of laser-ablated chromium atoms with dioxygen. Infrared spectra of CrO, OCrO, CrOO, CrO3, Cr(OO)(2), Cr2O2, Cr2O3 and Cr2O4 in solid argon," *J. Chem. Phys.* **1997**, *107*, 2798. b) Zhou, M. F.; Andrews, L., "Infrared spectra and density functional calculations of the CrO2-, MoO2-, and WO2- molecular anions in solid neon," *J. Chem. Phys.* **1999**, *111*, 4230. c) Andrews, L.; Rohrbacher, A.; Laperle, C. M.; Continetti, R. E., "Laser desorption/ionization of transition metal atoms and oxides from solid argon," *J. Phys. Chem. A* **2000**, *104*, 8173.

[31] a) Fan, J. W.; Wang, L. S., "Photoelectron-Spectroscopy of FeO- and Fe)2- - Observation of Low-Spin Excited-States of FeO and Determination of the Electron-Affinity of FeO2," *J. Chem. Phys.* **1995**, *102*, 8714. b) Wang, L. S.; Wu, H. B.; Desai, S. R., "Sequential oxygen atom chemisorption on surfaces of small iron clusters," *Phys. Rev. Lett.* **1996**, *76*, 4853. c) Wu, H. B.; Desai, S. R.; Wang, L. S., "Observation and photoelectron spectroscopic study of novel mono- and diiron oxide molecules: FeOy- (y=1-4) and Fe2Oy- (y=1-5)," *J. Am. Chem. Soc.* **1996**, *118*, 7434. d) Wang, Q.; Sun, Q.; Sakurai, M.; Yu, J. Z.; Gu, B. L.; Sumiyama, K.; Kawazoe, Y., "Geometry and electronic structure of magic iron oxide clusters," *Phys. Rev. B* **1999**, *59*, 12672. e) Gutsev, G. L.; Rao, B. K.; Jena, P.; Li, X.; Wang, L.-S., "Experimental and theoretical study of the photoelectron spectra of MnOx-(x=1-3) clusters," *J. Chem. Phys.* **2000**, *113*, 1473. f) Sun, Q.; Sakurai, M.; Wang, Q.; Yu, J. Z.; Wang, G. H.; Sumiyama, K.; Kawazoe, Y. "Geometry and electronic structures of magic transition-metal oxide clusters M9O6 (M = Fe, Co, and Ni)," *Phys. Rev. B* **2000**, *62*, 8500. g) Gutsev, G. L.; Jena, P.; Zhai, H.-J.; Wang, L.-S., "Electronic structure of chromium oxides, CrOn- and CrOn (n = 1-5) from photoelectron spectroscopy and density functional theory calculations," *J. Chem. Phys.* **2001**, *115*, 7935. h) Zhai, H.-J.; Wang, L.-S., "Electronic structure and chemical

bonding of divanadium-oxide clusters (V2Ox, x=3-7) from anion photoelectron spectroscopy," *J. Chem. Phys.* **2002**, *117*, 7882. i) Gutsev, G. L.; Bauschlicher, C. W., Jr.; Zhai, H.-J.; Wang, L.-S., "Structural and electronic properties of iron monoxide clusters FenO and FenO- (n = 2-6): a combined photoelectron spectroscopy and density functional theory study," *J. Chem. Phys.* **2003**, *119*, 11135. j) Zhai, H.-J.; Kiran, B.; Cui, L.-F.; Li, X.; Dixon, D. A.; Wang, L.-S., "Electronic Structure and Chemical Bonding in MOn- and MOn Clusters (M = Mo, W; n = 3-5): A Photoelectron Spectroscopy and ab Initio Study," *J. Am. Chem. Soc.* **2004**, *126*, 16134. k) Yang, X.; Waters, T.; Wang, X.-B.; O'Hair, R. A. J.; Wedd, A. G.; Li, J.; Dixon, D. A.; Wang, L.-S., "Photoelectron Spectroscopy of Free Polyoxoanions Mo6O192- and W6O192- in the Gas Phase," *J. Phys. Chem. A* **2004**, *108*, 10089. l) Zhai, H. J.; Huang, X.; Waters, T.; Wang, X. B.; O'Hair, R. A. J.; Wedd, A. G.; Wang, L. S., "Photoelectron spectroscopy of doubly and singly charged group VIB dimetalate anions: M2O72-, MM ' O-7(2-), and M2O7- (M, M ' = Cr, Mo, W)," *J. Phys. Chem. A* **2005**, *109*, 10512. m) Zhai, H.-J.; Huang, X.; Cui, L.-F.; Li, X.; Li, J.; Wang, L.-S., "Electronic and Structural Evolution and Chemical Bonding in Ditungsten Oxide Clusters: W2On- and W2On (n = 1-6)," *J. Phys. Chem. A* **2005**, *109*, 6019. n) Huang, X.; Zhai, H. J.; Li, J.; Wang, L. S. "On the structure and chemical bonding of tri-tungsten oxide clusters W3On- and W3On (n=7-10): W3O8 as a potential molecular model for O-deficient defect sites in tungsten oxides," *J. Phys. Chem. A* **2006**, *110*, 85. o) Zhai, H. J.; Wang, L. S. "Probing the electronic properties of dichromium oxide clusters Cr2On- (n=1-7) using photoelectron spectroscopy," *J. Chem. Phys.* **2006**, *125*, 164315. p) Zhai, H. J.; Wang, L.-S., "Probing the Electronic Structure and Band Gap Evolution of Titanium Oxide Clusters (TiO2)n- (n = 1-10) Using Photoelectron Spectroscopy," *J. Am. Chem. Soc.* **2007**, *129*, 3022.

[32] a) Wenthold, P. G.; Jonas, K. L.; Lineberger, W. C., "Ultraviolet photoelectron spectroscopy of the chromium dioxide negative ion," *J. Chem. Phys.* **1997**, *106*, 9961. b) Ramond, T. M.; Davico, G. E.; Hellberg, F.; Svedberg, F.; Salen, P.; Soderqvist, P.;

Lineberger, W. C., "Photoelectron spectroscopy of nickel, palladium, and platinum oxide anions," *J. Mol. Spec.* **2002**, *216*, 1. c) Ichino, T.; Gianola, A. J.; Andrews, D. H.; Lineberger, W. C., "Photoelectron spectroscopy of AuO- and AuS-," *J. Phys. Chem. A* **2004**, *108*, 11307.

[33] a) Yang, D. S.; Hackett, P. A., "ZEKE spectroscopy of free transition metal clusters," *J. Elec. Spectros. Relat. Phenom.* **2000**, *106*, 153. b) Yang, D. S. "Photoelectron spectra of metal-containing molecules with resolutions better than 1 meV," Coord. *Chem. Rev.* **2001**, *214*, 187.

[34] Green, S. M. E.; Alex, S.; Fleischer, N. L.; Millam, E. L.; Marcy, T. P.; Leopold, D. G., "Negative ion photoelectron spectroscopy of the group 5 metal trimer monoxides V3O, Nb3O, and Ta3O," *J. Chem. Phys.* **2001**, *114*, 2653.

[35] a) Pramann, A.; Nakamura, Y.; Nakajima, A.; Kaya, K., "Photoelectron Spectroscopy of Yttrium Oxide Cluster Anions: Effects of Oxygen and Metal Atom Addition," *J. Phys. Chem. A* **2001**, *105*, 7534. b) Pramann, A.; Koyasu, K.; Nakajima, A.; Kaya, K., "Photoelectron spectroscopy of cobalt oxide cluster anions," *J. Phys. Chem. A* **2002**, *106*, 4891. c) Pramann, A.; Koyasu, K.; Nakajima, A.; Kaya, K., "Anion photoelectron spectroscopy of VnOm- (n=4-15; m=0-2)," *J. Chem. Phys.* **2002**, *116*, 6521.

[36] Yoder, B. L.; Maze, J. T.; Raghavachari, K.; Jarrold, C. C., "Structures of Mo2Oy- and Mo2Oy (y=2, 3, and 4) studied by anion photoelectron spectroscopy and density functional theory calculations," *J. Chem. Phys.* **2005**, *122*, 094313.

[37] a) von Helden, G.; Kirilyuk, A.; van Heijnsbergen, D.; Sartakov, B.; Duncan, M. A.; Meijer, G., "Infrared spectroscopy of gas-phase zirconium oxide clusters," *Chem. Phys.* **2000**, *262*, 31. b) van Heijnsbergen, D.; von Helden, G.; Meijer, G.; Duncan, M. A., "Infrared resonance-enhanced multiphoton ionization spectroscopy of magnesium oxide clusters," *J. Chem. Phys.* **2002**, *116*, 2400. c) van Heijnsbergen, D.; Demyk, K.; Duncan,

M. A.; Meijer, G.; von Helden, G., "Structure determination of gas phase aluminum oxide clusters," *Phys. Chem. Chem. Phys.* **2003**, 5, 2515.

[38] a) Fielicke, A.; Meijer, G.; von Helden, G., "Infrared spectroscopy of niobium oxide cluster cations in a molecular beam: Identifying the cluster structures," *J. Am. Chem. Soc.* **2003**, *125*, 3659. b) Fielicke, A.; Meijer, G.; von Helden, G., "Infrared multiple photon dissociation spectroscopy of transition metal oxide cluster cations - Comparison of group Vb (V, Nb, Ta) metal oxide clusters," *Eur. Phys. J. D* **2003**, *24*, 69. c) Fielicke, A.; Mitric, R.; Meijer, G.; Bonacic-Koutecky, V.; von Helden, G., "The structures of vanadium oxide cluster-ethene complexes. A combined IR multiple photon dissociation spectroscopy and DFT calculation study," *J. Am. Chem. Soc.* **2003**, *125*, 15716. d) Demyk, K.; van Heijnsbergen, D.; von Helden, G.; Meijer, G., "Experimental study of gas phase titanium and aluminum oxide clusters," *Astron. & Astrophys.* **2004**, *420*, 547.

[39] a) Asmis, K. R.; Bruemmer, M.; Kaposta, C.; Santambrogio, G.; von Helden, G.; Meijer, G.; Rademann, K.; Woeste, L., "Mass-selected infrared photodissociation spectroscopy of V4O10+," *Phys. Chem. Chem. Phys.* **2002**, *4*, 1101. b) Brummer, M.; Kaposta, C.; Santambrogio, G.; Asmis, K. R., "Formation and photodepletion of cluster ion-messenger atom complexes in a cold ion trap: Infrared spectroscopy of VO+, VO2+, and VO3+," *J. Chem. Phys.* **2003**, *119*, 12700. c) Asmis, K. R.; Meijer, G.; Bruemmer, M.; Kaposta, C.; Santambrogio, G.; Woeste, L.; Sauer, J., "Gas phase infrared spectroscopy of mono- and divanadium oxide cluster cations," *J. Chem. Phys.* **2004**, *120*, 6461. d) Asmis, K. R.; Santambrogio, G.; Brummer, M.; Sauer, J., "Polyhedral vanadium oxide cages: Infrared spectra of cluster anions and size-induced d electron localization," *Angew. Chem. Int. Ed. Eng.* **2005**, *44*, 3122. e) Janssens, E.; Santambrogio, G.; Brummer, M.; Woeste, L.; Lievens, P.; Sauer, J.; Meijer, G.; Asmis, K. R., "Isomorphous substitution in bimetallic oxide clusters," *Phys. Rev. Lett.* **2006**, *96*.

[40] a) Sambrano, J. R.; Andres, J.; Beltran, A.; Sensato, F.; Longo, E., "Theoretical study

of the structure and stability of NbxOy and NbxOy+ (x = 1-3; y = 2-5, 7, 8) clusters," *Chem. Phys. Lett.* **1998**, *287*, 620. b) Calatayud, M.; Silvi, B.; Andres, J.; Beltran, A., "A theoretical study on the structure, energetics and bonding of VOx+ and VOx (x=1-4) systems," *Chem. Phys. Lett.* **2001**, *333*, 493. c) Calatayud, M.; Andres, J.; Beltran, A., "A systematic density functional. theory study of VxOy+ and VxOY (X=2-4, Y=2-10) systems," *J. Phys. Chem. A* **2001**, *105*, 9760. d) Sambrano, J. R.; Gracia, L.; Andres, J.; Berski, S.; Beltran, A., "A theoretical study on the gas phase reactions of the anions NbO3-, NbO5-, and NbO2(0H)(2)(-) with H2O and O-2," *J. Phys. Chem. A* **2004**, *108*, 10850. e) Sambrano, J. R.; Andres, J.; Gracia, L.; Safont, V. S.; Beltran, A., "DFT study of the water-assisted tautomerization process between hydrated oxide, MO(H2O)(+), and dihydroxide, M(OH)(2)(+) cations (M = V, Nb and Ta)," *Chem. Phys. Lett.* **2004**, *384*, 56. f) Gracia, L.; Andres, J.; Safont, V. S.; Beltran, A., "DFT study of the reaction between VO2+ and C2H6," *Organometallics* **2004**, *23*, 730.

[41] a) Veliah, S.; Xiang, K. H.; Pandey, R.; Recio, J. M.; Newsam, J. M., "Density functional study of chromium oxide clusters: Structures, bonding, vibrations, and stability," *J. Phys. Chem. B* **1998**, *102*, 1126. b) Xiang, K. H.; Pandey, R.; Recio, J. M.; Francisco, E.; Newsam, J. M., "A theoretical study of the cluster vibrations in Cr2O2,Cr2O3, and Cr2O4," *J. Phys. Chem. A* **2000**, *104*, 990.

[42] a) Reddy, B. V.; Khanna, S. N., "Chemically induced oscillatory exchange coupling in chromium oxide clusters," *Phys. Rev. Lett.* **1999**, *83*, 3170. b) Morisato, T.; Jones, N. O.; Khanna, S. N.; Kawazoe, Y., "Stable aluminum and chromium oxide clusters as precursors to nanoscale materials," *Comp. Mater. Sci.* **2006**, *35*, 366.

[43] Chakrabarti, A.; Hermann, K.; Druzinic, R.; Witko, M.; Wagner, F.; Petersen, M., "Geometric and electronic structure of vanadium pentoxide: A density functional bulk and surface study," *Phys. Rev. B* **1999**, *59*, 10583.

[44] Zimmermann, R.; Steiner, P.; Claessen, R.; Reinert, F.; Hufner, S.; Blaha, P.; Dufek, P., "Electronic structure of 3d-transition-metal oxides: on-site Coulomb repulsion versus covalency," *J. Phys.: Condens. Matter* **1999**, *11*, 1657.

[45] a) Vyboishchikov, S. F.; Sauer, J., "Gas-phase vanadium oxide anions: Structure and detachment energies from density functional calculations," *J. Phys. Chem. A* **2000**, *104*, 10913. b) Vyboishchikov, S. F.; Sauer, J., "(V2O5)(n) gas-phase clusters (n=1-12) compared to V2O5 crystal: DFT calculations," *J. Phys. Chem. A* **2001**, *105*, 8588. c) Vyboishchikov, S. F., "Gas-phase reactions of V2O5+ and V2O6+ ions with CH3CF3 studied by density functional theory," J. Mol. Struc. Theochem. **2005**, *723*, 53.

[46] Albaret, T.; Finocchi, F.; Noguera, C., "Density functional study of stoichiometric and O-rich titanium oxygen clusters," *J. Chem. Phys.* **2000**, *113*, 2238.

[47] Gutsev, G. L.; Andrews, L.; Bauschlicher, C. W., "Similarities and differences in the structure of 3d-metal monocarbides and monoxides," *Theo. Chem. Accts.* **2003**, *109*, 298.

[48] a) Guo, B. C.; Kerns, K. P.; Castleman, A. W., "Ti8C12+-metallo-carbohedrenes: a new class of molecular clusters?," *Science* **1992**, *255*, 1411. b) Guo, B. C.; Wei, S.; Purnell, J.; Buzza, S.; Castleman, A. W., "Metallo-carbohedrenes [M8C12+ (M = vanadium, zirconium, hafnium, and titanium)]: a class of stable molecular cluster ions," *Science* **1992**, *256*, 515. c) Guo, B. C.; Castleman, A. W., "Metallo-carbohedrenes: a new class of molecular clusters," *Adv. Met. Semicond. Clusters* **1994**, *2*, 137. d) Cartier, S. F.; May, B. D.; Castleman, A. W., "Formation, Structure, and Stabilities of Metallocarbohedrenes," *J. Phys. Chem.* **1996**, *100*, 8175.

[49] a) Pilgrim, J. S.; Duncan, M. A., "Beyond metallo-carbohedrenes: growth and decomposition of metal-carbon nanocrystals," *J. Am. Chem. Soc.* **1993**, *115*, 9724. b) Pilgrim, J. S.; Duncan, M. A., "Metallo-carbohedrenes: chromium, iron, and molybdenum analogs,"

J. Am. Chem. Soc. **1993**, *115*, 6958. c) Duncan, M. A., "Synthesis and characterization of metal-carbide clusters in the gas phase," *J. Cluster Sci.* **1997**, *8*, 239.

[50] Rohmer, M.-M.; Benard, M.; Poblet, J.-M., "Structure, Reactivity, and Growth Pathways of Metallocarbohedrenes M8C12 and Transition Metal/Carbon Clusters and Nanocrystals: A Challenge to Computational Chemistry," *Chem. Rev.* **2000**, *100*, 495.

[51] a) van Heijnsbergen, D.; von Helden, G.; Duncan, M. A.; van Roij, A. J. A.; Meijer, G., "Vibrational spectroscopy of gas-phase metal-carbide clusters and nanocrystals," *Phys. Rev. Lett.* **1999**, *83*, 4983. b) von Helden, G.; van Heijnsbergen, D.; Meijer, G., "Resonant ionization using IR light: A new tool to study the spectroscopy and dynamics of gas-phase molecules and clusters," *J. Phys. Chem. A* **2003**, *107*, 1671.

[52] a) Gueorguiev, G. K.; Pacheco, J. M., "Structural identification of metcars," *Phys. Rev. Lett.* **2002**, *88*, 115504. b) Gueorguiev, G. K.; Pacheco, J. M. "Shapes of cagelike metal carbide clusters: First-principles calculations," *Phys. Rev. B* **2003**, *68*, 241401.

[53] a) Liu, P.; Rodriguez, J. A.; Hou, H.; Muckerman, J. T., "Chemical reactivity of metcar Ti8C12, nanocrystal Ti14C13 and a bulk TiC(001) surface: A density functional study," *J. Chem. Phys.* **2003**, *118*, 7737. b) Liu, P.; Rodriguez, J. A.; Muckerman, J. T., "The chemical activity of metal compound nanoparticles: Importance of electronic and steric effects in M8C12 (M=Ti, V, Mo) metcars," *J. Chem. Phys.* **2004**, *121*, 10321. c) Liu, P.; Lightstone, J. M.; Patterson, M. J.; Rodriguez, J. A.; Muckerman, J. T.; White, M. G., "Gas-phase interaction of thiophene with the Ti8C12+ and Ti8C12 met-car clusters," *J. Phys. Chem. B* **2006**, *110*, 7449.

[54] a) Varganov, S. A.; Gordon, M. S., "Effects of strong electron correlations in Ti8C12 Met-Car," *Chem. Phys.* **2006**, *326*, 97. b) Varganov, S. A.; Dudley, T. J.; Gordon, M. S. "Predicted IR spectra of Ti8C12 and Ti8C12+," *Chem. Phys. Lett.* **2006**, *429*, 49.

[55] *Clusters of Atoms and Molecules Vol. I*; Haberland, H., Ed., Springer, Berlin, 1995. *Clusters of Atoms and Molecules Vol. II*; Haberland, H., Ed., Springer, Berlin, 1995.

[56] Johnston, R. L., *Atomic and Molecular Clusters*; Taylor & Francis, London, 2002.

[57] a) Ticknor, B. W.; Duncan, M. A., "Photodissociation of size-selected silicon carbide cluster cations," *Chem. Phys. Lett.* **2005**, *405*, 214. b) Jaeger, J. B.; Jaeger, T. D.; Duncan, M. A., "Photodissociation of Metal-Silicon Clusters: Encapsulated versus Surface-Bound Metal," *J. Phys. Chem. A* **2006**, *110*, 9310.

[58] Gaussian 03, Revision B.02, M. J. Frisch, G. W. Trucks, H. B. Schlegel, G. E. Scuseria, M. A. Robb, J. R. Cheeseman, J. A. Montgomery, Jr., T. Vreven, K. N. Kudin, J. C. Burant, J. M. Millam, S. S. Iyengar, J. Tomasi, V. Barone, B. Mennucci, M. Cossi, G. Scalmani, N. Rega, G. A. Petersson, H. Nakatsuji, M. Hada, M. Ehara, K. Toyota, R. Fukuda, J. Hasegawa, M. Ishida, T. Nakajima, Y. Honda, O. Kitao, H. Nakai, M. Klene, X. Li, J. E. Knox, H. P. Hratchian, J. B. Cross, C. Adamo, J. Jaramillo, R. Gomperts, R. E. Stratmann, O. Yazyev, A. J. Austin, R. Cammi, C. Pomelli, J. W. Ochterski, P. Y. Ayala, K. Morokuma, G. A. Voth, P. Salvador, J. J. Dannenberg, V. G. Zakrzewski, S. Dapprich, A. D. Daniels, M. C. Strain, O. Farkas, D. K. Malick, A. D. Rabuck, K. Raghavachari, J. B. Foresman, J. V. Ortiz, Q. Cui, A. G. Baboul, S. Clifford, J. Cioslowski, B. B. Stefanov, G. Liu, A. Liashenko, P. Piskorz, I. Komaromi, R. L. Martin, D. J. Fox, T. Keith, M. A. Al-Laham, C. Y. Peng, A. Nanayakkara, M. Challacombe, P. M. W. Gill, B. Johnson, W. Chen, M. W. Wong, C. Gonzalez, and J. A. Pople, Gaussian, Inc., Pittsburgh PA, 2003.

[59] Becke, A. D. *J. Chem. Phys.* **1993**, *98*, 5648.

[60] Lee, C.; Yang, W.; Parr, R. G. *Phys. Rev. B* **1988**, *37*, 785.

[61] Perdew, J. R.; Chevary, J. A.; Vosko, S. H.; Jackson, K. A.; Pederson, M. R.; Singh, D. J.; Fiolhais, C. *Phys. Rev. B* **1992**, *46*, 6671.

[62] Dunning, T.H.; Hay, P. J. *Methods of Electronic Structure Theory*, Vol. 2, H. F. Schaefer, ed., Plenum Press, **1977**.

[63] a) Hay, P. J.; Wadt, W. R. *J. Chem. Phys.* **1985**, *82*, 270. b) Hay, P. J.; Wadt, W. R. *J. Chem. Phys.* **1985**, *82*, 284. c) Hay, P. J.; Wadt, W. R. *J. Chem. Phys.* **1985**, *82*, 299.

[64] Cornett, D. S.; Peschke, M.; LaiHing, K.; Cheng, P. Y.; Willey, K. F.; Duncan, M. A., "A reflectron time-of-flight mass spectrometer for laser photodissociation," *Rev. Sci. Instrum.* **1992**, *63*, 2177.

[65] Molek, K. S.; Anfuso, C.; Duncan, M. A., work in progress.

[66] D.A. Dixon, private communication.

[67] Molek, K. S.; Reed, Z. D.; Ricks, A.M.; Duncan, M.A. "Photodissociation of Chromium Oxide Cluster Cations," *J. Phys. Chem. A* **2007**, *submitted*.

Chapter 5

Photodissociation of Iron Oxide Cluster Cations[1]

[1]Molek, K. S.; Anfuso-Cleary, C.; Duncan, M.A. "Photodissociation of Iron Oxide Cluster Cations," *J. Phys. Chem. A* 2007, submitted. Reprinted here with permission of publisher.

5.1 Abstract

Iron oxide cluster cations, $Fe_nO_m^+$, are produced by laser vaporization in a pulsed nozzle cluster source and detected with time-of-flight mass spectrometry. The mass spectrum exhibits a limited number of stoichiometries for each value of n, where $m \geq n$. The cluster cations are mass selected and photodissociated using the second (532 nm) or third (355 nm) harmonic output of a Nd:YAG laser. At either wavelength, multiphoton absorption is required to dissociate these clusters, which is consistent with their expected strong bonding. Cluster dissociation occurs via elimination of molecular oxygen, or by fission processes producing stable cation species. For each metal increment, n where $n < 6$, oxygen elimination proceeds until a terminal stoichiometry is reached. Clusters with the terminal stoichiometry do not eliminate oxygen, but rather undergo fission, producing smaller $Fe_nO_m^+$ species. Specific *cation* clusters are identified to be stable because they are produced repeatedly in the decomposition of larger clusters. In general, stable larger clusters, n $\geq$6, are not identified by a terminal stoichiometry, but rather by their repeated production in the dissociation of larger clusters. These combined results determine that that the n=m species of the form $Fe_nO_m^+$, where n = 2-13, have the greatest stability.

5.2 Introduction

Transition metal oxides are important in applications such as electronics,[1–4] catalysis,[3–7] and magnetic materials.[1–4] Numerous studies have focused on the properties of the bulk materials as well as the nanoparticle and gas phase cluster oxides. Nanoparticle oxides have applications in areas such as magnetism, catalysis, and medicine.[4,9–21] Iron oxide is particularly interesting because it consists of four major bulk phases, all of which exhibit unique properties. These properties allow it to be used in a variety of applications.[1–3] FeO, wüstite, has a rock salt-type structure with defects, generally referred to as $Fe_{1-x}O$.[13e] This phase is paramagnetic at room temperature and antiferromagnetic below 183 K.[17] It is used in semi-

conductors[1–3] and as a nonmagnetic precursor which is easily transferred into magnetite, Fe_3O_4, or maghemite, γ-Fe_2O_3.[17] Both magnetite and maghemite have a spinel structure and are ferromagnetic allowing them to be used for magnetic recording materials.[1–3] Interestingly, magnetite is the most magnetic of all the naturally occurring minerals on earth. Hematite, α-Fe_2O_3, has a corundum structure with weak ferromagnetism and is used as an antiferromagnetic insulator.[1–3] The films[11] and nanoparticles[12,13,16] of these various phases have been studied. Gas phase experiments have also been performed.[28,32,33,38,40–42,44,46] A variety of gas phase metal oxide experiments have probed properties of these systems such as bonding, reactivity, and structure.[22–54] Theory has provided a further understanding of the structures and stabilities of these clusters.[55–64] Mass spectrometry has been used to study these systems,[22–41] however, determining the relative stabilities remains problematic. In this study of iron oxide, we address this issue of stability using laser photodissociation of mass-selected cations.

Clusters stoichiometries and relative abundances of various transition metal oxide clusters have been determined using mass spectrometry.[22–41] Oxide clusters exhibit several stoichiometries for each metal increment, as opposed to "magic numbers" like metal carbides.[65–71] Castleman and coworkers have reported extensive studies of transition metal oxides and their reactivities with small hydrocarbons as well as carbon monoxide.[26–28] Additional experiments by Bernstein and coworkers investigated mass distributions using laser photoionization at vacuum ultraviolet wavelengths.[31,32] In both experiments the intensity patterns were used to infer relative cluster stability. The spectroscopy of small oxides has been studied with rare gas matrix isolation[42,43] and photoelectron spectroscopy of mass selected-ions.[44–51] Additional spectroscopy experiments have probed these systems using infrared techniques.[52–54] Our group in collaboration with Meijer and coworkers, used IR-resonance enhanced multiphoton ionization (IR-REMPI) to obtain the IR spectra for several metal carbide[66] and oxide[52] cluster systems. Additional infrared resonance enhanced multiphoton photodissociation (IR-

REPD) of mass-selected ions have been performed by Felicke, Meijer, and Asmis.[53,54] Theory has also been used to determine the structures of these transition metal oxide clusters.[55–64]

A variety of experiments have attempted to determine the stability of gas phase clusters such as metal oxides.[72,73] However many of these measurements use mass spectrometry, where problems due to unknown ionization potentials, fragmentation processes, and size-dependent cross sections are of concern. These same issues make it difficult to measure concentrations of neutral clusters in more recent photoionization experiments. Additional problems arise in cation experiments using energy-variable collision induced dissociation or photodissociation to determine the thresholds for bond breaking. Photodissociation relies on the absorption of light, which may not be efficient in the threshold region, and collisional measurements may suffer from significant kinetic shift effects at the threshold, especially for strongly bound clusters. Equilibrium measurements have been performed on the small vanadium oxide clusters,[22] photoionization has been employed on the neutral clusters,[31,32] collision induced dissociation has investigated various transition metal oxides[27,28] and photodissociation studies have been applied to vanadium, niobium, tantalum, and chromium.[26,29] The combined results from these experiments provide evidence for the relative cluster stabilities. Numerous experiments have studied the stability of vanadium-group and chromium oxides, but not iron oxide clusters.

We have shown repeatedly that photofragmentation studies of cluster cations can be used to determine relative stabilities.[29,66,74] Stable clusters are difficult to dissociate, however, they are often produced as fragment ions upon the dissociation of larger clusters. Although stable neutrals are not detected, they can be inferred from the neutral leaving groups via mass conservation. These methods have been used previously in our lab to study metal carbide[66] and metal oxide clusters.[29] The present experiments apply this same photodissociation methodology to iron oxides.

5.3 Experimental

Clusters are produced by laser vaporization in a pulsed nozzle cluster source and mass analyzed in a reflectron time-of-flight mass-spectrometer (TOF-MS) as described previously.[29,66,74] The second (532 nm) or third (355 nm) harmonic of a Nd:YAG laser (Spectra Physics GCR-11) is employed to vaporize iron from a rotating and translating metal rod. A helium mixture seeded with 20% oxygen is pulsed with a General Valve (150 psi backing pressure;1 mm orifice) through the sample rod holder. The oxide cluster cations grow from the laser-generated plasma, producing a molecular beam of clusters. This beam is expanded into a differentially pumped source chamber and skimmed into the mass spectrometer chamber, where cluster cations are sampled with a reflectron time-of-flight mass spectrometer using pulsed acceleration plates. Pulsed deflection plates in the first flight tube section are used to size-select the clusters of interest before they enter the reflectron. Photoexcitation employs a Nd:YAG laser (DCR-3) at 532 nm or 355 nm, which is timed to intersect the clusters at the turning point in the reflectron field. Subsequently, the parent and fragment ions are mass analyzed in the second drift tube section and detected using an electron multiplier tube and a digital oscilloscope (LeCroy 9310A). Data are transferred from the digital oscilloscope to a computer via an IEEE-488 interface. Different studies were performed as a function of laser wavelength and pulse energy for each cluster size. Photodissociation used 40-50 mJ/pulse of unfocused laser beam in a spot size of roughly 1 cm^2.

5.4 Results and Discussion

Figures 5.1 and 5.2 show the mass spectrum of $Fe_nO_m^+$ cation clusters produced in our experiment. Clusters containing up to 18 metal atoms and varying numbers of oxygen atoms are detected. The stoichiometries for each cluster correspond to a specific number of metal atoms, n, and oxygen atoms, m, where the most prominent mass peak within each group of clusters corresponds to $m \geq n$. For example, for n = 3 the mass peaks correspond to $Fe_3O_3^+$,

$Fe_3O_4^+$, $Fe_3O_5^+$, and $Fe_3O_6^+$. For each metal a similar trend is seen producing groups of peaks for n $<$ 10 and n $>$ 13. These groups correspond to the oxide clusters. A different behavior is seen in the most prominent peaks for n=10-13. These peaks have stoichiometries where $m = n$. The mass distributions that we measure are similar to the previously neutral measured by VUV photoionization by Bernstein and coworkers.[32] This is the best comparison available since there are no mass spectra measured for cation clusters larger than $Fe_3O_3^+$. To determine the relative stabilities of these various iron oxide clusters, we have mass-selected each cluster size with enough intensity, and photodissociated it with laser excitation at 532 nm and 355 nm. High laser fluences of 40 - 50 mJ /cm^2 pulse are necessary to achieve significant amounts of dissociation. These conditions indicate that multiphoton excitation is required to break the bonds, which is also consistent with our previous vanadium group and chromium oxide experiments.[29] Dissociation energies of the small clusters have been measured to be about 3-5 eV / bond[33,38,41,44] and density functional theory has calculated similar bond energies for larger clusters.[58] Therefore, it is understandable that multiphoton excitation might be required for dissociation. The absorption spectra of these clusters are also not known. It is possible that high fluence from the laser is required to overcome weak absorption at one or both of the wavelengths used. While dissociation is not efficient under any conditions, 355 nm gives the best signals, perhaps because of the greater photon energy or better absorption efficiency at this wavelength. Therefore the data shown throughout this paper are those obtained at 355 nm.

Selected examples of the photofragmentation mass spectra acquired from our experiment are presented throughout this chapter. All of the cluster ions photodissociated are listed in Table 5.1 along with the corresponding photofragments, where the most intense fragments are in bold.

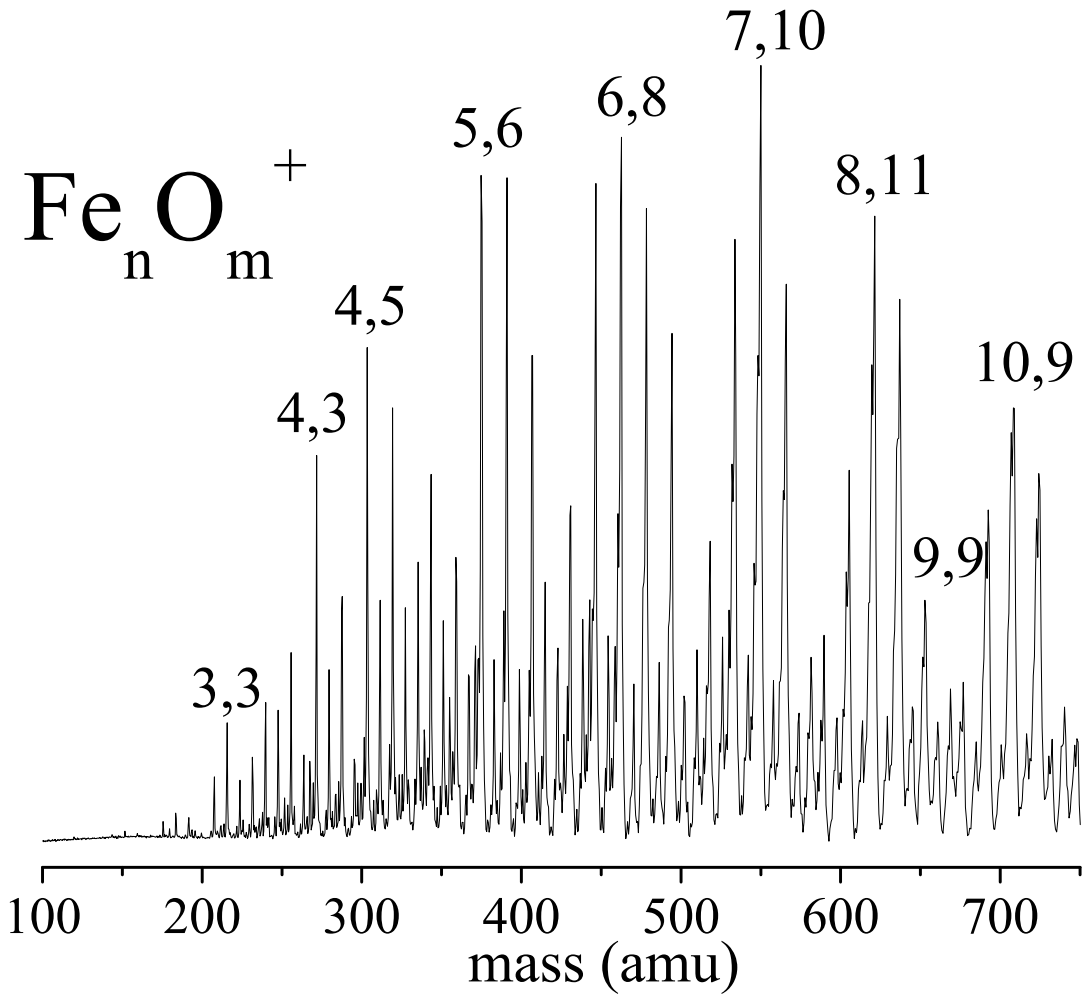

Figure 5.1: Time of flight mass spectrum for $Fe_nO_m^+$ clusters, in the lower mass range, formed in a He expansion.

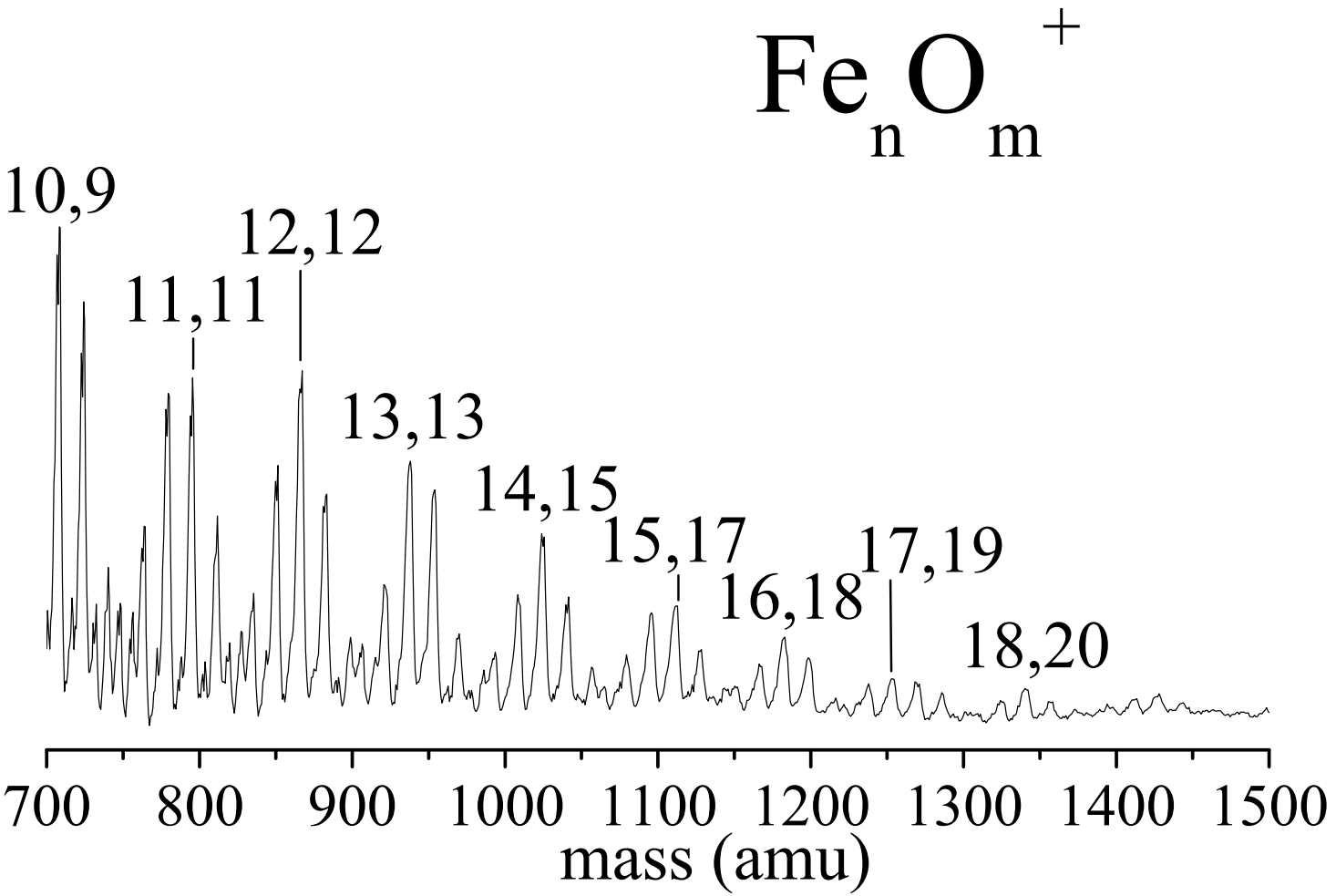

Figure 5.2: Time of flight mass spectrum for $Fe_nO_m^+$ clusters, in the higher mass range, formed in a He expansion.

Table 5.1: The iron oxide photofragments ($M_nO_m^+$ = n,m) detected using 532 nm and 355 nm. The stoichiometries indicated in bold were most prominent fragment ions detected.

Parent Cation Cluster	Fragment Clusters
1,4	1,2; **Fe^+**
1,6	**1,2**; Fe^+
2,2	2,1; **Fe^+**
2,3	2,2; 2,1; **Fe^+**
2,4	**2,2**; Fe^+
2,5	**2,3**; 2,2; 2,1; 1,2; **Fe^+**
2,6	2,2; **Fe^+**
2,8	**2,2**; 2,1; 1,2; **Fe^+**
3,3	2,2; 2,1; **Fe^+**
3,4	3,3; **2,2**; 2,1; Fe^+
3,5	3,3; **2,2**; 2,1; 1,2; **Fe^+**
3,6	3,4; 3,3; 2,2; 2,1; Fe^+
4,4	3,3; **2,2**; 2,1; Fe^+
4,5	4,4; **3,3**; 2,2; 2,1; Fe^+
4,6	**4,4**; 3,3; 2,2; 2,1; Fe^+
5,5	**4,4**; **3,3**; 2,2; 2,1; Fe^+
5,7	**5,5**; 4,4; 3,3; 2,2; 2,1; Fe^+
5,8	5,7; **5,6**; 5,5; 4,4; 3,3; 2,2; 2,1; Fe^+
6,6	6,5; 5,7; 5,6; 5,5; 4,4; **3,3**; 2,2; 2,1; Fe^+
6,7	**4,6**; 4,5; **4,4**; 3,3; 2,2; 2,1

Continued on next page...

Continued from previous page

Parent Cation Cluster	Fragment Clusters
6,8	**4,5**; 4,4; 3,3; 2,2; 2,1
7,8	6,6; **5,7**; 5,6; 5,5; **4,4**; 3,3; 2,2; 2,1
7,9	6,5; **5,6**; **4,4**; **3,3**; 2,2; 2,1
7,10	6,5; 5,8; 5,7; 5,6; 5,5; 4,4; **3,3**; 2,2; 2,1; Fe^+
8,6	6,4; 5,6; 5,5; 4,4; **3,3**; 2,2; 2,1
8,7	7,7; 7,5; 6,7; 6,6; 5,5; 4,4; **3,3**; 2,2; 2,1
8,8	7,8; 7,7; 7,6; 7,5; 6,7; 6,6; 5,5; 4,4; **3,3**; 2,2; 2,1
8,9	7,7; 7,6; 6,8; 6,7; 6,6; 5,5; 4,4; **3,3**; 2,2; 2,1
9,8	9,7; 9,6; 8,8; 8,7; 8,6; 7,6; 6,6; 5,5; 4,4; **3,3**; 2,2; 2,1
9,9	8,9; 7,9; 6,6; 5,5; 4,4; **3,3**; 2,2; 2,1
9,10	8,8; 6,6; 5,5; **4,4**; **3,3**; 2,2; 2,1
10,10	6,6; 5,5; **4,4**; **3,3**; 2,2; 2,1
10,11	10,10; 10,9; 10,8; 10,7; 9,9; 9,8; 9,7; 8,9; 8,8; 7,8; 7,7; 6,6; 5,5; **4,4**; **3,3**
10,12	10,11; 10,10; 10,9; 10,8; 9,10; 9,9; 9,8; 9,7; 8,9; 7,7; 6,6; 5,5; **4,4**; **3,3**
10,13	10,9; 9,9; 9,7; 8,8; 7,7; 6,6; 5,5; **4,4**; **3,3**; 2,2
11,11	11,9; 11,7; 10,10; 9,11; 9,8; 9,6; 8,9; 8,8; 7,10; 7,8; 7,7; 6,6; 5,5; **4,4**; **3,3**; 2,2; 2,1; Fe^+
11,13	11,11; 11,9; 10,10; 9,11; 9,10; 9,9; 9,8; 9,6; 8,8; 7,7; 6,6; 5,5; **4,4**; **3,3**; 2,2; 2,1; Fe^+
12,12	12,10; 11,11; 10,11; 10,9; 9,11; 9,10; 9,9; 9,8; 8,9; 8,8; 7,7; 6,6; 5,5; **4,4**; **3,3**; 2,2; 2,1; Fe^+

Continued on next page...

Continued from previous page

Parent Cation Cluster	Fragment Clusters
13,14	13,12; 11,11; 11,9; 10,11; 10,10; 9,10; 9,9; 8,8; 7,7; 6,6; 5,5; **4,4**; **3,3**; 2,2; 2,1; Fe^+
14,15	13,13; 12,12; 12,10; 11,11; 10,11; 10,9; 9,11; 9,10; 9,9; 9,8; 8,9; 8,8; 7,7; 6,6; 5,5; **4,4**; **3,3**; 2,2; 2,1; Fe^+
15,17	13,13; 13,11; 12,13; 11,11; 10,10; 9,9; 8,8; 7,7; 6,6; 5,5; **4,4**; 3,3; 2,2; 2,1; Fe^+
16,19	15,13; 14,15; 13,13; 12,13; 11,11; 10,10; 9,9; 8,8; 7,7; 6,6; 5,5; **4,4**; **3,3**; 2,2; 2,1; Fe^+
17,19	16,16; 15,15; 14,14; 13,13; 12,12; 11,11; 10,10; 9,9; 8,8; 7,7; 6,6; **5,5**; **4,4**; **3,3**; 2,2; 2,1; Fe^+

The photodissociation mass spectra are collected in a difference mode of operation, where spectra collected with the photodissociation laser off (only the selected parent ion present) are subtracted from the spectra collected with the photodissociation laser on (which contains fragment peaks and residual parent ion). This method produces a negative parent ion peak, showing depletion, and positive fragment ion peaks. Ideally the integrated intensities of the fragment ion peaks would equal the integrated intensity of the parent ion, displaying charge conservation. However, mass-discrimination effects within our instrument make it impossible to focus on both the parent and fragment ions with equal sensitivity and resolution.[75] Therefore, fragment ion peaks are amplified on the spectra which results in an off scale parent ion peak in the negative direction, so that we can show the more interesting fragment ions. We also use several focusing conditions to ensure that no fragment ions are missed. However, for these reasons, we do not report branching ratios for the various fragment ions. Instead, we only distinguish between strong and weak fragments.

Photodissociation mass spectra for the clusters $Fe_3O_3^+$, $Fe_3O_5^+$ and $Fe_3O_6^+$, hereafter designated as the 3,3; 3,5; and 3,6 species, respectively, are shown in Figure 5.3. The 3,5 and 3,6 fragment to 3,3 and 3,4 respectively via a loss of oxygen. Experimentally we do not have the capability to detect neutral clusters, although using mass conservation we can infer that the neutral leaving group in Figure 5.3 is oxygen. Throughout this chapter we use brackets to indicate our uncertainty of the neutral losses. For example, in Figure 5.3, the loss of two oxygen atoms could occur by losing either molecular or atomic oxygen. Therefore, this loss is indicated as $[O_2]$, although, it is safe to assume the loss of molecular oxygen, O_2, as this is the lower energy channel. Castleman and co-workers also observe that the inferred neutral loss of molecular oxygen, as opposed to atomic oxygen, is a preferred mechanism for collisional dissociation of oxygen rich iron oxide clusters.[28] This same behavior is seen for the n=2 group, in data not shown, where the 2,1; 2,2; and 2,3; fragment ions are produced from the parent 2,3; 2,4; and 2,5 clusters, respectively. Additionally the 2,6 and 2,8 parent clusters produce the 2,2 fragment ion via elimination of two and four units of $[O_2]$.

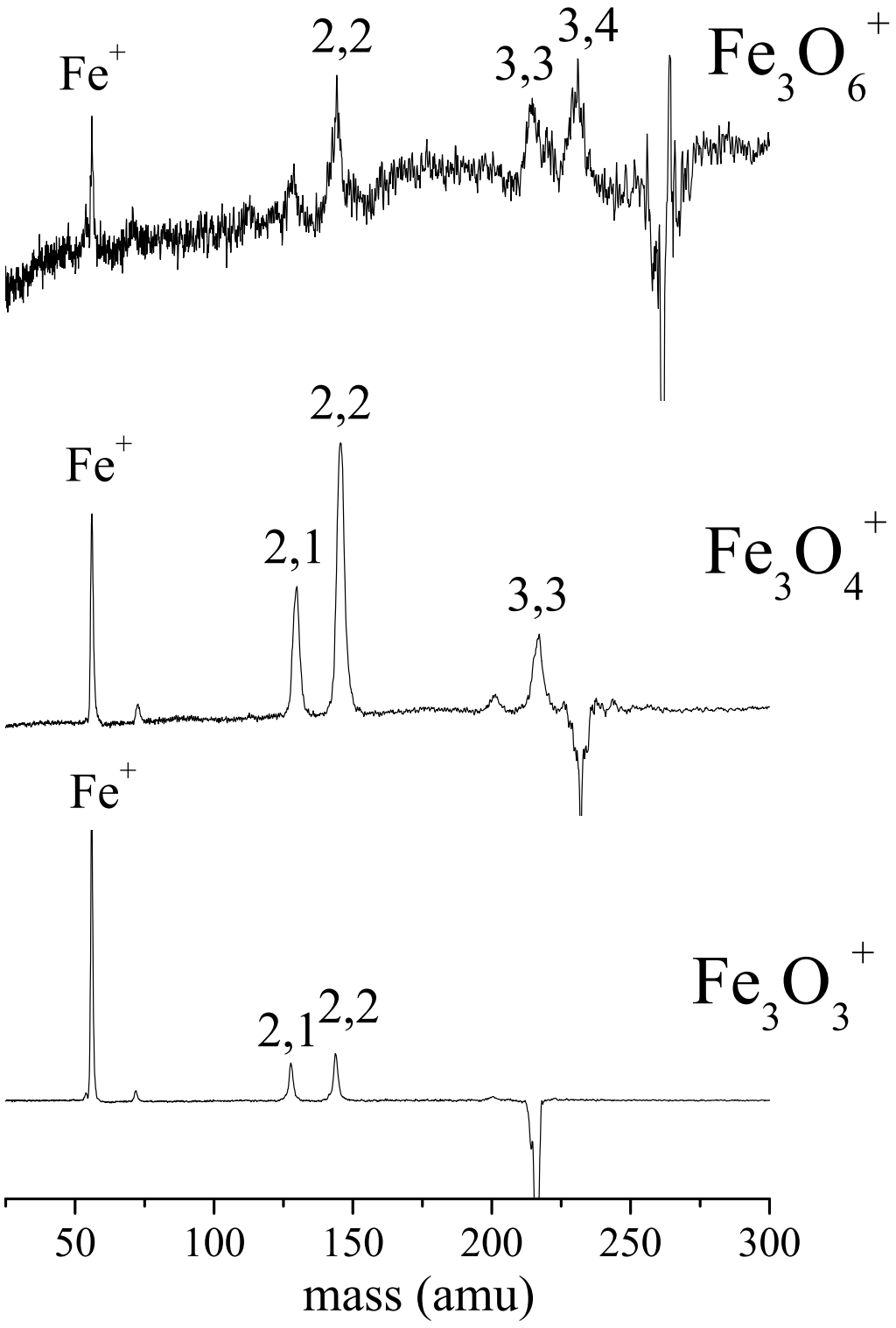

Figure 5.3: Photodissociation mass spectra of $Fe_3O_m^+$ clusters at 355 nm.

The loss of [O_2] ceases in the $Fe_3O_m^+$ complexes at the fragment ion 3,3 which is the smallest ion produced in the n=3 group. For this reason $Fe_3O_3^+$ is determined to be the terminal ion for this group. The repeated appearance of this ion as a fragment from those having the same number of metal and more oxygen indicates that this cluster is relatively more stable than other clusters within the n=3 group. We therefore designate the terminal ion 3,3 as the most stable cluster for the n=3 group. Upon examining the n=2 group, we can identify the terminal ion as the 2,2. Although some clusters produce fragment ions beyond this point with measurable intensity, the $Fe_2O_2^+$ cluster is prominent throughout all of the $Fe_2O_m^+$ dissociation, therefore it is defined as the "core" cluster for the n=2 group.

Once the terminal ion is reached within a specific group, dissociation occurs via fission with units of [FeO] eliminated. Again we indicate the inferred neutral loss in brackets. The photodissociation for the n=3 clusters show this, as the $Fe_3O_3^+$ fragment ion dissociates via the loss of [FeO] to produce the 2,2 and a small amount of 1,1 fragment ions. The elimination of [FeO] can occur through direct or sequential dissociation processes to produce the smaller mass fragment ions. Direct processes occur through the loss of the neutral atoms or molecules which produce the fragment ions. However, sequential processes occur through the stepwise elimination of multiple neutrals. For example, the dissociation of the parent cluster 3,3 producing the 2,2 and 1,1 fragment ions could be a sequential process or 2 direct processes occurring in parallel. Laser power or wavelength studies can be used to distinguish between sequential and direct processes. In our experiments we found that the prominent fragment ions are independent of the dissociation wavelength 532 nm or 355 nm. However, the laser power studies (over the range of 5 - 25 mJ/cm^2 pulse for 355 nm and 15 - 125 mJ/cm^2 pulse for 532 nm) provides compelling evidence for sequential processes. Laser power studies were performed on numerous parent cluster sizes from those with a single metal atom to 15 metal atoms. All of these studies, with the exception of a few small clusters($n \leq 3$), show that as the laser power decreased, fragment ions closest to the mass of the parent ion remained intense while the lower mass fragments disappeared. The production of the 2,1 and

Fe^+ fragment ions in the n=3 spectra are also consistent with sequential processes, as these fragments were also produced in the n=2 group. These two ions are produced throughout all the data presented here and will not be discussed further. Evidence for stable cation clusters are shown via the repeated production of these clusters from several different parent clusters. From this point on we only discuss those dissociation routes which are common to more than one cluster system.

These same dissociation patterns are seen in the $Fe_4O_m^+$ clusters (m=4,5,6), in data not shown, and the $Fe_5O_m^+$ clusters (m=5,7,8), shown in Figure 5.4. Within both of these groups $[O_2]$ is eliminated, producing the 4,4; 5,5 and 5,6 fragment ions from the 4,6; 5,7 and 5,8 parent clusters, respectively. Again the loss of $[O_2]$ ceases at the $Fe_4O_4^+$ and $Fe_5O_5^+$ clusters. Based on the power dependence studies, these clusters probably dissociate via the elimination of [FeO] units to produce the 3,3 and 2,2 fragment ions with the 4,4 also being produced from the 5,5 parent. For these reasons the 4,4 and 5,5 are determined to be the terminal ions for the n=4 and n=5 groups.

The fragmentation spectra of the $Fe_6O_m^+$ clusters (m= 6,7,8) and $Fe_7O_m^+$ clusters (m= 8,9,10) are shown in Figures 5.5 and 5.6, respectively. One noticeable difference in the fragmentation patterns of both groups is that the tendency to lose $[O_2]$ is not observed. Instead, for the 6,6 and all three n=7 parents, we see many more fragment ions at masses closer to that of the parent until a 1:1, or $n = m$, stoichiometry is reached at the 5,5. From the 5,5 the dissociation proceeds with inferred losses of [FeO] units, as seen earlier, producing the 4,4; 3,3; and 2,2 fragments. The top and middle frames of Figure 5.5, corresponding to the 6,8 and 6,7 parent clusters, do not show such extensive fragmentation. There are also several deviations in the fragment ions produced from the n=6 and n=7 parent clusters. Rather than producing the 1:1 stoichiometric clusters, the 6,7 parent cluster dissociates to the 4,4 and 4,6 fragment ions with comparable intensities and the 6,8 dissociates to the 4,5 fragment. Likewise, the 7,8 and 7,10 both display a prominent peak at the mass corresponding to the 5,7 fragment and the 7,9 displays a prominent peak for the 5,6 fragment. Since there is no

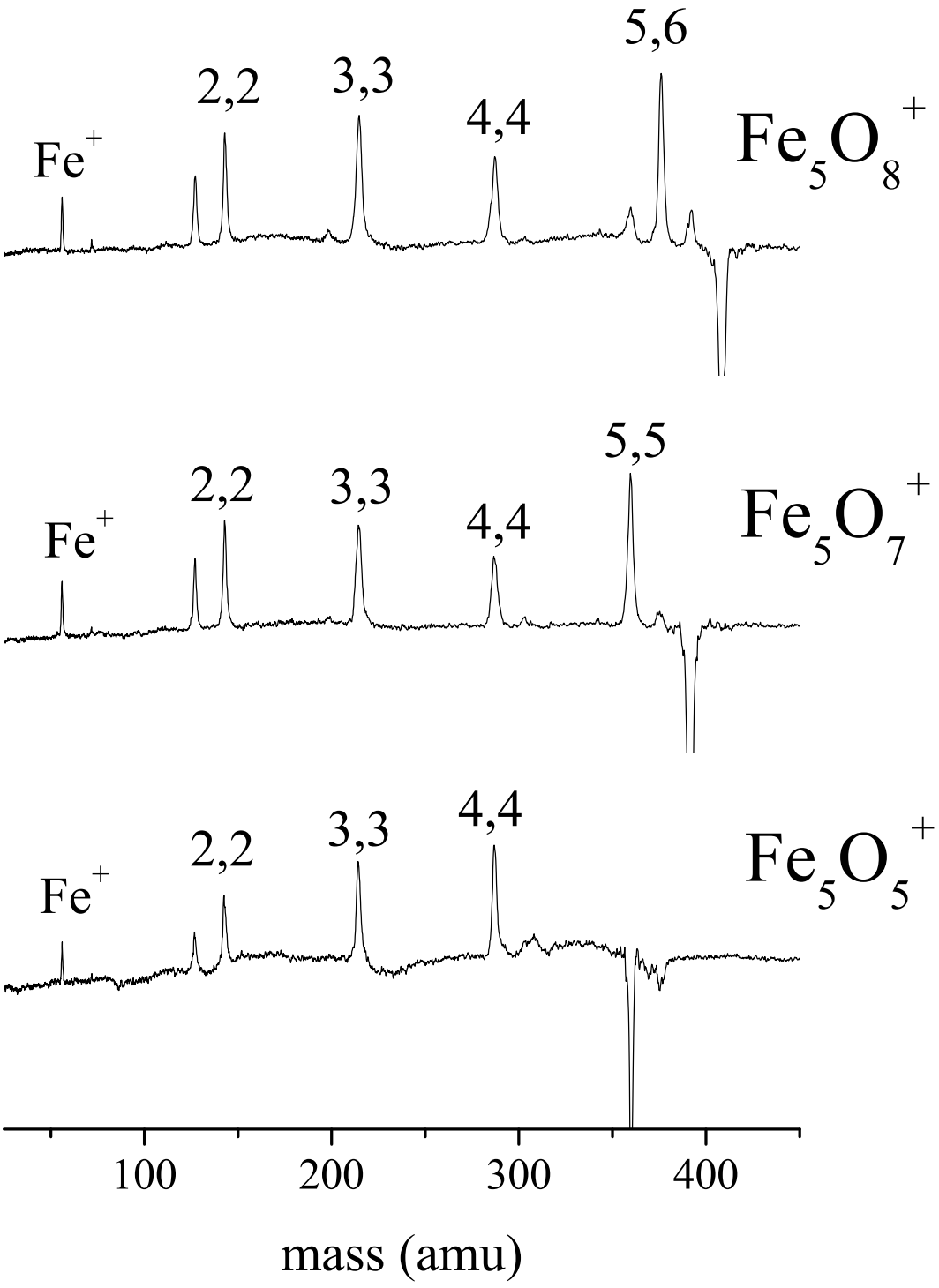

Figure 5.4: Photodissociation mass spectra of $Fe_5O_m^+$ clusters at 355 nm.

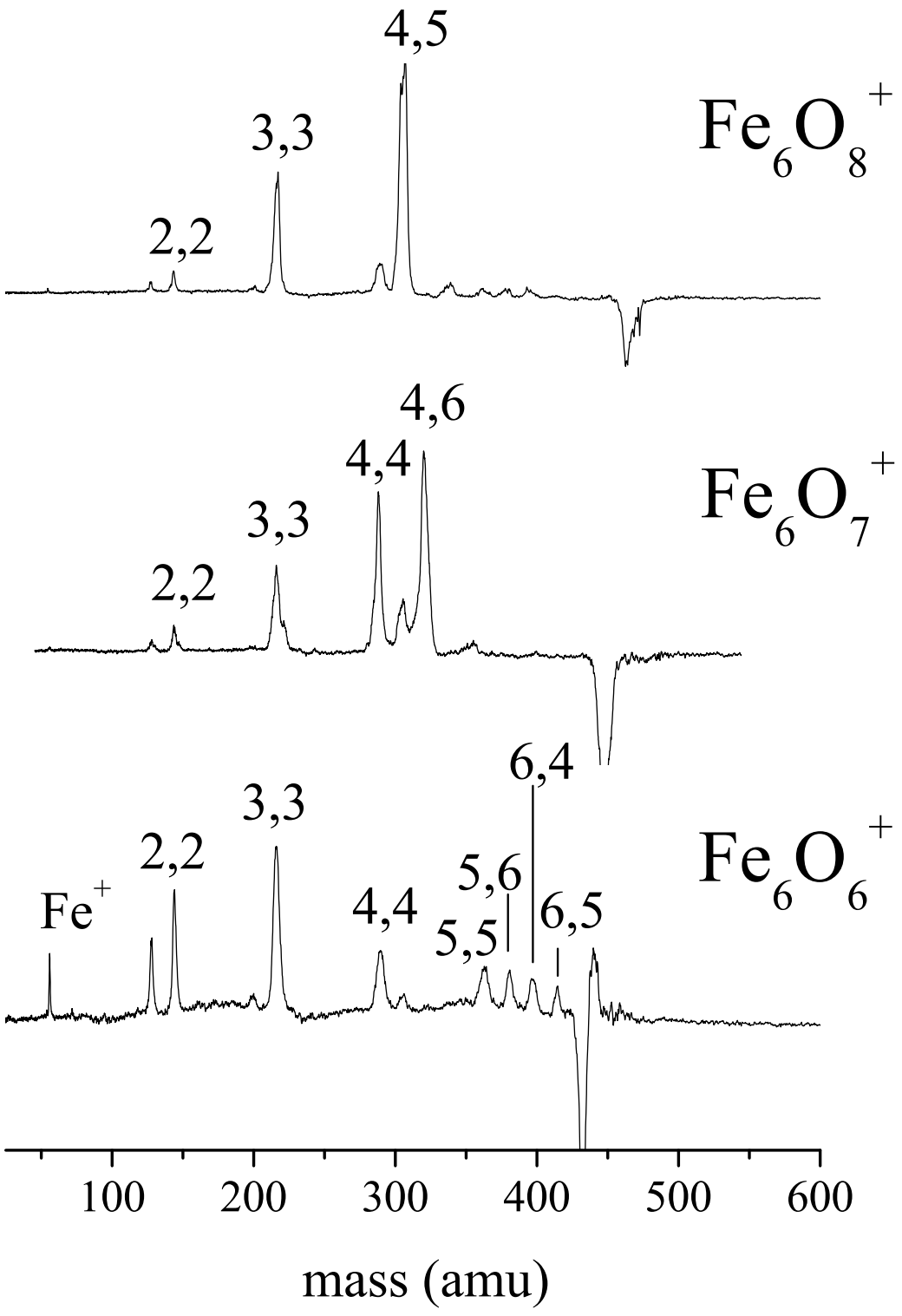

Figure 5.5: Photodissociation mass spectra of $Fe_6O_m^+$ clusters at 355 nm.

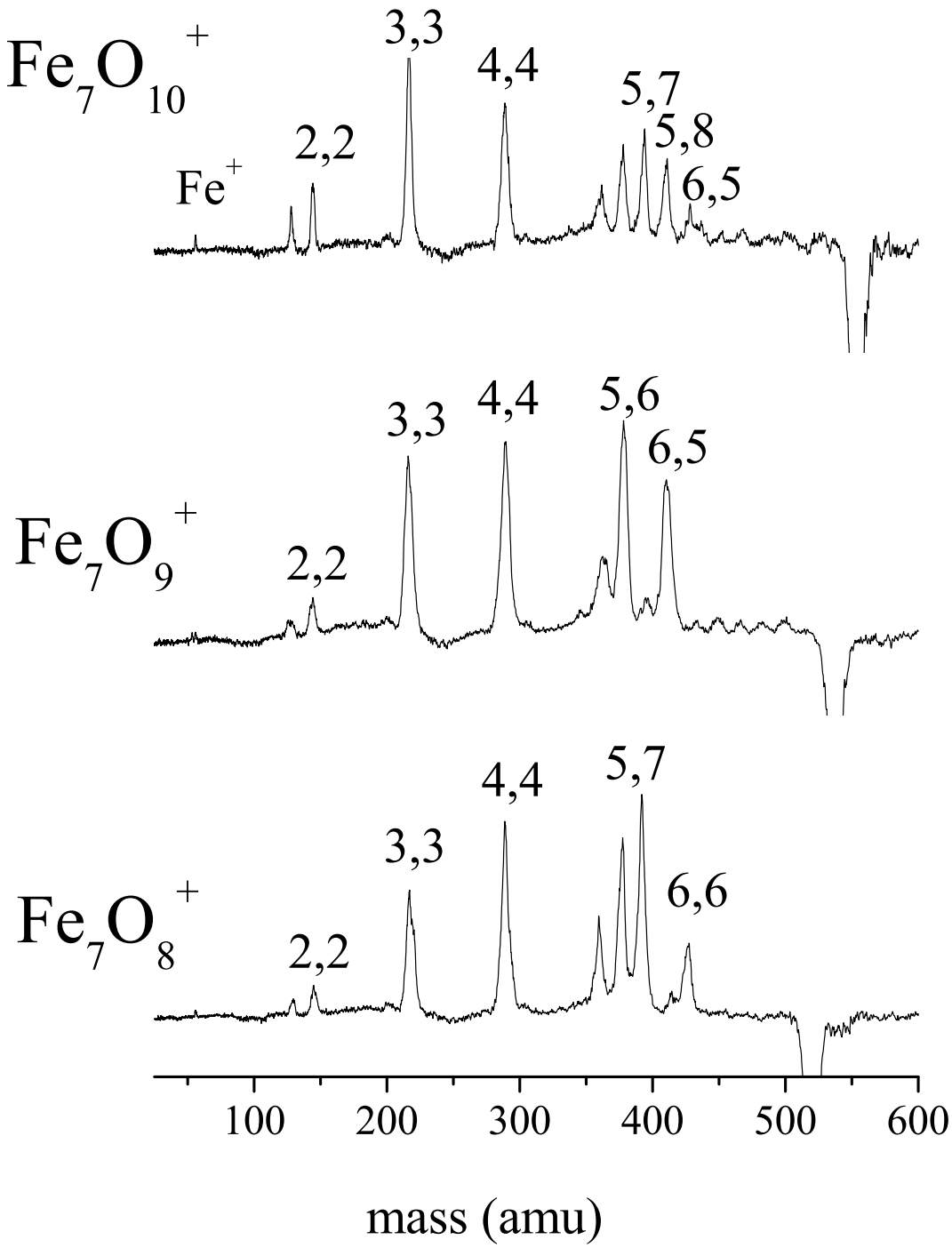

Figure 5.6: Photodissociation mass spectra of $Fe_7O_m^+$ clusters at 355 nm.

evidence for these ions in the fragmentation spectra of larger clusters, 6,7 → 4,6 and 7,8 → 5,7 were determined to be anomalies. However, the 4,5; 5,6 and 5,7 fragment ions, from the 6,8; 7,9; and 7,10 parents, all correspond to a loss of neutral [Fe_2O_3]. This is the first evidence seen for the neutral loss of the stable bulk stoichiometry Fe_2O_3. While this is interesting, there is some ambiguity regarding the significance of the [2,3] as a neutral loss channel. If this loss were significant, we would expect to see a prominent peak where a 1:1 fragment ion could be formed as a result of this loss from the parent cluster. Instead, comparable intensities for the 4,4 and 4,6 fragment ions are produced from the dissociation of the 6,7 parent cluster. Consistent with this, the most prominent fragment peak in the fragmentation spectrum for the 7,8 corresponds to the 5,7, rather than the 5,5. This is puzzling and suggests that perhaps the 4,6 and 5,7 are stable cations. However the dissociation of larger clusters as well as the smaller ones only shows the 4,4 and 5,5 fragment ion. Thus the conclusion remains that the 5,5 and 4,4 are the most stable cations for their groups. These larger clusters, where n > 5, do not exhibit the same behavior as the small clusters where losses of [O_2] cease with a specific terminal stoichiometry, instead the stable cation cluster for each group can be identified by its repeated appearance in the decomposition of larger clusters. Thus, the stable clusters for the n=6 and n=7 groups cannot be identified simply through the inspection of the corresponding groups dissociation spectra. Instead, reviewing the dissociation of larger clusters, as seen later, shows the relative stability of the $Fe_6O_6^+$ and $Fe_7O_7^+$clusters within their respective groups.

The photodissociation spectra of the $Fe_9O_m^+$ (m=8,9,10) clusters are shown in Figure 5.7. For this group as well as the n=8 group (data not shown), the extensive fragmentation subsides at the 6,6 fragment ion. Both groups also show the production of the common stable fragment clusters 5,5; 4,4; 3,3; and 2,2 probably via the loss of neutral [FeO] units. The dissociation of larger clusters show definitively that the $Fe_8O_8^+$ and $Fe_9O_9^+$ clusters are the most stable.

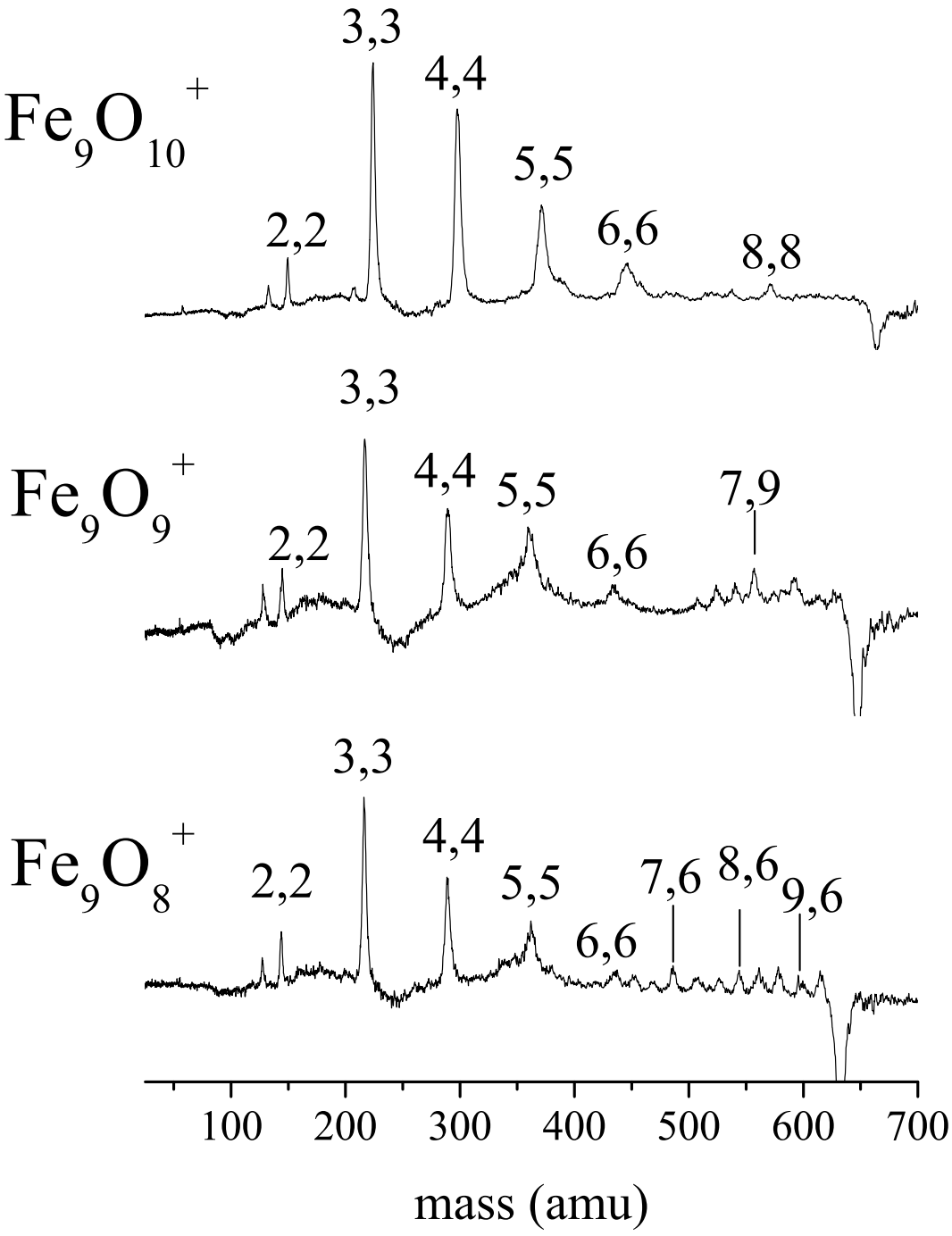

Figure 5.7: Photodissociation mass spectra of $Fe_9O_m^+$ clusters at 355 nm.

Losses of oxygen, both molecular and atomic, resume in the dissociation of the n=10 and n=11 groups of clusters, shown in Figure 5.8 and 5.9, respectively. This behavior is seen for all of the clusters dissociated in both groups with the exception of the 10,10 which does not lose oxygen. This might be due to the small parent cluster signal. However we cannot be certain because, at masses close to that of the parent, low intensity peaks appear to be visible in the noise region of the spectrum. For this reason, we conclude that the 10,10 parent probably dissociates by eliminating neutral [FeO] units to form the smaller $n = m$ clusters, where m < 7. The extensive fragmentation ceases at the 7,7 fragment in the spectra for both the n=10 and n=11 groups of clusters. Beginning with the 7,7 through the 2,2. the typical 1:1 stoichiometric mass peaks are produced for each group. The appearance of the 7,7 and 6,6 supports previous conclusions made that these are the most stable cations within their respective groups. It is also interesting to note that in the n=11 spectra the only fragment ions produced for the n=8 and n=10 groups are the 8,8 and 10,10, providing additional evidence for the stability of these clusters. Interestingly, the elimination of [Fe_2O_3] is again inferred from 10,11 → 8,8; 10,12 → 8,9 and 11,13 → 9,8 fragment ions. Additionally, the dissociation patterns of the larger clusters shows repeatedly that the 10,10 and 11,11 are the most stable cations for their groups.

In the n=11 spectra, we begin to see broadened fragment ion peaks, where n<8, which are beyond our instrument resolution. Presumably this is because the fragmentation events producing those fragment ions are slower on our instrument time scale. This makes sense based on the prior supposition that the fragmentation processes are sequential. According to RRKM, the weakest bond in the cluster will break first and the rate of dissociation depends on the amount of excess energy deposited above the dissociation threshold as well as the density of states near the level where excitation occurs.[76] Thus, larger clusters having a higher density of states and more avenues for the energy to redistribute, like those with more than 10 metals, require a longer time to dissociate and more energy. If the processes are in fact sequential, this means that the fragment ions closer to the parent mass will dissociate

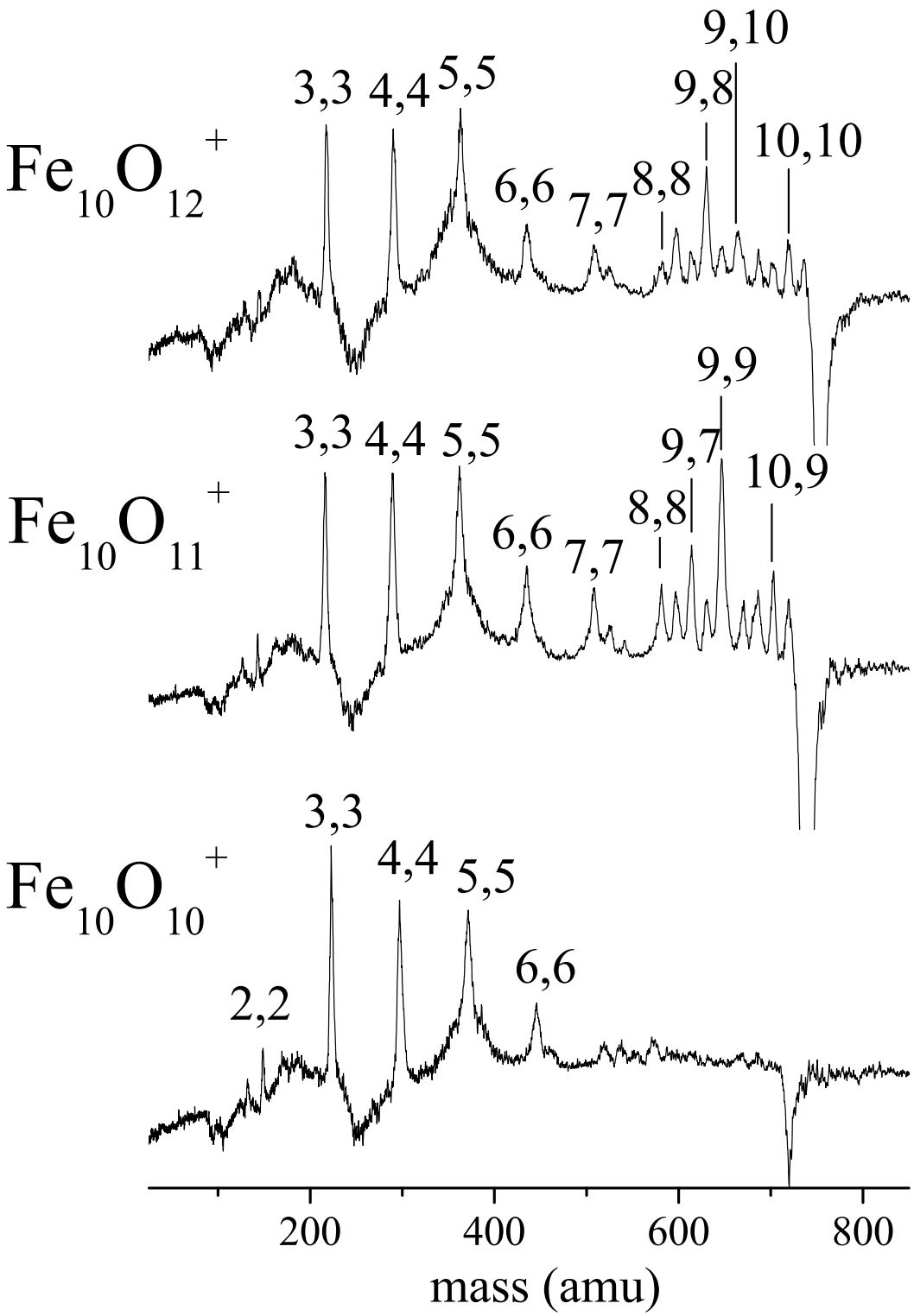

Figure 5.8: Photodissociation mass spectra of $Fe_{10}O_m^+$ clusters at 355 nm.

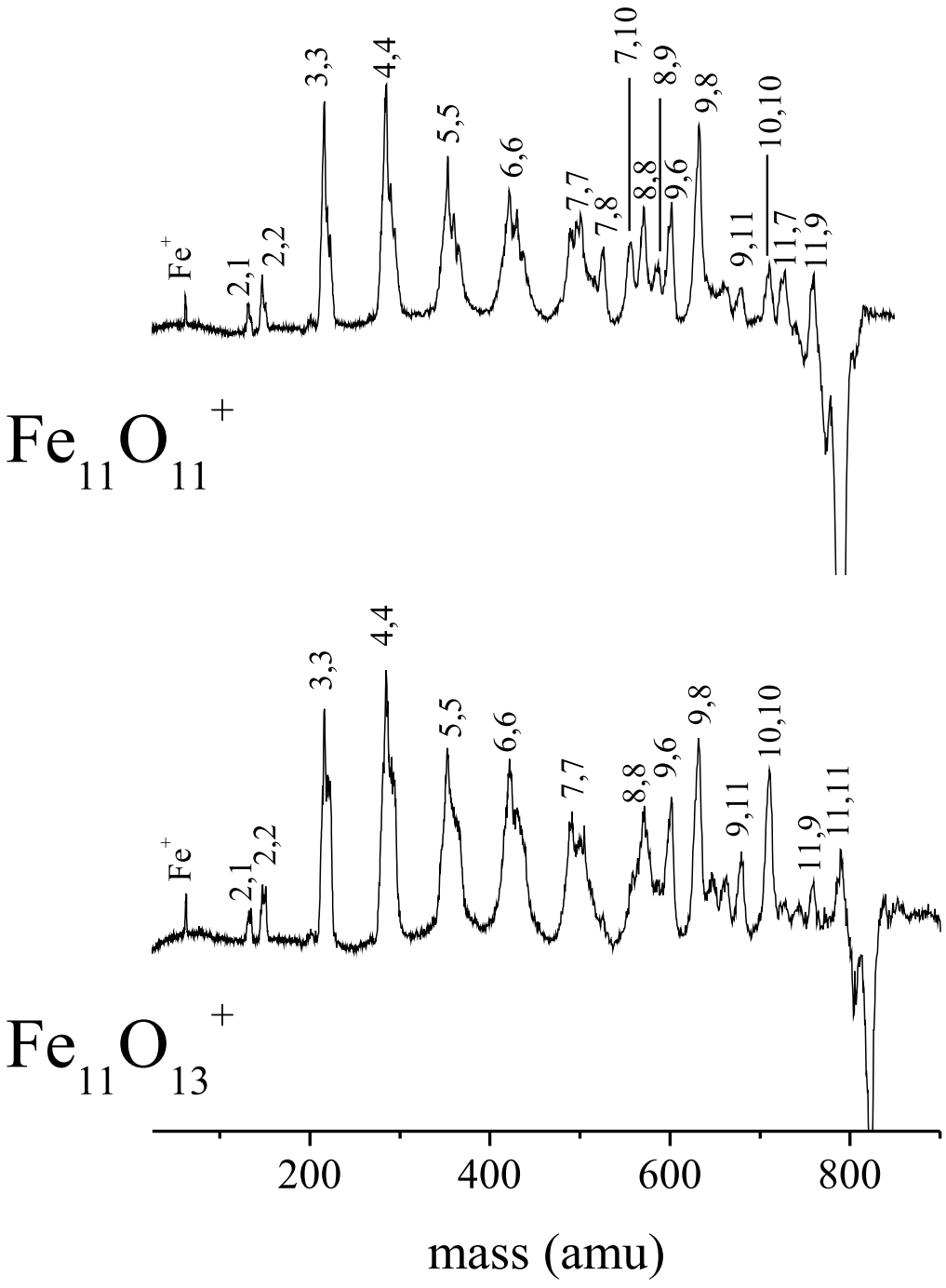

Figure 5.9: Photodissociation mass spectra of $Fe_{11}O_m^+$ clusters at 355 nm.

on a faster timescale relative to the smaller mass fragments. Additionally, if the majority of the energy is used up for the dissociation of the parent cluster to the larger mass fragment there will be less energy leftover to produce the smaller mass fragments. This would result in the larger mass fragments having more narrow widths than the smaller ones.

Figure 5.10 shows the fragmentation spectra of the $Fe_{12}O_{12}^+$, $Fe_{13}O_{14}^+$, and $Fe_{14}O_{15}^+$ clusters, and Figure 5.11 shows the fragmentation spectra of the $Fe_{15}O_{17}^+$, $Fe_{16}O_{19}^+$, and $Fe_{17}O_{19}^+$. All of these spectra show the same patterns of extensive fragmentation at the masses closest to the parent mass with a broadening of subsequent masses. The only peak that is not broadened in the 17,19 spectra corresponds to the 16,16 fragment ion. At first sight, the fragment mass peaks in the low mass range, where $n < 5$, do not appear to be broadened in these spectra. However when compared to those same mass peak widths from the dissociation of small clusters, it is apparent that these peaks are also broadened, although not as noticeably as those in the higher mass range. We also see the repeated production of the typical 1:1 stoichiometric clusters which begins at larger fragment sizes as the parent cluster size increases. For instance, the $Fe_{12}O_{12}^+$ parent cluster shows the 1:1 fragment ions beginning with the 8,8, whereas it begins at 13,13 in the dissociation of the $Fe_{16}O_{19}^+$ cluster. It is unrealistic to be confident of the assignments for the mass peaks which are broad enough to encompass several stoichiometries, e.g. the 10,10 fragment peak from the 16,19 parent could possibly be the 10,9 - 10,12. Although, 1:1 stoichiometric stable cluster cations for $n<13$ are repeatedly detected from dissociation spectra of parent clusters as large at 16,19. Therefore, it is reasonable to assume that, although the peaks in Figure 5.11 are broad enough to encompass multiple clusters for n=8 through n=12, they are probably due to the fragment ions having a 1:1 stoichiometry. An additional broadening of the fragment peaks for $n<16$ is seen from the 17,19 parent. This may be caused by the very small signal of the parent cluster or the requirement of more energy to dissociate the 17,19. Evidence for the elimination of neutral [2,3] is also shown from each parent cluster in Figure 5.11 producing 10,9; 11,11 and 12,12 which are the first intense fragment ion peaks in all three spectra respectively. We also see

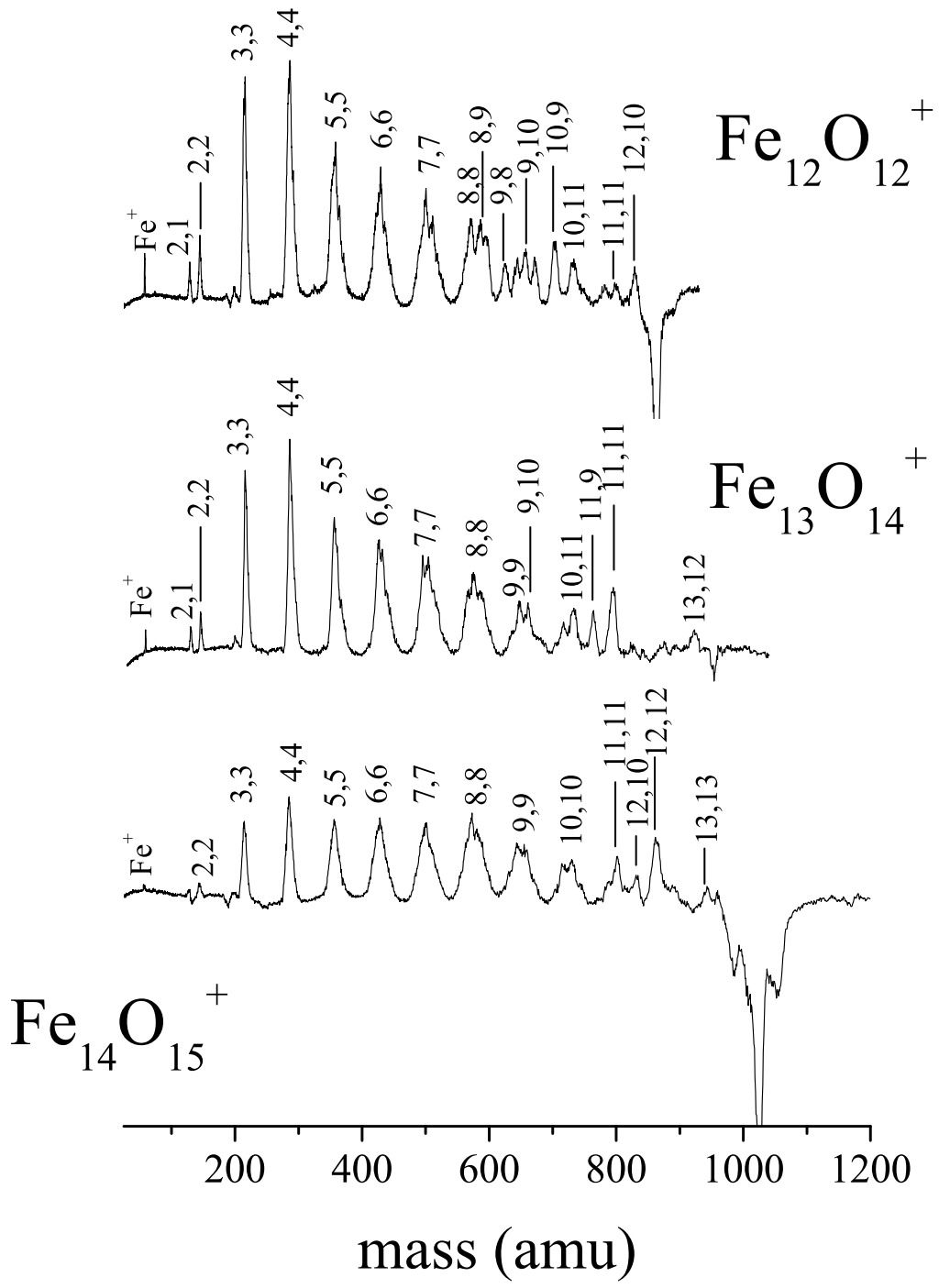

Figure 5.10: Photodissociation mass spectra of $Fe_{12}O_{12}^+$ (top), $Fe_{13}O_{14}^+$ (middle) and $Fe_{14}O_{15}^+$ (bottom) clusters at 355 nm.

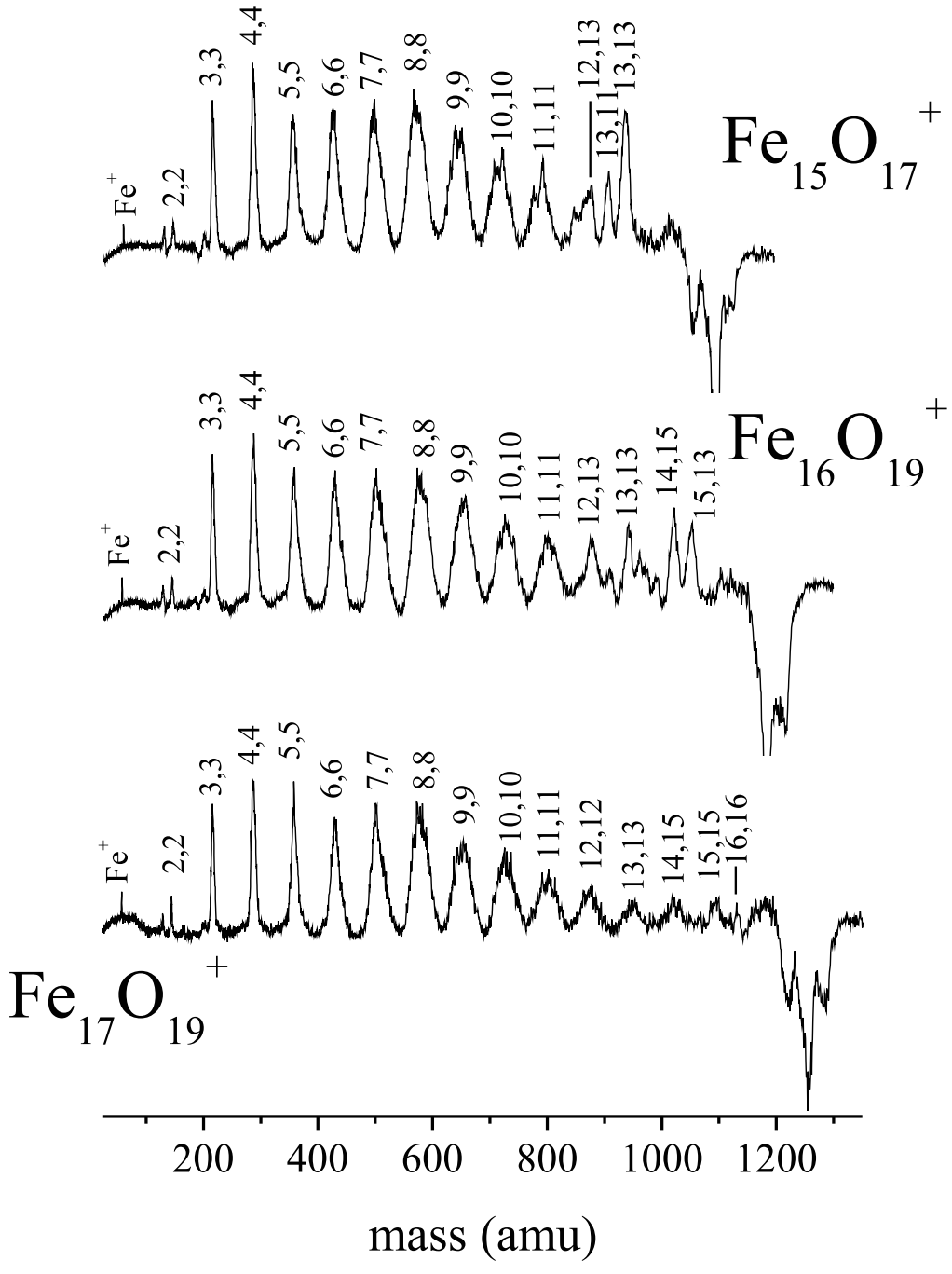

Figure 5.11: Photodissociation mass spectra of $Fe_{15}O_{17}^{+}$ (top), $Fe_{16}O_{19}^{+}$ (middle) and $Fe_{17}O_{19}^{+}$ (bottom) clusters at 355 nm.

the first evidence for the elimination of [3,4] from the 14,15 → 11,11, the 15,17 → 12,13 and the 17,19 → 14,15. Again, this is interesting because the bulk stoichiometries of iron oxide are FeO, $Fe_2O_3$and Fe_3O_4.[1–3]

These data show conclusively that the most stable cation clusters all have a 1:1 stoichiometry, where n < 14, for the $Fe_nO_m^+$ clusters. We have also shown that the inferred neutral stoichiometry FeO occurs repeatedly while Fe_2O_3 and Fe_3O_4 are seen occasionally. As in our previous work, we interpret the production of the stable species from a variety of parent ions and under different dissociation laser conditions (wavelength, power) to indicate the intrinsic relative stability of these clusters. Also consistent with this, some of these same stoichiometries are apparent as abundant species in the distribution of clusters which grew initially from the cluster source (e.g., 3,3; 11,11; 12,12; 13,13).

These patterns of cluster stability can be compared to previous experiments determining dissociation patterns,[26,33] reactivity studies[28] and neutral cluster distributions.[32] Schwarz and co-workers used collisional activated mass spectrometry to investigate the dissociation patterns of the small cation clusters where m $\leq$4 .[33] These results showed preferential inferred losses of FeO from the 1:1 clusters and losses of O_2 from the more oxygen rich clusters. The thermochemical data presented by Schwarz and co-workers for the smaller clusters, suggest the loss of FeO from Fe_3O_3 is $\sim$ 20 kcal/mole lower energy than the competitive channels of dissociation O_2 and FeO_2 and $\sim$ 30 kcal/mole lower energy than the loss of atomic O.[33] Castleman and co-workers have studied the reactivity of the small anion clusters (where n=1-2) with CO,[28] where the most reactive clusters were determined to be the oxygen rich species. The small stable cluster 2,2 (identified here) was found to be less reactive than its oxygen rich counterparts. Additionally, Castleman reported the inferred loss of molecular oxygen from $Fe_2O_6^-$ producing $Fe_2O_4^-$ which subsequently probably loses FeO or FeO_2. We also see the loss of [O_2], however we do not observe the inferred loss of [FeO] until two units of [O_2] are eliminated, leaving the 2,2 terminal ion. This might be attributed to our multiphoton conditions, but the power dependence studies of Fe_2O_6 provide compelling evidence that

Fe_2O_6 loses 2 units of [O_2] before [FeO] is eliminated. Lastly, we can compare our results with those of the photoionized neutral clusters reported by Bernstein and co-workers, where clusters were studied using three different wavelengths, 355 nm, 193 nm, and 118 nm.[32] All three wavelengths show distributions where 1:1 species are the most intense features within the mass spectra. Although cross sections are not known for these species, the ionization potential has been determined using vacuum ultraviolet photoionization studies, by Leone and co-workers, to be approximately 8.56 eV for FeO.[41] Additionally Khanna and co-workers calculated the ionization potentials to be approximately 7.5 eV for each n=m cluster, where n = 2-6.[58] These potentials show that multiphoton conditions are required in order to detect the neutral clusters using 193 nm and 355 nm. VUV photoionization, 118 nm, has the best chance to ionize clusters without fragmentation, and thus may be able to detect the most abundant neutral clusters formed. The 118 nm studies also showed that the most abundant clusters detected were those of the 1:1 stoichiometry.[32] However photoionization with VUV is could also be detecting those clusters which are easier to ionize as opposed to those that are the most stable. This possible bias in the photoionization measurements makes it impossible at present to resolve the issue of cation versus neutral stabilities.

Several groups have performed theoretical calculations on the anion and neutral species of the most stable geometric configurations for the clusters where n=1-6.[28,33,42,44,58,64] Castleman and co-workers have also performed DFT calculations on the smallest cation clusters, FeO_m^+(where m=1-3).[28] Khanna and co-workers have predicted structures for the neutral clusters which are found in Figure 5.12.[58] Khanna's results showed that clusters with the 1:1 stoichiometry were more stable than their more oxygen rich counterparts. Ring structures were found to be the most stable for clusters having metal atoms of n = 2-5. A further prediction stated that the $n = m$ species for 6,6 - 12,12 clusters are combinations of smaller rings in cages and tower structures, with weaker ring-ring bonding, such as those shown in Figure 5.12. While our data supports the 1:1 stoichiometric clusters being the most stable, we do not find evidence which supports the larger clusters being formed via rings of

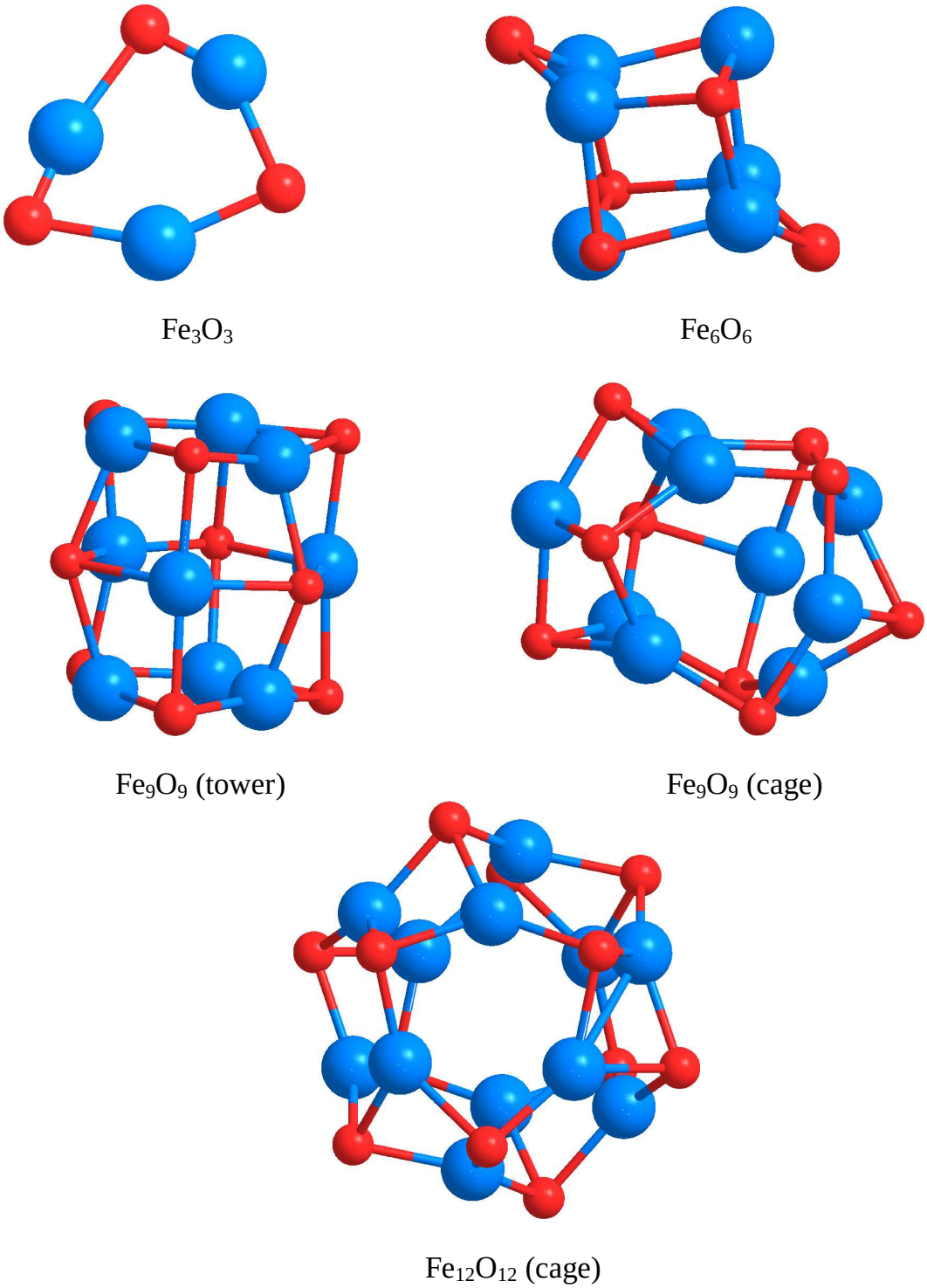

Figure 5.12: Calculated structures of Fe_nO_m by Khanna and co-workers.[58]

small clusters. For example, let's consider the 9,9 cluster. Khanna reported that the binding energy between the rings (3.45 eV) is less than the bond energy per atom (4.49 eV). If the 9,9 were comprised of three rings of 3,3 we would expect to see the bonds between the rings break first leaving the 6,6 and 3,3 as fragment ions and perhaps even prominent ones. The 3,3 is the most prominent peak in the dissociation spectrum of 9,9, however, the 6,6 peak is very small. We also see additional much more intense fragment ions corresponding to the 1:1 stoichiometries for the 5,5; 4,4 and 2,2 clusters, leading to the conclusion that it is unlikely that the 9,9 is comprised of three 3,3 rings.

It is also instructive to examine the predicted magnetism of those clusters which are found to be the most stable throughout our data. The theoretical magnetism of neutral Fe_nO_m clusters have been investigated using DFT.[64] The alignment of the magnetic moments on iron, for the $n = m$ clusters (where n=2-4), changed from a ferromagnetic to antiferromagnetic arrangement with an increasing number of oxygen atoms.[64] This confirms that perhaps these small 1:1 clusters are antiferromagnetic like the bulk solid.

In light of these structures we can make some final comparisons. The most stable clusters identified within each group can be rationalized based on the known inorganic chemistry of iron. Iron prefers the two oxidations states +2 and +3. Taking this into consideration, we can predict that the 1:1 clusters either have a mixed valence or a non-integer overall oxidation. For example the $Fe_2O_2^+$ could either have one metal with a +3 and one with a +2 or an average +2.5 oxidation state. Theoretical structures have only been calculated for the cations containing a single metal,[28] however we can speculate that the structure for the 2,2 cation is probably a symmetrical ring. This deduction is based on the theoretical calculations of the anion and neutral clusters and their typical agreement with those same cation clusters.[27,31,38,39,51,57] The ring structure indicates that the two metal atoms are equal, thus the overall oxidations state is probably +2.5, rather than the mixed valence oxidation state. This trend can be carried through all of the 1:1 clusters where the overall oxidation state becomes closer to +2 as the cluster size increases. For example, the 7,7 cluster would

have an overall oxidation state of +2.14 and the 12,12 would be +2.08. This trend was also noted by Schwarz and coworkers in the small cations clusters[33] and by Wang and co-workers for the small neutral clusters.[44] The structures calculated by Khanna and co-workers supports this idea as the rings where n=3-6 are symmetrical.[58] This is interesting because the bulk stoichiometries have a +2 oxidation state for FeO, +3 for hematite, Fe_2O_3, and a mixture of +2 and +3 in magnetite, Fe_3O_4.[1–3] In addition the inferred neutral cluster eliminated repeatedly, [FeO], and the occasional loss of [Fe_2O_3] maintain the stoichiometries found within two of the bulk iron oxide phases.

5.5 Conclusions

Iron oxide cluster cations produced by laser vaporization have been investigated with time-of-flight mass spectrometry and mass-selected photodissociation. A limited number of oxide stoichiometries are observed at each cluster size with a specific number of metal atoms. Photodissociation of these clusters is only possible via multiphoton excitation, consistent with strong metal oxide bonding. Dissociation produces a number of cation clusters repeatedly from many different parent ions, including $n = m$ clusters of the form $Fe_nO_m^+$, where n=2-13. These clusters are concluded to be significantly more stable than others in the same size region. Likewise, the neutral clusters FeO is observed repeatedly as a leaving group from a variety of parent cluster ions, and is concluded to be a stable neutral. The oxidation states implied by these data are the commonly found +2 and +3 states for iron. However, further theoretical investigations of the cation clusters structures and magnetic properties would be useful.

Finally, wüstite, the bulk FeO phase, has applications in the development of semiconductors. However, the stability of this phase is dependent on temperatures above 560 °C. The stable 1:1 clusters found in our results could possibly be used to compare the bulk phase and nanocluster materials. For this reason, further investigations into the possible isolation of

these nanoclusters at room temperature would be interesting. Perhaps these small nanoclusters exhibit some stability not seen in the bulk phase. If the 1:1 nanoclusters can be isolated at lower temperatures they would be even more useful for semiconductor applications.

5.6 References

[1] Cox, P. A. *Transition Metal Oxides*; Clarendon: Oxfrod, 1992.

[2] Rao, C. N.; Raveau, B. *Transition Metal Oxides*; Wiley: New York, 1998.

[3] Cotton, F. A.; Wilkinson, G.; Murillo, C. A.; Bochmann, M., *Advanced Inorganic Chemistry*, 6^{th} edition, John Wiley & Sons, New York, 1999.

[4] Hayashi, C.; Uyeda, R.; Tasaki, A. *Ultra-Fine Particles*; Noyes: Westwood, 1997.

[5] Henrich, V. E.; Cox, P. A. *The Surface Science of Metal Oxides*; Cambridge University Press: Cambridge, 1994.

[6] Somorjai, G. A. *Introduction to Surface Chemistry and Catalysis*; Wiley-Interscience: New York, 1994.

[7] Gates, B. C. "Supported Metal-Clusters - Synthesis, Structure, and Catalysis," *Chem. Rev.* **1995**, *95*, 511.

[8] a) Street, S. C.; Xu, C.; Goodman, D. W. "The physical and chemical properties of ultrathin oxide films," *Annu. Rev. Phys. Chem.* **1997**, *48*, 43. b) Rainer, D. R.; Goodman, D. W. "Metal clusters on ultrathin oxide films: model catalysts for surface science studies," *J. Mol. Catal. A: Chem.* **1998**, *131*, 259. c) St. Clair, T. P.; Goodman, D. W. "Metal nanoclusters supported on metal oxide thin films: bridging the materials gap," *Top. Catal.* **2000**, *13*, 5. d) Wallace, W. T.; Min, B. K.; Goodman, D. W. "The nucleation, growth, and stability of oxide-supported metal clusters," *Top. Catal.* **2005**, *34*, 17. e) Chen, M. S.; Goodman, D. W. "Catalytically active gold: From nanoparticles to ultrathin films," *Acc. Chem. Res.* **2006**, *39*, 739. f) Chen, M. S., Luo, K., Kumar, D., Wallace, W. T., Yi, C.-W., Gath, K. K., Goodman, D. W. "The Structure of ordered Au films on TiOx," *Surf. Sci.* **2007**, *601*, 632.

[9] Pope, M. T.; Mller, A. *Poloyoxometalate Chemistry From Topology via Self-Assembly to Applications*; Kluwer: Boston, 2001.

[10] *Metal Nanoparticles: Synthesis, Characterization, and Applications*; Feldheim, D. L.; Foss, C. A. J., Eds.; Marcel Dekker: New York, 2002.

[11] Crans, D. C.; Smee, J. J.; Gaidamauskas, E.; Yang, L. Q. "The chemistry and biochemistry of vanadium and the biological activities exerted by vanadium compounds," *Chem. Rev.* **2004**, *104*, 849.

[12] a) Dimitrov, D. V.; Unruh, K., Hadjipanayis, G. C.; Papaefthymiou, V.; Simopoulos, A. "Ferrimagnetism and defect clustes in $Fe_{1-x}O$ films," *Phys. Rev. B* **1999**, *59*, 499. b) Dimitrov, D. V.; Unruh, K., Hadjipanayis, G. C.; Papaefthymiou, V.; Simopoulos, A. "Defect clusters in $Fe_{1-x}O$ and their ferromagnetic properties," *J. Appl. Phys.* **2000**, *87*, 7022.

[13] a) Rockenberger, J.; Scher, E. C.; Alivisatos, A. P. "A new nonhydrolytic single-precursor approach to surfactant-capped nanocrystals of transition metal oxides," *J. Am. Chem. Soc.* **1999**, *121*, 11595. b) Puntes, V. F.; Krishnan, K. M.; Alivisatos, A. P. "Colloidal nanocrystal shape and size control: The case of cobalt," *Science* **2001**, *291*, 2115. c) Nolting, F.; Luning, J.; Rockenberger, J.; Hu, J.; Alivisatos, A. P. "A PEEM study of small agglomerates of colloidal iron oxide nanocrystals," *Surf. Rev. Lett.* **2002**, *9*, 437. d) Jun, Y. W.; Casula, M. F.; Sim, J. H.; Kim, S. Y.; Cheon, J.; Alivisatos, A. P. "Surfactant-assisted elimination of a high energy facet as a means of controlling the shapes of TiO2 nanocrystals," *J. Am. Chem. Soc.* **2003**, *125*, 15981. e) Casula, M. F.; Jun, Y. W.; Zaziski, D. J.; Chan, E. M.; Corrias, A.; Alivisatos, A. P. "The concept of delayed nucleation in nanocrystal growth demonstrated for the case of iron oxide nanodisks," *J. Am. Chem. Soc.* **2006**, *128*, 1675.

[14] Farrell, D.; Majetich, S. A.; Wilcoxon, J. P. "Preparation and characterization of monodisperse Fe nanoparticles," *J. Phys. Chem. B* **2003**, *107*, 11022.

[15] Ayers, T. M.; Fye, J. L.; Li, Q.; Duncan, M. A. "Synthesis and isolation of titanium metal cluster complexes and ligand-coated nanoparticles with a laser vaporization flowtube reactor," *J. Cluster Sci.* **2003**, *14*, 97.

[16] Roesky, H. W.; Haiduc, I.; Hosmane, N. S. "Organometallic oxides of main group and transition elements downsizing inorganic solids to small molecular fragments," *Chem. Rev.* **2003**, *103*, 2579.

[17] Redl, F. X.; Black, C. T.; Papaefthymiou, G. C.; Sandstrom, R. L.; Yin, M.; Zeng, H.; Murray, C. B.; O'Brien, S. P. "Magnetic, electronic, and structural characterization of nonstoichiometric iron oxides at the nanoscale," *J. Am. Chem. Soc.* **2004**, *126*, 14583.

[18] Cushing, B. L.; Kolesnichenko, V. L.; O'Connor, C. J. "Recent advances in the liquid-phase syntheses of inorganic nanoparticles," *Chem. Rev.* **2004**, *104*, 3893.

[19] Kang, E.; Park, J.; Hwang, Y.; Kang, M.; Park, J. G.; Hyeon, T. "Direct synthesis of highly crystalline and monodisperse manganese ferrite nanocrystals," *J. Phys. Chem. B* **2004**, *108*, 13932.

[20] Fernandez-Garcia, M.; Martinez-Arias, A.; Hanson, J. C.; Rodriguez, J. A. "Nanostructured oxides in chemistry: Characterization and properties," *Chem. Rev.* **2004**, *104*, 4063.

[21] Suzdalev, I. P.; Makismov, Y. V.; Imshennik, V. K.; Novichikhin, S. V.; Mateev, V. V.; Tretyakov, Y. D.; Lukashin, A. V.; Eliseev, A. A.; Avramenko, N. V.; Mayygin, A. A.; Sosnov, E. A. "Formation and properties of the nanocluster structure of iron oxides," *Russian Chem. Bulletin, Int. Ed.*, **2006**, *55*, 1755.

[22] a) Berkowitz, J.; Chupka, W. A.; Inghram, M. G. "Thermodynamics of the V-O System - Dissociation Energies of VO and VO_2," *J. Chem. Phys.* **1957**, *27*, 87. b) Inghram, M. G.; Chupka, W. A.; Berkowitz, J. "Thermodynamics of the Ta-O System - Dissociation Energies of Tao and Tao2," *J. Chem. Phys.* **1957**, *27*, 569.

[23] Farber, M.; Uy, O. M.; Srivastava, R. D. "Effusion-mass spectrometric determination of the heats of formation of the gaseous molecules V4O10, V4O8, VO2, and VO," *J. Chem. Phys.* **1972**, *56*, 512.

[24] Bennett, S. L.; Lin, S. S.; Gilles, P. W. "High-Temperature Vaporization of Ternary-Systems .1. Mass-Spectrometry of Oxygen-Rich Vanadium-Tungsten-Oxygen Species," *J. Phys. Chem.* **1974**, *78*, 266.

[25] Maunit, B.; Hachimi, A.; Manuelli, P.; Calba, P. J.; Muller, J. F. "Formation of iron oxides clusters induced by resonant laser ablation ionization," *Int. J. Mass Spectrom. Ion Processes* **1996**, *156*, 173.

[26] a) Kooi, S. E.; Castleman, A. W. "Photofragmentation of vanadium oxide cations," *J. Phys. Chem. A* **1999**, *103*, 5671. b) Bell, R. C.; Zemski, K. A.; Justes, D. R.; Castleman, A. W. "Formation, structure and bond dissociation thresholds of gas-phase vanadium oxide cluster ions," *J. Chem. Phys.* **2001**, *114*, 798.

[27] a) Deng, H. T.; Kerns, K. P.; Castleman, A. W. "Formation, structures, and reactivities of niobium oxide cluster ions," *J. Phys. Chem.* **1996**, *100*, 13386. b) Bell, R. C.; Zemski, K. A.; Kerns, K. P.; Deng, H. T.; Castleman, A. W. "Reactivities and collision-induced dissociation of vanadium oxide cluster cations," *J. Phys. Chem. A* **1998**, *102*, 1733. c) Bell, R. C.; Zemski, K. A.; Castleman, A. W. "Size-specific reactivities of vanadium oxide cluster cations," *J. Cluster Sci.* **1999**, *10*, 509. d) Zemski, K. A.; Bell, R. C.; Castleman, A. W. "Reactivities of tantalum oxide cluster cations with unsaturated hydrocarbons," *Int. J. Mass. Spectrom.* **1999**, *184*, 119. e) Zemski, K. A.; Bell, R. C.; Castleman, A. W. "Reactions of tantalum oxide cluster cations with 1-butene, 1,3-butadiene, and benzene (vol 104A, pg 5733, 2000)," *J. Phys. Chem. A* **2000**, *104*, 7408. f) Zemski, K. A.; Justes, D. R.; Bell, R. C.; Castleman, A. W. "Reactions of niobium and tantalum oxide cluster cations and anions with n-butane," *J. Phys. Chem. A* **2001**, *105*, 4410. g) Zemski, K. A.; Justes, D. R.; Castleman, A. W. "Reactions of group V transition metal oxide cluster

ions with ethane and ethylene," *J. Phys. Chem. A* **2001**, *105*, 10237. h) Zemski, K. A.; Justes, D. R.; Castleman, A. W. "Studies of metal oxide clusters: Elucidating reactive sites responsible for the activity of transition metal oxide catalysts," *J. Phys. Chem. B* **2002**, *106*, 6136. i) Justes, D. R.; Mitric, R.; Moore, N. A.; Bonacic-Koutecky, V.; Castleman, A. W. "Theoretical and experimental consideration of the reactions between VxOy+ and ethylene," *J. Am. Chem. Soc.* **2003**, *125*, 6289. j) Justes, D. R.; Moore, N. A.; Castleman, A. W. "Reactions of vanadium and niobium oxides with methanol," *J. Phys. Chem. B* **2004**, *108*, 3855. k) Bergeron, D. E.; Castleman, A. W., Jr.; Jones, N. O.; Khanna, S. N. "Stable Cluster Motifs for Nanoscale Chromium Oxide Materials," *Nano Lett.* **2004**, *4*, 261. l) Kimble, M. L.; Castleman, A. W. "Gas-phase studies of AunOm+ interacting with carbon monoxide," *Int. J. Mass. Spectrom.* **2004**, *233*, 99. m) Kimble, M. L.; Castleman, A. W., Jr.; Mitric, R.; Buergel, C.; Bonacic-Koutecky, V. "Reactivity of Atomic Gold Anions toward Oxygen and the Oxidation of CO: Experiment and Theory," *J. Am. Chem. Soc.* **2004**, *126*, 2526. n) Sun, Q.; Rao, B. K.; Jena, P.; Stolcic, D.; Kim, Y. D.; Gantefor, G.; Castleman, A. W. "Appearance of bulk properties in small tungsten oxide clusters," *J. Chem. Phys.* **2004**, *121*, 9417. o) Sun, Q.; Rao, B. K.; Jena, P.; Stolcic, D.; Kim, Y. D.; Gantefor, G.; Castleman, A. W. "Appearance of bulk properties in small tungsten oxide clusters (vol 121, pg 9417, 2004)," *J. Chem. Phys.* **2005**, *122*. p) Kimble, M. L.; Castleman, A. W.; Burgel, C.; Bonacic-Koutecky, V. "Interactions of CO with AunOm- (n $\geq$ 4)," *Int. J. Mass. Spectrom.* **2006**, *254*, 163. q) Kimble, M. L.; Moore, N. A.; Johnson, G. E.; Castleman, A. W.; Burgel, C.; Mitric, R.; Bonacic-Koutecky, V. "Joint experimental and theoretical investigations of the reactivity of Au2On- and Au3On- (n=1-5) with carbon monoxide," *J. Chem. Phys.* **2006**, *125*. r) Moore, N. A.; Mitric, R.; Justes, D. R.; Bonacic-Koutecky, V.; Castleman, A. W., Jr. "Kinetic Analysis of the Reaction between (V2O5)n=1,2+ and Ethylene," *J. Phys. Chem. B* **2006**, *110*, 3015.

[28] a) Reilly, N. M., Reveles, J. U., Johnson, G. E., Khanna, S. N., Castleman, A.W. Jr.

"Influence of charge state on the reaction of $FeO_3^{+/-}$ with carbon monoxide," *Chem. Phys, Lett.* **2007**, *435*, 295. b) Reilly, N. M., Reveles, J. U., Johnson, G. E., Khanna, S. N., Castleman, A.W. Jr. "Experimental and Theoretical Study of the Structures and Reactivity of $Fe_{1-2}O_{\leq 6}^-$ Clusters with CO," *J. Phys. Chem. A.* **2007**, *111*, 4158.

[29] a) France, M. R.; Buchanan, J. W.; Robinson, J. C.; Pullins, S. H.; Tucker, J. L.; King, R. B.; Duncan, M. A. "Antimony and Bismuth Oxide Clusters: Growth and Decomposition of New Magic Number Clusters," *J. Phys. Chem. A* **1997**, *101*, 6214. b) Molek, K. S.; Jaeger, T. D.; Duncan, M. A. "Photodissociation of vanadium, niobium, and tantalum oxide cluster cations," *J. Chem. Phys.* **2005**, *123*. c) Molek, K. S.; Reed, Z. D.; Ricks, A.M.; Duncan, M.A. "Photodissociation of Chromium Oxide Cluster Cations," *in press* **2007**.

[30] Oliveira, M. C.; Marcalo, J.; Vieira, M. C.; Ferreira, M. A. A. "Formation of some transition metal oxide cluster anions and reactivity towards methanol in the gas phase," *Int. J. Mass. Spectrom.* **1999**, *187*, 825.

[31] a) Foltin, M.; Stueber, G. J.; Bernstein, E. R. "On the growth dynamics of neutral vanadium oxide and titanium oxide clusters," *J. Chem. Phys.* **1999**, *111*, 9577. b) Foltin, M.; Stueber, G. J.; Bernstein, E. R. "Investigation of the structure, stability, and ionization dynamics of zirconium oxide clusters," *J. Chem. Phys.* **2001**, *114*, 8971. c) Matsuda, Y.; Shin, D. N.; Bernstein, E. R. "On the zirconium oxide neutral cluster distribution in the gas phase: Detection through 118 nm single photon, and 193 and 355 nm multiphoton, ionization," *J. Chem. Phys.* **2004**, *120*, 4142. d) Matsuda, Y.; Shin, D. N.; Bernstein, E. R. "On the copper oxide neutral cluster distribution in the gas phase: Detection through 355 nm and 193 nm multiphoton and 118 nm single photon ionization," *J. Chem. Phys.* **2004**, *120*, 4165. e) Matsuda, Y.; Bernstein, E. R. "On the titanium oxide neutral cluster distribution in the gas phase: Detection through 118 nm single-photon and 193 mn multiphoton ionization," *J. Phys. Chem. A* **2005**, *109*, 314.

f) Matsuda, Y.; Bernstein, E. R. "Identification, structure, and spectroscopy of neutral vanadium oxide clusters," *J. Phys. Chem. A* **2005**, *109*, 3803. g) Dong, F.; Heinbuch, S.; He, S. G.; Xie, Y.; Rocca, J. J.; Bernstein, E. R. "Formation and distribution of neutral vanadium, niobium, and tantalum oxide clusters: Single photon ionization at 26.5 eV," *J. Chem. Phys.* **2006**, *125*, 164318.

[32] a) Shin, D. N.; Matsuda, Y.; Bernstein, E. R. "On the iron oxide neutral cluster distribution in the gas phase. I. Detection through 193 nm multiphoton ionization," *J. Chem. Phys.* **2004**, *120*, 4150. b) Shin, D. N.; Matsuda, Y.; Bernstein, E. R. "On the iron oxide neutral cluster distribution in the gas phase. II. Detection through 118 nm single photon ionization," *J. Chem. Phys.* **2004**, *120*, 4157.

[33] a) Schrder, D.; Jackson, P.; Schwarz, H. "Dissociation patterns of small FemOn+ (m=1-4, n <= 6) cluster cations formed upon chemical ionization of Fe(CO)(5)/O-2 mixtures," *Eur. J. Inorg. Chem.* **2000**, 1171. b) Jackson, P.; Harvey, J. N.; Schrder, D.; Schwarz, H. "Structure and reactivity of the prototype iron-oxide cluster Fe2O2+," *Int. J. Mass. Spectrom.* **2001**, *204*, 233.

[34] a) Harvey, J. N.; Diefenbach, M.; Schroder, D.; Schwarz, H. "Oxidation properties of the early transition-metal dioxide cations MO2+ (M = Ti, V, Zr, Nb) in the gas-phase," *Int. J. Mass. Spectrom.* **1999**, *183*, 85. b) Schrder, D.; Schwarz, H.; Shaik, S. "Characterization, orbital description, and reactivity patterns of transition-metal oxo species in the gas phase," *Struct. Bonding* **2000**, *97*, 91. c) Jackson, P.; Fisher, K. J.; Willett, G. D. "The catalytic activation of primary alcohols on niobium oxide surfaces unraveled: the gas phase reactions of NbxOy- clusters with methanol and ethanol," *Chem. Phys.* **2000**, *262*, 179. d) Schroder, D.; Engeser, M.; Schwarz, H.; Harvey, J. N. "Energetics of the ligated vanadium dications VO2+, VOH2+, and [V,O,H-2](2+)," *Chemphyschem* **2002**, *3*, 584. e) Engeser, M.; Schlangen, M.; Schroder, D.; Schwarz, H.; Yumura, T.; Yoshizawa, K. "Alkane oxidation by VO2+ in the gas phase: A unique

dependence of reactivity on the chain length," *Organometallics* **2003**, *22*, 3933. f) Engeser, M.; Schroder, D.; Schwarz, H. "Gas-phase dehydrogenation of methanol with mononuclear vanadium-oxide cations," *Chemistry-a European Journal* **2005**, *11*, 5975. g) Koszinowski, K.; Schlangen, M.; Schroder, D.; Schwarz, H. "Formation, structure, and reactivity of gaseous Ni2O2+," *Eur. J. Inorg. Chem.* **2005**, 2464. h) Feyel, S.; Dobler, J.; Schroder, D.; Sauer, J.; Schwarz, H. "Thermal activation of methane by tetranuclear [V4O10](+)," *Angewandte Chemie-International Edition* **2006**, *45*, 4681. i) Feyel, S.; Schroder, D.; Rozanska, X.; Sauer, J.; Schwarz, H. "Gas-phase oxidation of propane and 1-butene with [V3O7](+): Experiment and theory in concert," *Angewandte Chemie-International Edition* **2006**, *45*, 4677. j) Feyel, S.; Schroder, D.; Schwarz, H. "Gas-phase oxidation of isomeric butenes and small alkanes by vanadium-oxide and -hydroxide cluster cations," *J. Phys. Chem. A* **2006**, *110*, 2647.

[35] Wang, X.; Neukermans, S.; Vanhoutte, F.; Janssens, E.; Verschoren, G.; Silverans, R. E.; Lievens, P. "Stability patterns and ionization potentials of CrnOm clusters (n=3-50, m=0, 1, 2)," *Appl. Phys. B: Lasers Opt.* **2001**, *73*, 417.

[36] Fielicke, A.; Rademann, K. "Stability and reactivity patterns of medium-sized vanadium oxide cluster cations $V_xO_y^+$ (4 <= x <= 14)," *Phys. Chem. Chem. Phys.* **2002**, *4*, 2621.

[37] Aubriet, F.; Muller, J. F. "About the atypical behavior of CrO3, MoO3, and WO3 during their UV laser ablation/ionization," *J. Phys. Chem. A* **2002**, *106*, 6053.

[38] a) Griffin, J. B.; Armentrout, P. B. "Guided ion beam studies of the reactions of Fe-n(+) (n=2-18) with O-2: Iron cluster oxide and dioxide bond energies," *J. Chem. Phys.* **1997**, *106*, 4448.

[39] a) Xu, J.; Rodgers, M. T.; Griffin, J. B.; Armentrout, P. B. "Guided ion beam studies of the reactions of V-n(+) (n=2-17) with O-2: Bond energies and dissociation pathways," *J. Chem. Phys.* **1998**, *108*, 9339. b) Griffin, J. B.; Armentrout, P. B. "Guided ion beam

studies of the reactions of Cr-n(+) (n=2-18) with O-2: Chromium cluster oxide and dioxide bond energies," *J. Chem. Phys.* **1998**, *108*, 8062. c) Vardhan, D.; Liyanage, R.; Armentrout, P. B. "Guided ion beam studies of the reactions of Ni-n(+) (n=2-18) with O-2: Nickel cluster oxide and dioxide bond energies," *J. Chem. Phys.* **2003**, *119*, 4166. d) Liu, F. Y.; Li, F. X.; Armentrout, P. B. "Guided ion-beam studies of the reactions of Co-n(+) (n=2-20) with O-2: Cobalt cluster-oxide and -dioxide bond energies," *J. Chem. Phys.* **2005**, *123*.

[40] Chestakov, D. A.; Parker, D. H.; Baklanov, A. V. "Iron monoxide photodissociation," *J. Chem. Phys.* **2005**, *122*.

[41] Metz, R. B.; Nicolas, C.; Ahmed, M.; Leone, S. R. "Direct determination of the ionization energies of FeO and CuO with VUV radiation," *J. Chem. Phys.* **2005**, *123*.

[42] a) Chertihin, G. V.; Saffel, W.; Yustein, J. T.; Andrews, L.; Neurock, M.; Ricca, A.; Bauschlicher, C. W. "Reactions of laser-ablated iron atoms with oxygen molecules in condensing argon. Infrared spectra and density functional calculations of iron oxide product molecules," *J. Phys. Chem.* **1996**, *100*, 5261.

[43] a) Chertihin, G. V.; Bare, W. D.; Andrews, L. "Reactions of laser-ablated chromium atoms with dioxygen. Infrared spectra of CrO, OCrO, CrOO, CrO3, Cr(OO)(2), Cr2O2, Cr2O3 and Cr2O4 in solid argon," *J. Chem. Phys.* **1997**, *107*, 2798. b) Zhou, M. F.; Andrews, L. "Infrared spectra and density functional calculations of the CrO2-, MoO2-, and WO2- molecular anions in solid neon," *J. Chem. Phys.* **1999**, *111*, 4230. c) Andrews, L.; Rohrbacher, A.; Laperle, C. M.; Continetti, R. E. "Laser desorption/ionization of transition metal atoms and oxides from solid argon," *J. Phys. Chem. A* **2000**, *104*, 8173. d) Wang, X.; Andrews, L. "Precious Metal-Molecular Oxygen Complexes: Neon Matrix Infrared Spectra and Density Functional Calculations for M(O2), M(O2)2 (M = Pd, Pt, Ag, Au)," *J. Phys. Chem. A* **2001**, *105*, 5812. e) Danset, D.; Manceron, L.;

Andrews, L. "Vibrational Spectra of Nickel and Platinum Dioxide Molecules Isolated in Solid Argon," *J. Phys. Chem. A* **2001**, *105*, 7205.

[44] a) Fan, J. W.; Wang, L. S. "Photoelectron-Spectroscopy of Feo- and Feo2- - Observation of Low-Spin Excited-States of Feo and Determination of the Electron-Affinity of Feo2," *J. Chem. Phys.* **1995**, *102*, 8714. b) Wang, L. S.; Wu, H. B.; Desai, S. R. "Sequential oxygen atom chemisorption on surfaces of small iron clusters," *Phys. Rev. Lett.* **1996**, *76*, 4853. c) Wu, H. B.; Desai, S. R.; Wang, L. S. "Observation and photoelectron spectroscopic study of novel mono- and diiron oxide molecules: FeO_y^- (y=1-4) and $Fe_2O_y^-$ (y=1-5)," *J. Am. Chem. Soc.* **1996**, *118*, 7434. d) Gutsev, G. L.; Bauschlicher, C. W., Jr.; Zhai, H.-J.; Wang, L.-S. "Structural and electronic properties of iron monoxide clusters FenO and FenO- (n = 2-6): a combined photoelectron spectroscopy and density functional theory study," *J. Chem. Phys.* **2003**, *119*, 11135.

[45] a) Wang, L.-S.; Wu, H.; Desai, S. R.; Lou, L. "Electronic structure of small copper oxide clusters: from Cu2O to Cu2O4," *Phys. Rev. B: Condens. Matter* **1996**, *53*, 8028. b) Gutsev, G. L.; Rao, B. K.; Jena, P.; Li, X.; Wang, L.-S. "Experimental and theoretical study of the photoelectron spectra of MnOx-(x=1-3) clusters," *J. Chem. Phys.* **2000**, *113*, 1473. c) Sun, Q.; Sakurai, M.; Wang, Q.; Yu, J. Z.; Wang, G. H.; Sumiyama, K.; Kawazoe, Y. "Geometry and electronic structures of magic transition-metal oxide clusters M9O6 (M = Fe, Co, and Ni)," *Phys. Rev. B* **2000**, *62*, 8500. d) Gutsev, G. L.; Jena, P.; Zhai, H.-J.; Wang, L.-S. "Electronic structure of chromium oxides, CrOn- and CrOn (n = 1-5) from photoelectron spectroscopy and density functional theory calculations," *J. Chem. Phys.* **2001**, *115*, 7935. e) Zhai, H.-J.; Wang, L.-S. "Electronic structure and chemical bonding of divanadium-oxide clusters (V2Ox, x=3-7) from anion photoelectron spectroscopy," *J. Chem. Phys.* **2002**, *117*, 7882. f) Zhai, H.-J.; Kiran, B.; Cui, L.-F.; Li, X.; Dixon, D. A.; Wang, L.-S. "Electronic Structure and Chemical Bonding in MOn- and MOn Clusters (M = Mo, W; n = 3-5): A Photoelectron Spectroscopy and ab Initio Study," *J. Am. Chem. Soc.* **2004**, *126*, 16134. g) Yang, X.; Waters, T.; Wang,

X.-B.; O'Hair, R. A. J.; Wedd, A. G.; Li, J.; Dixon, D. A.; Wang, L.-S. "Photoelectron Spectroscopy of Free Polyoxoanions Mo6O192- and W6O192- in the Gas Phase," *J. Phys. Chem. A* **2004**, *108*, 10089. h) Zhai, H. J.; Huang, X.; Waters, T.; Wang, X. B.; O'Hair, R. A. J.; Wedd, A. G.; Wang, L. S. "Photoelectron spectroscopy of doubly and singly charged group VIB dimetalate anions: M2O72-, MM ' O-7(2-), and M2O7- (M, M ' = Cr, Mo, W)," *J. Phys. Chem. A* **2005**, *109*, 10512. i) Zhai, H.-J.; Huang, X.; Cui, L.-F.; Li, X.; Li, J.; Wang, L.-S. "Electronic and Structural Evolution and Chemical Bonding in Ditungsten Oxide Clusters: W2On- and W2On (n = 1-6)," *J. Phys. Chem. A* **2005**, *109*, 6019. j) Huang, X.; Zhai, H. J.; Li, J.; Wang, L. S. "On the structure and chemical bonding of tri-tungsten oxide clusters W3On- and W3On (n=7-10): W3O8 as a potential molecular model for O-deficient defect sites in tungsten oxides," *J. Phys. Chem. A* **2006**, *110*, 85. k) Zhai, H. J.; Wang, L. S. "Probing the electronic properties of dichromium oxide clusters Cr2On- (n=1-7) using photoelectron spectroscopy," *J. Chem. Phys.* **2006**, *125*.

[46] Wang, Q.; Sun, Q.; Sakurai, M.; Yu, J. Z.; Gu, B. L.; Sumiyama, K.; Kawazoe, Y. "Geometry and electronic structure of magic iron oxide clusters," *Phys. Rev. B* **1999**, *59*, 12672.

[47] a) Wenthold, P. G.; Jonas, K. L.; Lineberger, W. C. "Ultraviolet photoelectron spectroscopy of the chromium dioxide negative ion," *J. Chem. Phys.* **1997**, *106*, 9961. b) Ramond, T. M.; Davico, G. E.; Hellberg, F.; Svedberg, F.; Salen, P.; Soderqvist, P.; Lineberger, W. C. "Photoelectron spectroscopy of nickel, palladium, and platinum oxide anions," *J. Mol. Spectrosc.* **2002**, *216*, 1. c) Ichino, T.; Gianola, A. J.; Andrews, D. H.; Lineberger, W. C. "Photoelectron spectroscopy of AuO- and AuS-," *J. Phys. Chem. A* **2004**, *108*, 11307.

[48] a) Yang, D. S.; Hackett, P. A. "ZEKE spectroscopy of free transition metal clusters," *J. Electron Spectrosc. Relat. Phenom.* **2000**, *106*, 153. b) Yang, D. S. "Photoelectron

spectra of metal-containing molecules with resolutions better than 1 meV," *Coord. Chem. Rev.* **2001**, *214*, 187.

[49] Green, S. M. E.; Alex, S.; Fleischer, N. L.; Millam, E. L.; Marcy, T. P.; Leopold, D. G. "Negative ion photoelectron spectroscopy of the group 5 metal trimer monoxides V3O, Nb_3O, and Ta_3O," *J. Chem. Phys.* **2001**, *114*, 2653.

[50] a) Pramann, A.; Nakamura, Y.; Nakajima, A.; Kaya, K. "Photoelectron Spectroscopy of Yttrium Oxide Cluster Anions: Effects of Oxygen and Metal Atom Addition," *J. Phys. Chem. A* **2001**, *105*, 7534. b) Pramann, A.; Koyasu, K.; Nakajima, A.; Kaya, K. "Photoelectron spectroscopy of cobalt oxide cluster anions," *J. Phys. Chem. A* **2002**, *106*, 4891. c) Pramann, A.; Koyasu, K.; Nakajima, A.; Kaya, K. "Anion photoelectron spectroscopy of VnOm- (n=4-15; m=0-2)," *J. Chem. Phys.* **2002**, *116*, 6521.

[51] Yoder, B. L.; Maze, J. T.; Raghavachari, K.; Jarrold, C. C. "Structures of $Mo_2O_y^-$ and Mo_2O_y (y=2, 3, and 4) studied by anion photoelectron spectroscopy and density functional theory calculations," *J. Chem. Phys.* **2005**, *122*, 094313/1.

[52] a) von Helden, G.; Kirilyuk, A.; van Heijnsbergen, D.; Sartakov, B.; Duncan, M. A.; Meijer, G. "Infrared spectroscopy of gas-phase zirconium oxide clusters," *Chem. Phys.* **2000**, *262*, 31. b) van Heijnsbergen, D.; von Helden, G.; Meijer, G.; Duncan, M. A. "Infrared resonance-enhanced multiphoton ionization spectroscopy of magnesium oxide clusters," *J. Chem. Phys.* **2002**, *116*, 2400. c) van Heijnsbergen, D.; Demyk, K.; Duncan, M. A.; Meijer, G.; von Helden, G. "Structure determination of gas phase aluminum oxide clusters," *Phys. Chem. Chem. Phys.* **2003**, *5*, 2515.

[53] a) Fielicke, A.; Meijer, G.; von Helden, G. "Infrared spectroscopy of niobium oxide cluster cations in a molecular beam: Identifying the cluster structures," *J. Am. Chem. Soc.* **2003**, *125*, 3659. b) Fielicke, A.; Meijer, G.; von Helden, G. "Infrared multiple photon dissociation spectroscopy of transition metal oxide cluster cations - Comparison

of group Vb (V, Nb, Ta) metal oxide clusters," *European Physical Journal D* **2003**, *24*, 69. c) Fielicke, A.; Mitric, R.; Meijer, G.; Bonacic-Koutecky, V.; von Helden, G. "The structures of vanadium oxide cluster-ethene complexes. A combined IR multiple photon dissociation spectroscopy and DFT calculation study," *J. Am. Chem. Soc.* **2003**, *125*, 15716. d) Demyk, K.; van Heijnsbergen, D.; von Helden, G.; Meijer, G. "Experimental study of gas phase titanium and aluminum oxide clusters," *Astronomy & Astrophysics* **2004**, *420*, 547.

[54] a) Asmis, K. R.; Bruemmer, M.; Kaposta, C.; Santambrogio, G.; von Helden, G.; Meijer, G.; Rademann, K.; Woeste, L. "Mass-selected infrared photodissociation spectroscopy of $V_4O_{10}^+$," *Phys. Chem. Chem. Phys.* **2002**, *4*, 1101. b) Brummer, M.; Kaposta, C.; Santambrogio, G.; Asmis, K. R. "Formation and photodepletion of cluster ion-messenger atom complexes in a cold ion trap: Infrared spectroscopy of VO^+, VO_2^+, and VO_3^+," *J. Chem. Phys.* **2003**, *119*, 12700. c) Asmis, K. R.; Meijer, G.; Bruemmer, M.; Kaposta, C.; Santambrogio, G.; Woeste, L.; Sauer, J. "Gas phase infrared spectroscopy of mono- and divanadium oxide cluster cations," *J. Chem. Phys.* **2004**, *120*, 6461. d) Asmis, K. R.; Santambrogio, G.; Brummer, M.; Sauer, J. "Polyhedral vanadium oxide cages: Infrared spectra of cluster anions and size-induced d electron localization," *Angewandte Chemie-International Edition* **2005**, *44*, 3122. e) Janssens, E.; Santambrogio, G.; Brummer, M.; Woste, L.; Lievens, P.; Sauer, J.; Meijer, G.; Asmis, K. R. "Isomorphous substitution in bimetallic oxide clusters," *Phys. Rev. Lett.* **2006**, *96*.

[55] a) Sambrano, J. R.; Andres, J.; Beltran, A.; Sensato, F.; Longo, E. "Theoretical study of the structure and stability of Nb_xO_y and $Nb_xO_y^+$ (x = 1-3; y = 2-5, 7, 8) clusters," *Chem. Phys. Lett.* **1998**, *287*, 620. b) Calatayud, M.; Silvi, B.; Andres, J.; Beltran, A. "A theoretical study on the structure, energetics and bonding of VOx+ and VOx (x=1-4) systems," *Chem. Phys. Lett.* **2001**, *333*, 493. c) Calatayud, M.; Andres, J.; Beltran, A. "A systematic density functional. theory study of VxOy+ and VxOY (X=2-4, Y=2-10) systems," *J. Phys. Chem. A* **2001**, *105*, 9760. d) Sambrano, J. R.; Gracia, L.; Andres,

J.; Berski, S.; Beltran, A. "A theoretical study on the gas phase reactions of the anions NbO3-, NbO5-, and NbO2(0H)(2)(-) with H2O and O-2," *J. Phys. Chem. A* **2004**, *108*, 10850. e) Sambrano, J. R.; Andres, J.; Gracia, L.; Safont, V. S.; Beltran, A. "DFT study of the water-assisted tautomerization process between hydrated oxide, MO(H2O)(+), and dihydroxide, M(OH)(2)(+) cations (M = V, Nb and Ta)," *Chem. Phys. Lett.* **2004**, *384*, 56. f) Gracia, L.; Andres, J.; Safont, V. S.; Beltran, A. "DFT study of the reaction between VO2+ and C2H6," *Organometallics* **2004**, *23*, 730.

[56] a) Veliah, S.; Xiang, K. H.; Pandey, R.; Recio, J. M.; Newsam, J. M. "Density functional study of chromium oxide clusters: Structures, bonding, vibrations, and stability," *J. Phys. Chem. B* **1998**, *102*, 1126. b) Xiang, K. H.; Pandey, R.; Recio, J. M.; Francisco, E.; Newsam, J. M. "A theoretical study of the cluster vibrations in Cr2O2,Cr2O3, and Cr2O4," *J. Phys. Chem. A* **2000**, *104*, 990.

[57] a) Reddy, B. V.; Khanna, S. N. "Chemically induced oscillatory exchange coupling in chromium oxide clusters," *Phys. Rev. Lett.* **1999**, *83*, 3170. b) Morisato, T.; Jones, N. O.; Khanna, S. N.; Kawazoe, Y. "Stable aluminum and chromium oxide clusters as precursors to nanoscale materials," *Comp. Mater. Sci.* **2006**, *35*, 366.

[58] a) Jones, N. O.; Reddy, B. V.; Rasouli, F.; Khanna, S. N. "Structural growth in iron oxide clusters: Rings, towers, and hollow drums," *Phys. Rev. B* **2005**, *72*. b) Jones, N. O.; Reddy, B. V.; Rasouli, F.; Khanna, S. N. "Structural growth in iron oxide clusters: Rings, towers, and hollow drums (vol 72, pg 165411, 2005)," *Phys. Rev. B* **2006**, *73*

[59] Chakrabarti, A.; Hermann, K.; Druzinic, R.; Witko, M.; Wagner, F.; Petersen, M. "Geometric and electronic structure of vanadium pentoxide: A density functional bulk and surface study," *Phys. Rev. B* **1999**, *59*, 10583.

[60] Zimmermann, R.; Steiner, P.; Claessen, R.; Reinert, F.; Hufner, S.; Blaha, P.; Dufek, P. "Electronic structure of 3d-transition-metal oxides: on-site Coulomb repulsion versus covalency," *J. Phys.: Condens. Matter* **1999**, *11*, 1657.

[61] a) Vyboishchikov, S. F.; Sauer, J. "Gas-phase vanadium oxide anions: Structure and detachment energies from density functional calculations," *J. Phys. Chem. A* **2000**, *104*, 10913. b) Vyboishchikov, S. F.; Sauer, J. "(V2O5)(n) gas-phase clusters (n=1-12) compared to V2O5 crystal: DFT calculations," *J. Phys. Chem. A* **2001**, *105*, 8588. c) Vyboishchikov, S. F. "Gas-phase reactions of V2O5+ and V2O6+ ions with CH3CF3 studied by density functional theory," *Journal of Molecular Structure-Theochem* **2005**, *723*, 53.

[62] Albaret, T.; Finocchi, F.; Noguera, C. "Density functional study of stoichiometric and O-rich titanium oxygen clusters," *J. Chem. Phys.* **2000**, *113*, 2238.

[63] a) Gutsev, G. L.; Rao, B. K.; Jena, P. "Systematic study of ore, peroxo, and superoxo isomers of 3d-metal dioxides and their anions," *J. Phys. Chem. A* **2000**, *104*, 11961. b) Gutsev, G. L.; Andrews, L.; Bauschlicher, C. W. "Similarities and differences in the structure of 3d-metal monocarbides and monoxides," *Theoretical Chemistry Accounts* **2003**, *109*, 298.

[64] a) Shiroishi, H.; Oda, T.; Hamada, I.; Fujima, N. "Structure and magnetism on iron oxide clusters Fe_nO_m (n=1-5): Calculation from first principles," *European Physical Journal D* **2003**, *24*, 85. b) Shiroishi, H.; Oda, T.; Hamada, I.; Fujima, N. "Structure and magnetism on sanion iron oxide clusters $Fe_nO_m^-$ (n=1-2)," *Molecular Simulation* **2004**, *30*, 911.

[65] a) Guo, B. C.; Kerns, K. P.; Castleman, A. W., Jr. "Ti8C12+-metallo-carbohedrenes: a new class of molecular clusters?," *Science* **1992**, *255*, 1411. b) Guo, B. C.; Wei, S.; Purnell, J.; Buzza, S.; Castleman, A. W., Jr. "Metallo-carbohedrenes [M8C12+ (M = vanadium, zirconium, hafnium, and titanium)]: a class of stable molecular cluster ions," *Science* **1992**, *256*, 515. c) Guo, B. C.; Castleman, A. W., Jr. "Metallo-carbohedrenes: a new class of molecular clusters," *Adv. Met. Semicond. Clusters* **1994**, *2*, 137. d) Cartier,

S. F.; May, B. D.; Castleman, A. W., Jr. "Formation, Structure, and Stabilities of Metallocarbohedrenes," *J. Phys. Chem.* **1996**, *100*, 8175.

[66] a) Pilgrim, J. S.; Duncan, M. A. "Beyond metallo-carbohedrenes: growth and decomposition of metal-carbon nanocrystals," *J. Am. Chem. Soc.* **1993**, *115*, 9724. b) Pilgrim, J. S.; Duncan, M. A. "Metallo-carbohedrenes: chromium, iron, and molybdenum analogs," *J. Am. Chem. Soc.* **1993**, *115*, 6958. c) Duncan, M. A. "Synthesis and characterization of metal-carbide clusters in the gas phase," *J. Cluster Sci.* **1997**, *8*, 239.

[67] Rohmer, M.-M.; Benard, M.; Poblet, J.-M. "Structure, Reactivity, and Growth Pathways of Metallocarbohedrenes M8C12 and Transition Metal/Carbon Clusters and Nanocrystals: A Challenge to Computational Chemistry," *Chem. Rev.* **2000**, *100*, 495.

[68] a) van Heijnsbergen, D.; von Helden, G.; Duncan, M. A.; van Roij, A. J. A.; Meijer, G. "Vibrational spectroscopy of gas-phase metal-carbide clusters and nanocrystals," *Phys. Rev. Lett.* **1999**, *83*, 4983. b) von Helden, G.; van Heijnsbergen, D.; Meijer, G. "Resonant ionization using IR light: A new tool to study the spectroscopy and dynamics of gas-phase molecules and clusters," *J. Phys. Chem. A* **2003**, *107*, 1671.

[69] Gueorguiev, G. K.; Pacheco, J. M. "Structural identification of metcars," *Phys. Rev. Lett.* **2002**, *88*; Gueorguiev, G. K.; Pacheco, J. M. "Shapes of cagelike metal carbide clusters: First-principles calculations," *Phys. Rev. B* **2003**, *68*.

[70] a) Liu, P.; Rodriguez, J. A.; Hou, H.; Muckerman, J. T. "Chemical reactivity of metcar Ti8C12, nanocrystal Ti14C13 and a bulk TiC(001) surface: A density functional study," *J. Chem. Phys.* **2003**, *118*, 7737. b) Liu, P.; Rodriguez, J. A.; Muckerman, J. T. "The chemical activity of metal compound nanoparticles: Importance of electronic and steric effects in M8C12 (M=Ti, V, Mo) metcars," *J. Chem. Phys.* **2004**, *121*, 10321. c) Liu, P.; Lightstone, J. M.; Patterson, M. J.; Rodriguez, J. A.; Muckerman, J. T.; White, M. G. "Gas-phase interaction of thiophene with the Ti8C12+ and Ti8C12 met-car clusters," *J. Phys. Chem. B* **2006**, *110*, 7449.

[71] Varganov, S. A.; Gordon, M. S. "Effects of strong electron correlations in Ti8C12 Met-Car," *Chem. Phys.* **2006**, *326*, 97; Varganov, S. A.; Dudley, T. J.; Gordon, M. S. "Predicted IR spectra of Ti8C12 and Ti8C12+," *Chem. Phys. Lett.* **2006**, *429*, 49.

[72] a) *Clusters of Atoms and Molecules Vol. I*; Haberland, H., Ed.; Springer: Berlin, 1995; Vol. 52. b) *Clusters of Atoms and Molecules Vol. II*; Haberland, H., Ed.; Springer: Berlin, 1995; Vol. 52.

[73] Johnston, R. L. *Atomic and Molecular Clusters*; Taylor & Francis: London, 2002.

[74] a) Ticknor, B. W. D.; M. A. "Photodissociation of size-selected silicon carbide cluster cations," *Chem. Phys. Lett* **2005**, *405*, 214. b) Jaeger, J. B. J., T. D.; Duncan, M. A. " Photodissociation of Metal-Silicon Clussters: Encapsulated versus Surface-Bound Metal," *J. Phys. Chem. A* **2006**, *110*, 9310.

[75] Cornett, D. S.; Peschke, M.; LaiHing, K.; Cheng, P. Y.; Willey, K. F.; Duncan, M. A., *Rev. Sci. Instrum.* **1992**, *63*, 2177.

[76] Baer, T., Hase, W. *Unimolecular Reaction Dynamics*; Oxford University Press: New York, 1996.

Chapter 6

Conclusions

Vanadium, niobium, tantalum, chromium and iron oxide cluster cations are produced in laser vaporization pulsed nozzle cluster source and investigated with time-of-flight mass spectrometry and mass-selected photodissociation. Photodissociation experiments of these transition metal oxide cluster cations are the first thorough investigations of its kind, providing insights into the most stable cluster motifs of these oxides. The ability to select each cluster individually allowed the fragmentation mass spectrum for each cluster to be examined, providing significant insights into the relative stability of these oxide clusters. The most stable clusters can be compared to the stable theoretical structures. The stable cluster cations have also revealed information valuable for experiments used to isolate the corresponding nanocluster materials.

A limited number of oxide stoichiometries are observed at each cluster size with a specific number of metal atoms. Chromium also has an especially large abundance of $Cr_4O_{10}^+$ in the cluster distribution produced by the source. The cluster cation distributions are similar, as has also been noted by previous workers. Photodissociation of these clusters is only possible via multiphoton excitation, consistent with strong metal oxide bonding. We have determined two general types of dissociation. Some clusters eliminate excess oxygen in units of O_2 such as vanadium, chromium and iron, whereas niobium and tantalum oxide clusters lose atomic oxygen. Clusters with excess oxygen eliminate oxygen until a terminal oxide stoichiometry is reached at which point further fragmentation occurs via fission. Fission occurs by loss of stable metal oxide fragments. The vanadium group oxides eliminate MO_2, MO_3 and M_2O_5 as stable neutrals, chromium oxides eliminate CrO_3, Cr_2O_5 and Cr_4O_{10} and iron oxides eliminate FeO, with occasional losses of Fe_2O_3 observed. These neutral stoichiometries are noteworthy as they are found in the corresponding bulk materials. The terminal cations identified at each metal size increment, n, also repeatedly appear as abundant photofragments from larger clusters for different metals. The most stable cation stoichoimetries established for the vanadium group oxides are MO_2^+, $M_2O_4^+$, $M_3O_7^+$, $M_4O_9^+$, $M_5O_{12}^+$, $M_6O_{14}^+$ and $M_7O_{17}^+$. Vanadium is an anomaly as $V_3O_6^+$ has a comparable stability to $V_3O_7^+$. The most stable

cation clusters determined for chromium are very similar to those of the vanadium group, including CrO^+, $Cr_2O_4^+$, $Cr_3O_6^+$, $Cr_3O_7^+$ and $Cr_4O_{10}^+$. However, the most stable iron cluster stoichiometries are different than those of the vanadium group or chromium as the $n = m$ clusters of the form $Fe_nO_m^+$, where n=2- 13, were found to have exception stability for iron. It is also worth noting that the Cr_4O_{10} cluster exhibits a strong stability as both a neutral and an ion. This may be in part attributed to the high symmetry of its structure.

Our data implies that the vanadium group and iron oxide clusters exhibit oxidation states which are commonly found in the corresponding bulk oxides. The vanadium group clusters imply oxidation states of +4 and +5 whereas the iron clusters suggest the commonly found +2 and +3 states. In contrast, the most stable chromium clusters suggest +4 and +5 oxidation states which are not common in its solid oxide materials.

Where applicable, these conclusions agree with other data on the same oxide cluster cations. There is evidence that neutral clusters of these same metals follow the same stability. Further work is needed to confirm this. Despite the new data on structures of the small clusters, additional work from both theory and experiment is needed to establish the structures that correspond to these stable clusters and to explain the source of their stability. For example the detailed comparison of the per-bond energetics for chromium oxide clusters of different sizes does not provide as clear and compelling a picture of the most stable clusters as the experiment does. In addition, further theoretical investigations of iron cation cluster structures and magnetic properties would be useful.

The laser vaporization, pulsed nozzle cluster source, coupled with photodissociation experiments, has proven to be a powerful technique used to study strongly bound clusters. These experiments would be useful in studying other transition metal oxides such as zinc and cobalt, both of which are relevant for their electronic and magnetic properties, respectively. Additional experiments studying multi-metal oxide clusters would be useful such as $Au(M_nO_m^+)$. These experiments might reveal the bonding nature of the gold onto the metal oxide which is useful for catalytic applications where metals are supported on metal oxides.

Other experiments using infrared photodissociation would be useful to determine the structures of these stable cation clusters. As mentioned previously, such experiments are limited by the inherent strong binding in these clusters as well as the method used to produce such clusters. In the near future, our lab will have the capability of producing these oxide clusters in a cold source which will minimize the production of hot clusters. The cold source, cooled by liquid helium, will be attached to the rod holder used to generate the oxide clusters. Buffer gas collisions with the walls of the cooled rod holder will help dissipate the heat generated from the high laser fluences required to produce these clusters. In so doing the source will cool the oxide clusters enough to possibly rare gas tag. Our group has demonstrated the practicality and usefulness of employing rare gas tagging for weakly bound clusters which are still too strongly bound for single photon infrared spectroscopy. The methods routinely used to produce these weakly bound clusters cannot produce large strongly bound clusters. However the addition of a cold source to our laser vaporization pulsed nozzle source will increase the chances of producing these large strongly bound clusters with rare gas tagging. Such clusters can then be probed using infrared photodissociation experiments. These IR experiments will allow their structures to be determined which can then be compared to the corresponding theoretical structures. These and other future experiment related to those mentioned here will provide detailed information at the fundamental level which will hopefully answer questions that remain in these metal oxide systems.